Winegrowing Futures

Final report

Theme 4

Optimising resource use and protecting the environment





The National Wine and Grape Industry Centre is a research centre within Charles Sturt University in alliance with the Department of Primary Industries NSW and the NSW Wine Industry Association

Contents

Abstract 1

Summary 2

Background 3

Aims 8

Targets 9

Experiments 10

Experiment 4.1 Soil-water flux and nitrogen movement in Australian vineyards 10

Materials and method 10

Results and discussion 12

Outcome and conclusion 15

Experiment 4.2 The use of bromide as a nitrate analogue to trace its movement in irrigated soils 16

Materials and method 16

Results and discussion 18

Outcome and conclusion 20

Experiment 4.3 Validation of a novel dual tensiometric drainage meter 20

Materials and method 20

Results and discussion 23

Outcome and conclusion 26

Experiment 4.4 Predictive modelling of grapevine production using remote sensing techniques 26

Introduction 26

Materials and method 35

Results and discussion 53

Outcome and conclusion 70

Experiment 4.5 Grapevine nutrient reserves and their impact on grape yield variability and yield estimation 75

Introduction 75

Materials and method 77

Results and discussion 81

Outcome and conclusion 89

Outcomes/Conclusions 90

Theme outcomes 90

Theme outputs 91

Theme milestones 91

Recommendations 92

Aerial remote sensing for yield forecasting 92

Appendices 96

Appendix 1 Communications 96
Appendix 2 Intellectual property 100
Appendix 3 References 101
Appendix 4 Staff 110
Appendix 5 Other relevant material 111
Appendix 6 Budget reconciliation 112

THEME 4 Optimising resource use and protecting the environment

Abstract

Optimising viticultural resource use for economic and environmental sustainability broadly requires knowledge of the impact of resource use practices, and opportunities to improve them. Research in Theme 4 was thus directed along two streams; one which determined the impact of water and nitrogen use in warm, irrigated inland vineyards and the other which revealed opportunities to use new tools, including remote sensing and spatial technologies to understand and optimise the use of those resources for achieving production and environmental goals. This report describes the four projects that led to those advances.

One study examined the soil solution nitrogen concentration and determined how irrigation and fertiliser management can affect the loss of both water and nitrogen from vineyards. It has highlighted the importance of both soil water and fertiliser monitoring and application practices in avoiding losses from the vineyard system. That study also created a web-based irrigation scheduling tool which normalised data from a range of different soil water measuring devices. The tool was successfully tested by farmers and consultants. A second study used bromide as a tracer to examine transport of solutes under a drip emitter for different soil types. That research has provided base line information about the movement of water soluble anions (nitrate and chloride) in a major vineyard soil type. A third study, used a dual tube tensiometer to measure the soil-water flux in the rootzone of an irrigated vineyard. This study showed that the dual tube tensiometric drainage meter is a robust, low maintenance device that may be used to provide accurate measures of soil water potential for the determination of soil water potential gradients under near-saturation conditions. Those soil water potential gradients provide useful indications of relative, vertical soil water fluxes. Combined with knowledge of the hydraulic conductivity function of soils at the measurement depth, soil water potential gradients determined with the drainage meter may be used quantify soil water fluxes and deep drainage over specified periods.

Significantly, despite the generally minimal deep drainage in drip irrigated vineyards surveyed in project 4.1, we found that even in a typical, drip irrigated vineyard in the Riverina, drainage of water beyond the root zone may occur throughout the growing season and is largely determined by the frequency and duration of irrigation. Although this finding was from a single vineyard it may indicate further opportunities to reduce water use in the region using in-situ measurement of soil water potential and drainage.

The fourth study, predictive modelling for yield forecasting, progressed in three distinct areas. (1) Incorporation of spatial data improved efficiency in yield forecast sampling; using either vineyard soil conductivity or visible-NIR remotely sensed canopy maps to target samples sites, half the number of samples were required to produce similar yield estimation errors as random sampling. (2) Vineyard remote sensing data over current and preceding seasons improved spatial yield forecasts; early season canopy growth in the preceding season added considerable skill to simple forecast models. (3) A statistical modelling protocol was developed as a winegrape forecasting tool; climate anomalies explained significant region-scale yield temporal variability.

The fifth study evaluated grapevine nutrient reserves and their impact on grape yield variability and yield estimation. The project continued research on carbohydrate reserves in relation to the management of vine productivity and fruit quality. Work undertaken to complement the predictive modelling project, together with further analysis of existing data, suggests that more immediate benefit may be obtained from the measurement of reserves as a predictor of yield rather than deliberate management. Over-wintering reserve status can be a predictor of canopy growth potential and aspects of reproductive development, while changes in reserve concentrations during a season may be indicative of internal carbon availability and cropping capacity. To facilitate incorporation of reserves into commercial vineyard management practices or future yield forecasting models, a rapid ATR-FT-IR spectrometry method was developed for perennial grapevine tissues.

Information and methods described in each of the projects may be used by individual wine businesses or at the whole of industry scale in the development of improved resource use environmental management systems.

Summary

Knowledge of soil-water movement in vineyards is essential for the management of irrigation, soil nutrition and salinity. This research aimed to determine the extent of water and nutrient losses from vineyards under differing irrigation and fertiliser strategies, the factors that determine those losses and how to measure deep drainage in real-time based on in-situ measurement of water potential gradient as input to general models of soil water movement.

The extent of water and nutrient losses from vineyards was researched in three complementary projects involving:

1. The extension of a multi-vineyard study to determine the typical concentrations of nitrogen in the soil-water solution and runoff from vineyards;
2. A study of solute movement in soil using bromide as a tracer to simulate nitrate and chloride transport under drip emitters; and
3. The use of a dual tube tensiometer and soil hydraulic flow models to determine deep drainage from the rootzone from changes in soil water potential between two points.

The multi-vineyard field study examined soil nitrogen (N) dynamics in both drip and furrow-irrigated vineyards, on three soil types. Nitrogen concentrations combined with the number of days in which drainage below the rootzone was likely indicated that subsurface pathways represent a potential N export risk from vineyards. The risk of leaching N from vineyards was related to its concentration of the soil-water solution, and fertiliser application and irrigation practices. As grapevines in most vineyards had more than adequate N the study revealed a significant opportunity to reduce the risk of environmental impacts and production costs by reducing applications of N. A web-based irrigation scheduling tool which normalised data from a range of different soil water measuring devices was developed to assist grapegrower participants in this study. That tool was successfully tested by farmers and consultants and led to modification of grower practices for greater efficiency of water use in drip irrigated vineyards. The study identified regional differences in irrigation and fertiliser associated with particular production targets and thus highlighted the need for a regional approach to nitrogen and water management in vineyards.

The bromide tracer experiment revealed that drip emitter rate was seldom the dominant factor in the movement of monovalent mineral anions through the soil. The results showed the initial soil-water content played a larger role in anion movement through the soil.

The prototype dual tube tensiometer, developed by Hutchison and Bond, was able to accurately measure the soil-water potential gradient between two points in the rootzone over long periods as input to existing general models of soil water movement. The use of several of those models was compared revealing significant differences and highlighting inadequacies in each that limit their use, at least for predicting deep drainage from dual tube tensiometer output.

As intended the results from this research form the basis of guidelines for best practice fertiliser and irrigation management, along with new elements to add to regional on-farm environmental risk management systems.

The application of aerial remote sensing to improve grape yield forecasting was investigated over three consecutive seasons. Data describing environmental, yield and quality components was collected at two vineyard sites (Hunter and Riverina). Sampling schemes captured the spatial variability of the two study sites using nested cluster algorithms with either EM38 maps or remotely sensed canopy vigour maps as input. Using spatial data to help select sites significantly increased the sampling efficiency in all three years in both vineyards. The overall potential error for yield forecasts due to vineyard spatial variability was, however, high (±20% using 9 sample sites selected with the aid of spatial information; about 30 samples were required with the aid of spatial information for an error of ±5%).

Vineyard sample data was collected at both sites at harvest, and associated winemaking and berry analysis was completed over three years at the two vineyards. Remotely-sensed vineyard canopy data (collected four times per season over three years at two study sites) were processed using a specially designed remote-sensing vineyard imagery discretisation algorithm. Best subset regression analysis revealed that remotely sensed canopy data from the preceding two years in conjunction with elevation data consistently explained 40–50% of the variability in the sampled yield. Application of the best models to whole of vineyard remotely sensed and environmental data to estimate whole of vineyard spatial variability in yield were produced.

Aggregated yield and climate data were produced for all major viticultural regions of Australia. A neural network modelling protocol was developed as a regional yield forecasting tool. The modelling protocol was applied to 1982–2007 Australian Chardonnay yield. Cross-validation indicated that about 50% of the temporal variability in yield was explained by the climate data. Indicators of yield at various stages leading up to harvest were identified from the analysis of the national climate and yield data, for example temperature at fruit set in the preceding seasons. All climate data used in the forecasting model was updated with newly available BOM pre-interpolated datasets. A paper was produced discussing the merits of different temperature based viticulture-climate indices using this new data.

A synthesis of key results of the various components of the project produced options for yield forecasting using different methods and data at various times before harvest. Important forecast variables include canopy growth rates in the preceding season, canopy size at around veraison and temperature indicators in late winter/ early spring of previous years.

The research undertaken on grapevine carbohydrate reserves since its integration into this Theme of the Winegrowing Futures Program in 2009 was largely aimed at consolidating and extending the findings of project CSU 05/01 'Management of carbohydrate reserve accumulation as a tool for regulating vine productivity and fruit quality'. One component of the research concerned the impact of over-wintering carbohydrate reserves on shoot growth and yield in the following season, and whether a direct measure of carbohydrates could provide an input for yield forecasting models. The second component of the research focussed on the influence of within season carbohydrate reserve dynamics and vine carbohydrate balance on fruit composition and wine quality.

During winter 2005, 2006 and 2007 a survey of 32 commercial Shiraz and Chardonnay blocks was undertaken across southern NSW to determine the impact of management practice and climate on carbohydrate and nutrient reserve storage in cane, wood and root tissue. Bud-dissections were undertaken at the same time, and yield data was collected for each vineyard to assess the potential value of a carbohydrate and nutrient reserve test as a yield forecasting tool. An initial statistical analysis of the large dataset produced by this survey was presented in the CSU 05/01 final report, but a new multivariate analysis incorporating climatic modelling in being undertaken for the publication of this work. During the 2009-10 season the opportunity was taken to combine a study of vine carbohydrate, nutrition and fruitfulness with spatial and remote sensing data being collected from the Shiraz trial site at Yenda as part of Project 4.4. This study included a substantial microscopy component, and complemented the earlier survey by providing a detailed understanding of bunch initiation and primary bud necrosis at the vineyard level.

To assess the influence of carbohydrate reserve status and carbohydrate supply on fruit composition and wine quality, field trials were undertaken in the Riverina from 2006 to 2010 that used a combination of crop thinning, deficit irrigation and defoliation treatments to manipulate vine carbon balance. The results demonstrate that carbohydrate reserve dynamics can differ significantly between seasons, and that even when crop load is the same, the internal carbohydrate supply may differ between years. Wine colour density and tannin concentrations of Shiraz wines were higher in the season with higher reserves between flowering and veraison, raising the possibility that carbohydrate availability during early berry development may have a greater impact on wine composition than previously appreciated. As part of the experimental approach to test this hypothesis, large potted vines are being established on a fixed trellis in the new NWGIC bird-proof enclosure, and a whole vine assimilation chamber developed to manipulate photosynthesis through varying CO_2 concentrations at various stages during berry development.

As a step towards providing the industry with a rapid method for measuring carbohydrate and nutrient reserves, staff in Project 4.5 have been working with other researchers based at the NWGIC to develop an FTIR protocol for starch, sucrose, glucose, fructose and nitrogen in wood and root tissue. A calibration based on 1880 samples has been produced for starch and total N on dried ground tissue, and work is in progress for the individual sugars and to evaluate the method with fresh intact tissue samples.

Background

Although the impact of irrigation on yield and basic fruit composition parameters (tannins and phenolics) is well understood in red wine grape varieties, the complex interactions of spatial and temporal environmental variations (soil characteristics and climatic conditions that drive water use) on grapevine

growth, yield and flavour profiles in white wine is not. Growers wanted to know how this can be managed to minimise vineyard water use whilst maximising yield for defined quality targets. Likewise, classical approaches to estimating grapevine yield are inherently inaccurate (±30%) because they suffer from similar sources of variation due both to effects of environment on grapevine growth in the previous year as well as growth and development within the current growing season.

The use of remote sensing and spatial analysis techniques to model vineyard water use, improved interpretation of data output from soil moisture monitoring equipment and yield prediction with remotely sensed data over several years might lead to improved WUE and more reliable yield forecasting. This would require a thorough analysis of the components of grapevine yield, and the application of field treatments to manipulate yield in the vineyard.

The average absolute difference between grower estimates of seasonal winegrape production and winery deliveries has been reported to be 33% (Dunn and Martin 2003). The impact of this mismatch is high, not only for wineries, where preparations for the annual vintage and harvest logistics involve significant expenditure, but also for suppliers trying to match inventory to demand and for seasonal grape price negotiations that generally rely on accurate supply forecasts. One estimate puts the collective costs of uncertainty in grape supply volume to Australian wineries at $200m each year. Clearly, greater levels of accuracy in forecasting seasonal grapevine yield will be of considerable benefit to wine producers and other sectors of the industry.

National and regional grape yield forecasts are generally based on the area of bearing vines together with an estimate of seasonal factors on grape development. Improving forecast accuracy using that approach seems achievable but only with better information on the impacts of climate on grape development.

Individual vineyard yield estimates presently rely on random and/or stratified sampling of vines and their developing grape bunches between budburst and harvest (see Clingeleffer *et al.* 2001; Dunn and Martin 1998; Martin *et al.* 2003). The average of the yield-indicating parameters, namely, bunch number and bunch weight per vine, of the sample set is then multiplied by the number of vines in the block to produce the forecast for the whole block. Dunn and Martin (2003) found that for forecasts made in January, the average absolute difference could be reduced to 20% and potentially to 10–15% by using improved protocols. However, they noted resistance to their current improvements due to the cost and effort required in the vineyard. These impediments may be overcome by reducing the number of sampled vines by segregating the vine population into zones of known variation using precision technologies such as electromagnetic (EM) surveying of soil conditions, aerial remote sensing of vine canopies or harvest yield monitoring, and, at least for sampling after fruit set, by substituting the total fruit load of each sample vine for the sub-sampling of the developing crop of the sample vine.

Further Details

In reviewing prior research and identifying knowledge gaps in the area of water use efficiency it was recognised that vineyard water use practices interacted with soil nutrition and nutrient leakage below vine root zones. Thus efficiency of both water and fertiliser (most notably nitrogen) were inseparably linked, both in terms of grapevine performance and economic and environmental impacts. We searched key databases including AGRICOLA, CAB and ASFA for both national and international papers on the movement of nutrients in surface runoff or deep drainage. The literature indicated that the leakage of nitrogen below the rooting zone of most agricultural plants is highly likely, with greater losses occurring in higher rainfall environments. There was no specific information that related to the movement of nitrogen or phosphorous in soil or water from below the roots of vines. However, compelling evidence from Western Australia (Sharma *et al.* 1994) indicated that 50% of the total water used in irrigated horticulture ends up as drainage water and about 40% of the applied N is leached below the root zone.

Publications in this area were extremely limited and hence the need for the research we undertook. The most informative piece of work on vineyards linking fertiliser use with the nitrogen contamination of waterways had been conducted by Schaller (1991) who presented groundwater pollution data from nitrate use in German vineyards at the International Symposium on Nitrogen in Grapes and Wine. He concluded that management practices such as minimum tillage could reduce N losses associated with runoff and that better N efficiencies could be achieved with better application techniques and breeding.

Although irrigation water in the Murrumbidgee Irrigation Areas (MIA) of NSW is considered to be of high quality with low salt content, excessive irrigation can contribute to ground water accessions resulting in either increased tile drainage effluent from existing relatively shallow water tables or increased accessions to the groundwater mound that brings salt from depth into the drainage water. The Vineyard Leakiness workshop held by the GWRDC in January 2002 also provided reports showing evidence that vineyards are variable and ultimately prone to leak water and nutrients. Previous studies (Bramley and Lanyon 2002) had shown a large variability in soil type and water use within vineyards, which indicates that leakage of water does occur and is influenced by soil type. However, nutrient loss and the influence of soil type on nutrient loss had not been addressed.

Soil moisture and transpiration are important for nutrient uptake, as is the composition and concentration of the soil nutrient solution (Mengel 1991). Root density is also important for nutrient uptake and is dependent on soil structure and soil chemical properties (salinity, pH, ion toxicity). Nutrient use efficiency (NUE) is the total uptake per plant of a particular nutrient (dry matter production per unit nutrient in the dry matter) and is dependent on the plant itself and the environment, particularly soil moisture (Marschner 1995). Nitrogen uptake, storage and mobilisation within grapevines varies with the stage of phenological development of vines (Wermelinger 1991). Further knowledge in matching nutrient availability and the relative uptake by the vines throughout their annual growth cycle will be important for developing a sustainable vineyard system.

Past research on grapevine nutrition and irrigation has stressed the benefits of nitrogen (Holzapfel and Treeby 1999) and irrigation management (McCarthy 1998; Loveys *et al.* 1998) for grapevine vigour control and for improving berry composition and a large field trial in the Riverina on irrigation and nutrition management (Wade *et al.* 2000) demonstrated the significance of interacting nutrition and irrigation effects on berry composition (Wade *et al.* 2001 and 2002).

Previous drainage studies in the Riverina have shown that water is leaking beyond the rootzone of grapevines. This leakage, or deep drainage, is detrimental to the environment because the resultant drainage water can contain harmful solutes such as salt and fertiliser. Analysis of tile drainage records and watertable elevations in vineyards show that on average 50% of deep drainage occurs in spring (McCaffery 1999) and in the case of one furrow irrigated vineyard, 30% of deep drainage occurred with the first irrigation of the season (Christen and Skehan 1999). A high proportion of this drainage occurring in spring is caused by irrigating too early and too heavily on a rootzone that is near to full with water, following winter rains. At this time evaporation is low due to cool conditions and canopy leaf area is small. Water applied at that time is unused by grapevines and it moves beyond the root system. Early irrigations are thought to be a response by grapegrowers to the perceived high risk of fruit loss due to inadequate soil moisture from budburst through to flowering. Excessive irrigation at this time contributes to groundwater accessions resulting in either increased tile drainage effluent from existing relatively shallow watertables or increased accessions to the groundwater mound that brings salt from depth into the drainage water.

Conventional flood irrigation practice can exacerbate this problem through excessive application of water that subsequently contributes to raising the watertables and increasing rootzone salinity (Christen and Hutchinson 2002). Consequently, these practices have to be changed to save water, which is an increasingly limited resource, and to ensure grapevine productivity is sustainable into the future by maintaining healthy soils. In addition, nitrogen is another core input in grape production. It is viewed as the most important nutrient pollutant emanating from the major Australian viticultural regions (Harrison 1994). Salt and nitrate levels in downstream river water used for drinking could become a health concern if contaminated discharges from drainage basins or aquifers enter the Murray Darling Basin Catchment (MDBC). Such outcomes have been observed in Europe and are considered threatening to the health of river systems (Schaller 1991; Schaller *et al.* 1993).

Previous studies on nutrient movement in sandy-loam soils have shown that nitrogen generally leaches readily while phosphorous is bound to clay and organic matter surfaces (Kirkby *et al.* 1997) and the concentration of phosphorous dissolved in soil-water increases when the soil's adsorption capacity is exceeded (Barrow 1989; Holford 1989). However, the movement of nutrients through duplex soils of sandy loam over clay is more complex and less well understood (Sharma *et al.* 1994).

Around the world fresh water is a scarce natural resource, this is especially true in Australia, which has only 5% of the world's fresh water (United Nations 2003). The demand on these water resources is increasing due to population and industry growth as well as increased pressure to provide water for the maintenance of aquatic environments. Associated with this increased demand for fresh water is a growing need to manage not only the quantity of water, but to maintain or improve quality.

Water moving from agricultural land can contribute to reduced water quality in inland water systems, through the transport of sediment and chemicals including nutrients, herbicides, pesticides and heavy metals. Eutrophication, accumulation of nutrients (nitrogen and phosphorous) which contribute to the development of algal blooms, is one of the key water quality issues identified in catchments throughout Australia (Atech Group 2000; Cottingham *et al.* 1995) and the world (Heathwaite *et al.* 2005; Sharpley and Tunney 2000). A number of catchments in south-eastern Australia have set nutrient reduction targets (Anon. 2004; Port Phillip and Westernport CMA 2004) with increasing pressure being applied to all sectors which contribute nutrients to the water systems, including agriculture, to meet these targets. Nutrients transported from vineyards and a range of other sources within a catchment contribute to the eutrophication of inland water. Previous work has shown that N and P may be exported from vineyards through surface and sub-surface pathways. For example (Ramos and Martinez-Casasnovas 2004), reported significant N, P and K export in surface runoff from a vineyard in Spain during a storm event, while significant losses of N to groundwater from vineyards has been reported in various viticultural regions (Muller *et al.* 1985) overseas.

The Australian viticultural sector has become increasingly aware of the need to understand and reduce the offsite impacts of its production systems, not only to meet legislative or catchment targets but also to ensure the sustainability of their properties and maintain a 'clean and green' marketing advantage. The location of many vineyards in Australia has grown out of the need to both satisfy access to water and specific climates. Many vineyards are located close to rivers or streams or within valleys that contain major watercourses that feed other agricultural industries and urban communities. The proximity of vineyards to inland water systems suggests that water and nutrients exported from the vineyard have the potential to reach inland water systems, presenting a significant offsite risk to inland water quality.

The goal of identifying irrigation and nutrition strategies that ensure minimal drainage and groundwater contamination whilst producing high quality grapes and wines required additional knowledge on the fate of water and solutes within vine root zones. The impact of irrigation and nutrient strategies on water and nutrient movement in Australian vineyard soils was largely unknown, particularly during spring and after harvest. To enhance current best practice for sustainable grape growing, a complete understanding of water and nutrient movement through vineyard soils and development of tools to facilitate adoption of modified cultural techniques was needed. Environmental and economic benefits to both the grape industry and the rural and regional communities where grapes are grown were envisaged.

Environmental management in viticulture is becoming a mandatory requirement for marketing wine in certain markets (Reedman 2001) and implementation of environmental management systems (EMS) is becoming essential (Baker 2001). Sustainable vineyard systems, incorporating the Australian and New Zealand standard for environmental management systems developed in accord with the ISO 14000 series (1996), are a useful framework for managing and assessing the impacts of an industry or farm on the environment, by integrating environmental management into an enterprise's daily operations.

This work was undertaken to assist in determining changes to environmental performance as a consequence of newly developed irrigation and fertiliser management systems. State regulations underpinning the NSW water reform issues are documented in reports such as Stressed Rivers (NSW Land and Water 1998) and they indicate the need for better environmental management. The MIA Districts Community Land and Water Management Plan (EnviroWise®) identifies a number of problems (e.g. drainage, waterlogging and salinity) in this major grapegrowing area. Similar issues are of concern in north east Victoria, the Sunraysia and Riverland production regions of south-east Australia, as well as the Padthaway region of South Australia, where increasing salinisation of irrigation water has been identified by the state's DWLBC.

The Australian viticultural industry has taken a lead role in environmental stewardship by seeking

to understand and reduce the impact that grape and wine production has on the environment. This is important, because management at the farm level is increasingly being evaluated on the basis of its environmental footprint and impact on catchments. Through the Cooperative Research Centre for Viticulture (CRCV) and the Grape and Wine Research and Development Corporation (GWRDC), a number of risk assessment tools (Baker 2004) and multi-tiered approaches to EMS (Fisher 2004) have been developed for the industry. Alongside this, some of the larger viticultural companies have been proactive in developing and introducing EMS derivatives into their management, using a range of tools from self-assessments to fully audited ISO 14000 systems.

One important environmental consideration for vineyards is water and nutrient management, as they represent costly inputs to the productions system that can negatively impact on the environment. While EMS programs such as VERA (Baker 2004) address the issues of nutrient and water management, they were not designed to provide detailed decision support trees or monitoring tools for water and nutrient management. A paucity of data on water and nutrient movement from vineyards through surface and sub-surface pathways makes it difficult to identify management priorities and benchmarks. This paucity also makes it difficult to show how management actions implemented on farm can give measurable improvements in the paddock, and even more so at the catchment scale.

Monitoring tools for risk assessment, developed previously in the grains industry EMS pilots (Ridley *et al.* 2003; Newton and Hastings 2003) are being adapted for viticulture. However, the perennial and deep rooting habit of *Vitis vinifera* required use of a range of plant and soil based monitoring methods to manage fertilisers for both productivity and the environment. Development of these monitoring tools also builds on previous research and farmer surveys (Goodwin 2002). The tools allow structured interpretation of data gathered in case studies at each of the field sites and enable evaluation of vineyard environmental impact within an EMS framework. Tools based on expert knowledge and farmer practicality, and which can show economic benefits, are most likely to influence changes in management that may lead to (a) water savings and water use efficiency, (b) improved water quality, (c) protection of the soil resource and (d) reduced environmental footprint.

There was a need to better understand the movement of nutrients applied in viticulture for a range of soils in wine growing regions of southern Australia (NE-Vic, SW-NSW and SE-SA). An important consideration is plant-soil interactions that relate to water and nutrient uptake and the mineral composition of grapes.

Tracing solute movement in soil

Monitoring the movement solutes such as nitrogen through soils is a challenging task. Solute transport through soil has been successfully assessed by using tracers to indicate the movement of water and NO3-N. Probably the most popular non-reactive conservative tracer is bromide (Br^-) which is often applied as a potassium salt (KBr) (Bowman 1984). Several studies have confirmed that NO_3^-N and Br^- concentrations are comparable (Abit *et al.* 2008; Gasser *et al.* 2002). Field solute transport studies are presented with present numerous challenges and it can be difficult to account for the many factors that affect tracer movement. For instance, previous studies have found numerous effects that can complicate tracer experiments, such as accounting for plant uptake (Gasser *et al.* 2002), differences in soil structure (Walton *et al.* 2000), changes in soil texture (Kazemi *et al.* 2008) and the presence of a shallow water table (Abit *et al.* 2008). Nevertheless, given the time scale over which transport processes of chemical movement occur the tracer approach provides a robust manner to further understand solute and nutrient transport.

Measuring deep drainage in situ

Drainage from soils is an attribute that is difficult to measure, however is required due to the risk of salt accumulation and potential of waterlogging the soil. On the other hand, drainage can leach mineral nutrients beyond the rootzone, which can lead to the contamination of natural systems. Soil water drainage follows by soil-water potential gradients and occurs over a small range of soil-water potentials at saturation. Lysimetry is the standard method for measuring drainage, however it is a costly and invasive method that lacks in-field truthing. Drainage at a field-scale is volumetrically measured from the water flowing from sub-surface drains, if available. This volumetric measurement in imprecise as the proportion of the water flow captured is questionable and sub-surface drains are used minimally across cultivated land. More recently, suction plates were developed but provide single-point measurements of drainage (van Grinsven *et al.* 1988; Masarik *et al.* 2004). Drainage can be calculated as the residual sum from a soil-water balance, which incorporates

evapotranspiration, rainfall, irrigation, runoff and the change in soil-water content (Hillel 1998). This balance method is risky as there is a large amount of uncertainty when calculating evapotranspiration.

The lack of ability to calculate drainage has led to a number of methods and meters being developed to measure soil-water flux, however fine textured soils (clay dominated) still provide the biggest challenge. The Dual Tensiometric Flux Meter whereby two tensiometers, vertically separated, are installed in situ to measure soil-water potential gradients, has been specifically designed for measuring soil-water potential near saturation. If hydraulic conductivity of the soil is unknown the measurements obtained from this meter may be used to provide an indication of water flux at various states of hydration. We tested a prototype dual tensiometric drainage meter and its ability to measure drainage from an irrigated vineyard.

Research in this Theme was thus directed toward providing baseline data on soil-water and nutrient movement, providing information on relationships between management, nutrient and water transport from vineyards across a range of grape growing regions to inform best management practice (BMP) for grape productivity and wine quality, and to develop monitoring tools for interpretation in an EMS framework. It was aimed at addressing: the drainage issues relevant to environmentally sustainable vineyard irrigation and delivering solutions to minimise off-site drainage impacts within the inland production regions of southern Australia.

The work undertaken in Project 4.5 since integration into Theme 4 in 2009 was largely aimed at consolidating and extending the findings of project CSU 05/01 'Management of carbohydrate reserve accumulation as a tool for regulating vine productivity and fruit quality'. One component of the research concerned the impact of over-wintering carbohydrate reserves on shoot growth and yield in the following season, and whether a direct measure of carbohydrates could provide an input for yield forecasting models. The second component of the research focussed on the influence of within season carbohydrate reserve dynamics and vine carbohydrate balance on fruit composition and wine quality.

During winter 2005, 2006 and 2007 a survey of 32 commercial Shiraz and Chardonnay blocks was undertaken across southern NSW to determine the impact of management practice and climate on carbohydrate and nutrient reserve storage in cane, wood and root tissue. Bud-dissections were undertaken at the same time, and yield data was collected for each vineyard to assess the potential value of a carbohydrate and nutrient reserve test as a yield forecasting tool. An initial statistical analysis of the large dataset produced by this survey was presented in the CSU 05/01 final report, but a new multivariate analysis incorporating climatic modelling in being undertaken for the publication of this work. During the 2009-10 season the opportunity was taken to combine a study of vine carbohydrate, nutrition and fruitfulness with spatial and remote sensing data being collected from the Shiraz trial site at Yenda as part of Project 4.4. This study included a substantial microscopy component, and complemented the earlier survey by providing a detailed understanding of bunch initiation and primary bud necrosis at the vineyard level.

Project 4.5 was developed to assist the other projects in this Theme, particular yield estimation by providing a physiological basis for the research and for interpreting the responses. Further preparations were undertaken to allow measurements of whole vine assimilation and also setting the basis for the project submitted previously to GWRDC on vine balance titled 'Optimising production sustainability and grape quality through a physiological definition of vine balance'. Over-winter vine carbohydrate reserves play a major role in influencing vine productivity and are an important element of predictive modelling. Information collated from data on grapevine carbohydrate reserves collected during the previous GWRDC project entitled 'Management of carbohydrate reserve accumulation as a tool for regulating vine productivity and fruit quality' contributed to this research.

Aims

To achieve the following aims and performance targets of this Theme, five inter-related projects were established.

4. Determine the extent of water and nutrient losses from vineyards under differing nutrition and irrigation strategies).
5. Develop a strategy to normalise data output from soil moisture sensors independent of sensor type deployed.
6. Describe rootzone stratification of salinity and nutrient status under various climatic, irrigation, water quality and soil conditions.

7. Develop guidelines for irrigation and fertiliser management strategies to reduce nutrient loss in drainage water.
8. Develop a practical on-farm EMS plan-do-check-act cycle to suit vineyard best management practices (BMPs).
9. Stratify vineyard sampling for yield prediction on the basis of remote sensing data and analyse remotely sensed data of individual grapevines at key phenological stages.
10. Correlate remote sensing data, yield components, sensory data and climatic data over consecutive growing seasons.
11. Determine optimum time to forecast yield with greatest accuracy and least error.
12. Produce a crop forecasting model and evaluate against industry best practice.

Experiment		Aim/s addressed
4.1	Soil-water flux and nitrogen movement in Australian vineyards	1, 2, 3, 4, 5
4.2	The use of bromide as a nitrate analogue to trace its movement in irrigated soils	1, 4, 5
4.3	Validation of a novel dual tensiometric drainage meter	1, 4, 5
4.4	Predictive modelling of grapevine production using remote sensing techniques	6, 7, 8, 9
4.5	Grapevine nutrient reserves and their impact on grape yield variability and yield estimation vines	7, 8, 9

Targets

1. Match seasonal irrigation schedules and fertiliser application to grapevine requirements for sustainable grape production
2. Develop a BMP that will minimise the environmental footprint of wine grape production in the warm inland irrigated regions of Australia
3. Review classical approaches to crop estimation
4. Improve yield prediction using remote sensing techniques

Experiments

Experiment 4.1
Soil-water flux and nitrogen movement in Australian vineyards

Materials and method

This project investigated the nitrogen export through surface pathways and the potential for nitrogen to be exported via subsurface pathways from irrigated vineyards. Seven vineyards were monitored to investigate the interaction between method of irrigation and fertiliser application on the possibility of nitrogen being lost from the vineyard environment. The measurements were taken for 3 years and were analysed in terms of the potential of off-site impacts on drainage water quality exported from vineyards. This section describes the measurements undertaken.

Site Description and Climate

Riverina, New South Wales and Rutherglen, Victoria were the focus of this research. The Riverina is a very hot grape growing region (Iland and Gago 1997) with a mean January temperature of 23.9°C and a mean annual rainfall of 406 mm. Rutherglen is a hot grape growing region (Iland and Gago 1997) with a mean January temperature of 23.3°C and a mean annual rainfall of 590 mm.

Six Chardonnay vineyards in the Riverina and one Shiraz vineyard in Rutherglen were investigated. *Table 4.1* presents details relating to irrigation, planting, block size, spacings, rootstock, cordons and pruning. Predominantly, recently planted vineyards were chosen due their limited root development and generally high fertiliser and irrigation inputs due to economic pressure to bring young vines into early production. The vineyards were all managed and operated as commercial enterprises.

Two irrigation methods were analysed: furrow or flood irrigation (F) and drip irrigation (D). Three soil types were selected within each irrigation method including: Eutrophic, Red Chromosol with a sandy loam field texture (S); Supracalcic, Red Dermosol with a loam field texture (L); and Epipedal, Grey Vertosol with a clay-loam field texture (CL) (Isbell 1996). *Table 4.1* illustrates the codes that each vineyard will be referred to hereafter.

Vineyard sampling and instrumentation

An electromagnetic induction (EM38) survey was used to select monitoring sites by identifying soil variability. The EM38 device was calibrated with electrical conductivity data to identify low, medium and high salinity, which is indicative of potentially high, medium and low leaching fractions, respectively. Monitoring was conducted in the furrow-irrigated vineyards (F) where medium salinity levels were found at both the head (H) and tail (T) of the furrow. In the drip-irrigated vineyards three sites were chosen in the middle and towards either end of the vineyard, with the middle site of medium salinity being the main site (M). Two satellite sites were also chosen in the drip-irrigated vineyard to represent low and high salinity levels.

A root distribution study was undertaken at commencement to determine the depth of the

Table 4.1 Vineyard descriptions for drip (D and DR) and furrow irrigated vineyards on sandy (S), loam (L) and clay loam (CL) soils.

Vineyard	Region	Grape variety	Irrigation type	Year planted	Block size (ha)	Spacing (m)		Rootstock	Other
						Vine	Row		
D_S	Riverina	Chardonnay	Drip	2001	2.7	2.5	3.0	Ruggeri 140	Double cordon, spur pruned
D_L	Riverina	Chardonnay	Drip	2002	2.9	1.8	3.6	Own-roots	Single cordon, spur pruned
D_{CL}	Riverina	Chardonnay	Drip	1994	33.5	2.3	3.6	Ramsey	Single cordon, hedge pruned
DR_S	Rutherglen	Shiraz	Drip	2003	2.4	2.0	4.0	Schwarzmann	Single cordon, spur pruned
F_S	Riverina	Chardonnay	Flood	2002	3.4	2.3	3.6	Ramsey	Single cordon, spur pruned
F_L	Riverina	Chardonnay	Twin furrow	2002	2.3	2.4	3.7	Ramsey	Single cordon, spur pruned
F_{CL}	Riverina	Chardonnay	Twin furrow	2002	12.6	2.3	3.6	Ramsey	Single cordon, spur pruned

vineyard rootzone. The average root length density was 0.65–0.95 cm cm^3 for all rootstocks and irrigation delivery methods (Hutton *et al.* 2007). Also, the majority of roots (73%) were above 0.5 m. Generally no roots were found below 90 cm, except in one vineyard where there was a shallow watertable at about 1.2 m below the surface. Therefore, the rootzone was defined as being above 1 m.

Prior to the start of irrigation, in September in the first season, Watermark ® (Irrometer Co., Riverside, USA) and ceramic cup soil solution samplers were installed. In the furrow irrigated vineyards the water sensors were installed at the H and T sites, while the samplers were installed at H, M and T sites and once in the satellite site. For the drip-irrigated vineyards the water sensor was installed only at the M site, while the samplers were installed directly under the dripper. The water sensors were installed at depths of 0.25, 0.50, 0.75 and 1.00 m below the soil surface, and readings were automatically recorded at hourly intervals at all depths and locations. The solution samplers were installed at depths of 0.5, 0.75 and 1.00 m for furrow irrigation and 0.25, 0.50 and 1.00 m for drip irrigation. Soil solution was sampled when the soil was at or above the upper limit (about −10 kPa), to ensure the highest possibility of downward water movement. The samples were obtained by applying 60 kPa suction to the ceramic cup sampler for about 24 h and then extracting the sample.

The surface pathway of nitrogen was monitored in two vineyards (one drip (DR_S) and one furrow (F_{CL})) between September and June in each season. The runoff was collected from a 1 ha subcatchment at the DR_S site. A galvanised U-channel at the bottom of the slope became the monitoring point. Surface runoff (DR_S) was monitored using a 300 mm H Flume (Ackers *et al.* 1978) and an ISCO storm monitoring system (ISCO Inc., Lincoln, Nebraska, USA) comprising of a 4230 bubbler flow meter and a 3700 automatic sampler. At the F_{CL} site a 5.9 ha subcatchment was measured by collecting runoff in an earthen drain, at the end of each irrigation furrow. Surface runoff (F_{CL}) was monitored using a 200 mm H Flume (Ackers *et al.* 1978) and an ISCO storm monitoring system (ISCO Inc., Lincoln, Nebraska, USA) comprising of a 4230 bubbler flow meter and a 3700 automatic sampler. Each of the monitoring systems provided measurements of flow at 1-minute time step intervals and 1–20 water samples per event greater than 1000 L.

Soil and water analysis

Initial soil samples were collected in September in the first season at 0–20, 20–40, 40–60, 60–80 and 80–100 cm depths using a tractor mounted, 4.4 cm diameter hydraulic soil coring machine. Approximately 6 cores were collected and bulked for each vineyard. The soils were analysed for electrical conductivity (EC), ammonium-N (NH_4^+-N), nitrate-N (NO_3^--N) using standard methods (Rayment and Higginson 1992) and for particle size under the International System (White 1987).

Water collected from the ceramic cups (soil solution) and from the surface runoff was filtered within 12 hours of collection (50 mL through a 0.45 µm Durapore ® membrane filter; Millipore Australia Pty Ltd, Australia). If nutrient analysis could not be conducted immediately the filtered samples were frozen. All water samples were analysed for nitrate plus nitrite ($N_{(nitrate + nitrite)}$) using the Griess-Ilosvay chemistry (Rayment and Higginson 1992) on a LaChat Quickchem 8000 flow injection system with a cadmium column (Zellweger Analytics Inc., USA). Total dissolved Nitrogen (TDN) was analysed on selected samples using an alkaline persulphate digestion procedure and the LaChat Quickchem 8000 flow injection system.

Irrigation, fertiliser application and vine n status

The vineyard managers controlled the irrigation and fertiliser application at each site, using a range of fertiliser products and application methods. In the furrow-irrigated vineyards, the fertiliser was ripped into the irrigation furrow in either spring/autumn or both. On the drip-irrigated vineyards, the fertiliser was either banded under the vines or fertigated through the dripper system. Most vineyards fertilised post harvest (April/May) and again in October/November, except for DS which applied fertiliser 4–5 times a year (*Table 4.2*).

Irrigation and fertiliser application were generally applied according the vineyard managers' historical records. The rates of nitrogen applications were sometimes modified in the second and subsequent seasons after the results from the petiole nitrogen analysis were provided to the managers. Total nitrogen concentrations of the irrigation water were less than 0.25 mg N L^{-1} across all vineyards and seasons.

The amount of nitrogen exported from the vineyard was determined from hand-harvesting four replicated sites. The fresh weight of the harvested fruit

Table 4.2 Summary of water and nitrogen inputs (harvest to harvest for 2004-05 and 2005-06) and nitrogen exported from drip (D and DR) and furrow (F) irrigated vineyards on sandy (S), loam (L) and clay loam (CL) soils.

	Vineyard						
	D_S	D_L	D_{CL}	DR_S	F_S	F_L	F_{CL}
2004-05							
Inputs							
Fertiliser N (kg N ha^{-1})	32.5	54.9	59.6	22.5	81.1	87.6	95.9
Timing	Oct, Nov, Dec, Jan	May, Oct	May, Nov	Nov	Apr	May, Nov	May, Oct
Irrigation Water (ML ha^{-1})	6.5	2.2	5.3	1.5	5.0	6.0	4.9
Rainfall (ML ha^{-1})	2.5	2.5	2.5	4.6	2.5	2.5	2.5
Export							
Fruit N (kg N ha^{-1})	58.7	40.6	72.2	13.9	46.5	51.7	40.4
Balance (input–export) N (kg N ha^{-1})	-26.2	14.3	-12.6	8.6	34.6	35.9	55.5
2005-06							
Inputs							
Fertiliser N (kg N ha^{-1})	66.2	45.4	26.6	0	81.1	29.6	81.1
Timing	Mar, Apr, Nov, Dec, Jan	Apr, Nov	Apr, Aug		Apr	Apr	Apr
Irrigation water (ML ha^{-1})	4.2	2.1	4.9	1.5	5.2	5.2	5.5
Rainfall (ML ha^{-1})	3.6	3.6	3.6	4.7	3.6	3.6	3.6
Export							
Fruit N (kg N ha^{-1})	43.7	38.0	42.0	7.9	44.2	52.1	48.3
Balance (input–export) N (kg N ha^{-1})	22.5	7.4	-15.4	-7.9	36.9	-22.5	32.8

was measured and a subsample of the whole bunches (about 2 kg) was taken. The subsample was washed with phosphate free detergent and distilled water, oven dried at 90°C to result in the fresh to dry weight (DW) conversion. The dried sample was then coarse ground using a Cyclotec 1093 mill (Foss, HillerØd, Denmark) and then further ground to 0.12 mm with an ultra-centrifugal mill (Retsch ZM100, Haan, Germany). Following the grinding, the total nitrogen content was determined using a total combustion gas chromatograph (Carlo Erba NA 1500, Italy). The calculation of fruit nitrogen exported from vineyards at harvest was calculated using nitrogen concentration multiplied by fruit yield per ha to give kg of nitrogen per hectare.

Results and discussion

Over the two seasons (2004-05 and 2005-06) of monitoring, the irrigation volume ranged from 1.5 to 6.5 ML ha^{-1}, with the furrow-irrigated vineyards applying more water. The nitrogen fertiliser inputs varied significantly between vineyards. The adequate range for petiole nitrogen concentrations is 0.8–1.1% DW for own-rooted vines and 0.9–1.25% DW for vines on Ramsey rootstock (Robinson *et al.* 1997). The vineyards D_L, F_{CL}, F_S and F_L all were above this adequate range, while D_{CL} and DR_S were close to or within the range and D_S was deficient in both seasons. In general, the vineyards with higher nitrogen fertiliser application had higher mineral concentrations in the soil and nitrogen concentrations in the soil solution, suggesting the application rate of fertiliser affects the nitrogen leaching from vineyards (Muller 1993; Wahl *et al.* 1997).

The petiole nitrogen concentrations increased linearly with nitrogen application, but the yield remained unaltered by nitrogen inputs. The excessive nitrogen may have been used for higher vegetative growth, such as shoots. Also, the nitrogen concentrations in the root and wood samples increased with more nitrogen fertiliser, which further supports the excessive nitrogen application is utilised for vegetative growth. It is suggested that nitrogen application rates should not exceed 40–50 kg N ha^{-1}, and rates above 60 kg N ha^{-1} are prone to higher concentrations of soil solution nitrogen being leached.

A simple nitrogen balance indicates the annual nitrogen fertiliser inputs ranged from 0–96 kg N ha^{-1}, with less than this being exported as produce. This occurred for 5 vineyards in 2004-05 and 4 in 2005-06, suggesting there is a greater potential for nitrogen

loss from these sites via atmospheric, surface and subsurface pathways. The mature vineyard had a greater ability to buffer the nitrogen imports and exports, due to the nitrogen reserves in the older vines (Bates *et al.* 2002).

Where greater nitrogen fertiliser inputs were experienced, a higher mineral nitrogen concentration in the soil was found (*Table 4.3*). Up to a depth of 80 cm the nitrogen content was positively correlated (r>0.6) with fertiliser rate. Nitrogen sources are generally concentrated at the soil surface (Wild 1988), which was found for D_{CL}, DR_S and F_{CL} vineyards, some accumulation further down the profile was experienced at F_S, F_L and F_{CL} vineyards. This accumulation of nitrogen down the profile indicates the mobility of fertiliser nitrogen and mineral nitrogen within the soil profile.

The annual surface runoff for the 2-year period 2004-05 and 2005-06 for DR_S was 12.9 and 3.9 kL ha^{-1} and for F_{CL} 77.7 and 191 kL ha^{-1} respectively (*Table 4.4*). The runoff for DR_S was associated with rainfall events, while the runoff from F_{CL} was associated with irrigation events. On F_{CL}, approximately 5 ML ha^{-1} of irrigation water was applied with less than 5% being exported via surface runoff. The nitrogen concentration in the surface runoff ranged from 0.01 to 8.3 mg N L^{-1}, with the annual flow weighted mean concentration less than 3 mg N L^{-1} (*Table 4.4*). When these samples were analysed for nitrite concentration it was found that nitrite was general less than 5% of the nitrate and nitrite combined concentration. Nitrate and nitrite concentrations accounted for 20–75% of the TDN (<0.45 µm) in the runoff water, which suggests other forms of nitrogen, including organic and colloidal Nitrogen, are significant. The flow weighted annual nitrogen concentrations were generally higher than the in-stream environmental trigger value of 0.5 mg N L^{-1} (ANZECC and ARMCANZ, 2000). These results indicate the annual export of nitrogen by surface runoff (0–0.3 kg N ha^{-1}) is not a significant pathway of nitrogen loss from the monitored sites. It should be noted that management factors, including irrigation management and fertiliser application rates, could significantly affect nitrogen export from vineyards.

The soil-water measurements were used to identify conditions for growth and provide an indication of the potential for drainage below the rootzone (*Table 4.5*). All the vineyards experienced periods where the soil matric potential greater than −10 kPa, which is indicative of field capacity and the most conducive for downward movement of water. Between 0 and 205 days were experience with a matric potential of greater than −10kPa. The furrow-irrigated vineyard

Table 4.3 Soil properties, including electrical conductivity (EC), mineral nitrogen (nitrate, nitrite and ammonium) and particle size analysis by depth for the drip (D and DR) and furrow (F) irrigated vineyards on sandy (S), loam (L) and clay loam (CL) soils .

		Mineral N (mg N kg^{-1})					Particle size analysis (% sand:silt:clay)				
		Depth (cm)					Depth (cm)				
Vineyard	EC1:5 (µS/cm)	0–20	20–40	40–60	60–80	80–100	0–20	20–40	40–60	60–80	80–100
D_S	292	2.00	0.59	0.67	4.37	4.48	82:5:13	84:5:11	85:4:11	75:8:17	79:6:15
D_L	200	0.52	0.61	0.46	0.55	1.05	51:10:39	39:12:49	56:14:30	44:28:28	42:15:43
D_{CL}	150	15.35	1.32	0.43	0.27	1.01	47:9:44	47:10:43	35:9:56	19:12:69	30:9:61
DR_S	230	4.58	1.58	1.25	1.80	0.25	66:15:19	61:15:24	59:13:28	59:13:28	68:9:23
F_S	215	11.63	11.75	17.08	6.21	4.16	76:10:14	73:7:20	71:8:21	62:14:24	54:15:31
F_L	183	1.63	5.48	12.06	8.38	4.42	43:38:19	66:17:17	32:23:45	28:18:54	28:17:55
F_{CL}	274	51.31	28.20	20.67	8.55	3.37	47:11:42	31:9:60	32:15:53	33:10:57	33:7:60

Table 4.4 Nitrogen concentrations and load exported as surface runoff (July to June) from drip (D and DR) and furrow (F) irrigated vineyards on sandy (S), loam (L) and clay loam (CL) soils.

			Concentration (mg N L^{-1})		
Vineyard	Year	Surface runoff (kL ha^{-1})	Total dissolved nitrogen*	Nitrate and nitrite*	Nitrate and nitrite range
DR_S	2004-05**	12.9	0.54	0.12	-
	2005-06**	3.9	8.20	2.90	-
F_{CL}	2004-05	77.7	1.60	1.20	0.01-8.3
	2005-06	191.0	0.83	0.63	0.01-4.0

* Annual flow-weighted mean concentration

** Only one runoff event

generally experienced a greater number of days where drainage was likely compared to the drip-irrigated vineyard (57 and 37 days, respectively). Due to the variability between the vineyards there was no significant difference between the irrigation methods (P>0.2). Even with the limitations of single point measurements and averaging the soil matric potential across the depths, the data suggests there is a risk of drainage for some of the vineyards in some years.

Nitrate and nitrite concentrations varied significantly over time for the drip and furrow-irrigated vineyards (*Table 4.6*). The greater variation occurred between the years and individual samplings than the variation between vineyards. The majority of variation occurred between sites on a vineyard and between the replicated sites at M, H and T. The D_S, D_L and F_S vineyards displayed a significant nitrogen concentration variation between the sampling sites (P<0.015), which can be accounted by the soil Nitrogen, soil-water content and soil physical property variations and sampling frequency (time and number of samples). The between sample variations show no significant effect of the timing of fertiliser, time of year or soil matric potential at the time of sampling on the soil nitrogen concentration. The nitrate and nitrite concentrations, even at 1 m, were generally higher than the trigger value of 0.5 mg N L^{-1} (ANZECC and ARMCANZ, 2000) indicating there is a potential for leachate to drain and degrade water quality. Another interesting value is at 1 m the nitrate and nitrite concentrations range 0.64–82 mg N L^{-1}, which highlights the ability for mineral nitrogen to be mobilised within the soil profile and potentially

Table 4.5 The number of days the soil profile, to 1 m, had an average matric potential above –10 kPa and the optimum zone of –10 to –80 kPa for drip (D and DR) and furrow (F) irrigated vineyards on sandy (S), loam (L) and clay loam (CL) soils.

		Soil Matric Potential 0 to –10 kPa (days per year)		Soil Matric Potential –10 to –80 kPa (days per year)	
Vineyard		**2004-05***	**2005-06**	**2004-05***	**2005-06**
DS	M	58	32	225	329
DL	M	2	2	276	353
DCL	M	94	63	184	297
DRS	M	0	58	159	129
FS	H	125	205	159	155
	T	0	16	229	334
FL	H	52	15	116	296
	T	79	200	209	130
FCL	H	59	64	219	291
	T	48	10	235	320

*2004-05 "year" from September to June included 285 days of monitoring data

Table 4.6 Combined average concentrations of nitrate and nitrite (mg N L^{-1}), both mean and range shown, in soil solution for drip (D and DR) and furrow (F) irrigated vineyards on sandy (S), loam (L) and clay loam (CL) soils.

		Depth (m)							
Vineyard	**Season**	**0.25**		**0.50**		**0.75**		**1.00**	
D_S	2004	5.97	0.04–36	5.56	0.10–36			17.20	0.10–88
	2005	11.69	0.00–47	13.19	0.04–54			5.71	0.00–38
D_L	2004	12.75	0.10–69	5.01	0.10–51			6.08	0.10–39
	2005	27.05	0.05–155	57.16	0.24–149			5.80	0.10–14
D_{CL}	2004	4.96	0.10–68	0.84	0.10–8			0.64	0.10–6.8
	2005	22.12	0.08–141	21.71	0.02–114			12.30	0.04–97
DR_S	2004	14.98	0.08–69	4.14	0.62–19			4.87	1.40–12
	2005	1.98	0.01–16	0.34	0.01–4.8			1.12	0.00–8.5
F_S	2004			44.66	0.10–138	45.48	0.10–104	37.77	0.10–76
	2005			27.07	0.10–121	47.36	0.10–215	40.32	8.60–150
F_L	2004			4.65	0.10–54	5.91	0.02–98	5.27	0.02–74
	2005			17.70	0.09–154	12.07	0.00–91	4.01	0.00–67
F_{CL}	2004			109.14	0.10–266	54.25	0.10–116	38.54	0.11–138
	2005			98.31	0.10–222	83.72	0.10–225	82.33	0.10–155

degrade water systems. However, the magnitude of the nitrogen export reaching the water system depends on the location to the water system, nitrogen load exported and the level of dilution beyond the vineyard.

Overall four main areas were analysed in this project for their effects on nitrogen concentrations, including soil type, irrigation method, fertiliser application and nitrogen form in the soil solution. Three soil textures were analysed using an ANOVA of solution nitrogen concentration at 1 m below the surface, where it was found the soil type did not significantly affect soil solution ($P>0.05$). The concentration of nitrogen in the soil solution was significantly higher in the furrow than drip-irrigated vineyard ($P<0.01$). This difference may be due to irrigation method and from the higher nitrogen application rates for the furrow-irrigated vineyards. The fertiliser nitrogen inputs varied from 0–96 kg N ha^{-1}, where in general the vineyards with a higher fertiliser nitrogen input caused an increase in mineral nitrogen concentrations in the soil solution. Selected samples revealed 95% of nitrogen measured was nitrate. From the DR_S vineyard, the TDN comprised between 25–80% nitrate and nitrite, depending on sampling time. These concentrations indicate other forms of nitrogen, such as ammonium, organic nitrogen or colloidal material, were contributing significantly to total nitrogen concentrations. Therefore, all the vineyards could be adversely affecting water quality from nitrogen leaching and can be exacerbated by higher soil nitrogen concentrations and fertiliser application rates.

Outcome and conclusion

The soil nitrogen concentration study has revealed that the amount of nitrate nitrogen leaving both drip and furrow-irrigated vineyards by surface runoff is about 5%. Most nitrogen losses were occurring in the soil solution through drainage. The data collected from 6 vineyards revealed the timing, quantity and method of water application have significant effects on nitrogen leaching from vineyards. The nitrogen content of soil was positively correlated ($r>0.6$) with fertiliser rate up to a depth of 80 cm. From the observations made in this study, application rates of 40–50 kg N ha^{-1} appeared sufficient to achieve optimal vegetative growth and fruit N composition. N removal in harvest fruit generally accounted for only half the seasonal application rates thus indicating an opportunity to reduce production costs and the risk of N losses beyond the rootzone.

The normalisation of soil-water sensor output data was developed into a web-based software tool, which was extensively taken up by vineyard managers and consultants. This provides a tool that outputs soil-water fluctuations regardless of the soil moisture sensor.

There was no evidence of rootzone stratification of salinity in this study. However the concentration of mineral nitrogen was generally highest further down the profile in sand and loam soils; in contrast to the clay-loam soils where it was highest at 0–20 cm.

Stratification of salts within the rootzone may be caused by that accession of salt by rising water tables. However this is becoming less of a risk with the rapid adoption of drip irrigation in the Riverina and other major irrigated winegrape production regions. Evidence obtained in this project showed that the average EC of the soil solution throughout the soil profile at all sites was well below threshold for effects of salinity on water availability to grapevines and there was no evidence (either visual or analytical) of specific salt toxicity at any site. However with trends toward less water application in regions with saline irrigation water it would be prudent to monitor for salt accumulation in the rootzone and to promote appropriate leaching irrigations.

Experiment 4.2
The use of bromide as a nitrate analogue to trace its movement in irrigated soils

Materials and method

The experiment was conducted in the Riverina, NSW where the irrigation was controlled by the vineyard property owner and scheduled according to commercial practice. Three treatments were established, whereby different irrigation volumes were applied using pressure compensated drip emitters (Netafim, Melbourne Australia) with different discharge rates. The three discharge rates were 1.0, 1.6 and 2.3 L h^{-1} (T1, T2 and T3). The drippers were spaced 0.6 m apart. The duration of irrigation on each occasion was the same as that of rest of the vineyard which received water at T2 rates. The irrigation volume on each sampling date is given in *Table 4.8*. Irrigation began on 26 September 2008 and ceased on 30 April 2009. The experiment used a complete randomised block design, with four replicates. Each treatment block was 25 m long and three vine rows wide.

Experimental site description

The experimental site for this research was located within a 2.7 ha commercially managed vineyard near Griffith, NSW. The vineyard was planted with Chardonnay grapes (*Vitis vinifera* L.), with a row spacing of 3.6 m and vine spacing of 2.5 m, using a single cordon, spur pruned and drip irrigated system. The site is typical of the Riverina region including low relief and deep alluvial sediments with some sandy sections, which were deposited by prior/ancient streams. The soil is classified as a Brown Dermosol according to the Australian Soil Classification System (Isbell 2002), which indicates the surface soil (0–15 cm) is clay-loam in texture with a sandy clay-loam below. This soil is well-drained and common in the Riverina. For the research a number of soil parameters were measured using standard methodology, including bulk density using the core method (McKenzie *et al.* 2002), particle size analysis using the hydrometer method (Gee and Or 2002) and electrical conductivity and pH (Piper 1942 and Rayment and Higginson 1992). *Table 4.7* below shows all the results from these measurements for six depths.

The climate in the Riverina is typically semi-arid, and characterised by hot and dry summers with mild winters experiencing occasional frosts. The average rainfall is 406 mm, which is spread evenly throughout the year. The Riverina typically has large evaporative losses and low relative humidity during summer, and irrigation is essential to maintain grapevine productivity. An automatic weather station at the experimental site, measured temperature, relative humidity, solar radiation and rainfall. Using this data, a modified Penman equation was used to calculate the potential evapotranspiration (ET_o) (Meyer *et al.* 1999). The crop evapotranspiration (ET_c) was calculated by incorporating a crop coefficient (K_c) value, which changed according to the size of the canopy of the grapevine (Nicholas 2004) (*Table 4.8*).

Bromide tracer application

To determine the rate and extent of nutrient losses a bromide ion tracer (Br^-) was used to detect and measure the movement down the soil profile. A bromide tracer was chosen as it is a conservative, non-reactive anion and had been successfully applied in other leaching and solute transport studies (Flury and Paprtiz 1993). An aqueous solution of potassium bromide (KBr) was applied on 7 November 2008, close to flowering when fertiliser is usually applied, at a rate of 32 mg Br^- cm^{-2}. This bromide concentration is comparable with that used in other tracer studies (Tilahun *et al.* 2005). The tracer was applied using an animal health vaccinator (NJ Phillips Pty Ltd). Injections of 5 mL was applied 5 cm apart in a square grid layout (625 m^2) at a depth of 20 mm below the soil surface (*Figure 4.1*). The centre of the injection grid was immediately below a drip emitter. Fifteen injection sites were used for

Table 4.7 Soil characteristics by depth for the soil found at the field experimental site.

Depth (cm)	EC (dS m^{-1})	pH (1:5 water)	Bulk density (g cm^{-3})	Sand percent (2-0.02 mm)	Silt percent (0.02-0.002 mm)	Clay percent (< 0.002 mm)
0–10	0.13	7.09	1.40	48.5	8.9	42.6
10–20	0.21	7.19	1.40	40.3	7.9	51.9
20–45	0.48	7.24	1.46	28.9	7.7	63.3
45–60	0.64	8.21	1.27	27.9	11.3	60.9
60–75	0.46	8.91	1.30	31.6	10.5	57.9
75–100	0.36	9.44	1.37	40.1	11.8	48.2

Table 4.8 Rainfall, crop evapotranspiration and irrigation volumes for the three drip emitter rates (T1, T2 and T3) for the field experimental site at the five sampling times for Br-.

Dates	Days after experiment start	Cumulative rainfall (mm)	Cumulative ET_c (mm)	Cumulative irrigation volume (mm)		
				T1	T2	T3
14/11/2008	7	29.0	21.8	1.4	2.2	3.2
3/12/2008	26	59.0	76.0	39.8	63.7	91.6
23/12/2008	46	105.2	145.0	71.3	114.1	164.0
29/01/2009	83	114.4	318.2	188.4	301.5	433.4
18/03/2009	131	130.8	500.2	322.7	516.3	742.2

each treatment to accommodate for five sampling times. Since all sampling was destructive there was no repeat sampling.

To measure the concentration of bromide through the soil profile, soil cores were taken at predetermined locations along each treatment on five occasions during the 2008-09 growing season (7, 26, 46, 83 and 131 days after the solution was injected). The background bromide concentration, determined prior to tracer injection, was within 1.5×10^{-4} to 9.6×10^{-3} mg Br^- cm^{-3}. The soil cores were collected directly below the drip emitter using a tractor-mounted hydraulic corer. Soil cores were obtained and divided into eight depth increments: 0–5, 5–10, 10–20, 20–30, 30–40, 40–60, 60–80 and 80–100 cm. Soil samples were oven dried for 48 hours at 105°C and passed through a 2 mm sieve. An aqueous soil extract solution, of a 1:1 ratio was prepared using 20 g of dried soil and 20 mL of deionised water. Each sample was shaken using a rotating laboratory shaker, centrifuged and filtered (0.48 µ) into vial and analysed for bromide using chromatography (Dionex ICS-2500 system).

Soil-water and watertable measurements

The bromide concentration method can be used to measure the gravimetric soil water content, which is determined from the oven dried soil core samples. Following this the volumetric soil water content can be calculated by accounting for bulk density. The measurement of the volumetric soil water content provided a direct soil-water observation at each sampling time. Simultaneously, an additional record of soil moisture dynamics was recorded with granular matrix resistant sensors (Watermark Irrometer Co., USA) at three depths of 25, 50 and 75 cm below the middle row of each treatment. Four test wells were installed, one in each treatment and one control outside the irrigated vine area, to monitor the changes in the watertable height.

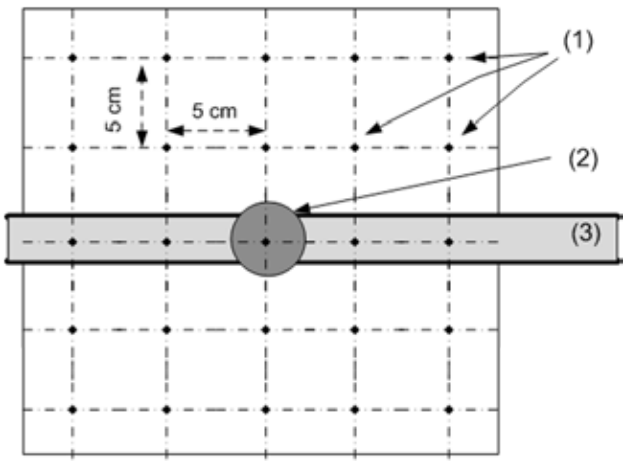


Figure 4.1 Location of bromide tracer injection points (1) relative to drip emitter location (2) and drip line (3).

Plant measurements, CLT model and statistical analysis

Remotely sensed images were used to estimate the crop canopy area (m^2). For each treatment, the fruit yield was calculated at harvest on 28 January 2009 and shoot weights (kg m^{-2}) measured in the following winter.

The Convective Log-normal Transfer (CLT) function model developed by Jury and Roth (1990) assumes the soil consists of a series of stream tubes, in which the travel time of solute particles to a reference depth *L* is a random variable distributed log-normally (Biggar and Nielsen, 1976). Hence, for a narrow pulse of a tracer such as Br^- applied to the surface soil, we assume that the time *t* for a particle of solute to reach a given depth *L* is a random variable distributed log-normally, that is:

$$\ln t \sim N(\mu, \sigma^2) \quad \text{[Equation 1]}$$

where $\mu = E[\ln t]$ and $\sigma^2 = \mathrm{Var}[\ln t]$. The travel time pdf $f_L(t)$ is then:

$$f_L(t) = \frac{1}{\sigma t\sqrt{2\pi}} \exp\left[-\frac{(\ln t - \mu)^2}{2\sigma^2}\right] \quad \text{[Equation 2]}$$

This model assumes there is no mixing (i.e. dispersion) between these stream tubes. The CLT model has often been found to be most appropriate for field solute transport experiments with resident concentration data (Ellsworth *et al.* 1996; Jury and Sposito 1985; Vanderborght *et al.* 1996). The CLT model has been used to make estimates for transport parameters of different net applied water volumes to predict differences in the risk of NO_3-N leaching (Mallawatantri and Mulla, 1996). Mallawatantri and Mulla found a large variation in predicting leaching risk according to whether plot or field-scale data were used. Gasser *et al.* (2002) were able to modify the CLT model with source and sink terms for N to allow estimates of NO_3-N flux concentrations at 1 m depth, while Butters and Jury (1989) found that a CLT model calibrated at 0.3 m could estimate the leading of the applied solute (Br^-) to a depth of 25 m. Hence, we find that the CLT can be applied to a range of data and is able to provide a useful approach to mathematically describe the solute transport processes in soils.

Analysis of Variance (ANOVA) statistical analysis was carried out to determine the differences between the treatments at each sampling time, for all measurements conducted. A statistically significant difference was set at the five percent level ($p<0.05$) using GenStat software (Lawes Agricultural Trust 2005).

Results and discussion

The results from the bromide tracer experiment are given in *Figure 4.2*, for each treatment (T1, T2 and T3) at each of the five sample times. The greatest amount of solute movement occurred during the first seven days by which time there was tracer at a depth of 30 cm. This movement is likely to have been assisted by rainfall (20 mm) that occurred a day after the tracer was applied. The relatively rapid movement of the bromide tracer was probably also due to the well-structured nature of the Brown Dermosol.

Approximately three weeks after the tracer application, the tracer had leached from the top-soil and the solute front (location of the peak concentrations) had moved to a depth of 30 cm for T2. At that time, the concentration peak was highest for T3 indicating the drip emitter rate directly affects the movement of solutes. The sampling on day 46 shows the peak for all three treatments around 30-50cm, and with some higher concentrations further down the profile. On day 83 the peak was around the 60–90 cm depth, which is close to the bottom of the rootzone of grapevines in this soil type. Finally at day 131, all treatments had returned to nearly the background bromide concentration to a depth of 40 cm and the only treatment showing significant bromide concentrations was T1 at the lowest depths. This may indicate the lower drip emitter rate slows the speed of solute and water movement through the soil.

The mass balance analysis of the bromide tracer as a percentage of the applied amount is given in *Figure 4.3*. The results show the soil leached strongly after the start of the experiment and a strong recovery of 70–80% was obtained. However, as the experiment progressed lateral spreading and considerable variability of the applied tracer caused the recovery of bromide tracer to decrease with time. The mass balance displays small variation between the treatments, which indicates that the irrigation volume did not strongly affect the bromide tracer movement. The low recovery rates of bromide tracer may be due to by-pass or preferential flow (White *et al.* 1986). The low recovery of bromide tracer is not uncommon and the values obtained here are consistent with other studies (Bandaranayake and Arshad 2006; Flemming and Butters 1995). It is common for field tracer experiments recover less than 100% of the tracer applied (Skaggs *et al.* 2002).

The results from the CLT modelling are presented in *Table 4.9*. The only significant difference between treatments was on the 26th day for T3. Considering T3 had the highest drip emitter rate, the relatively small values for z (depth) are unusual since the higher the drip emitter rate the deeper the expected solute depth. The lack of a strong relationship between the derived parameters and the treatments was not unexpected as those derived parameters relate to the whole profile

Table 4.9 Parameter estimates (μ and σ) from the least squares of the time-travel of the CLT model, for each treatment at the first 3 sample times after Br- was applied (days).

Sample time (days from start)	Treatment	π†	σ
7	1	3.06 (±0.08)	0.74
7	2	3.12 (±0.09)	0.83
7	3	2.96 (±0.09)	0.85
26	1	3.15 (±0.08)	0.81
26	2	3.00 (±0.09)	0.85
26	3	3.30* (±0.08)	0.73
46	1	3.36 (±0.08)	0.81
46	2	3.39 (±0.09)	0.83
46	3	3.43 (±0.07)	0.70

† Standard error of the mean is given in brackets for μ .
* $p<0.05$

and the transient nature of the soil water movement is more likely to lead to differences between depths.

When comparing the results from the CLT model with actual field measurements we find a similar outcome. *Figure 4.4* gives the normalised bromide concentration, which was fitted for the CLT model for the three treatments at 26 days.

The results from the measurement of the soil-water content were used to determine bromide concentration. The first three samples are shown in *Figure 4.5*. Those are the most relevant for comparison with the bromide tracer data. At the first sampling, the greatest difference in the soil-water was found across the whole soil profile, but as the soil became saturated those differences decreased and the soil-water content became more uniform. The only data

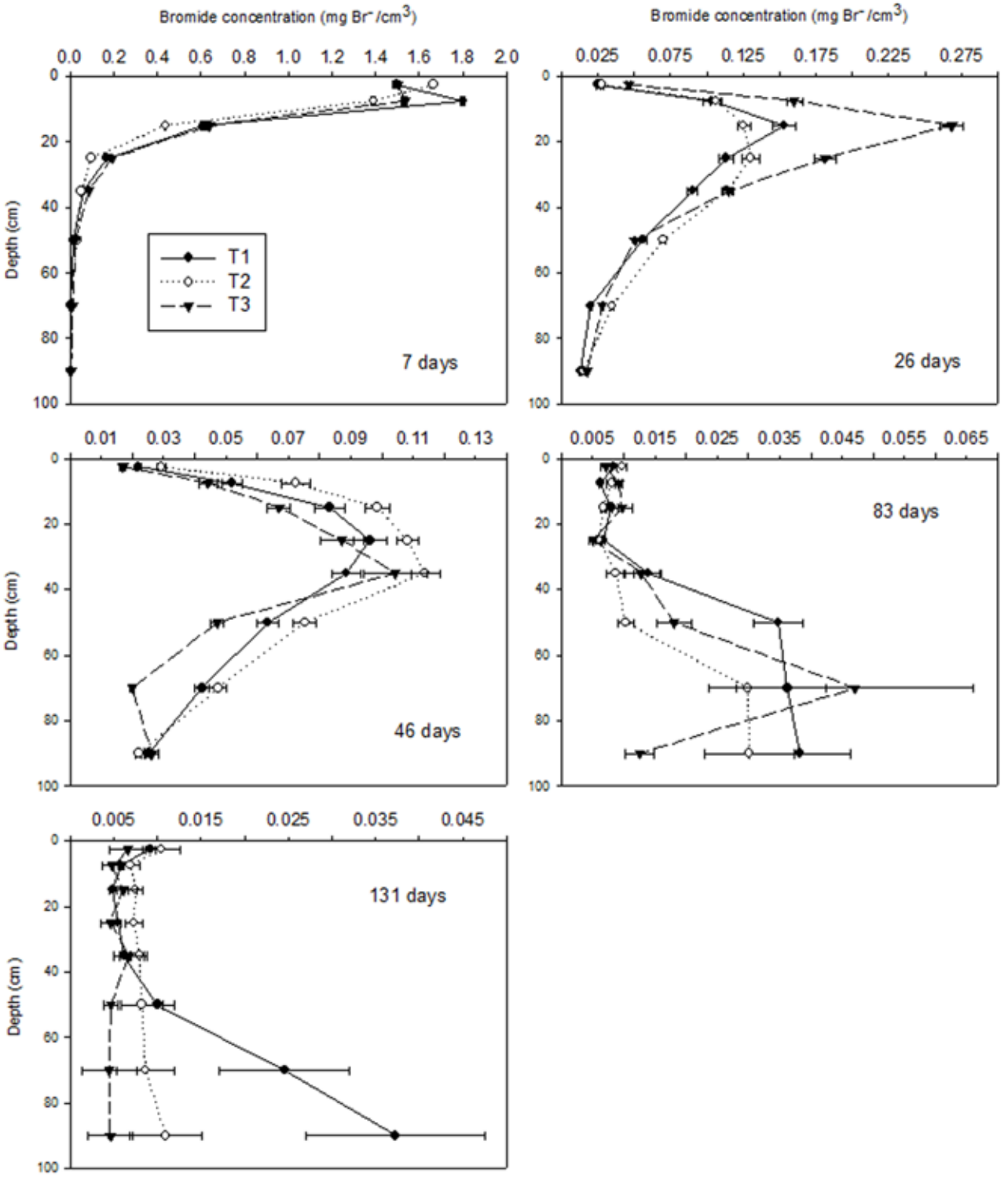


Figure 4.2 Bromide concentration (mg Br^- cm^{-3}) by depth (with SE bars) for T1, T2 and T3 at five sampling times after the bromide tracer was applied.

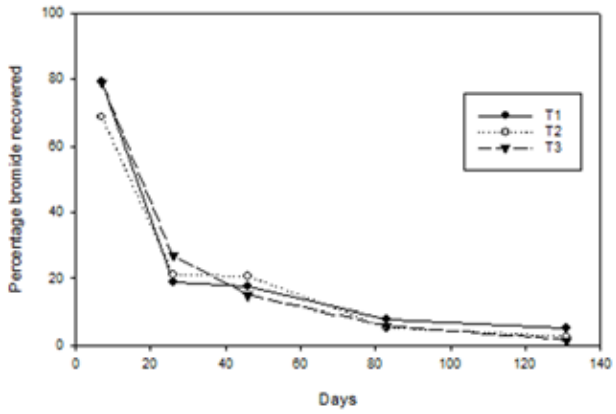


Figure 4.3 The percentage bromide recovered as a percentage of the amount applied at five sampling times for three different irrigation volume treatments (T1, T2 and T3).

showing a significant difference was for the sample time after 26 days where T3 (with the higher drip emitter rate) had the wettest soil. These results are comparable with the bromide tracer where T3 at 26 days had the highest concentration of bromide tracer.

Outcome and conclusion

The bromide tracer research conducted in the Riverina demonstrated a robust methodology to calculate and determine soluble nutrient losses to deep drainage beyond the rootzone. In this instance, it was determined the nutrient movement was the highest for the T2 and T3 drip emitter rates. The most significant data was obtained on the 26th day after tracer injection. Therefore, the drip emitter rate did not affect the nutrient and water movement in the soil profile but rather the soil properties. The results from this study isolated the importance of clay content and soil bulk density as important soil properties, which have a significant influence on the mobile water content and the movement of highly mobile nutrients such as nitrate. These results emphasise the need to manage vineyard soils according to their unique properties. This is especially relevant for the application of fertilizers and subsequent irrigation scheduling.

Experiment 4.3
Validation of a novel dual tensiometric drainage meter

Materials and method

The drainage meter

The drainage meter comprises two vertically separated tube tensiometers mounted within a single PVC housing (9 cm diameter, *Figure 4.6*) (Hutchinson and Bond 2001). The tube tensiometer is a narrow vertical tube containing a porous, diatomaceous earth.

A measurement of in situ soil-water potential (h) is taken adjacent to each sensing tip (*Figure 4.7*, *part 11* and *12*) over the range –L<h<0 cm, where L is the tube length plus the height of the sensing tip, by measuring the pressure at the bottom of the tube (*Figure 4.7*, *part 8*). The pressure transducers (at the bottom of the tube) are calibrated against soil-water suction over a range of temperatures, to an accuracy of ±0.5 cm of water. When the measurement of soil-water potential is performed, a simultaneous temperature measurement is performed using the thermistor mounted near the pressure transducer. The data from the pressure transducers is converted to soil-water potential based on the calibration of the pressure transducers. Electrical cables provide a power supply to the pressure transducers and to transmit a digital output (mA) to a data logger (Elsema Pty Ltd, Smithfield, NSW, Australia). Nylon tubes vent the transducers to atmospheric pressure. If the tensiometer is below the maximum measured value the tensiometer is able to re-wet itself, which makes this meter low maintenance if the field is dry for long periods of time. This meter has the added feature of being able to inject and withdraw fluid to/from the soil for analysis.

Site Description

The experiment was conducted in a drip-irrigated vineyard near Hanwood in the Riverina. The vineyard comprised mature, own-rooted *Vitis vinefera* cv Chardonnay, planted 1.8 m apart in rows 3 m apart.

The soil, locally known as Hanwood loam, is well structured and free draining (Butler 1979). It typically has a loam textured A horizon above a light clay subsoil with various amounts of sandy soil. The profile is typically uniform to a depth of 0.6 m, after which small amounts of carbonate material is found. Hanwood loam is classed as a Brown Dermosol (Isbell 2002) and as a Calcic Haploxeralf (Soil Survey

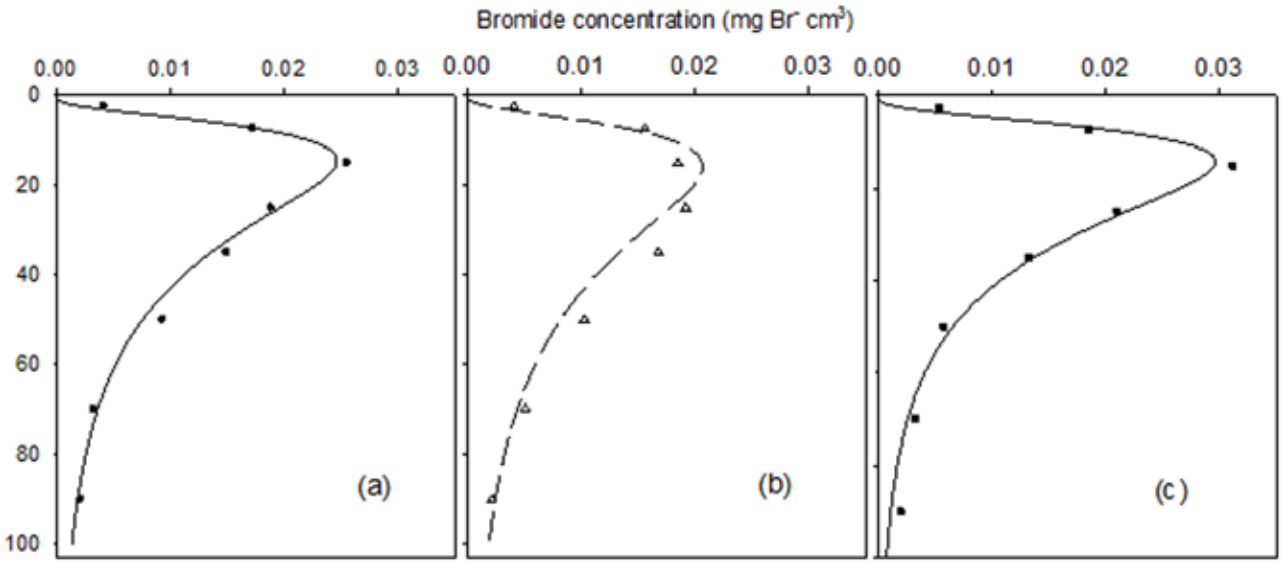


Figure 4.4 The normalised resident Br^- concentration using the fitted CLT model for (a) T1, (b) T2 and (c) T3 at the second sampling time (26 days).

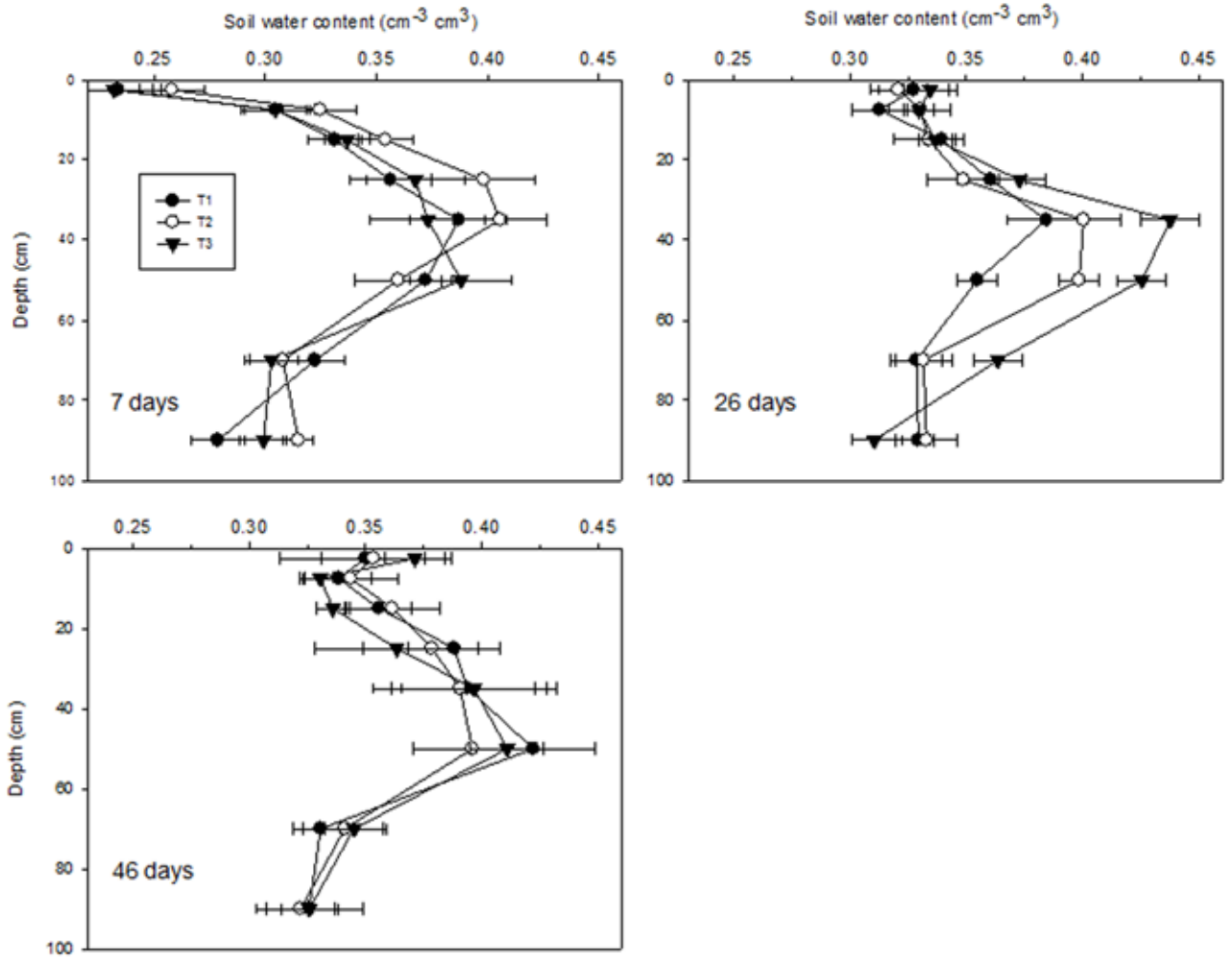


Figure 4.5 Soil water content ($cm^3\ cm^{-3}$) for each treatment at the first three sampling times after the bromide tracer was applied.

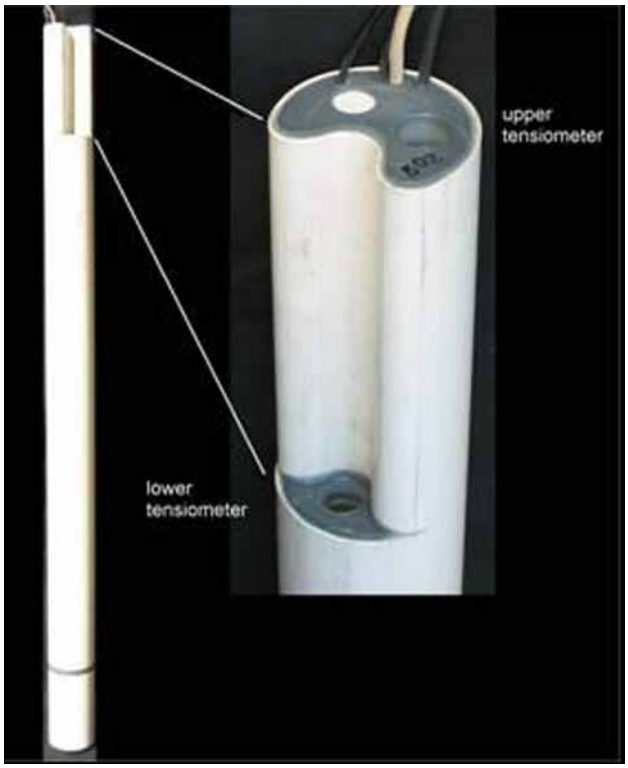


Figure 4.6 Drainage meter showing the upper and lower tensiometer sensing tips.

Staff 2010). The soil properties measured as the study site are given in *Table 4.10*.

Measurements

The drainage meter was installed at a depth of 67.5 cm, which corresponded to the depth of the rootzone of the grapevines. Regular measurements of soil-water potential gradient were recorded, and corrected for temperature. The dates and duration of irrigations were recorded and used to calculate volumes of irrigation per hectare.

An automatic weather station at the study site recorded humidity, temperature, wind speed and solar radiation at hourly intervals. A tipping bucket rain gauge was also installed, which logged any rainfall greater then 0.2 mm every hour. The potential evapotranspiration (ET_o) was calculated using the FAO 56 equation and this data (Allen *et al.* 1998).

Parameter estimation using an inverse modelling approach

The HYDRUS software (Šimůnek *et al.* 2006) offers several soil hydraulic models to simulate variably saturated non-linear flow through porous media. The method employed by HYDRUS involves an inverse parameter optimisation procedure. Thus, the objective function Φ was minimised using a weighted least-squares approach that is based upon the Levenberg-Marquardt technique. Here Φ is the difference between measured values (from the drainage meter) and predicted values of soil water potential, h for a particular measured parameter w:

$$\phi(\beta) = \sum_{i=1}^{n} w_i \left[q_i^* - q_i(\beta) \right]^2 \qquad \text{[Equation 3]}$$

To solve Equation 3 transient flow data from the lower tensiometer of the drainage meter was used. Water was pumped at a low flow rate (200 mL h^{-1}) into the top of the drainage meter to produce a subsurface spheroidal source. This provided a wetting response that changed h for the upper and lower tensiometers. *Figure 4.8a* shows water flowing into the drainage meter over five distinct cycles that lasted >1200 h. These cycles are referred to as the pump-down procedure which was commenced once the soil profile had dried to just beyond an *h* value of 100 cm. Drying the soil profile was undertaken to avoid the complicated effects of hysteresis. The cumulative volume (cm^3) of water pumped (*Figure 4.8b*) onto the top of the drainage meter was modelled numerically using HYDRUS with the lower tensiometer observations (h).

The model domain specified vertical flow over a two-dimensional plane that was 200 cm high and 100 cm wide, which was segmented into a finite element size of 2.5 cm. A free drainage condition was applied at the lower horizontal boundary of the domain, while no flux was permitted from the two vertical boundaries or the upper horizontal boundary. The upper tube tensiometer of the drainage meter (length 120 cm, diameter 1.8 cm) was included and diatomaceous earth material was specified over this

Table 4.10 Key chemical and physical properties of the soil at selected depths.

Depth (cm)	EC (dS m^{-1})	pH (1:5 water)	Clay (%)	Silt (%)	Sand (%)	Bulk density (mg cm^{-3})
0-10	0.23	8.15	23.9	17.9	58.2	1.49
30-40	0.08	8.37	30.7	19.7	49.6	1.43
50-60	0.22	9.10	26.9	27.9	45.2	1.36
80-100	0.37	9.88	20.6	24.6	54.9	1.52

area of the domain. A variable flux condition was set at the top of the tube tensiometer and this was also diatomaceous earth, which acted as a hydraulic bridge (with an area of 22.5 cm^2). It was over this area that the model domain allowed water to be pumped into the drainage meter. The rest of the domain was specified as a single material to represent the surrounding soil profile. The initial soil water conditions were set to an h value of 100 cm. The modelling procedure involved optimising parameter estimates of soil hydraulic properties in a step-wise manner. It was assumed that the variances of the errors in the measured data were equal and a weighting coefficient of 1 was applied.

Results and discussion

Data was recorded from the 1 September 2006 until the 31 March 2007. The data was graphed both as soil-water potential and the soil-water potential gradient (*Figure 4.11*). Two distinct wetting events and two drying periods are evident. Prior to the initiation of irrigation (12 October 2006) the measurements of soil-water potentials revealed a drying trend (*Figure 4.11a*), however after irrigation commenced a rapid increase in soil-water potential is apparent (both tensiometers). Up to 23 October the increase continued, however following this date a fluctuating cycle was experienced. The fluctuating cycle was over arched by a regime of diminishing soil-water potential until 28 January 2007. The fluctuations corresponded with irrigations, which did not fully replace soil-water lost through evapotranspiration. Drainage occurred at times when the soil-water potential was high (i.e. greater than 0), which was evident until early December where the gradient was also positive (*Figure 4.11b*). The total rainfall contributed to soil saturation (66 mm) but did show a distinct response at the depth of the drainage meter (*Figure 4.11c*).

The second major wetting up of the soil occurred on 28 January, after the grapevines were harvested and irrigation was increased (*Figure 4.11a*). Following harvest, the evaporative demand of the grapevine decreases, due to fruit removal and leaf losses from

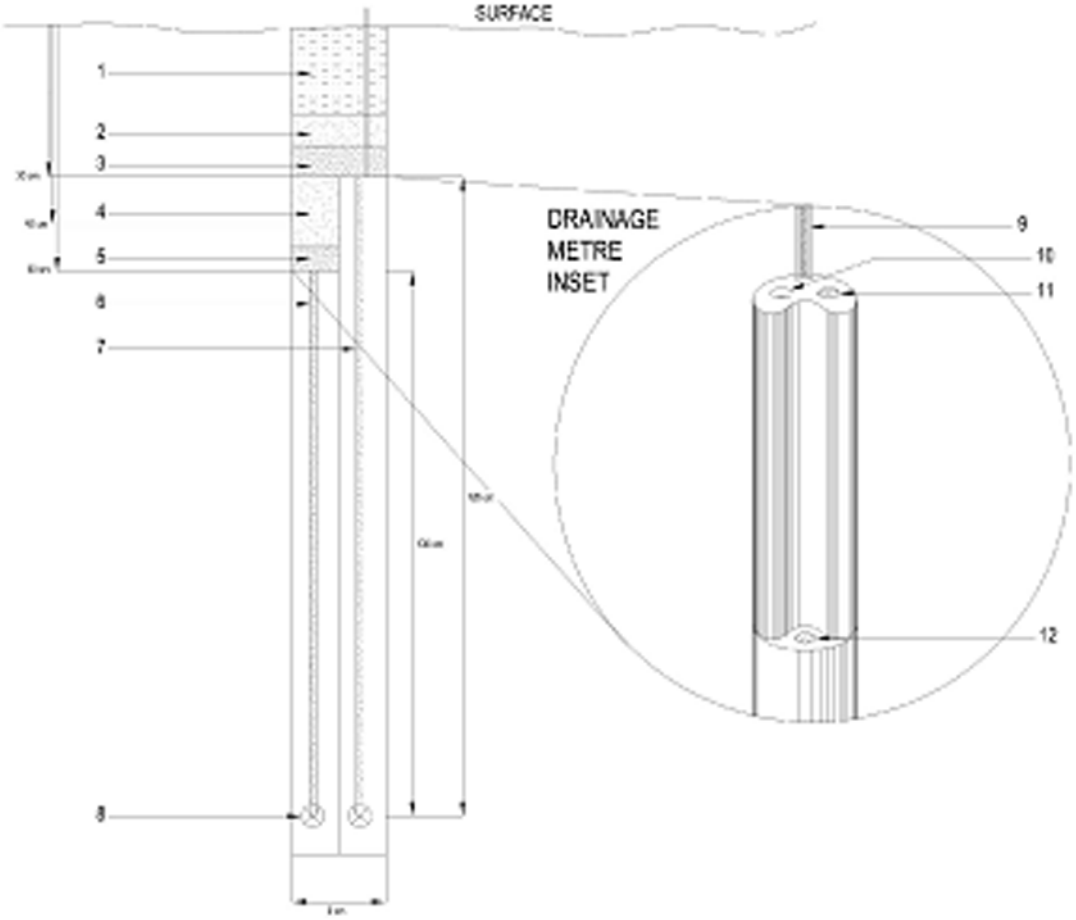


Figure 4.7 Drainage meter with two tube tensiometers: subsurface installed view (a) and close-up view of the tensiometer sensing tips (b). A cross-sectional view (a) of an installed drainage meter with repacked soil (1), upper bentonite seal (2), diatomaceous earth for upper tensiometer (3), lower bentonite seal (4), diatomaceous earth for lower tensiometer (5), tube for lower tensiometer (6), tube for upper tensiometer (7) and pressure transducers (8). The inset (b) shows the electrical cables and plastic tubes (9), ceramic disc (10), sensing tip of upper tensiometer (11) and sensing tip of lower tensiometer (12).

pre-harvest trimming and machine harvesting. Following harvest, the soil-water potential and soil-water potential gradient fluctuated in correspondence with irrigation scheduling (*Figure 4.11a* and *b*).

The soil-water potential gradient data was used to calculate the amount of drainage measured on an unscaled basis, i.e. units not defined (*Figure 4.9*). From the graph, the dots indicate there was a steady amount of drainage during the observation period. On only seven days no drainage occurred, while high drainage occurred on two occasions viz. in mid-October 2006 and the end of January 2007. Following harvest, a sharp rise in cumulative drainage occurred (after 26 January 2007).

Estimates of the soil hydraulic properties were made (*Table 4.11*) using the inverse modelling procedure within the HYDRUS software. Using observations of h from the lower tensiometer and the volume of water applied from the pump-down procedure (*Figure 4.11*) estimates of soil hydraulic properties were calculated

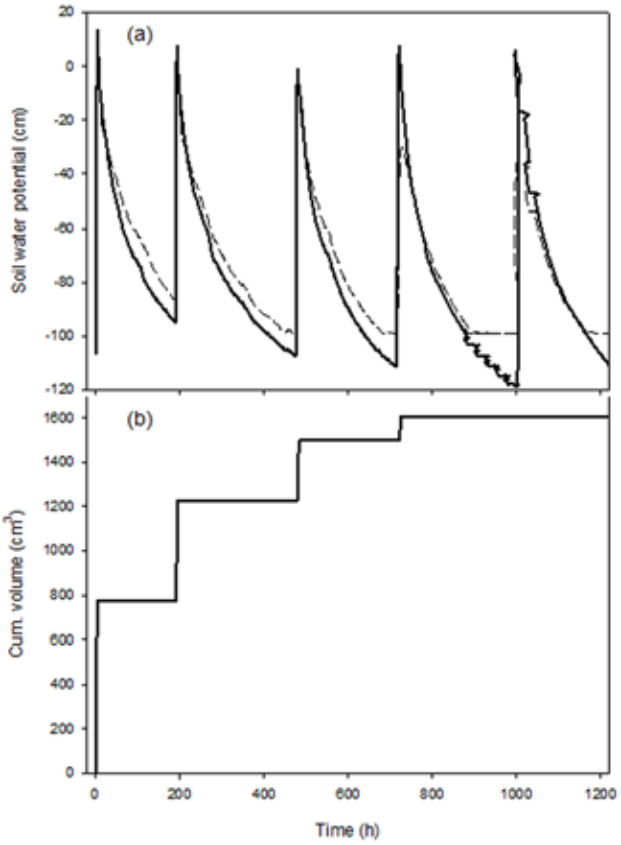


Figure 4.8 (a) Observed soil water potential (cm), h for the upper (solid line) and lower (dashed line) tensiometer of the drainage meter with (b) the cumulative volume of water (solid line) pumped.

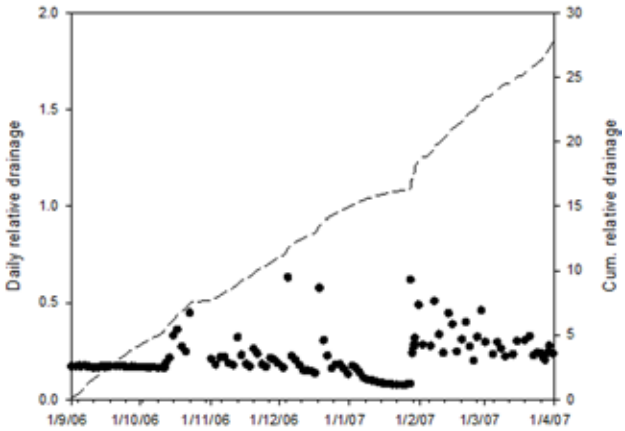


Figure 4.9 Changes in daily relative drainage (•) and cumulative relative drainage (- - -) based on the soil water potential gradient values from 1 September 2006–31 March 2007.

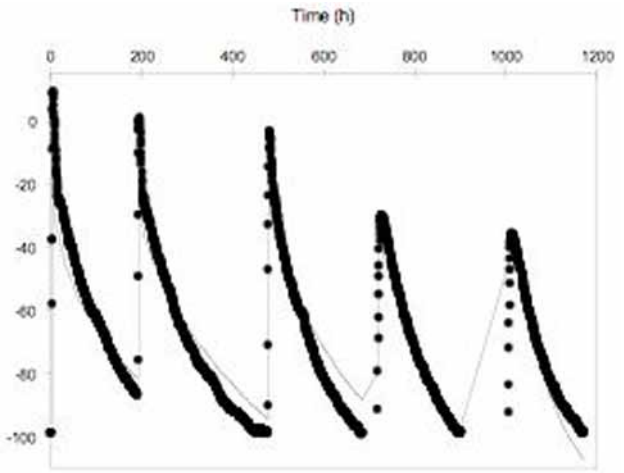


Figure 4.10 Lower tensiometer observations (•) with modelled values (solid line) of soil water potential during the pump down procedure.

Table 4.11 Final parameter estimates of soil hydraulic properties.

			95% Confidence limits	
Parameter	**Final estimate value**	**S.E. Coeff.**	**Lower**	**Upper**
α (cm^{-1})	9.0e-06	6.0E-07	8.2E-06	1.05E-05
N	1.083	0.003	1.076	1.089
K_s (cm h^{-1})	18.1	1.28	15.59	20.61
L	0.1	0.05	0.00	0.20
w_2	0.038	1.15E-03	0.03	0.04
α_2	0.114	4.28E-03	0.11	0.12
n_2	3.416	0.06	3.34	3.58

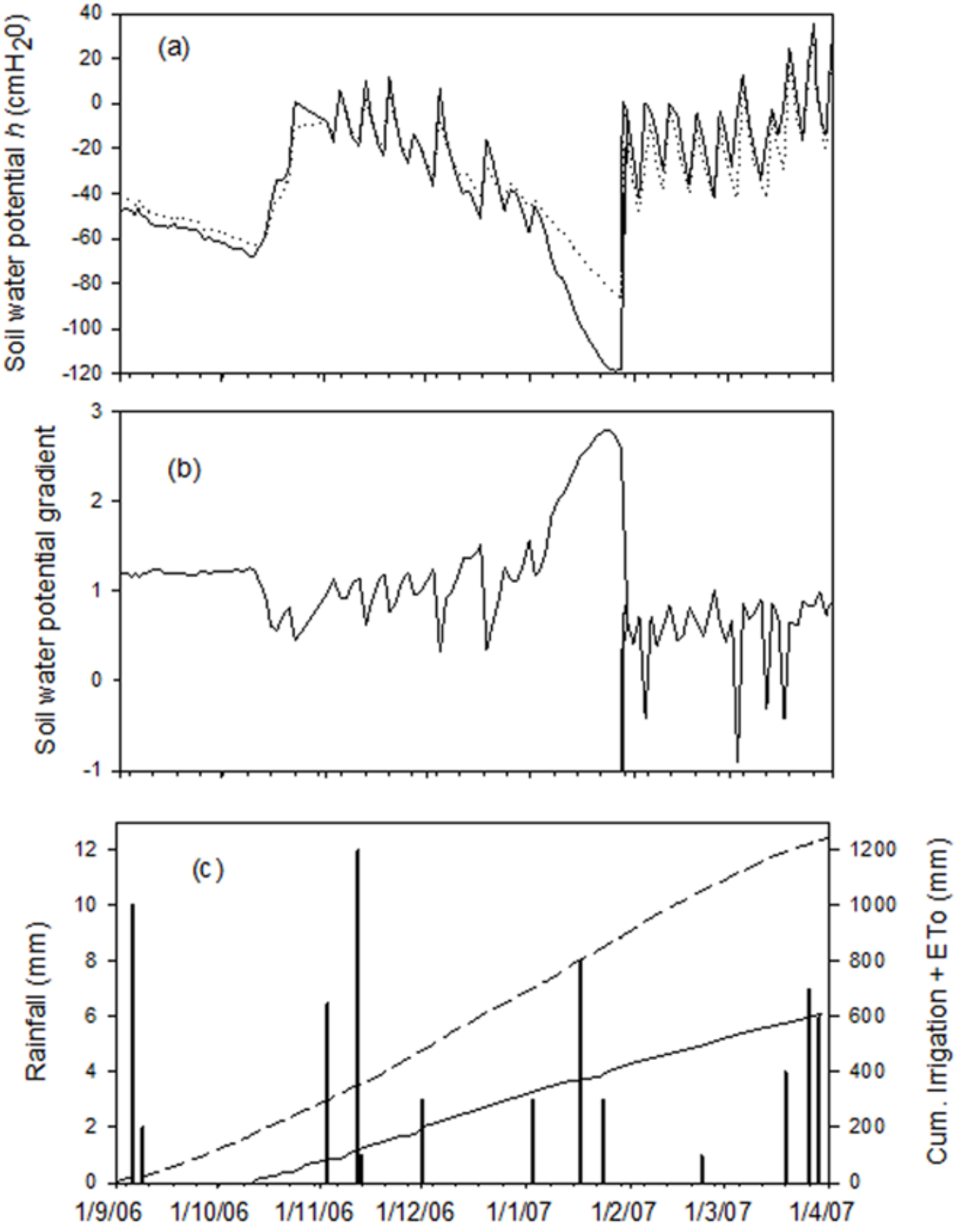


Figure 4.11 Seasonal field measurements from a drainage meter of: (a) soil water potential h (cm of H_20) for the upper (solid line) and the lower (dotted line) tube tensiometer; (b) calculated soil water potential gradient; (c) daily rainfall (mm), cumulative irrigation (solid line, mm) and potential evapotranspiration ET_o (dashed line, mm) in a vineyard, Hanwood, NSW from 1 September 2006–31 March 2007.

based upon initial values given in *Table 4.10*. The estimates from the HYDRUS model gave an R2 value of 0.89 and the predicted values of h were close to the observed values from the lower tensiometer during the pump down procedure (*Figure 4.10*).

The results given here demonstrate the application of the dual tensiometric drainage meter. The measurements obtained from the meter assist in the understanding of the soil-water balances in irrigated vineyards. Frequent drainage is experienced throughout the growing season, particularly when large amounts of irrigation are applied and the grapevines are not transpiring the volume of water applied, for example after harvest. Inverse modelling of transient flow data was undertaken successfully and parameter estimates were made of soil hydraulic properties. Nevertheless, it is possible to improve estimates of soil hydraulic properties by applying alternative models with differing soil hydraulic conductivity functions. This novel research provides insights into how the soil-water balance can be better managed to prevent near-saturated conditions, which have the potential to leach water and nutrients from the soil profile.

Outcome and conclusion

We conclude from this study that the dual tube tensiometric drainage meter is a robust, low maintenance device that may be used to provide accurate measures of soil water potential for the determination of soil water potential gradients under near-saturation conditions. Those soil water potential gradients provide useful indications of relative, vertical soil water fluxes. Combined with knowledge of the hydraulic conductivity function of soils at the measurement depth, soil water potential gradients determined with the drainage meter may be used quantify soil water fluxes and deep drainage over specified periods.

Significantly, despite the generally minimal deep drainage in drip irrigated vineyards surveyed in Project 4.1, we found that even in a typical, drip irrigated vineyard in the Riverina, drainage of water beyond the root zone may occur throughout the growing season and is largely determined by the frequency and duration of irrigation. Although this finding was from a single vineyard it may indicate further opportunities to reduce water use in the region using in-situ measurement of soil water potential and drainage.

Experiment 4.4
Predictive modelling of grapevine production using remote sensing techniques

Introduction

Section 1

The predictive modelling stream progressed in three distinct areas. Each of these areas is represented in subsections. Incorporation of spatial data improved efficiency in yield forecast sampling (*Section 1*). Vineyard remote sensing data over current and preceding seasons improved spatial yield forecasts (*Sections 2a, b*). Climate anomalies explained significant region-scale temporal yield variability (*Sections 3a, b*).

Using spatial information to improve vineyard sampling

Whole of vineyard assessment for ripeness and yield forecasting is common practice, often employing spatially randomised sampling. However, the level of spatial variability in yield and fruit composition within vineyard management blocks can be high, meaning that, unless many samples are collected, large potential errors in derived estimates are likely. We investigated whether vineyard sampling procedures that incorporate knowledge of vineyard spatial information that relates to yield and fruit composition variability would better estimate both the true ripeness level and the final yield.

Previous studies have demonstrated patterns of quantifiable measures of vineyard spatial variability, such as canopy vigour and soil electrical conductivity, correspond to patterns of future yield and grape composition at harvest. Targeted sampling was conducted over two years, guided by a geographic information system's nested-cluster analysis of remotely sensed imagery in one vineyard and EM38 soil maps in another. Subset modelling of targeted schemes with various numbers of samples produced significant efficiency improvements over equivalent random sampling. However, the level of variability in these vineyards was too high to produce accurate estimates of fruit composition and yield with a number of samples that would be considered reasonably practical using either random or targeted sampling strategies. Precision viticulture tools may nonetheless be able to further reduce potential sampling error by weighting samples according to the area of the vineyard that has similar characteristics to the sample locations, and by providing better

estimates of vineyard spatial variability in yield and ripening.

This section of the report describes two related experiments, each spanning three years, to produce targeted sampling schemes that improve yield forecasting. In one experiment, information on the potential spatial variability in yield was inferred from soil electrical conductivity. Sample sites were spatially fixed for the three years of the study and were selected using a nested cluster algorithm. In the other experiment, information on the potential spatial variability in yield was inferred from optical remote sensing of the vineyard canopy. Canopy vigour of each individual grapevine within the vineyard was derived from imagery acquired at veraison in each year. The grapevines were ranked and a sample set of vines were selected at equal intervals of the list of ranked vines. The error intervals in estimates, produced using Monte Carlo simulations of subsamples of all sampled vines using knowledge of the potential spatial variability in yield, were compared to the sampling error that would have occurred if using random sampling. The targeted sampling schemes performed consistently better than the random sampling schemes. An increase in sampling efficiency resulted in both experiments; for the same level of error in estimates produced using random sampling, the number of samples required in a targeted sampling scheme fell by about 40% (using soil EC) and by about 20% (using remote sensing). The level of error was still very high, with 36 targeted sample sites required to reduce the potential error to ±10%. Due to the high level of spatial variability and the desire to reduce the sampling effort further, the recommendation is to study spatiotemporal variability of sites to derive sample locations that best match inter-annual variability in yield of the whole block.

Viticultural context

The average absolute difference between grower estimates of seasonal winegrape production and winery deliveries has been reported to be 33% (Dunn and Martin 2003). The impact of this mismatch is high, not only for wineries, where preparations for the annual vintage and harvest logistics involve significant expenditure, but also for suppliers trying to match inventory to demand and for seasonal grape price negotiations that generally rely on accurate supply forecasts. One estimate puts the collective costs of uncertainty in grape supply volume to Australian wineries at $200m each year. Clearly, greater levels of accuracy in forecasting seasonal grapevine yield will be of considerable benefit to wine producers and other sectors of the industry. A key cause of inaccuracy in yield forecasting is the inherent spatial variability within vineyard blocks. Up to 10 fold variation was typical within Cabernet Sauvignon vineyards in a yield monitoring study of several regions of Australia (Bramley and Hamilton, 2004). Extensive sampling is necessary in order to produce data that is representative of the spatial variability within vineyards.

Individual vineyard yield estimates presently rely on random and/or stratified sampling of vines and their developing grape bunches between budburst and harvest (see Clingeleffer *et al.* 2001; Martin *et al.* 2003; Dunn and Martin 1998). The average of the yield-indicating parameters, namely, bunch number and bunch weight per vine, of the sample set is then multiplied by the number of vines in the block to produce the forecast for the whole block. Dunn and Martin (2003) found that for forecasts made in January, the average absolute difference could be reduced to 20% and potentially to 10–15% by using improved protocols. However, they noted resistance to their current improvements due to the cost and effort required in the vineyard. These impediments may be overcome by reducing the number of sampled vines by segregating the vine population into zones of known variation using precision technologies such as electromagnetic (EM) surveying of soil conditions, aerial remote sensing of vine canopies or harvest yield monitoring. This section of the report presents results of a study investigating the relative benefits of using spatial information to reduce the number of samples required to describe the variability of yield within a vineyard block and hence reduce the sampling time for accurate yield estimation procedures.

Section 2a

Using remote sensing to increase yield forecasting accuracy

Predictive mapping of within-vineyard winegrape yield, quality and ripeness, using high spatial resolution optical remotely-sensed imagery of grapevine canopy, is an emerging practice in precision viticulture. The process relies upon relationships between image-derived canopy vigour measures and potential fruit composition elements and yield components (i.e. berry weight, berries per bunch and bunch counts). Regular image acquisition of two contrasting vineyard sites (one hand-pruned with relatively small canopies, and one machine-pruned with relatively

large canopies) over a three year period enabled an analysis of annual variation in correlations between remotely sensed image-derived grapevine canopy descriptors and yield and fruit composition sampled at harvest in characteristically different vineyards. An image processing algorithm to segment row crop canopy imagery into single grapevine objects was developed for vineyard canopy mapping. Various remote sensing vegetation indices that could be calculated from 4-band colour infrared imagery for each grapevine object revealed that indices sensitive to high vegetation densities, such as the triangular vegetation index and enhanced vegetation index, performed significantly better at predicting fruit composition and yield elements than the commonly used normalised difference vegetation index. In the larger canopy, machine-pruned vineyard, derived canopy vigour measures consistently positively correlated with yield and negatively correlated with the key quality indicator, grape anthocyanin content. In addition, fruit ripeness, indicated by berry sugar content, was negatively correlated with canopy vigour descriptors but only in relatively low yielding years. Similar correlations were observed in the hand-pruned lower vigour vineyard, but were significantly weaker and inconsistent. The level of information about canopy vigour in the pixels (i.e. number of pure grapevine canopy pixels and the proportion of grapevine canopy within mixed pixels) that made up each vine object may have contributed to effecting differences in observed correlations between the two vineyards; imagery containing fewer canopy pixels resulted in weaker relationships between remotely sensed canopy information and fruit yield and composition elements. The ability of optical remote sensing to successfully map within vineyard variability in winegrape composition and yield may vary depending upon vineyard characteristics and management as well as temporal variability in overall vineyard production.

Abbreviations

α	probability of Type I error
θ	vineyard row orientation
φ	field orientation (perpendicular to θ)
a, b	parameters used in models that describe location and direction of individual vineyard rows
d_{vine}	spacing of individual grapevines along a vineyard row
d_{row}	spacing of vineyard rows
n	number of vineyard rows in the vineyard region of interest
m	number of segment areas (individual grapevines) in a vineyard row
r	correlation coefficient
r^2	coefficient of determination
x, y	pixel coordinates in horizontal and vertical directions respectively
δx, δy	distance between samples on a row in horizontal and vertical directions respectively
B	binary array, describing location of grapevine canopy and inter-row space
R_w	reflectance of waveband w
T	transformed coordinate array describing location of individual vineyard rows
X, Y	horizontal and vertical pixel coordinate arrays
EC_a	apparent electrical conductivity (of soil)
EVI	enhanced vegetation index
LAI	leaf area index
NDVI	normalised difference vegetation index
ROI	region of interest
SR	simple ratio
TA	titratable acidity
TSS	total soluble solids
TVI	triangular vegetation index
VARI	visible atmospherically resistant index
VI	vegetation index

Viticultural context

Detailed spatial knowledge about vineyard performance enables targeted management of water, fertiliser and spray application and selective harvesting to produce uniform quality fruit deliveries (Bramley and Hamilton 2004). An increasingly common source of this information is in the form of remotely sensed imagery (Hall *et al.* 2002; Metternicht 2003; Tisseyre *et al.* 2007). The development of low-cost acquisition systems are decreasing costs and increasing accessibility to high spatial resolution imagery for precision agriculture and viticulture practice (e.g. Morais *et al.* 2008). The utility of remotely sensed aerial colour-infrared imagery of vineyards is reliant upon the relationships that can be established between derived image products and viticultural variables of management significance. Relationships between image-derived quantitative vegetation metrics and canopy vigour have been variously established (Johnson *et al.* 2003; Tisseyre *et al.* 2008; Hall *et al.* 2008), indicating the utility of optical remote sensing in describing spatial patterns of canopy vigour. In addition, relationships between ground-based measures of canopy vigour and yield and quality are also established (e.g. Mabrouk and Sinoquet 1998; Smart 1985). Those grapevines within

a vineyard that have relatively larger canopies generally produce higher yields (Tisseyre *et al.* 2008), and early-season grapevine canopy size can be indicative of yield in the following season (Cunha *et al.* 2010). Canopy vigour has also been demonstrated to affect fruit composition indicative of quality and eventual wine value (Lamb *et al.* 2004; Cortell *et al.* 2007; Johnson *et al.* 2001).

Two commonly measured compositional elements of winegrapes are acidity and total soluble solids (TSS) (Hamilton and Coombe 1988). Acidity decreases and TSS, indicative of berry sugar content, increases during the phenological stage of veraison (when berries colour and soften). Total carbohydrate production in the grapevine, a key factor in the ripening process, is dependent on total photosynthesis, which is in turn dependent on the total level of sun-exposed vegetative canopy (Howell 2001). Spatially variable environmental conditions within a vineyard management block (i.e. soil composition, soil depth, irrigation and management variability) engender spatial differences in canopy growth. Different rates of ripening are experienced in response to differences in vine balance, e.g. those vines with large fruit loads and relatively small canopies ripen more slowly than those vines with smaller fruit loads with relatively large canopies (Holzapfel *et al.* 2010). The spatial differences in ripening rates are expressed as spatial variability in fruit ripeness (i.e. acidity and TSS) at a single harvest time. The relationship between canopy characteristics and ripeness can be expected to be complex, because the level of carbohydrate reserves present in the vine, accumulated or depleted in previous growing seasons, affect yield and ripening potential (Holzapfel *et al.* 2010) in addition to the current season's canopy characteristics.

In addition to TSS and acidity, phenolic compounds are key compositional elements of red winegrapes and subsequently in extracted juice, playing an important role in the quality and value of finished wines (Harbertson and Spayd 2006). Two key subgroups of phenolic compounds are flavonols, common in both red and white varieties, and anthocyanins, which are specific only to red grape varieties. Studies on the microclimate of the fruiting zone have shown that anthocyanin concentration is highly dependent upon temperature of the fruit during ripening (Bergqvist *et al.* 2001; Spayd *et al.* 2002), and berry temperature increases linearly with sunlight exposure (Smart and Sinclair 1976; Bergqvist *et al.* 2001). As well as canopy shape and density affecting a grapevine's light interception efficiency, the microclimate of the fruiting zone, which is commonly situated below the canopy within the mid-section of the grapevine, is dependent upon vine trellising method the canopy growth (Smart 1985). It is generally the case that trellising type is consistent throughout single vineyard management units, thus the determinant of within vineyard variability in microclimate of the fruiting zone is likely to be effected by canopy growth variability.

Clearly grapevine canopy affects winegrape composition and thus large scale delineation of management zones has been achieved either qualitatively (e.g. Proffitt *et al.* 2006) or by using geostatistical techniques to objectively deliver zones with significantly difference management requirements (Kitchen *et al.* 2005; Acevedo-Opazo *et al.* 2008; Schepers *et al.* 2004; Fridgen *et al.* 2004; Pedroso *et al.* 2010) based on vineyard canopy imagery. Narrow-band indices derived from hyperspectral vineyard imagery are beginning to receive attention as possible indicators of grapevine physiology that may in future be able to map grape quality (Zarco-Tejada *et al.* 2005; Martin *et al.* 2007). In this study, we focus on indices that can be produced from low-cost multispectral systems with blue, green, red and near-infrared spectral bands. A segmentation algorithm was developed specific to vineyard imagery and applied to produce discrete groups of pixels equivalent to the size of a single grapevine plant. The segmentation of pixels into objects (e.g. Walter 2004) enables object based image analysis (OBIA) (Blaschke 2010) where reflectance information from a number of pixels describes a single object, in this case, individual grapevines. The advantage of OBIA for this study was to enable calculation of various indices to describe vegetative canopy for individual grapevine objects coincident with the size of the fruit sampling locations in the vineyard.

The normalised difference vegetation index (NDVI) is a commonly used VI in precision viticulture that can be derived using a simple multispectral system. For vineyards with LAI ranging between 0 and 3 and NDVI below 0.5, Johnson *et al.* (2003) reported a strong linear relationship between LAI and NDVI (r^2=0.73). In a comparison of relationships between grapevine LAI and three different VIs, Dobrowski *et al.* (2002) reported similar strength relationships in vertically shoot-positioned vineyards from canopy NDVI values averaging about 0.6 using a 0.5 m pixel size. The NDVI was originally produced for a study

using LandSat multispectral scanner imagery (with a spatial resolution of 79 m) to assess biomass on rangelands (Rouse *et al.* 1973). The relatively low level of vegetation biomass of each pixel suited the index in this use, but the NDVI is less suited to studies of dense vegetation due to index saturation when leaf area index is high (Wang *et al.* 2005; Huete *et al.* 1999). At high spatial resolutions for large canopy grapevines (such as that used in this study), pure pixels of grapevine canopy are common, which have very high LAI, ranging between 2 and 4 for mature canopies in a previous study by Hall *et al.* (2008). In that study, at the mature canopy stage, the NDVI of pure canopy pixels was typically greater than 0.8, and the consequent fit of linear relationships between canopy NDVI and LAI was poor. Using NDVI for assessing vegetation density in canopies with high levels of leaf area may therefore be less useful than indices that are less prone to saturation.

In addition to investigating the utility of vegetation indices other than NDVI in characterising spatial variability in vineyard performance, the effects of image acquisition timing and inter-annual variability in winegrape production volumes on the strength of correlations between remote-sensing image-derived canopy descriptors and fruit yield and composition were examined. By collecting imagery four times per season and harvest data over three years at two contrasting vineyards, a comprehensive analysis of yield component and fruit composition relationships with grapevine canopy descriptors over consecutive years was enabled. The correlation strengths between remotely sensed derived canopy descriptors and fruit yield and quality appeared relatively poor overall. However, the level of correlation required for whole-of-vineyard harvest-segmentation to achieve a significant difference in grape quality is shown to be satisfied at relatively low levels of correlation.

Section 2b

Supplementary study on forecasting grape yield with high spatial resolution optical remote sensing

Quantitative descriptors of 52 Cabernet Sauvignon grapevine canopies from a single vineyard block in the Riverina (NSW, Australia) were derived from high spatial resolution (0.25 m) vegetation index images acquired on nine occasions over two growing seasons. Two canopy descriptors were derived from the imagery: one to describe grapevine canopy area and the other vegetation density. The descriptors were compared to yield data collected from the same vines at harvest in both years. The strength and type of the relationships varied with phenological stage. Significant ($p<0.05$) correlations between canopy density and yield collected in the same year were observed, which were negative for descriptors derived from imagery collected pre-veraison then positive for descriptors derived from imagery collected at veraison. In addition there was a strong negative correlation between canopy density from imagery acquired at flowering in year 1 and yield in year 2. The relative change in the area and density of the grapevine canopy between adjacent imaging missions was also calculated using the remotely sensed canopy descriptors. The relationship between the relative change in canopy density between adjacent imaging missions during year 1 and yield in year 2 produced the greatest magnitude correlation in the study. A best subsets regression analysis of the remotely sensed canopy descriptors produced a three variable model to estimate year 2 yield data with an adjusted-R^2 of 0.69, suggesting forecasting grape yield from variability in vine canopies detected by high spatial resolution optical remote sensing is achievable.

Viticultural context

The relationships between grapevine canopy descriptors derived from remotely sensed imagery and fruit composition are now established (Hall *et al.* 2008a; Lamb *et al.* 2004), enabling forecasts of spatial variability in quality related fruit composition variables across vineyards. This section of the report presents work in which remotely sensed imagery of grapevine canopy is investigated with respect to forecasting future grape yield at the single vineyard management block scale.

Future grape yield may be indicated by canopy size and density either by its effect on grape development by altering the light microclimate in the fruiting zone (Dokoozlian and Kliewer 1996; Haselgrove *et al.* 2000), or by expressing the utilisation and/or storage of water, nutrients and carbohydrate reserves. At inflorescence initiation (before flowering in the season preceding their maturity, see Watt *et al.* 2008), the development of inflorescence primordia is dependent upon shade in the canopy; highly shaded shoots are less likely to produce inflorescence primordia (May 1965; Sanchez and Dokoozlian 2005). Restraining shoot growth from approximately a month after fruit set (by restricting soil water) can result in an increased number of clusters per vine and increased berry number per bunch over the long term (Neja *et al.* 1977). During flowering, fruit set can be reduced by shaded conditions and vigorous shoot

growth, reducing the availability of assimilates to the inflorescence (May 2004). As the season progresses, shade in the canopy and vigorous shoot growth causes reduced berry growth since assimilate allocation is restricted (Ollat *et al.* 2002). Close to harvest, dense canopies can encourage the incidence of botrytis that commonly reduces yield (Smithyman *et al.* 1998).

Airborne remote sensing can be a relatively inexpensive technology, on a per-hectare basis, for acquiring vineyard canopy data of vineyard management blocks. Quantifiable differences in grapevine vigour (foliage density and extent) are assessable from remotely sensed images of vineyards (Dobrowski *et al.* 2002; Hall *et al.* 2003; Johnson *et al.* 1996; Johnson *et al.* 1998). Recent developments in grapevine image processing and the greater accessibility of very high spatial resolution (<0.5 m pixel size) imagery (Hall *et al.* 2003; Tisseyre *et al.* 2007) now enables more comprehensive canopy descriptors to be derived from imagery than in the past (Hall *et al.* 2003). Moreover, Hall *et al.* (2008b) demonstrated that in a minimally pruned vineyard, remotely sensed descriptors of canopy area were found to have strong relationships with ground-based measurements of leaf area index (LAI).

Section 3

Predictive modelling of winegrape yield at the regional scale

Winegrape yield data of three major varieties grown in Australia for the period 1985 to 2007 and climate data for the period 1982 to 2007 were collated to analyse the effect of weather anomaly data (i.e. deviation of recorded meteorological data from the mean climate) from the four preceding years for 28 Australian viticultural regions of interest (ROI). Temperature, precipitation and selected atmospheric pressure based index anomalies were calculated for each region at daily time intervals. Data were temporally-averaged into phenological periods using heat accumulation totals as well as monthly, 3-monthly and annual periods. First and second order linear models revealed mean temperature, the Southern Oscillation Index and the Indian Ocean Dipole correlated most strongly with grapevine yield. The strongest correlations occurred for data representing winter and early springtime (July, August and September) in the growing season leading up to harvest and at the same time of year in the three preceding years. Splitting the data set into warm regions and cool regions affected the level of correlation of yield with many weather variables but were mainly associated with similar variables. Weather conditions during bud initiation are important in determining ultimate yield approximately 18 months later. Fluctuations in the bud initiation process may further affect yield three years later suggesting a link with accumulation and depletion of grapevine carbohydrate reserves. Neural network models using sets of variables found to have significant linear or quadratic relationships with yield were found, through cross-validation, to predict up to 50% of the variance in the yield data.

Viticultural context–spatial analysis of climate in winegrape growing regions in Australia

Air temperature during the growing season is considered one of the most important factors in quality winegrape production. Temperature characteristics of wine producing regions have been repeatedly studied and quantified in many different ways. One of the consequences of these disparate studies is a lack of consistent data describing temperature-related winegrape growing conditions that can be directly compared between regions and countries. This section of the report describes the temperature regimes of Australian winegrape growing regions (Geographic Indications, GIs) as described by the Australian Wine and Brandy Corporation (2008) with the addition of two further regions, North and South Tasmania (*Figure 4.12*). Four temperature-derived indices using the same calculation method used in a recent publication that similarly described the temperature regimes of winegrape growing regions of the western United States have been calculated (Jones *et al.* 2010). Similar efforts are underway to describe the winegrape growing region climates of other parts of the globe (Jones *et al.* 2009). With these data, the Australian growing conditions can be directly compared with those of the western United States and in the near future with those of other regions.

In addition to enabling comparisons to be drawn across regions, the data presented in this section of the report estimates the range of index values within individual regions that occur due to spatial variability. Common practice in the past has been to select a climate station representative of a region and calculate temperature indices for that location. Here, temperature data were interpolated (i.e., estimated from point data to produce a continuous surface) to cover all the climate regions with a resolution of 0.05 decimal degrees (~26 km^2 at 35°S). Index values were then calculated for every one of the smallest resolvable areas (known as pixels) within the winegrape growing regions. Summary data were

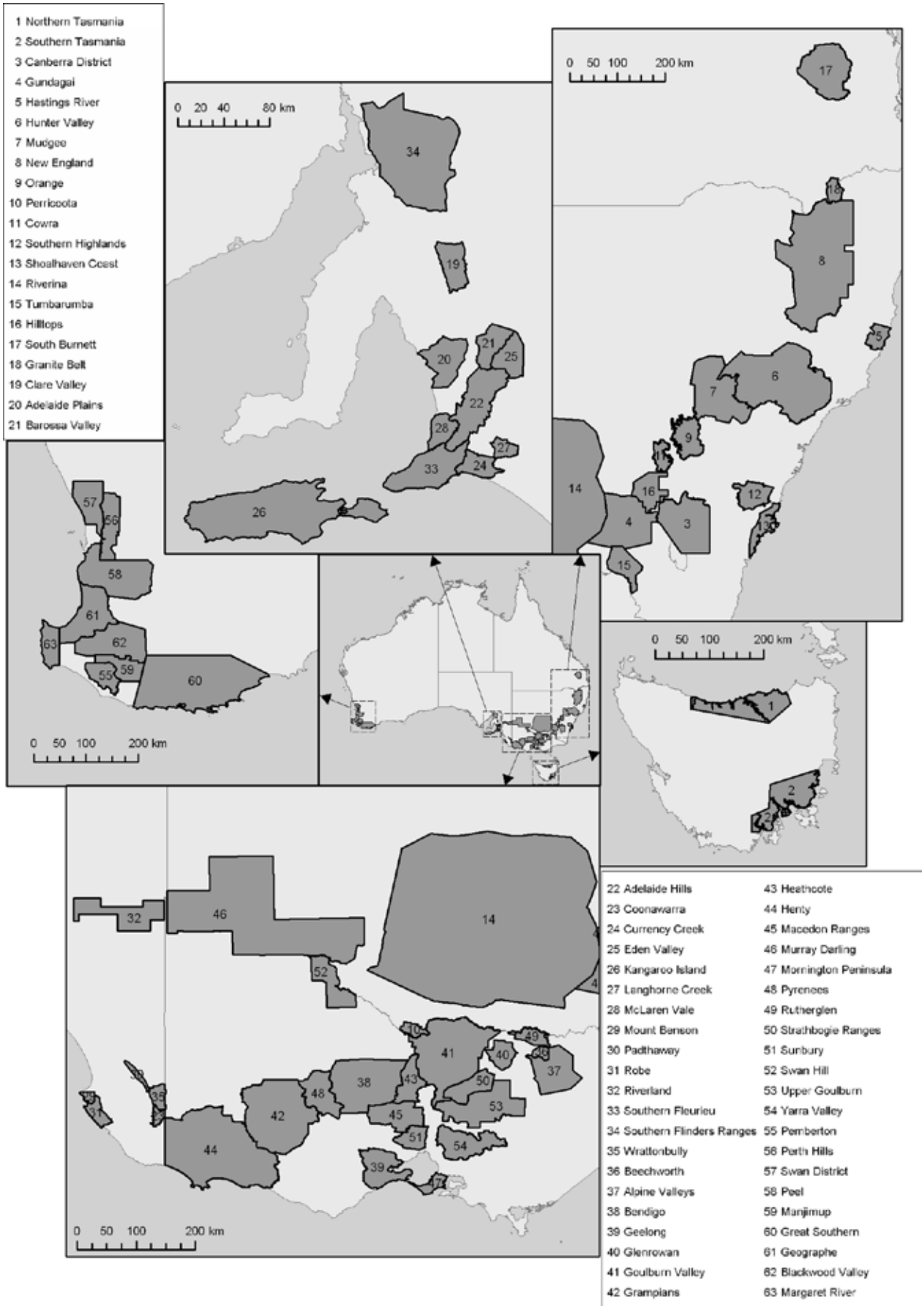


Figure 4.12 Australian Geographical Indications (GIs). Note: North and South Tasmania regions used in this study are not officially established GIs, but created by the authors from existing map sources and known areas of vineyards. (Data Source: Australian Wine and Brandy Corporation 2008)

Table 4.12 Climate variables derived, and the median index classification frequencies of the Australian GIs.

Variable	Equation	Months	Class Limits†	Count	Frequency
Average growing season temperature (GST)	$\frac{\sum_{d=1}^{n}[T_{max}+T_{min}]/2}{n}$	1 October–30 April	Too cool < 13°C	0	0 %
			Cool =13–15°C	2	3.2 %
			Intermediate =15–17°C	14	22.2 %
			Warm = 17–19°C	28	44.4 %
			Hot = 19–21°C	16	25.4 %
			Very hot = 21–24°C	3	4.8 %
			Too hot >24°C	0	0 %
Growing degree-days (GDD)‡	$\sum_{d=1}^{n}\max[(T_{max}+T_{min})/2-\mathbb{0}\ ,0]$	1 October–30 April	Too cool <850	1	1.6 %
			(Region I) 850–1389	5	7.9 %
			(Region II) 1389–1667	24	38.1 %
			(Region III) 1667–1944	16	25.4 %
			(Region IV) 1944–2222	10	15.9 %
			(Region V) 2222–2700	7	11.1 %
			Too hot >2700	0	0 %
Huglin index (HI)	$\sum_{d=1}^{n}\max[(T_{mean}-\mathbb{0}\ +T_{max}-\mathbb{0}\ )/2,0]K$ where K is an adjustment for latitude/day length§	1 October–31 March	Too cool <1200	0	0 %
			Very cool =1200–1500	2	3.2 %
			Cool =1500–1800	8	12.7 %
			Temperate =1800–2100	22	34.9 %
			Warm temperate =2100–2400	12	19.1 %
			Warm =2400–2700	14	22.2 %
			Very warm =2700–3000	5	7.9 %
			Too hot >3000	0	0 %
Biologically effective degree-days (BEDD)	$\sum_{d=1}^{n}\min[\max([T_{max}+T_{min}]/2-\mathbb{0}\ ,0)K+\mathbb{R}_{adj},9]$ where and K is an adjustment for latitude/day length§	1 October–30 April	<1000	2	3.2%
			1000–1200	4	6.4%
			1200–1400	22	34.9%
			1400–1600	22	34.9%
			1600–1800	12	19.1%
			1800–2000	1	1.6%
			>2000	0	0%

† Note that the class names given in the table are not directly comparable (e.g., GST cool does not necessarily compare to HI cool).

‡ Note that the GDD classes are based upon rounded °F limits as defined by Winkler et al (1974) (in parentheses), which produce non-rounded classes in °C units.

§ K is a latitude coefficient that takes into account increasing day lengths starting from 1.0 at 34° increasing incrementally pole ward and is based upon day lengths using Julian day and latitude.

then calculated to describe the spatial variability that occurs within each of the regions.

The four climate indices chosen for the analysis are described in *Table 4.12*. The indices discussed in this section of the report are simple indicators of the long-term suitability of a climate for the successful commercial production of winegrapes. Because of their simplicity, there will be climate types classified as suitable by these indices, while, in reality, aspects of their climates may make them unsuitable for commercial winegrape production. For example, flowering grapevines in highly continental climates that are subject to high levels of air mass variability may be persistently decimated by spring frosts despite having a warm growing season. Alternatively, extreme heat events during the ripening period may regularly occur, but high temperature variability results in the average temperature falling within a suitable classification category. Further terroir considerations, such as slope and aspect that can change solar radiation loading at a particular site or cultural practices evolved to deal with cool or hot climate conditions, can also extend the suitability range.

Growing season temperature (GST) is the simplest of the indices: the mean air temperature of all days between 1 October and 30 April. Since temperature is generally recorded as minimum and maximum temperatures each day, growing season temperature is an estimate of the average temperature. Actual average temperature (i.e. the average of a constantly recorded temperature) may vary a little from this estimate (McIntyre *et al.* 1987). In general terms, growing season temperatures between 13 and 21°C are considered suitable for quality winegrape production with different varieties being more suitable to different temperature regimes (Jones 2006).

The growing degree-days (GDD) index is a measure of heat summation. The accumulation of heat units over time is a common method of describing the suitability of growing crops in different climates. It is calculated by subtracting a base temperature (10°C for winegrapes) from the average temperature recorded each day from 1 October to 30 April (in the Southern Hemisphere) and then summating all values above zero. The first extensive use of heat unit calculation for viticulture was conducted by Winkler *et al.* (1974) for California. The region classifications originally determined by Winkler *et al.* (1974) have been retained in this study (*Table 4.12*). However, no upper or lower bounds to these classifications were originally specified. Any climate with a seasonal accumulation of less than 1389°C-days was classified as Region I, and any climate with a seasonal accumulation of more than 2222°C-days was classified as Region V. Upper and lower limits to quality winegrape production are used in this section of the report based on observations made by Jones *et al.* (2010) in the western United States winegrape growing regions, with a *Too Cold* class for GDD totals below 850°C-days and a *Too Hot* class for GDD totals above 2700°C-days. Note that these limits are not absolute and may not be applicable everywhere.

The Huglin Index (HI) (Huglin 1978) is a variation on the GDD, differing in three ways. Instead of using average temperature over a 24-hour period, the HI effectively uses an estimate of the daytime temperature by taking the mean of the average and maximum temperatures in its calculation. The daytime temperature may be considered to be of greater interest in terms of predicting plant growth, since this is the time during which photosynthesis occurs (Went 1957). In addition, a length of day ("longueur du jour") coefficient, *K*, is incorporated into the calculation, which Huglin (1978) varied from 1.02 to 1.06 at 40–50° latitude. Finally, HI is calculated using a 6-month period (1 October to 31 March, for the Southern Hemisphere) rather than a 7-month period used in the calculation of the other indices. For regions with high annual temperature ranges, indices calculated using a 7-month period are likely to have a lower index value than if using the 6-month period, since April temperatures are likely to be the coolest of the 7-month period. Indices calculated for areas that experience greater annual ranges in temperature will be more greatly modulated by including this cooler seventh month. Thus by using the six-month period, the effect on the index of the magnitude of the annual temperature range is reduced.

The biologically effective degree-day (BEDD) index (Gladstones 1992) is another variant on calculating heat summation. It incorporates both an adjustment for diurnal temperature range and a day length correction similar to the HI, but by using different methods. Instead of estimating the daytime temperature as used in the HI, the BEDD index incorporates a factor based directly on the diurnal temperature range; the index is adjusted upward if the diurnal temperature range is greater than 13°C and downward if less than 10°C (*Table 4.12*). The factor adjusting for day length is similar, but slightly different to HI's *K*, varying from 1.00 at 40° of latitude

to 1.045 at 50°. The BEDD index additionally differs to the HI in terms of it using the standard seven-month period (1 October to 30 April), thus retaining the potentially modulating effect on the index caused by variations in annual temperature ranges.

Section 3b

Identification of weather anomalies over preceding four growing seasons that significantly affect Australian winegrape yields

Yield forecasting of grapevines is the subject of numerous research projects. Grapevine physiology has been subject to in-depth study with the goal of adding to the knowledge that could be applied to increase accuracy of yield forecasts. The reproductive cycle of grapevines spans two years, and weather events at specific phases of development are thought to have a significant effect on berry cluster development during this time (Vasconcelos *et al.* 2009; Watt *et al.* 2008). Grapevines located in warmer regions are able to access more energy for growth and reproduction.

A study of Chardonnay (Watt *et al.* 2008) found that inflorescence primordia differentiation varied with climate, with grapevines located in hot climate buds being larger and exhibiting more secondary branching than grapevines located in relatively cool climates. The number of inflorescences produced by a grapevine is a major cause of temporal yield variability (Clingeleffer *et al.* 2001).

The normal partitioning of assimilates into vine growth or reproductive processes (what would happen if all environmental conditions remained average) at any stage, are influenced by external forces. At the regional scale, the key external forcing mechanism is climate. Carbohydrate reserves that are accumulated or depleted in previous seasons limit or extend the energy available to grapevines. Reserve levels at various stages at various grapevine reproductive stages may affect the end yield. The effect of previous seasons' climate on reproductive process is a key factor in determining reserve status of grapevines. The post-harvest period has been shown to be more important in relatively warmer climates (see (Field *et al.* 2009; Holzapfel *et al.* 2006).

Materials and method

Section 1

Field Data Collection

The study used two trial sites, one in the Hunter Valley and the other in the Riverina. Planting density and area of the two blocks had quite different characteristics (*Table 4.13*). Both are single management blocks of mature (more than 10 years old) Shiraz grapevines. The Hunter Valley site is hand pruned to lateral canes and the Riverina site is mechanically pruned. At both blocks, 54 sample sites (1 m of the cordon) were hand-harvested within a week before the blocks are commercially harvested with the total fruit weight of each site recorded. Each of the sample sites was carefully selected based upon the spatial variability characteristics of the blocks. The Hunter Valley site had fixed sample sites selected to most fully represent the spatial variability mapped by an EM38 soil survey conducted while the soil profile was relatively moist (*Figure 4.13a*). Geographic Information System (ESRI ArcGIS 9.2) software was used to split the block into three zones of equal variability (*Figure 4.13b*). Each of these three zones was further similarly divided into six sub-zones. Three grapevines were selected from within each of the sub-zones to produce 54 sample sites (*Figure 4.13c*). The Riverina site had 54 similarly categorised sample sites, but these were instead selected each season using canopy vigour data derived from remotely sensed imagery of the site (*Figure 4.14*). Each grapevine was individually described using a computer program derived from Hall *et al.* (2003) and ranked by canopy vigour. Sample grapevines are then selected at intervals of the ranked list of grapevines to best characterise the overall variability of the block. Each grapevine in the Riverina trial is placed into categories that are equivalent to the Hunter Valley site's zone, and sub-zone designations.

Table 4.13 Vineyard block information

Site	Pruning	Block area (ha)	Vine count	Approx. planting density (m^2/vine)	Row spacing (m)	Vine spacing along rows (m)	Total length of rows (m)
Riverina	Machine pruned only (hedge)	12.2	19824	6.2	3.35	1.85	36680
Hunter Valley	Hand- pruned to one or two canes	3.39	11214	3.0	3.00	1.00	11210

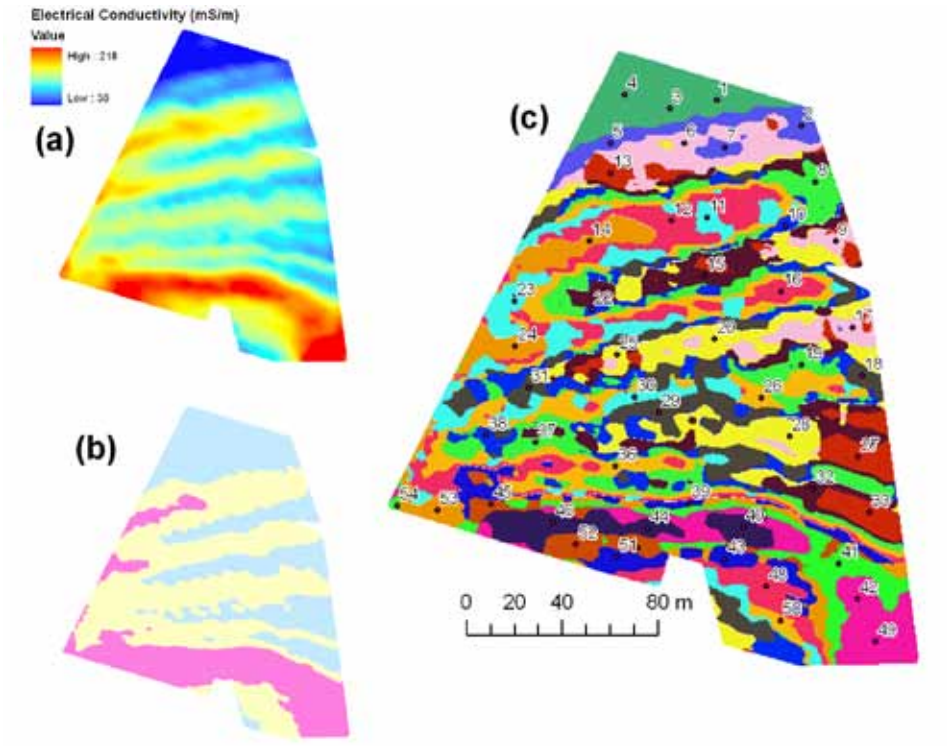


Figure 4.13 (a) EM38 soil survey of Hunter Valley vineyard site; (b) 3 zone map defined by EM38 data of equal variance; (c) 18 sub-zone map (6 zones within each zone as shown in (b)) and the 54 sample sites selected on the basis of 3 within each sub-zone.

Monte Carlo Simulation

A Monte Carlo simulation of selecting sets of sample sites on a semi-random basis that incorporated rules that take advantage of knowledge of the spatial variability in the block was conducted. *Table 4.14* describes the rules. For each number of sample sites (3, 6, 9, 12, 18, 24 and 36), 10,000 estimates of yield were generated. The mean and the 2.5% and 97.5% quantiles of the set of 10,000 simulated estimates of yield (the means) were then calculated. The error (E_t) was calculated as half the 95% quantile range. In effect different methods of estimating the error are necessary for the random sampling method to compare it against the targeted sampling method. Although not directly comparable (*Table 4.15*), the methodology does provide a good indication of the differences in error.

Calculation of equivalent error using random sampling

To compare the sampling technique used in this study with established random sampling techniques, a rearrangement of the equation for random sampling intensity was used. The number of randomly selected samples (n) to acquire in a study of a population can be estimated using:

$$n = \left(\frac{z_{\alpha/2}\sigma}{E} \right)^2 \quad \text{[Equation 4]}$$

where z_α is the critical z-score on the normal distribution that allows a type I error of α, σ is the

Table 4.14 Rules for the semi-random selection of sample sets used in the Monte Carlo simulation.

Number of Sample Sites	Rules for the semi-random selection of sample sets
3 sites	1 from each zone
6 sites	2 from each zone (with 1 from sub-zones 1, 2 or 3 and 1 from sub-zones 4, 5 and 6)
9 sites	3 from each zone (with 1 from sub-zones 1 or 2, 1 from sub-zones 3 or 4 and 1 from sub-zones 5 or 6)
12 sites	4 from each zone (with 1 from sub-zones 1 or 2, 1 from sub-zones 3 or 4, 1 from sub-zones 5 or 6 and any 1 of the remaining unselected samples within the zone)
18 sites	6 from each zone (with 1 from each sub-zone)
24 sites	8 from each zone (with 1 from each sub-zone and 2 further remaining unselected samples, with 1 from sub-zones 1, 2 or 3 and 1 from sub-zones 4, 5 and 6)
36 sites	12 from each zone (with 2 from each sub-zone)

population standard deviation and *E* is the maximum sample error (Freund and Simon 1997, p. 320). Use of *Equation 4* requires a normally distributed population and known σ. With 54 samples, the estimate of the population standard deviation ($\hat{\sigma}$) may be assumed to be little different to σ. However, a more rigorous calculation for n uses Student's t-distribution to take into account uncertainty in σ:

$$n = \left(\frac{t_{\alpha/2,\nu}\hat{\sigma}}{E} \right)^2 \quad \text{(Equation 5)}$$

where *t* is the critical value on Student's t-distribution with *v* degrees of freedom and probability of a type I error, α (Steel *et al.* 1997, pp. 124–125). The value for $t_{\alpha,v}$ in this study was derived using the qt function of S-PLUS v8.1.1 (TIBCO Software, 2008), where α=0.05 and *v*=N–1.

Non-negative data sets that have high variability relative to their means, such as sampled intra-vineyard yield data, are likely to fall into log-normal distributions. The distribution of the yield data sets were examined by constructing histograms using both the raw data and the log-transformed data (*Figure 4.15*). *Figure 4.15* indicates that most sets of the log-transformed and the raw yield data could both fall into normal distributions. The Shapiro-Wilk test for normality (S-PLUS v8.1.1) indicated no statistical difference between the levels of normality between the sets of log-transformed or raw yield data (*Table 4.16*). Those log transformed data distributions that did result in low W values were strongly influenced by a few low value outliers (Figure 3(i) and (j)). There was therefore no strong evidence that the distributions were either log-normally or normally distributed. However, in order to avoid the possibility of modelling error intervals extending below zero, the yield data was log-transformed.

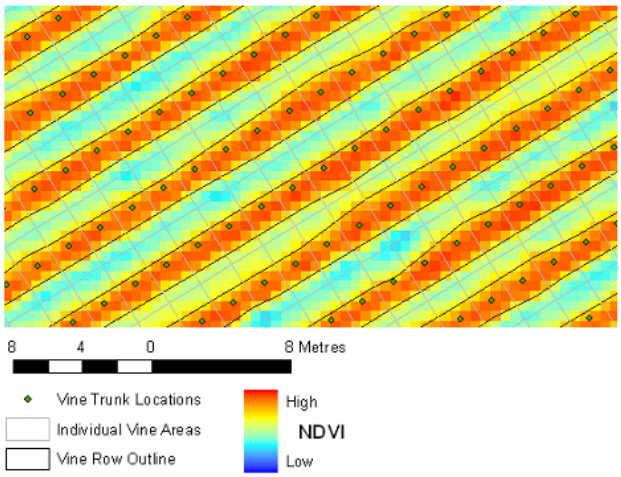


Figure 4.14 Close-up of remotely sensed NDVI image of vineyard with computer generated vine location information. Spectral reflectance information describing canopy characteristics of each individual vine can be rapidly extracted by the computer.

The estimated population standard deviations were calculated using the samples on each of the six sampling occasions:

$$\hat{\sigma} = \sqrt{\frac{\sum_i (\mathrm{h}\ x_i - \hat{\mu})^2}{N}} \quad \text{[Equation 6]}$$

where *x* is the set of sample data, *N* is the number of samples and $\hat{\mu}$ is the mean of the log-transformed yield data, i.e.

Table 4.15 Statistical considerations for each estimation method.

Method	Estimating confidence interval	Variance parameter	Student's t
Random sampling *without* prior knowledge of variability	Normal or log-normal distribution	Sample variance can be accurately calculated, but assumptions are made about the distribution of the population	Variable, depending on number of samples. If only 3 samples, t=4.303, but quickly decreases for increasing sample size, e.g. n=6, then t=2.571
Random sampling *with* prior knowledge of variability	Normal or log-normal distribution	Sample variance can be accurately calculated, but assumptions are made about the distribution of the population	Constant, regardless of number of samples, based on all targeted samples. Degrees of freedom (v) is constant 53, therefore t is a constant 2.006 for p=0.05
Targeted sampling	Monte Carlo	Samples are not randomly selected; the selection process is designed to characterise variation with greatest efficiency. This artificially reduces the variance parameter and thus the confidence intervals	Non-parametric; not applicable

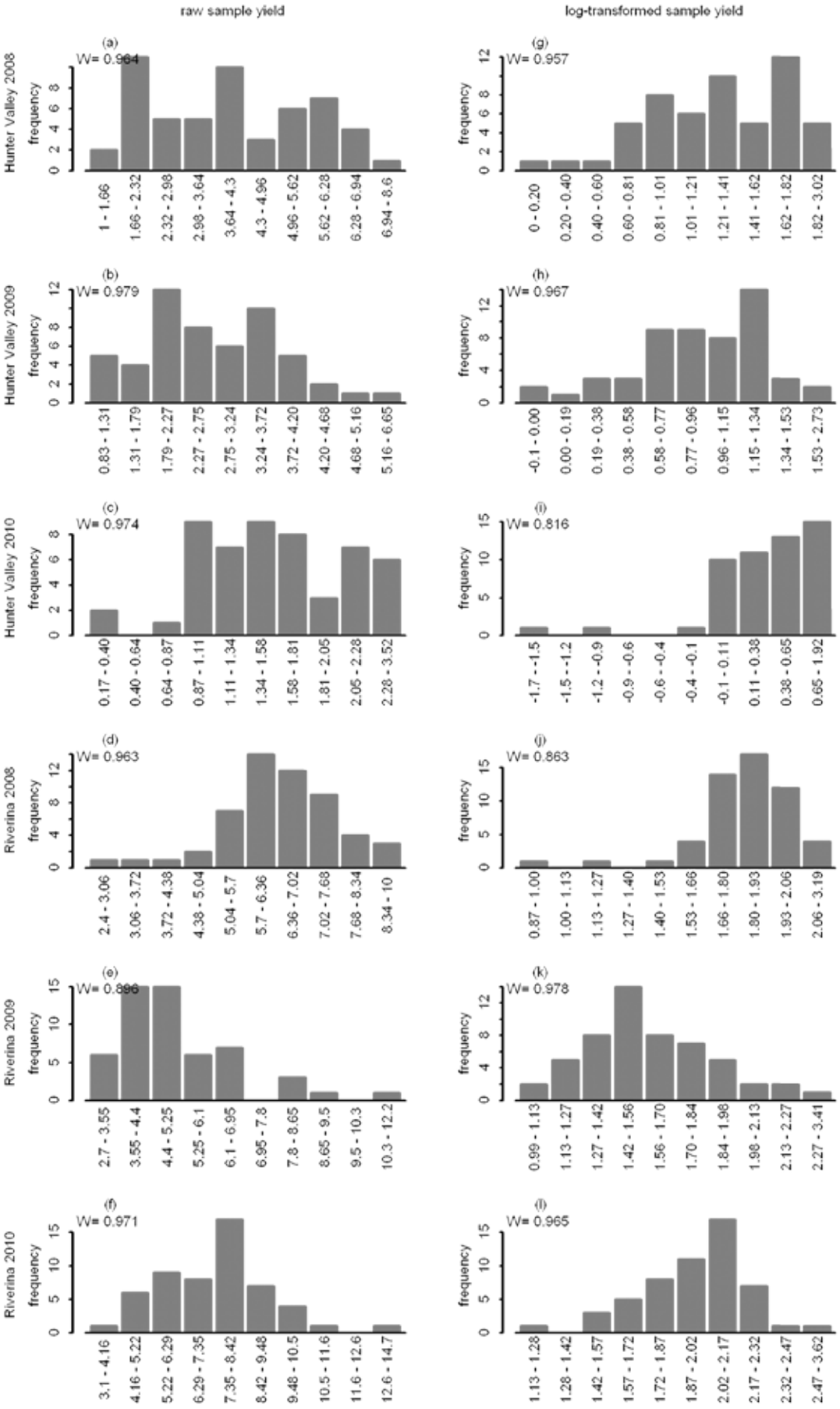


Figure 4.15 Sample yield distributions collected during each of the six harvests. Raw data are presented in the histograms on the left and the equivalent log-transformed data are on the right. The Shapiro-Wilk statistic (*W*) indicates the level of likelihood the samples come from a normal distribution. Small *W* values indicate samples are less likely to be from a normally distributed population.

Table 4.16 Comparisons of results of tests for normality (Shapiro-Wilk) on raw yield data and log-transformed yield data. Higher Shapiro-Wilk statistics (*W*) indicated greater probabilities (*p*) that the data comes from a normal distribution.

	W (raw data)	*W* (log-transformed data)	*p* (raw data)	*p* (log-transformed data)
Hunter 2008	0.964	0.957	0.11	0.05
Hunter 2009	0.979	0.967	0.28	0.15
Hunter 2010	0.974	0.816	0.32	<0.01
Riverina 2008	0.963	0.863	0.09	<0.01
Riverina 2009	0.896	0.978	<0.01	0.46
Riverina 2010	0.971	0.965	0.23	0.12

$$\hat{\mu} = \frac{\sum_i \ln x_i}{N} \quad \text{[Equation 7]}$$

A rearrangement of *Equation 2* delivered the log-transformed expected error that would result from randomly sampling yield using *n* sample vines:

$$E_r = \sqrt{\frac{t_{0.025,n-1}^{\ 2} \cdot \hat{\sigma}^2}{n}} \quad \text{[Equation 8]}$$

The geometric 0.025 and 0.975 quantiles of the expected log-normal distribution can then be calculated:

$$q_{0.025} = \exp(\ln \mu - E_r) \quad \text{[Equation 9]}$$

$$q_{0.975} = \exp(\ln \mu + E_r) \quad \text{[Equation 10]}$$

where, μ is the true mean yield per vine of the whole vineyard (note that this is not the mean yield of the sampled vines, $\hat{\mu}$). True mean yield per vine is a known variable; it is the total grape yield for the vineyard block, recorded at weigh-stations after machine harvesting of the blocks divided by the total number of vines in the vineyard.

To compare the vineyards to Wolpert and Vilas's (1992) quoted variability, coefficients of variation were calculated as the ratios of the population standard deviations to the means:

$$\hat{c}_v = \frac{\hat{\sigma}}{\mu} \quad \text{[Equation 11]}$$

Section 2a

Vineyard study sites

The study vineyards were located in the Riverina and Hunter Valley viticultural districts of New South Wales, Australia. The key characteristics of each vineyard are described in *Table 4.17*. Both were single management blocks of the red winegrape variety *Vitis vinifera* cv. Shiraz. Both study vineyards comprised vines of the same age, planted in 1999, and subject to drip irrigation. Measurements of apparent soil electrical conductivity (EC_a) were completed using a Geonics EM38RT unit (Geonics Ontario, Canada) operated in vertical dipole mode. The device was towed behind a quad bike on a custom built sleigh coupled to a differential GPS that also recorded elevation. Georeferenced measurements of EC_a were recorded every few seconds to produce roughly evenly spaced measures at a spatial density of approximately 1250 points per hectare. The point data were interpolated to a 0.5 m grid using ordinary kriging with a variable search radius comprising 12 points (ArcMap, version 9.3.1, ESRI: Redlands California). Spatial variability in EC_a of the soil (34–203 dS m^{-1}) and topography (elevation range 15.3 m) was greatest at the Hunter Valley site. The Riverina vineyard, by contrast, lay on flat land (elevation range <2 m) and exhibited much less variability in soil EC_a (107–156 dS m^{-1}). Although EM surveying was conducted under similar conditions at both sites, a few days after moderate rainfall, ranges of EC_a vary depending upon overall soil moisture conditions and cannot therefore be directly compared across the two sites. The large difference between the ranges at the two sites, nevertheless, indicated a greater level of variability in EC_a at the Hunter Valley vineyard. Soil electrical conductivity

Table 4.17 Study vineyards' characteristics.

	Hunter Valley Vineyard	Riverina Vineyard
Pruning Method	Spur pruned	Machine pruned
Vineyard area (ha)	3.4	12.2
Vine planting density (m^2 $vine^{-1}$)	3.0	6.2
Approx. long-term mean yield (t ha^{-1})	6	12
Yield (t ha^{-1}) 2008	9.85	13.77
Yield (t ha^{-1}) 2009	6.38	10.35
Yield (t ha^{-1}) 2010	3.13	13.58

and topography have been shown to be key drivers of within vineyard spatial variability (Acevedo-Opazo *et al.* 2008; Tisseyre *et al.* 2007), as it is indicative of soil compactness, salinity and water holding capacity. In addition to soil EC_a variability, a key difference between the sites was the pruning method, with the Hunter Valley site subject to spur-pruning, which entails careful excision by skilled vineyard workers of the previous year's woody growth to leave behind two buds at spurs evenly placed along the cordon. The Riverina site, on the other hand, was subject to machine pruning, entailing mechanical hedging of each vine row. In addition to the differences in the characteristics of the two vineyards, total production at each vineyard varied significantly across the three years of the study (*Table 4.17*). The greatest productivity changes occurred at the Hunter Valley site, with the 2010 production being less than one-third of the 2008 production.

Airborne multispectral imaging

A custom-built multispectral airborne digital imaging system was employed to acquire vineyard imagery. The system comprised four identical digital video cameras with 994×1014 pixel arrays attached to an image capturing PC mounted within a Cessna 310. Each camera lens was filtered to produce four spectral bands, centred at 450, 550, 675 and 800 nm (having 25 nm band widths for all but the 800 nm filter, which had a 40 nm band width). Images were acquired at an altitude of 1525 m (5000 ft) above ground level delivering a pixel resolution of ca. 0.5 m (see *Figure 4.16* for example imagery). Imagery was collected four times per growing season across three years at both vineyard sites within an hour of solar noon, minimising shadow. High, low and medium brightness near-Lambertian reflectance targets of known spectral characteristics, each measuring 3×3 m, were placed on the ground at the time of imaging to be included in the vineyard scene. Digital numbers extracted from the calibration panels in the raw imagery were related to the known reflectance values of the panels to produce a linear model to transform the whole image from digital numbers to reflectance values. The geographic co-ordinates of eight ground control points located at the edges and corners of the vineyard blocks were used to register the images to map coordinates using a spatial warping function from commercial image processing software (ENVI 4.7 (Linux 64), ITT Visual Information Solutions: Boulder, Colorado).

With image pre-processing completed (conversion from digital number to reflectance values and correction for radiometric and geometric distortion), ENVI was used to manually define the region of interest (ROI), i.e. the vineyard block, and to determine the row orientation (θ, clockwise from grid north). The image ROI was subsequently exported for input into the image processing algorithm (described in the following section). The process of defining vineyard blocks can be automated with vineyard recognition and mapping algorithms that include estimates of inter-row width and row orientation (Da Costa *et al.* 2007; Delenne *et al.* 2008); these may be integrated with the algorithm

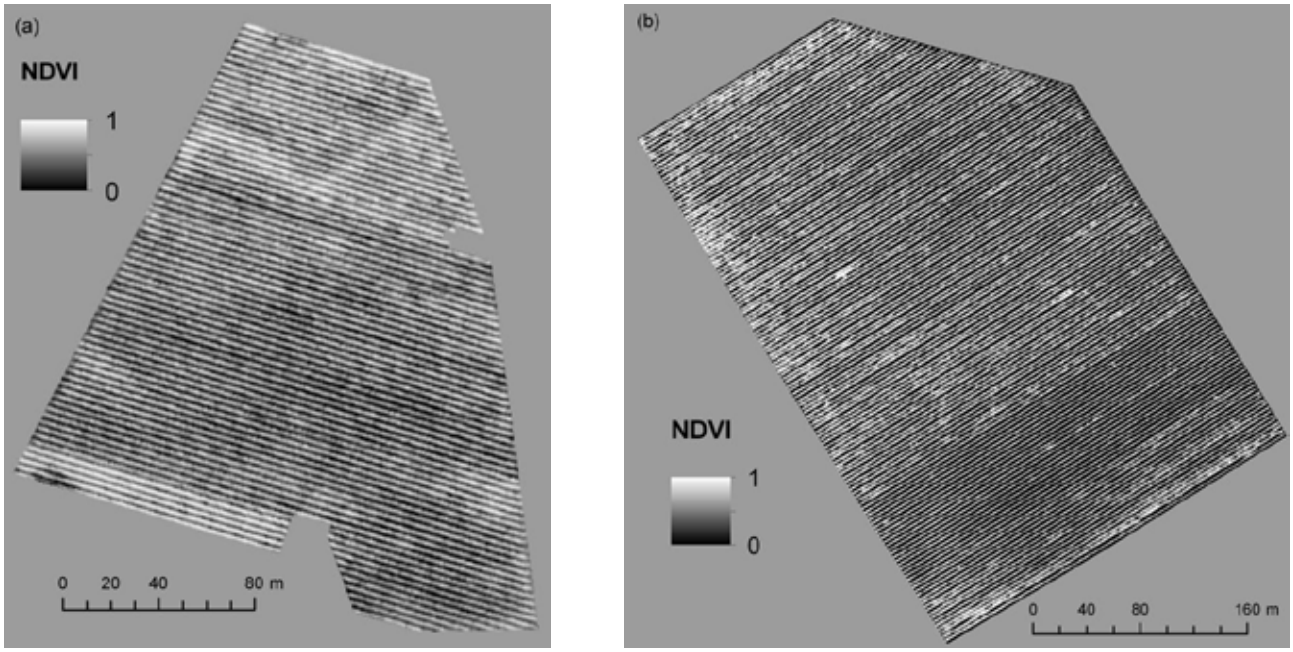


Figure 4.16 NDVI images of study blocks at veraison (greatest canopy extent) in study year 1, clipped to vineyard management unit extent. (a) Hunter Valley vineyard, 20 Feb 2008. (b) Riverina vineyard, 19 Feb 2008.

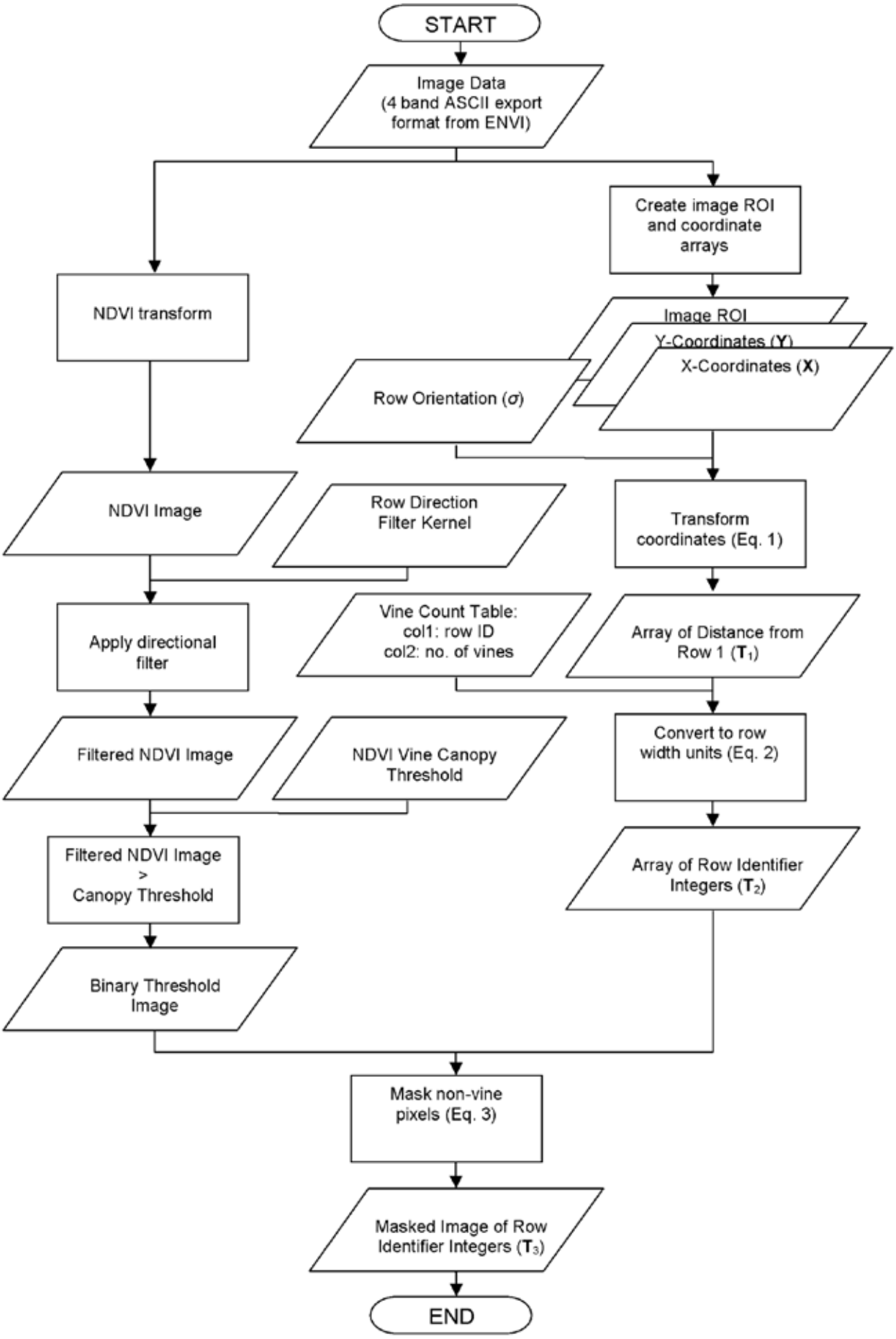


Figure 4.17 Flowchart describing image processing steps to determine vineyard row identification integers.

presented here. The timing of the image acquisition in terms of cumulative growing degree days (GDD, a convenient estimated measure of phenological progress, GDD=max[0, $(T_{max} + T_{min})/2$ -10], where T_{max} and T_{min} are the local daily maximum and minimum temperatures (Winkler *et al.* 1974) using data from the closest government climate recording station (Australian Bureau of Meteorology 2010)) since budbreak are presented in *Table 4.18*.

Image processing

The purpose of the image processing was to segment vineyard imagery into individual grapevine plant areas from which reflectance information could be extracted. The first stage comprised a semi-automatic process for determining the start and end points of each vineyard row, and the second stage entailed automatic splitting of each vine row into single plant unit areas or objects. With each pixel effectively assigned row and vine coordinates, extraction of reflectance information for each vine unit was a simple process. The major steps of the process are presented in the flow chart in *Figure 4.17* and described in detail in the following paragraphs. Note that the process of assigning row and vine coordinates to each image pixel was conducted using the NDVI, but that image information extracted at the end of the process was the reflectance values of the original imagery.

Image processing was conducted in S-plus (Spotfire S+ Version 8.0.4 for Linux, TIBCO Software Inc.: Palo Alto, California). The red and NIR bands were converted to a normalised difference vegetation index (NDVI) image (Rouse *et al.* 1973). The NDVI image was filtered with a 5×5 kernel directional filter, which was produced using the directional filter tool in Envi (Version 4.8 for Linux 64, ITT Visual Information Systems: Boulder, Colorado). A new kernel was produced for each image to be aligned with the angle of the row orientation, θ. Application of the directional filter produced a sharper image of the rows (*Figure 4.18*). The filtered image was converted to a binary image, **B**, where all pixels greater than a threshold value were assigned 1 and those below were assigned 0. The threshold value was initially set to 0, but was altered depending upon the canopy to soil area ratio effect on the contiguousness of vine rows in the resultant binary image. Contiguousness of pixels with a value of 1 along vine rows without joins to other rows was the most desirable result. Note that the threshold value was not an NDVI value, rather it was a value from the filtered image, the mean pixel value of which was zero with higher values indicating denser vegetation.

A coordinate transformation was used to assign a value to each pixel, representing its distance from the first row of the vineyard block ($\mathbf{T}_1$), i.e.

$$\mathbf{T}_1 = \mathbf{Y} - \mathbf{X}\sin\varphi \qquad \text{[Equation 12]}$$

where **X** and **Y** are the horizontal and vertical pixel coordinate arrays and φ is the angle perpendicular to the row direction). $\mathbf{T}_1$ was transformed to corresponded to units of row widths ($\mathbf{T}_2$), i.e.

Table 4.18 Schedule of field data collection.

	Hunter Valley Vineyard				Riverina Vineyard			
Year	Event	Date	GDD since budbreak	Days since budbreak	Event	Date	GDD since budbreak	Days since budbreak
1	Flight 1	19/10/2007	349	59	Flight 1	17/10/2007	234	47
	Flight 2	11/01/2008	1279	143	Flight 2	17/12/2007	1024	98
	Harvest	8/02/2008	1631	171	Flight 3	19/02/2008	1995	172
	Flight 3	20/02/2008	1748	183	Harvest	20/02/2008	2010	173
	Flight 4	31/03/2008	2146	223	Flight 4	31/03/2008	2527	213
2	Flight 1	17/10/2008	259	46	Flight 1	15/10/2008	226	38
	Flight 2	9/12/2008	736	99	Flight 2	25/11/2008	620	79
	Flight 3	14/01/2009	1173	135	Flight 3	13/01/2009	1245	128
	Harvest	5/02/2009	1512	157	Harvest	18/02/2009	1873	164
	Flight 4	13/05/2009	2490	254	Flight 4	17/03/2009	2212	191
3	Flight 1	20/10/2009	321	57	Flight 1	19/10/2009	238	52
	Flight 2	16/12/2009	1000	114	Flight 2	2/12/2009	873	96
	Flight 3	20/01/2010	1450	149	Harvest	15/02/2010	2070	171
	Harvest	22/01/2010	1483	151	Flight 3	16/02/2010	2084	172
	Flight 4	21/04/2010	2539	240	Flight 4	22/03/2010	2542	206

$$\mathbf{T}_2 = \left\lfloor n \frac{\mathbf{T}_1 - \min(\mathbf{T}_1)}{\max(\mathbf{T}_1)} \right\rfloor \quad \text{[Equation 13]}$$

where n is the number of vine rows in the vineyard block.

The binary image was then used to mask out the pixels not classified as vine, i.e.

$$\mathbf{T}_3 = \mathbf{B}\mathbf{T}_2 \quad \text{[Equation 14]}$$

An image of $\mathbf{T}_3$ was inspected to ensure each row had the same row identification integer, consisted of contiguous canopy pixels along rows, and was clearly separate from adjacent rows. Appropriate changes to the binary threshold value and the row orientation parameter (θ) were made if required.

Each row was then divided into a defined number of segments the width of the along-row vine spacing. The process began by creating an image of a single row ($\mathbf{T}_{row}$ with coordinates c) by selecting those pixels in $\mathbf{T}_3$ that were equal to the identifying integer associated with that row. A linear first order model was produced to describe the location and direction of the row, i.e.

$$\mathbf{Y}_{row} = a\mathbf{X}_{row} + b \quad \text{[Equation 15]}$$

where a and b were model parameters fitted using least squares regression. Minimum and maximum values of $\mathbf{X}$ and the corresponding values of $\mathbf{Y}$ resulting from the row description model were calculated from the single row image to determine start and end point locations of the vineyard row. Sets of coordinates of the central points of the segments along the row (X_i, Y_i) were then produced:

$$\mathbf{X}_i = \{\delta x, 2\delta x, ..., m\delta x\},\ \mathbf{Y}_i = \{\delta y, 2\delta y, ..., m\delta y\} \quad \text{[Equation 16]}$$

where

$$\delta x = \frac{\max(\mathbf{X}_{row}) - \min(\mathbf{X}_{row})}{m} \quad , \quad \delta y = \frac{\max(\mathbf{Y}_{row}) - \min(\mathbf{Y}_{row})}{m} \quad \text{[Equation 17]}$$

and m was the number of segments (individual grapevines) in each row. Four vertices of the contiguous bounding rectangles of each segment the width of the rows were calculated using

$$\{x_{v1}, y_{v1}\} = \left\{ x_i + \frac{d_{row}}{2}\cos\varphi - \frac{d_{vine}}{2}\sin\varphi, y_i + \frac{d_{row}}{2}\sin\varphi + \frac{d_{vine}}{2}\cos\varphi \right\} \quad \text{[Equation 18]}$$

$$\{x_{v2}, y_{v2}\} = \left\{ x_i + \frac{d_{row}}{2}\cos\varphi + \frac{d_{vine}}{2}\sin\varphi, y_i + \frac{d_{row}}{2}\sin\varphi - \frac{d_{vine}}{2}\cos\varphi \right\} \quad \text{[Equation 19]}$$

$$\{x_{v3}, y_{v3}\} = \left\{ x_i - \frac{d_{row}}{2}\cos\varphi - \frac{d_{vine}}{2}\sin\varphi, y_i - \frac{d_{row}}{2}\sin\varphi + \frac{d_{vine}}{2}\cos\varphi \right\} \quad \text{[Equation 19]}$$

$$\{x_{v4}, y_{v4}\} = \left\{ x_i - \frac{d_{row}}{2}\cos\varphi + \frac{d_{vine}}{2}\sin\varphi, y_i - \frac{d_{row}}{2}\sin\varphi - \frac{d_{vine}}{2}\cos\varphi \right\} \quad \text{[Equation 20]}$$

where $\mathbf{d}_{row}$ was the between-row spacing (the perpendicular distance between the rows), $\mathbf{d}_{vine}$ was the sample spacing (the distance between each segment's centre along the rows) and φ was the field orientation (the angle perpendicular to the vine row orientation, θ, i.e. $\varphi = \theta - \pi/2$). Those pixels with centroid coordinates inside each bounding rectangle were identified and associated with each vine unit in the vineyard. Using the original georectified imagery (i.e. not the filtered image), the mean reflectance values of all pixels in each vine object were then determined. Pure soil pixels, pure vine pixels and mixed pixels (containing both soil and vine reflectance information) were thereby aggregated to produce single reflectance values for each radiometric band per vine object.

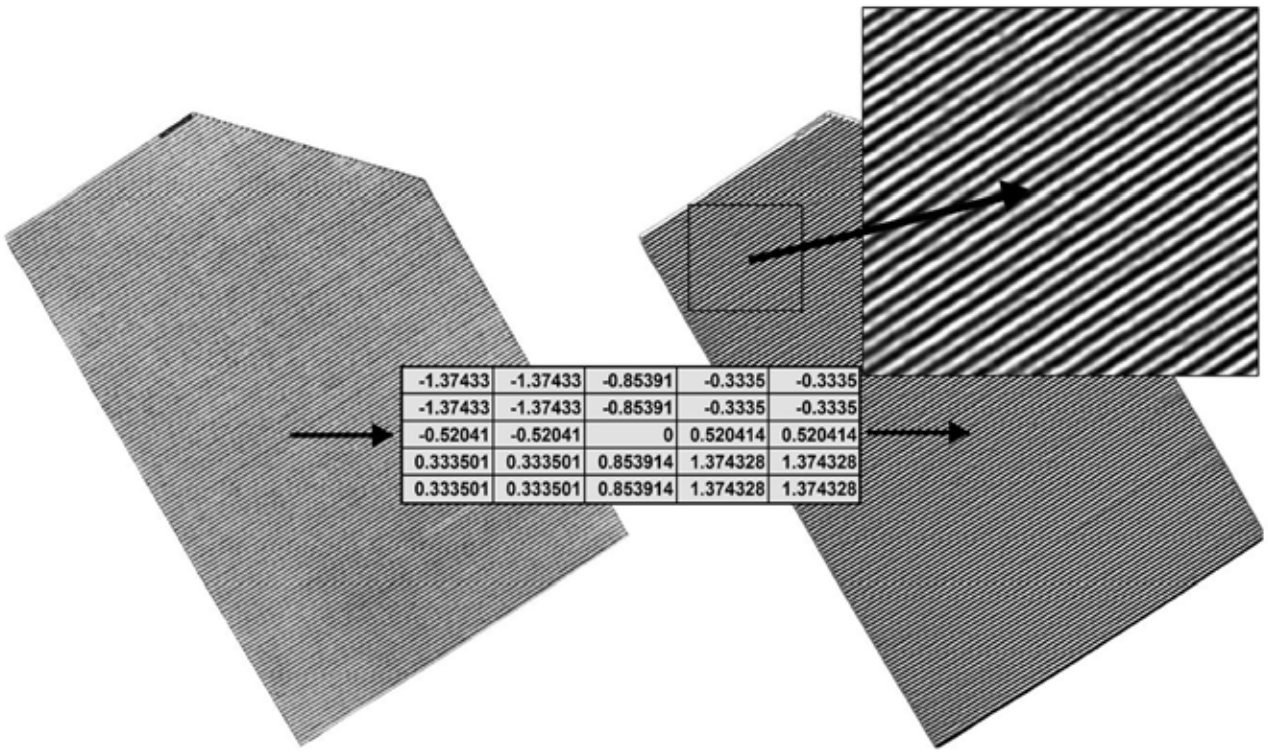


Figure 4.18 Directional filter applied to vineyard NDVI image enabled easier isolation of vine rows from inter-row space. Note that filtered imagery was only used in vineyard mapping processes; original imagery was used to define photosynthetically active biomass.

A number of vegetation indices (*Table 4.19*) were calculated using the mean reflectance data of each vine object. The utility of each VI to describe canopy that best estimated winegrape yield and composition was then investigated. The selected VIs comprised those that utilise bands included in typical low-cost 4-band colour-infrared multispectral imaging systems (i.e. blue, green, red and NIR bands). In addition, a vegetation abundance measure, estimated by a partial spectral unmixing procedure (Homayouni *et al.* 2008) and a vine canopy size measure, a count of the number of pixels above a threshold NDVI value (Hall *et al.* 2003), were produced.

On-ground data collection

Sample site selection was designed to achieve a good level of spatial coverage of each vineyard block while distributing sample sites to characterise overall environmental variability within the blocks. An isodata cluster algorithm ("Iso Cluster", Spatial Analyst, ArcMap, version 9.3.1, ESRI: Redlands California) was nested to first split each vineyard into three major zones and then six further subzones per major zone. Three sample vines were randomly selected from each subzone to produce a total of 54 samples per vineyard. The input to the cluster algorithm at the Hunter Valley site was a map of soil EC_a. The input to the cluster algorithm at the Riverina site, which exhibited low spatial variability in soil EC_a, was the NDVI image acquired closest to veraison (previously demonstrated to be the time at which strongest correlations between NDVI and grape colour within the year occurred in a Cabernet Sauvignon vineyard (Lamb *et al.* 2004)) before harvest operations of that year.

Fruit yield and composition descriptors were collected at each sample vine within one week before commercial harvesting operations. All grape clusters along 1 metre of the cordon, centred at the vine trunk of the sample vine locations, were hand harvested. The fruit was assessed in the field and in later laboratory analysis to determine: yield (total fruit weight) and its component parts (number of bunches, mean berry weight, number of berries per bunch), and key fruit quality measures that are indicative of final wine quality and potential value (total soluble solids, pH, titratable acidity (TA), anthocyanin content and total phenolic content). Grape yield was measured on location (kilograms of grapes per sample vine) and a sub-sample of approximately 100 berries from each sample vine was immediately packed in a cool box and then frozen for later laboratory analysis. Berry weight was determined by weighing 50 berries randomly selected from each sample. Total soluble solids (TSS) were measured with a bench refractometer (PR-101 ATAGO, Tokyo, Japan) from settled juice extracted from the grape samples. Anthocyanins (an

important quality indicating sub-group of phenolics in red wines, often simply referred to as 'colour') and total phenolics were assessed by spectrophotometer (UV-2101PC, Shimadzu, Kyoto, Japan): milligrams of anthocyanins per gram of berry weight and absorbance units per gram of berry weight (a relative measure of total phenolics). Grape sample juice pH and TA were assessed using a TIM800 Titration Manager coupled to a SAC080 Sample Changer and ABU901 Autoburette (Radiometer Copenhagen, Copenhagen, Denmark). Colour, phenolics, pH and TA measurements followed the procedure described by Iland *et al.* (2000). Berry sample solutions for assessment of anthocyanins and total phenolics were created through extraction using 10 mL of 50% v/v aqueous ethanol and 1 g of berry homogenate. The extract solutions, diluted in a 1:10 ratio with 1 M hydrochloric acid, were analysed with the spectrophotometer. The level of absorption at 520 nm and 280 nm was used to estimate anthocyanins and total phenolics, respectively. Acidity (pH) and TA samples were determined from 5 mL of settled grape juice diluted in 15 mL of de-ionised water. The initial pH of each sample was measured. Then samples were titrated using 0.1M sodium hydroxide. The volume of sodium hydroxide required to reach a pH of 8.2 was used to calculate TA. See Iland *et al.* (2000) for detailed information on calculations and procedures.

Statistical analysis

Correlation coefficients between all harvested grape character variables and the canopy descriptors derived from each VI in all three years (10 grape character variables×12 vineyard image data sets×3 study years=360 correlation coefficients per VI) were calculated. Thus correlations between all imagery and all fruit data were calculated regardless of year of collection. Of most relevance to this study are the correlations between image-derived canopy descriptors and fruit composition variables within the same year, which are analysed in detail in the results and discussion sections. However, cross-seasonal effects of canopy characteristics on fruit are potentially of interest, particularly because of factors related to carbohydrate reserve storage and utilisation. Therefore, in assessing each VI's predictive capacity all 360 correlation coefficients were considered. Although statistically significant correlations between grapevine canopy descriptors and variables describing fruit yield and quality might be identified, low magnitude coefficients imply a low level of prediction capability. For example, on a single vine basis where r=0.225 (statistically significant at α=0.05, 1-tail, n = 54), only 5.06% of the variability in a fruit descriptor is explained by the differences in canopy. However, in practice, a vineyard management block may only be split into two harvest zones.

To demonstrate the potential level of difference in a fruit descriptor variable for which various levels of correlation are found, a bootstrap simulation was conducted. Two sets of 54 random numbers were drawn from a normal distribution with mean 0 and standard deviation 1 using the rnorm function of

Table 4.19 Vegetation indices and descriptors of grapevine canopy examined in this study. R is the corrected reflectance in the band indicated by the subscript.

Index Name	Abbreviation	Equation
Vegetation Abundance (Homayouni *et al*. 2008)	Abundance	N/A
Enhanced Vegetation Index (Huete *et al*. 1997)	EVI	$EVI = G\frac{R_{nir} - R_{red}}{R_{nir} + C_1R_{red} - C_2R_{blue} + L}(1+L)$ where G=2.5, C_1=6.0, C_2=7.5 and L=1.0
Normalised Difference Vegetation Index (Rouse *et al*. 1973)	NDVI	$NDVI = \frac{R_{nir} - R_{red}}{R_{nir} + R_{red}}$
Vine Canopy Size (Hall *et al*. 2003)	Size	N/A
Simple Ratio (Birth and McVey 1968)	SR	$SR = \frac{R_{nir}}{R_{red}}$
Triangular Vegetation Index (Broge and Leblanc 2000)	TVI	$TVI = 0.5\left(125\left(R_{nir} - R_{green}\right)\right) - 250\left(R_{red} - R_{green}\right)$ [a]
Visible Atmospherically Resistant Index (Gitelson *et al*. 2002)	VARI	$VARI = \frac{R_{green} - R_{red}}{R_{green} + R_{red} - R_{blue}}$

[a] Note the parameters for the TVI calculation were altered to account for differences between the spectral bands used in this study and the bands used by Broge and Leblanc (Gitelson *et al*. 2002).

S-plus (TIBCO Spotfire S+ Version 8.0.4 for Linux, TIBCO Software Inc.: Palo Alto, California). The correlation coefficient between the two sets was calculated. The second set of numbers was placed in ascending order of the first set of numbers, simulating a prediction of a fruit quality/yield variable (the second set) based on the values of canopy descriptors (the first set). The dummy quality/yield variables were then split into two groups based on this order, with the first 27 ordered values placed into subset 1 and the second 27 ordered values placed into subset 2. A *t*-test was then conducted to determine any significant difference in the means of the two subsets. The simulation was repeated 1 million times. The p-values of the t-tests from the bootstrap simulation results for which correlation coefficients exceeded significance levels at α=0.1, 0.05, 0.01, 10^{-3} and 10^{-4} (corresponding to r>0.176, 0.225, 0.312, 0.405 and 0.475, when n=54) were examined. A difference between the means was considered to have occurred if $p<0.05$.

Section 2b

A minimally pruned block (ca. 1 ha) of Cabernet Sauvignon on own roots subject to spatially uniform management in Wagga Wagga, Australia was used in this study. Vines were trellised on a single wire with a row spacing of 3.6 m and an inter-vine spacing of 1.8 m. The block lay on a gentle (<10°) incline, sloping towards the east with rows planted perpendicular to the slope. Fifty-two individual sample grapevines were selected for sampling within the block using a stratified scheme based on canopy differences observed in earlier multispectral airborne imagery acquired of the vineyard. The sample vines were harvested at the conclusion of the successive 2000-01 (year 1) and 2001-02 (year 2) growing seasons just before commercial harvesting commenced. Grape yield was measured on location (kilograms of grapes per sample grapevine).

High spatial resolution (0.25 m) georectified and radiometrically corrected airborne normalised difference vegetation index (NDVI) images of the target vineyard site were acquired using the same remote sensing system and protocol outlined by Hall *et al.* (2008b). In year 1, three imaging over-flights were timed to coincide with flowering, veraison and maturity (just prior to harvest). In year 2 a further six imaging overflights were conducted: at flowering, midway between flowering and veraison, veraison, midway between veraison and maturity and maturity (*Table 4.20*). Any vegetation growing between and under the vines was removed with herbicide spray in the weeks prior to the imaging overflights. This ensured that most photosynthetically active vegetation detected in the vineyard block would be from vines alone.

Table 4.20 Timing of imaging overflights and designation of phenological stages.

	Days post-budbreak	Designation	Abbreviation
Year 1	60	Flowering	F1
	107	Veraison	V1
	156	Maturity	M1
Year 2	31	post-Budbreak	pB2
	48	Flowering	F2
	67	post-Flowering	pF2
	124	Veraison	V2
	140	post-Veraison	pV2
	165	Maturity	M2

Given that for highly vegetated targets, the NDVI value is close to unity, while for non-vegetated targets the NDVI is close to zero, a threshold NDVI value was calculated for each NDVI image to classify vine pixels and inter-row space pixels following the procedure of Hall *et al.* (2003). Images were processed to effectively remove pixels below the threshold NDVI value. The Vinecrawler algorithm (Hall *et al.* 2003) was then applied to collect spatially-referenced, single pixel-wide cross-sections along each vine row. Two quantitative canopy descriptors (Hall *et al.* 2003) were calculated for each NDVI slice: canopy area (CA), the number of pixels above the threshold NDVI; and canopy density (CD), the mean NDVI of those pixels above the threshold NDVI. The means of the canopy descriptors of the slices were calculated to provide whole sample single grapevine descriptors. *Figure 4.19* illustrates how the descriptors were derived. A full description of the Vinecrawler algorithm is given in Hall *et al.* (2003) and a further summary description in Hall *et al.* (2008b).

In addition to the two canopy descriptors described in *Figure 4.19*, two canopy descriptor derived indices were calculated for each sample site. Canopy density change (CDC),

$$CDC = \frac{D_t}{D_{t-1}} \qquad \text{[Equation 22]}$$

and canopy area change (CAC),

$$CAC = \frac{A_t}{A_{t-1}} \qquad \text{[Equation 23]}$$

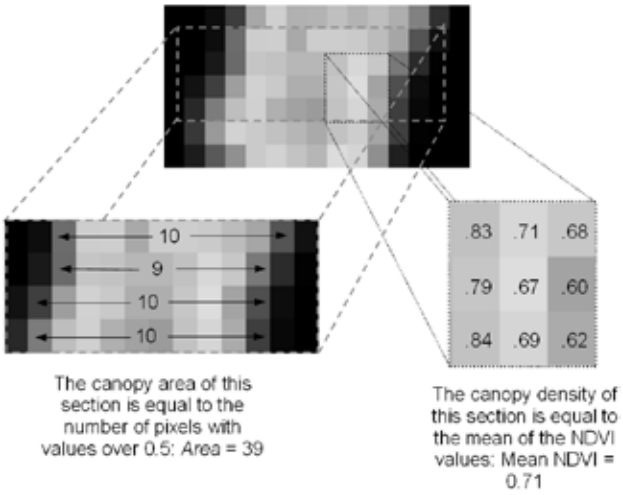


Figure 4.19 Canopy area and canopy density defined in terms of NDVI imagery (after Hall *et al*. 2008b).

where t is a sequential integer that refers to each imaging mission. Each index characterises the magnitude of canopy change between successive imaging missions.

Two best subset regression analyses were conducted using canopy area in one analysis and canopy density in the other. Yield in Year 2 was the response variable and each set of either canopy area or canopy density data (at all stages except post-veraison and maturity, which were acquired after mid-season trimming) and yield in year 1 were the predictor variables. Models for every possible combination of one, two or three predictor variables were derived using least squares regression.

Section 3a

Decadal-scale climatic variability results in indices describing viticultural growing conditions varying over time. Comparisons made between regions using ad-hoc calculations, particularly between regions in different countries, can result in indices being derived using data from unlike time-periods. A common time-period for the assessment of climate indices enables comparisons to be made spatially only, without the confounding affect of climatic temporal variability. A common period of 30 years from 1971 to 2000 is used here, same as the reference period employed in the Intergovernmental Panel on Climate Change Fourth Assessment Report (IPCC 2007). Interpolated maximum and minimum temperature grids (0.05 decimal degree resolution) generated for Australia were acquired from the Australian Bureau of Meteorology website (Bureau of Meteorology 2010) for each day from 1 October to April 30 for the years 1971 to 2000. A high resolution (3 arc-second) digital elevation map of Australia was also acquired (Jet Propulsion Laboratory 2004).

A grid of growing season temperature was simply calculated as the mean of all the daily temperature surfaces. The temperature grids where then used to calculate the three climate indices (GDD, HI and BEDD) per *Table 4.12*. Each index was calculated for the whole of Australia retaining the 0.05 decimal degree resolution. All the daily maps for each index were summed, then averaged by the total number of years to produce mean annual index totals for GDD, HI and BEDD, and averaged by the total number of days to produce mean GST (*Figure 4.20*). Pixels, whose centroid geographic coordinates were within a Geographic Indication (GI, Australian Wine and Brandy Corporation 2008), were extracted from the DEM and the four index maps, creating spatially appropriate data to assess the statistical properties of each GI's elevation and climate. The data describing the indices of the set of pixels extracted from each GI were summarised by five values: the maximum and minimum, the median (the second quartile) and the first and third quartiles (*Table 4.21*).

A common feature of both the HI and the BEDD is a latitude correction factor, which effectively adjusts the indices to account for differences in day length. Longer day lengths result in a greater proportion of a 24 hour period being closer to the maximum recorded temperature than the minimum recorded temperature. Since the daily average temperature is actually an estimate based on the mean of the minimum and maximum temperatures, the latitude correction factor increases the index value to account for the extra heat accumulation that results from longer day lengths that occur at higher latitudes during summer. The HI latitudinal correction (K) was developed for the latitudes of European viticulture as a linear response to increasing day lengths at higher latitudes (Huglin 1978). Equations to calculate day

Table 4.21 Significance levels of coefficients of determination for sample sizes typical in this study.

Alpha 1-tail	r^2, n=271	r^2, n=335
0.05	0.010	0.009
0.01	0.020	0.017
0.001	0.035	0.029
0.0001	0.050	0.041
0.00001	0.065	0.053
0.000001	0.080	0.065
3.9×10^{-8}	0.1	
1.1×10^{-9}		0.1

length used in this analysis are given by Glarner (2006). Day lengths (in hours) at latitude, *Lat*, for Julian day, *Jday*, were calculated using the exposed radius part between the sun's zenith and the sun's circle, *m*:

$$dayLength_{Lat_{JDay}} = \frac{\arccos\left(1 - m_{Lat_{JDay}}\right)}{\pi} \cdot 24 \qquad \text{[Equation 24]}$$

where

$$m_{Lat_{Jday}} = 1 - \tan(Lat) \cdot \tan\left(Axis \cdot \cos\left[\frac{\pi \cdot Jday}{182.625}\right]\right) \qquad \text{[Equation 25]}$$

where *Axis* is the obliquity of the ecliptic (currently, ~0.409 rad), and *JDay* is the Julian day assumed to begin on 21 June (Southern Hemisphere).

The total length of daylight for the six-month period 1 October (Julian Day 103) to 31 March (Julian Day 284) at a given latitude ($totalSeasonDayLength_{Lat}$) is

$$totalSeasonDayLength_{Lat} = \sum_{Jday=103}^{284} dayLength_{Lat_{JDay}} \qquad \text{[Equation 26]}$$

Using the upper and lower values of K given by Huglin and Schneider (1998), i.e. $K_{40°}$=1.02, $K_{50°}$=1.06, and equivalent $totalSeasonDayLength_{Lat}$, an equation describing *K* as a function of *totalSasonDayLength* was derived using least squares:

$$K_{Lat} = 2.8311 \times 10^{-4} \cdot totalSeasonDayLength_{Lat} + 0.30834 \qquad \text{[Equation 27]}$$

K for latitudes 0–65° at 0.05° intervals was then calculated. *K*, calculated in this way, is less than unity at latitudes lower than 33.3° (reaching 0.930 at the Equator). In this study, where *K* was less than unity, the latitude adjustment was not applied.

Galdstones's (1992, p. 63) adjustment for latitude/day length is functionally similar to K (*Figure 4.21*). A first-order linear function describes the relationship between the two parameters ($R^2 \approx 1$):

$$BEDDLatitudeAdjstmentFactor = 1.1135K - 0.13520 \qquad \text{[Equation 28]}$$

Although, both adjustment factors were based on day length/latitude, their respective magnitudes seem to have been decided arbitrarily. However, since this is an index, the absolute values derived are less important than the relative differences that the adjustment factors engender. The steeper gradient of the function of *BEDDLatitudeAdjustmentFactor* with respect to latitude (*Figure 4.21*) causes it to have a greater impact on heat sum calculation than *K*. The calculations used in this study have employed *K* as the latitude adjustment element for both heat sum calculations. This effectively modifies Gladstones's original BEDD, slightly reducing the effect of latitude in its calculation.

Section 3b

Winegrape yield data were obtained from the Australian Bureau of Statistics for the 25 vintages between 1983 and 2007. The three major grapevine cultivars of Australia are Chardonnay, Cabernet Sauvignon and Shiraz (also known as Syrah). Their total yield and mean yield per hectare of bearing area for these years are illustrated in *Figure 4.22*.

Geographic Indication (GI) regions of Australia were used to aggregate Statistical Local Areas (SLA) into 30 groupings representative of the wine growing regions of Australia, henceforth called regions of interest (ROI). Data on grape production area (obtained from the Australian Bureau of Statistics, ABS) and yield were aggregated from the SLAs into the 30 ROIs (*Figure 4.23*). Yield per hectare was calculated for each variety in each ROI spanning 25 vintages from 1983 to 2007. Data was adjusted for technological improvement in yield (linear trend removal) and for inter-annual oscillation in yield.

Each grouping was spatially aggregated and then clipped using the GIs to produce polygons spatially representative of the winegrape growing areas of the 30 regions of interest. Climate data were then interpolated for the polygons representing the ROIs. These climate data included daily temperature, rainfall, humidity, SOI, and the Dipole Mode Index (DMI, which describes the Indian Ocean Dipole. Climate data were aggregated into phenological time groupings of 100 BEDD intervals from the season start date (defined as day on which BEDD total has reached 10), individually calculated for each ROI. Potential advantages of using ENSO and IOD as predictors of yield are that these indices are commonly modelled to produce forecasts. ENSO and IOD forecasts can be plugged into the yield models to produce future yield forecasts.

Season start date is defined here as the day of 50% budbreak (check references Moncur, Coombe, McIntyre) averaged for a region. The method of determining budbreak was derived from the method of Moncur (1989) and used springtime daily temperature records. Moncur *et al.* (1989) determined the base temperature for heat sum calculations for budbreak to be on average 3.5°C. The heat sum total required to initiate budbreak was calculated by Moncur *et al.* (1989) to be on average 10300 degree hours for a (limited) range of locations and varieties. Since for this study only daily temperature data is available the equivalent degree day total used was 430 degree days (i.e. 10300/24).

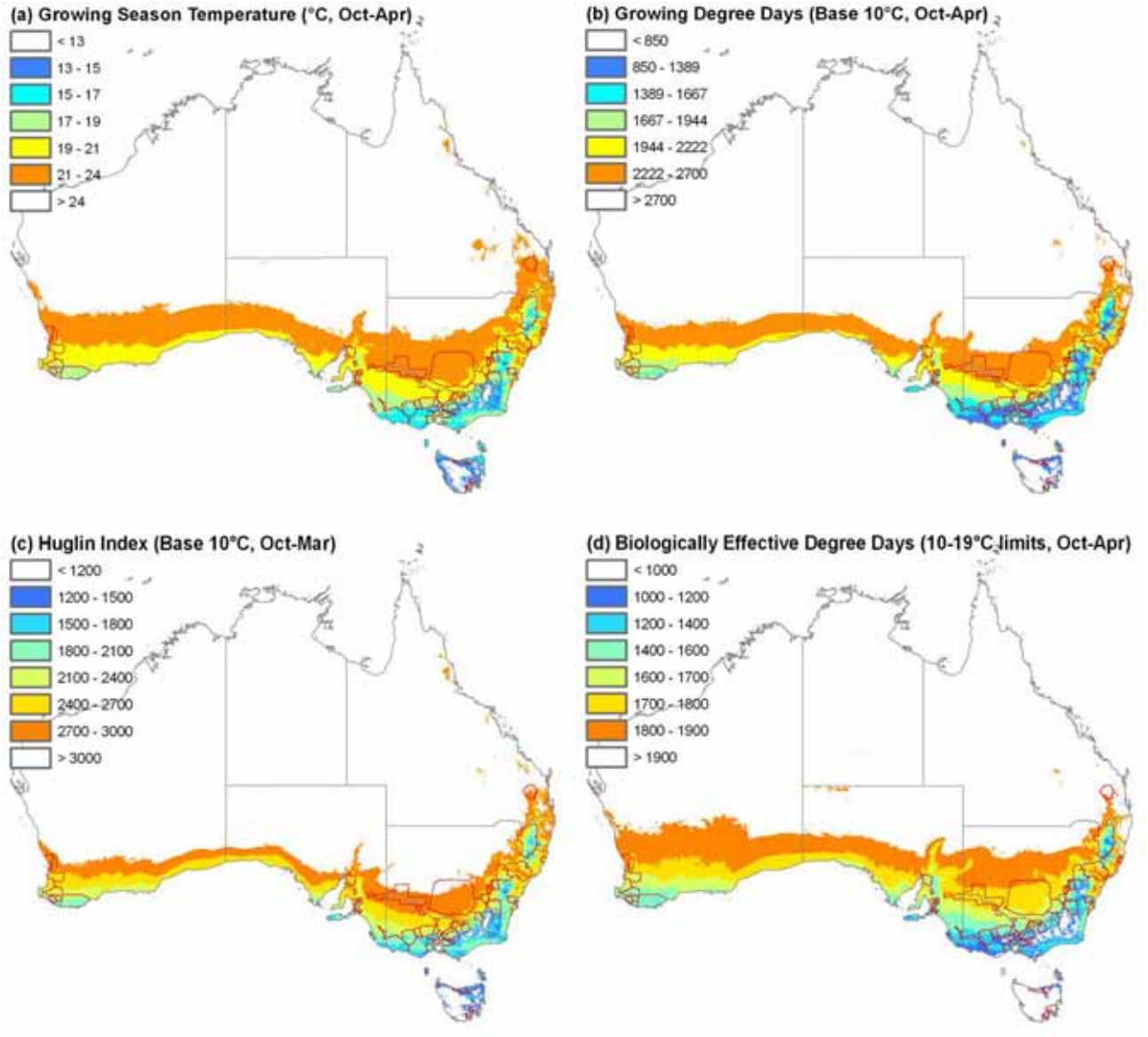


Figure 4.20 Maps of (a) growing season average temperatures (GST), (b) growing degree-days (GDD), (c) the Huglin Index (HI), and (d) biologically effective growing degree-days (BEDD), for Australia, 1971–2000. GI outlines are superimposed in red onto each map.

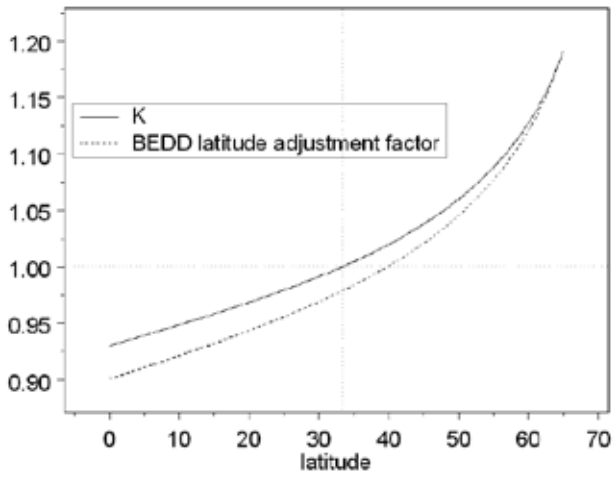


Figure 4.21 Comparison of Huglin's (*K*) and Gladstones's latitude adjustment factor for viticulture heat summation calculations.

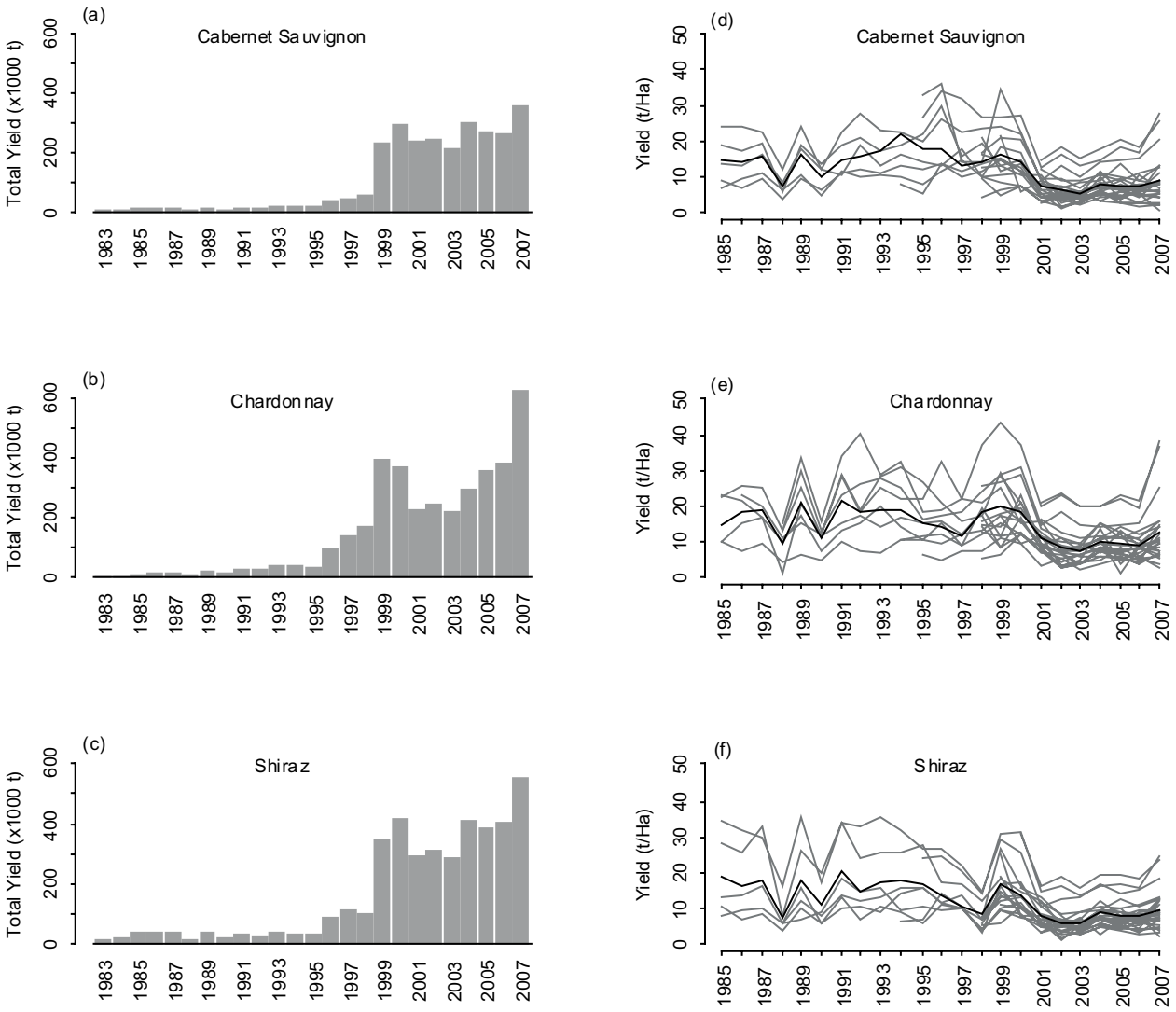


Figure 4.22 Total grapevine yield from 1983-2007 (a, b, c) and yields per hectare for each of the 28 regions in this study (grey lines) and the yield per hectare of all regions (black line) from 1985-2007 (d, e, f) for the varieties Cabernet Sauvignon, Chardonnay and Shiraz, respectively.

In addition the following derived climate indices were calculated:

- *Temperature variability index* (Gladstones 1992):

  $$TVI=(TD_{max}-TD_{min})+(TM_{max}-TM_{min})$$

  where TD_{max}/TD_{min} are the average daily maximum/minimum and TM_{max}/TM_{min} are the average highest maximum/minimum of the month. This can be modified to become a TVI for any period of contiguous days.

- *Spring frost index* averaged for October to November:

  $$SFI=TD_{mean}-TM_{min}$$

  where TD_{mean} is the average mean and TM_{min} is the average lowest minimum. TM_{min} was modified to the lowest minimum for the thermal time period.

- *Heat stressfulness index* (Gladstones 2004) averaged for January to March

  $$HSI=TM_{max}-TD_{mean}$$

  TM_{max} was modified to be the highest maximum for the thermal time period.

Data was normalised by calculating the mean of each temporal series of each variable and subtracting this from each data item in the series. Both the response variable (Yield) and the predictor variables were normalised. By using normalised data in the models result in an analysis of the effect of deviation in climate data from the mean in determining yield deviation from the mean is revealed. Models resulting from this process have the greatest predictive power for annual yields.

The yield (Y) of variety v in region r and time period t, $Y_{v,t,r}$ is the sum of all yield of variety v in time period t that are from all SLAs (s) within the region, i.e.

$$Y_{v,t,r}=\sum_{s} Y_{v,t,s},\ s\ \varepsilon\ r$$

Each time-period organised variable set was standardised to a mean of 0 and standard deviation of 1:

$$x_{v,t,r}=\frac{X_{v,t,r}-\overline{X_{v,t}}}{\sigma_{X_{v,t}}}$$

Single weather variables were regressed against Yield using both first and second order polynomials. Since a high number of predictor variables were produced from the base climate data (>4000), it is important to guard against Type I error. With a large number of samples coefficients of determination that describe how well models fit the data can be statistically significant at relatively small magnitudes. If using alpha=0.05, out of 4000 series of random data, 200 could be considered significantly related to the response variable, yet would have no value as predictor variables. *Table 4.21* contains the coefficients of determination that are required to be significant at various alpha levels for two sample sizes typical of this study. A coefficient of determination of only 0.009 is significant at α=0.05. If there were only one predictor variable for which a reasonable hypothesis can explain a relationship with the response variable then this would be a significant result, i.e. it would be a reasonable conclusion that the predictor variable does influence the response variable (the probability of Type I error would p=0.05). The level of significance increases rapidly as the coefficient of determination increases. When r^2 reaches 0.08, the probability of a relationship occurring by chance for a single variable is about one in a million ($\alpha=1\times10^{-6}$, $r^2=0.080$, $N=271$), and for 4000 series of predictor variables the probability of a relationship occurring by chance is about one in 250. The threshold r^2 chosen for this study is 0.065, which at the lower end of samples used in the study results in p≈0.00001. For 4000 random series, the probability that at least one will correlate with a response variable is p≈0.04.

Although the level of significance of a relationship is high at relatively low coefficients of determination, the predictive power of such relationships remains low. The proportion of variance in the response variable that is explained by a predictor variable with a coefficient of determination of 0.1 is 10%. Although it gives some indication of the probably outcome of a predicted response variable, it does not provide much predictive power. For example, for a model where $r^2=0.1$, the probability that the model correctly predicts that the response variable will be either less than or greater than the mean of the response variable series used to make the model is 55%.

Adjusted coefficients of determination (r^2_{adj}) were used to assess model skill. Adjusted coefficients of determination take into consideration the number of samples (n) and parameters (p) used in the model:

$$r^2{}_{adj}=1-(1-r^2)\frac{n-1}{n-p-1}$$

where p is the number of predictor variables and n is the sample size. The cross-validation process produces coefficients of determination that characterise the fit of the predicted yields to the actual yields in the validation set of samples.

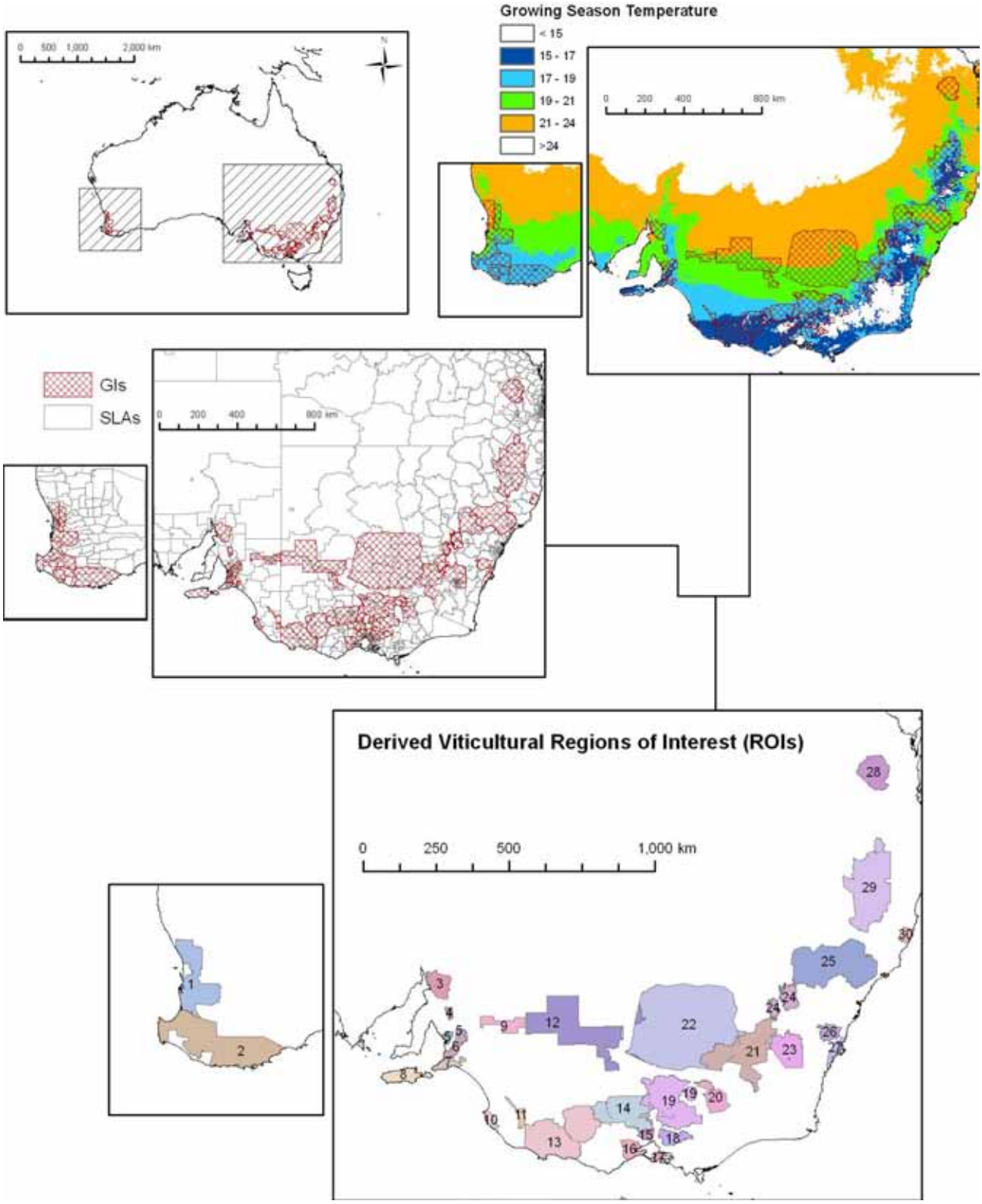


Figure 4.23 Derivation of viticultural regions of interest (ROIs) used in this study. ROIs are based on Geographic Indications (GIs). Statistical Local Areas (SLAs) (in which yield data is organised by the Australian Bureau of Statistics) that are wholly or partially within the GIs were grouped by GI. Those GIs that contained SLAs that significantly crossed over to different GIs led to amalgamation of GIs into single ROIs. The process was further guided by growing season temperature, i.e. adjacent GIs with similar growing season temperatures were amalgamated into single ROIs.

Neural network model

Neural networks are highly flexible (Venables and Ripley 2002), and are strong for predictive applications. However, they are black box systems that contain many parameters in hidden layers and are therefore weak for data interpretation. The preceding section discussed some key individual variables' relationships with winegrape yield and offers hypotheses for their influence on grapevine reproductive processes. In this section, a subset of the key variables is used to train neural network models to produce yield forecasts.

Neural networks are non-linear regression models that take the form

$$z = \varphi\left(\sum_{i=1}^{n} \omega_i x_i + b\right)$$

Where ω_i is the weight applied to x_i for sample *i* of *n* samples, and φ is the activation function, for which we applied the commonly used sigmoid function:

$$output = \frac{1 - e^{-z}}{1 + e^{-z}}$$

with the parameters fitted using an iterative optimisation process.

Neural networks are often conceptualised as a number of layers with the first layer being the predictive variables followed by a number of hidden computation layers and finally the layer of response variables. A simple neural network structure was employed in this study, with one hidden layer and one response variable (i.e. the yield of a single grape variety) used at any one time (*Figure 4.24*). The hidden layer can have any number of nodes. The neural network fitting process was conducted repeatedly using 1 to 10 nodes for each set of predictor variables

Neural networks are computationally expensive. The time taken to fit a neural network increased geometrically as the number of predictor variables increased. Initially, each run was conducted with 3 to 20 variables. A parsimonious approach was taken, employing a single layer feed forward neural network and reducing predictor variables. All weather variables (both unchanged and quadratic forms) correlated with yield and placed in order of strongest *correlation*. Neural networks were fit to the first three variables in the list, then the first four, etc., up to 20 variables.

Cross-validation is an important step in the production of predictive models (Picard and Cook 1984). Ten-fold cross validation is a commonly used form and is employed in this study. Ten-fold cross validation has been shown to be no better and less computationally expensive than "leave-one out" cross-validation (Kohavi 1995). The cross validation process is involves splitting the data is validation sets and training sets. The *Validation* data set is a randomly selected 10% of data samples. The remaining 90% of data is the *Training* data set. The neural network parameters are optimised using the training set data. The predictor variables from the validation data set are then used to produce model outputs. These are compared with response variables from the validation set. The mean sum of squares (MSS) between modelled output and actual yield data is calculated to provide a measure of the degree of fit achieved by the neural network. The process is stochastic, therefore the above process needs to repeated many (100) times and the MSS values are averaged.

Results and discussion

Section 1

Significant differences between the actual yield recorded at the weigh bridge after machine-harvesting and the hand-harvested estimate were found (*Table 4.22*). To correct for the discrepancy between the actual machine harvested yield and the hand-harvested estimate, a simple linear model (first order polynomial) was constructed using all actual machine harvest yields and hand-harvested estimates normalised by calculating their ratio to the mean values collected at each site over all three years. The model was used to produce machine-harvest estimates from the hand-harvest estimate data. Using all 54 sample vines, a good level of accuracy was produced (*Table 4.22*).

The comparisons between the targeted sampling and equivalent random sampling for each sample set size are presented in *Table 4.23*. Comparisons for a subset of sample sizes are presented visually in *Figure 4.25*.

The potential error (PE) of the different instances of the four yield forecasts is high when few sample sites were used in the Monte Carlo estimation modelling. When three samples were used, three of the four instances had a PE above 33% (reported as the average absolute difference between grower estimates of seasonal winegrape production and winery deliveries (Dunn and Martin 2003)) with the greatest PE of ±44.3% occurring at the Hunter Valley site in 2008. The PE fell as the number of samples was increased: by about 30% lower when six samples were used,

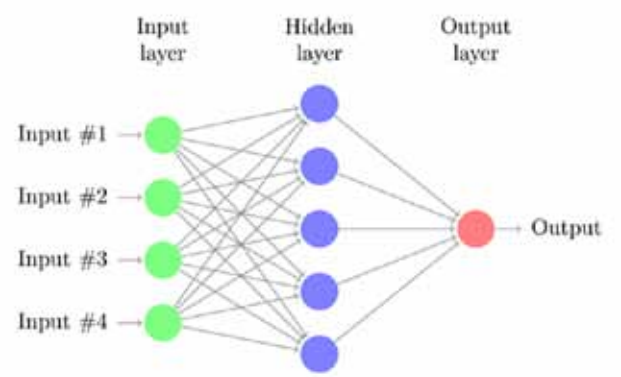


Figure 4.24 Conceptual model of a generic feed-forward artificial neural network structure (Fauske 2006). Each of the inputs is a climate anomaly variable for a wine region and year and the output is the corresponding yield anomaly data.

about 50% lower when nine samples were used, about 70% lower when 18 samples were used and about 85% lower when 36 samples were used. The overall level of potential error is mainly determined by the variability in yield of the site in that year, represented by the coefficient of variation (CV). The greater the level of spatial variability in yield, the grater the number of samples that are required in order to get a comparably accurate yield forecast to a site with a low level of spatial variability in yield.

The key comparison in this study is between the number of sample sites used to produce a yield estimate that incorporates spatial data and the number of sample sites that would be required to produce the same potential accuracy if sample site locations were selected randomly. The values are presented in the first and last columns of *Table 4.23*. The first column ("Number of Sample Sites") represents the number of sample sites used in the Monte Carlo simulation to produce estimates of the potential error when spatial data is incorporated into the sample selection procedure. The potential error here is then used along with the coefficient of variation of yield across all 54 sample sites to calculate the number of randomly selected samples required to achieve an estimate that has the same percentage error (n). The number of random samples required is consistently greater than the equivalent number of samples selected using spatial information (*Figure 4.25*). The level of advantage of using a sampling method that incorporates spatial data varied between years, but was always advantageous, and varied depending on the number of sample sites used, generally increasing for increasing sample sizes. This indicates a significant gain in estimation accuracy, if the same number of samples is used, or in sampling efficiency, allowing fewer samples to be collected to achieve the same level of potential error.

Section 2a

The results of the bootstrap simulations are summarised in *Table 4.24*. At a correlation significance level of $\alpha = 0.05$, the average difference between the subsets was 0.442 standard deviations, and the percentage of subsets with significantly different means was 48.3%. Thus, for vineyards with remotely sensed canopy descriptors correlating with a fruit quality or yield variable at $r>0.225$ ($\alpha=0.05$) that are split into equally sized sets of individual vines based on canopy density, the quality or yield variable of fruit harvested from those two sets will, on-average, differ by about 0.442 standard deviations and have a 48.3% chance of being significantly different. As the level of correlation increased, larger differences between the means of the subsets became more likely, and the probability of significant differences between the means increased. At $r>0.312$ ($\alpha=0.01$), the probability of a significant difference between the means of the subsets was 74.2%, with

Table 4.22 Total block machine harvest yield estimation variables for (a) the Riverina study site and (b) the Hunter Valley study site using all 54 sample vines.

Vintage	Hand-harvest estimate, M (t)	Machine-harvest estimate, $\hat{Y}$ (t)	Actual machine-harvest yield, Y (t)	Estimation accuracy, ε	Machine harvested yield per metre, μ (kg)	Hand harvested yield per metre, μ_h (kg)
(a) Riverina study site						
2008	233.0	155.1	168.0	-7.7%	4.580	6.352
2009	186.3	122.0	126.3	-3.4%	3.443	5.079
2010	272.1	182.8	165.6	+10.4%	4.515	7.418
(b) Hunter Valley study site						
2008	45.0	32.8	33.4	-2.0%	2.979	4.014
2009	30.5	21.7	21.6	+0.7%	1.927	2.721
2010	16.5	11.1	10.6	+4.8%	0.946	1.472

*Harvest Multiplier is the average of the preceding years' hand-machine ratios.

Table 4.23 Results of Monte Carlo modelling to determine error (E_m) when using a sub-set of sample sites subject to the conditions described in *Table 4.14* and the corresponding random sampling error (E_r) calculated using Equation 8 using the same number of samples. Data is presented for the Hunter Valley site in (a) 2008, (b) 2009 and (c) 2010.

	Targeted sampling system					**Equivalent random sample**		
N	$\bar{x}_m$	s_m	$q_{0.025,m}$	$q_{0.975,m}$	iqr_m	$q_{0.025,r}$	$q_{0.975,r}$	iqr_r
(a) Hunter Valley 2008 (μ=4.014 kg m^{-1}, =0.1126)								
3	4.007	0.9279	2.333	5.968	3.634	1.307	12.33	11.02
6	4.023	0.6184	2.800	5.267	2.467	2.498	6.449	3.950
9	3.993	0.4690	3.044	4.900	1.856	2.836	5.681	2.844
12	3.975	0.3981	3.208	4.742	1.534	3.012	5.349	2.336
18	4.014	0.2744	3.472	4.528	1.056	3.206	5.025	1.819
24	4.011	0.2600	3.500	4.508	1.009	3.317	4.858	1.541
36	4.016	0.1379	3.753	4.303	0.550	3.445	4.677	1.232
(b) Hunter Valley 2009 (μ=2.721 kgm^{-1}, =0.1485)								
3	2.709	0.5361	1.766	3.887	2.120	0.997	7.426	6.429
6	2.734	0.3638	2.058	3.485	1.427	1.780	4.158	2.378
9	2.708	0.2746	2.193	3.238	1.045	1.994	3.712	1.718
12	2.733	0.2444	2.282	3.224	0.943	2.105	3.518	1.413
18	2.717	0.1580	2.394	3.012	0.617	2.226	3.327	1.101
24	2.716	0.1537	2.422	3.026	0.603	2.294	3.227	0.933
36	2.716	0.0850	2.552	2.878	0.326	2.373	3.120	0.747
(c) Hunter Valley 2010 (μ=1.472 kg m^{-1}, =0.3227)								
3	1.538	0.2980	0.953	2.094	1.141	0.452	4.791	4.338
6	1.542	0.2107	1.138	1.962	0.824	0.894	2.423	1.529
9	1.541	0.1704	1.206	1.869	0.663	1.022	2.121	1.099
12	1.550	0.1475	1.260	1.833	0.573	1.089	1.991	0.902
18	1.542	0.1008	1.344	1.733	0.389	1.162	1.864	0.702
24	1.549	0.0875	1.376	1.716	0.340	1.204	1.799	0.594
36	1.548	0.0503	1.451	1.644	0.194	1.253	1.729	0.475

the mean difference between the subsets being 0.560 standard deviations. At r>0.475 (α=10^{-4}), a non-significant difference between the subsets became very unlikely (≈0.7% probability) and the mean difference between the subsets was estimated to be 0.809 standard deviations. A full economic analysis of the implications of these differences in practice is beyond the scope of this study. Nevertheless, it was demonstrated that, even at low levels of correlation between canopy and fruit quality or yield variables, practical levels of differentiation between fruit quality or yield variables can be achieved in the field. If the data required for a segmented harvest is collected as a matter of course, and even if the correlation is only significant at α=0.1, then approximately 1 year in 3 (a 34.4% chance was indicated by the simulation) a significant differentiation in the selected fruit quality attribute will be achieved. In practice, natural breaks in the data sets and non-normal distributions of remotely sensed canopy metrics would result in non-equal sized splits of grapevines likely being selected based on viewing imagery, which would likely result in stronger differentiation of fruit characteristics than this simulation has suggested.

The number of significant correlations between the remotely sensed canopy descriptors and the fruit quality and yield data out of the 360 calculated for each VI are summarised in *Table 4.25* at three different levels of significance. This table indicates the VIs best suited to predicting fruit composition and yield overall. The VI that correlated (α=0.05) with the most fruit descriptors was TVI, with 209 combined across both sites. There were more significant correlations at the Riverina vineyard at all significance levels for all VIs. In addition, the counts of significant correlations varied between the VIs at a greater level at the Riverina vineyard: the range of counts of significant correlations (α=0.05) at the Hunter Valley vineyard was 59 (VARI) to 86 (Abundance), whereas at the Riverina vineyard the range was 65 (VARI) to 128 (TVI).

Table 4.24 Results of a bootstrap simulation to estimate probability of a significant difference between an equally sized split of 54 dummy response variables (analogous to a grape quality or yield variable) placed in the ascending order of 54 dummy predictor variables (analogous to a grapevine canopy descriptor variable) at five different levels of correlation. One million variable sets were randomly selected from a normal distribution with mean 0 and standard deviation 1.

α	r	Count of significant correlations	Mean of subsets with significant correlations (standard deviations from the mean)		Mean difference between subsets with significant correlations (standard deviations)	Count of subsets with significant correlations that had significantly different means at alpha=0.05	Percentage of subsets with significant correlations that had significantly different means at alpha=0.05
			Subset 1	Subset 2			
0.1	0.176	100937	-0.189	0.188	0.379	34892	34.6
0.05	0.225	50538	-0.221	0.221	0.442	24416	48.3
0.01	0.312	10776	-0.280	0.280	0.560	7995	74.2
10-3	0.405	1176	-0.349	0.343	0.692	1102	93.7
10-4	0.475	145	-0.414	0.395	0.809	144	99.3

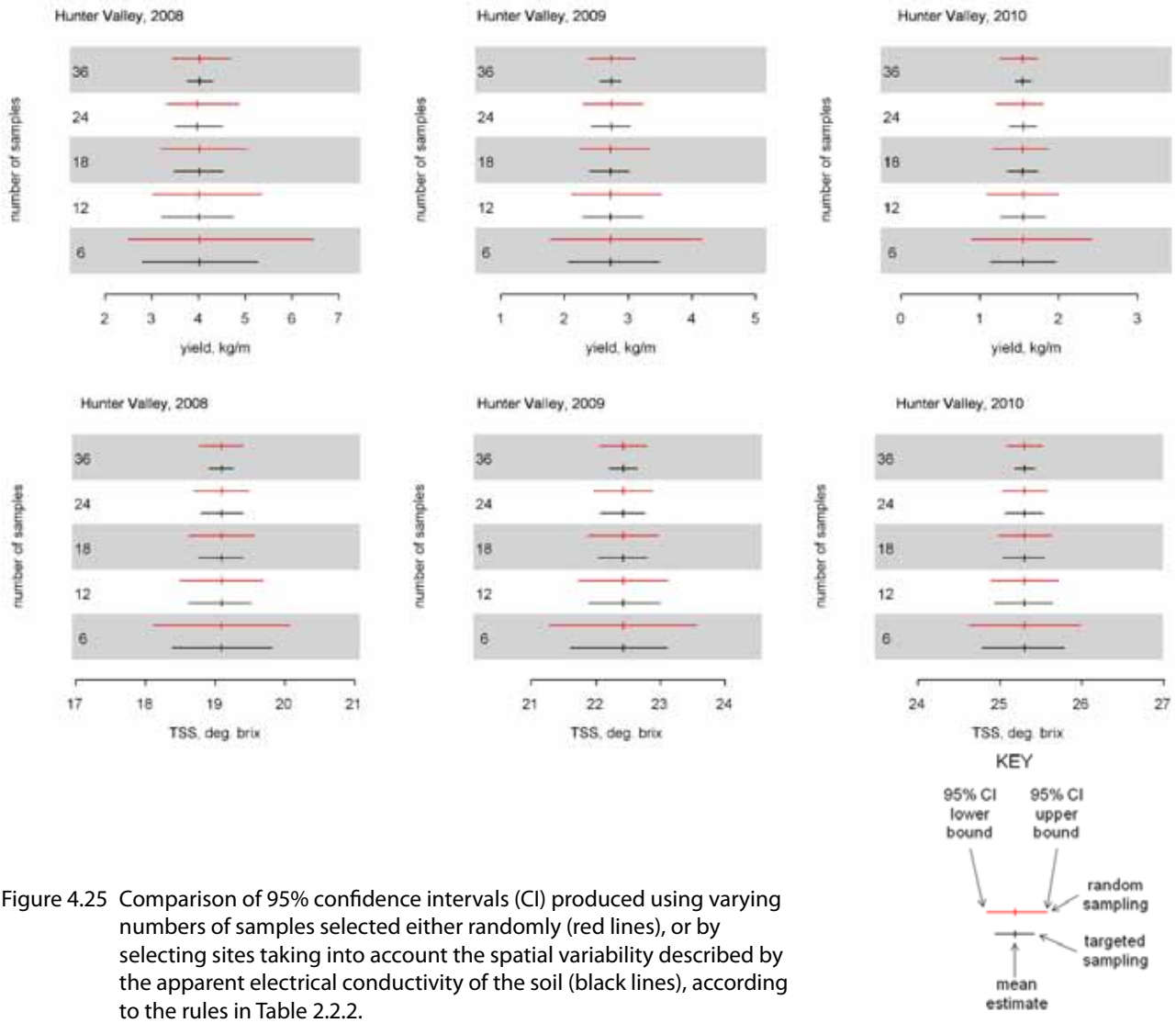


Figure 4.25 Comparison of 95% confidence intervals (CI) produced using varying numbers of samples selected either randomly (red lines), or by selecting sites taking into account the spatial variability described by the apparent electrical conductivity of the soil (black lines), according to the rules in Table 2.2.2.

Of all the vegetation indices investigated, the TVI produced canopy descriptors that had the greatest count of significant correlations with harvested fruit yield and composition variables. Analysis of temporal variability in correlation strengths therefore proceeded using the canopy descriptors derived from TVI only. Correlation coefficients between all three years' grape harvest data and the TVI canopy descriptors were produced and are presented in a series of charts (one chart for each viticultural variable) in *Figure 4.26* for the Riverina vineyard and *Figure 4.27* for the Hunter Valley vineyard. The x-axes on the charts are accumulated growing degree days (GDD), which were considered superior indicators of phenological progress through each growing season than a simple count of days after budbreak. The 1-tail significance level at $\alpha = 0.05$ is presented on the charts as solid horizontal lines. Vines with larger canopies were expected to produce greater yields and related yield components (bunch counts, berry weights and berries/bunch). Vines with smaller canopies were expected to produce fruit with higher colour and total phenolic levels (Lamb *et al.* 2004). Relationships between canopy and TSS, pH and TA are more complicated because of an interaction with yield. A lack of balance between photosynthetic capacity and yield may lead to positive or negative correlations depending upon whether canopies tend towards having greater photosynthetic capacity with lower yields, leading to positive correlations between berry sugar accumulation and canopy vigour, or lower photosynthetic capacity with greater yields, leading to positive correlations between berry sugar accumulation and canopy vigour (Intrieri *et al.* 1997). Furthermore, high yields can result in delayed maturation, resulting in spatial variability in berry sugar levels at harvest that is dependent upon crop load (Holzapfel *et al.* 2006). For TSS, pH and TA, both positive and negative significant correlation lines have therefore been included on the charts.

The NDVI values of the pixels from the original vineyard imagery acquired closest to veraison are presented as density plots in Figure 4.28. The bimodal distributions are typical of VI vineyard imagery, with the first peak representing the inter-row space, which in these vineyards was regularly-mowed grass. The Riverina vineyard histograms' thin and tall second peaks across all years indicate very dense grapevine canopies with the centre of the peak having an NDVI value above 0.8. *Figure 4.29* compares the relationships between the canopy descriptors of all grapevines derived using the various VIs. As NDVI derived canopy descriptor values increase, the rate of increase in EVI and TVI derived canopy descriptors becomes greater. The EVI and TVI were therefore more suited to describing grapevine canopy vegetation density because these indices were more sensitive to quantifying relative differences in dense vegetation.

Comparison of vegetation indices' utility to estimate fruit composition and yield

Of all the VIs employed, canopy descriptors derived from the TVI had the highest combined total counts of significant correlations between canopy density and fruit composition and yield (209 at α=0.05, *Table 4.26*). The commonly used NDVI was little different at the $\alpha = 0.05$ significance level (182, *Table 4.25*), but TVI had more than 50% more correlations significant at the α=0.001 level (64 cf. 40, *Table 4.26*) indicating a potentially superior ability to more accurately forecast spatial patterns of vineyard fruit quality and yield. The differences between the indices were most apparent at the Riverina vineyard, where both the TVI and the EVI produced more significant correlations than the NDVI, with the relative differences between the counts increasing as the level of significance increased (*Table 4.26*).

At high vegetation densities, NDVI saturation resulted in little variability in NDVI values of the grapevine canopy pixels (evidenced by the narrow right-hand peaks in *Figure 4.30d, e and f*). Thus with the NDVI, only a small range of values for grapevine canopy convey little information about relative differences in vegetation density. A greater influence on descriptor variability resulted from changes in canopy size or the density of the inter-row vegetation. The EVI, on the other hand, has been demonstrated to be more sensitive to relative differences in dense vegetation (Huete *et al.* 2002). Therefore, information about differences in dense grapevine canopy was more likely to be included in canopy descriptors derived using this index. Canopy descriptors derived from TVI had the greatest number of significant correlations with fruit quality and yield, with a particularly high number at the vineyard with the more vigorous canopy (Riverina, 128 cf. the average count of 102, *Table 4.26*). Like EVI, TVI appeared to better differentiate between very dense vegetation than the other indices.

Canopy descriptors derived using VARI were included in this study to examine the utility of imagery that does not include a near-infrared reflectance band. Despite strong correlations with the other VIs,

Table 4.25 Count of significant correlations of each canopy descriptor with fruit composition and yield descriptors (total yield, bunch count, mean bunch weight, berries per bunch, mean berry weight, total soluble solids, colour, total phenolics, pH and titratable acidity) collected at harvest from 54 sample vines at each site across all three years of the study. When the data sets from both sites are combined, TVI achieves the most correlations with fruit quality and yield descriptors at all levels of significance.

	Hunter Valley vineyard			Riverina vineyard			Both vineyards combined		
	α=0.05	α=0.01	α=0.001	α=0.05	α=0.01	α=0.001	α=0.05	α=0.01	α=0.001
Abundance	86	44	13	93	51	16	179	95	29
EVI	79	38	16	117	80	39	196	118	55
NDVI	75	35	12	107	6	28	182	101	40
Size	69	34	6	97	47	18	166	81	24
SR	72	35	9	107	63	21	179	9	30
TVI	81	45	17	128	85	47	209	130	64
VARI	59	28	13	65	41	18	124	69	31
Total	521	259	86	714	433	187	1235	692	273

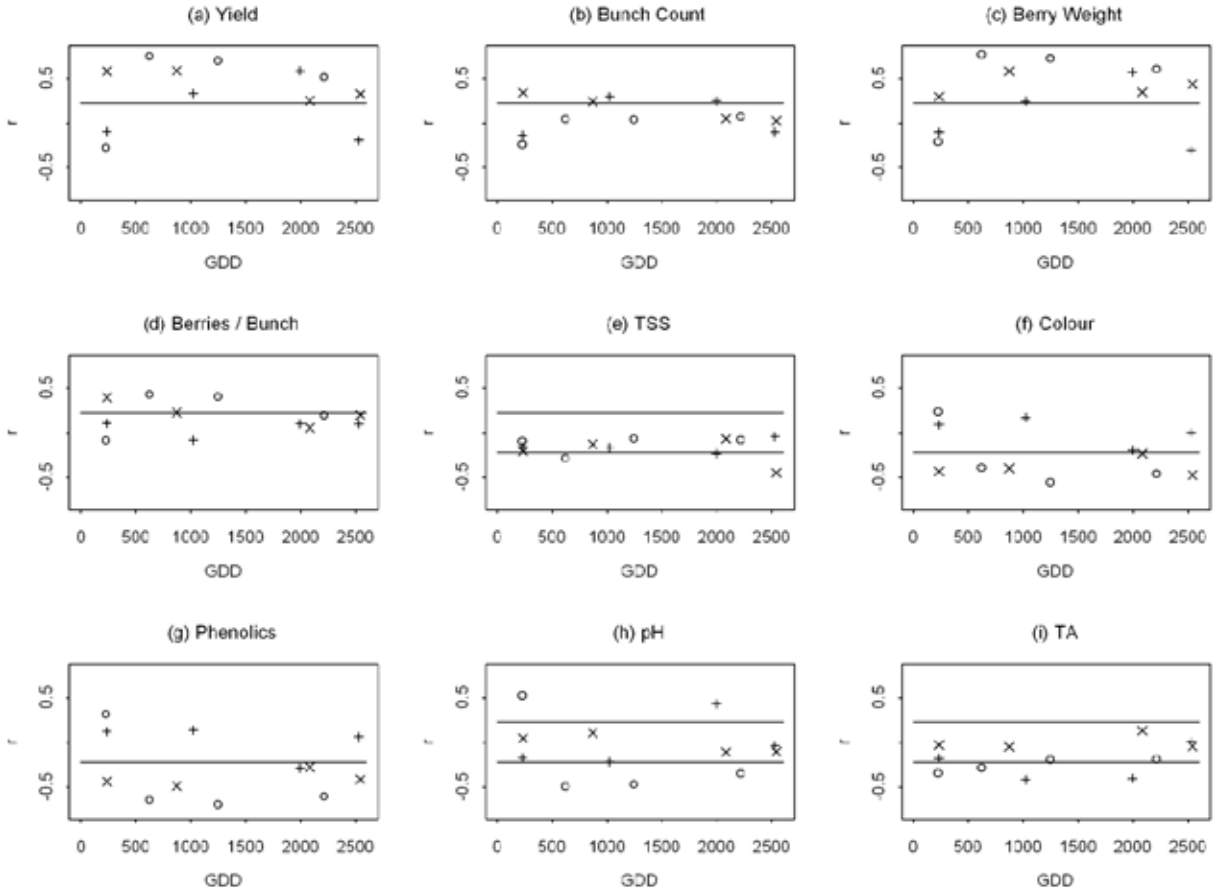


Figure 4.26 Correlation coefficients between canopy described by the triangular vegetation index (TVI) for 54 sample sites in the Riverina vineyard and (a) yield, (b) bunch count, (c) berry weight, (d) berries/bunch, (e) total soluble solids (TSS), (f) anthocyanins (colour), (g) total phenolics, (h) pH, (i) titratable acidity (TA) plotted against accumulated growing degree days (GDD) since budbreak. Symbol type indicates year in which imagery and harvested fruit data described by the point were collected: + year 1; o year 2; × year 3. The horizontal line at r=±0.225 indicates a significant 1-tail correlation at α=0.05.

Table 4.26 Summary of sampled yield data (kg m^{-1}).

	Riverina vineyard			Hunter Valley vineyard		
	Year 1	Year 2	Year 3	Year 1	Year 2	Year 3
Mean	6.4	5.1	7.3	4.9	2.7	1.5
Standard Deviation	1.2	1.7	1.6	1.6	1.0	0.54
Coefficient of Variation	0.19	0.33	0.22	0.33	0.37	0.36
Maximum	9.0	11.2	10.6	7.9	5.7	2.5
Minimum	2.4	2.7	3.1	2.0	0.83	0.17

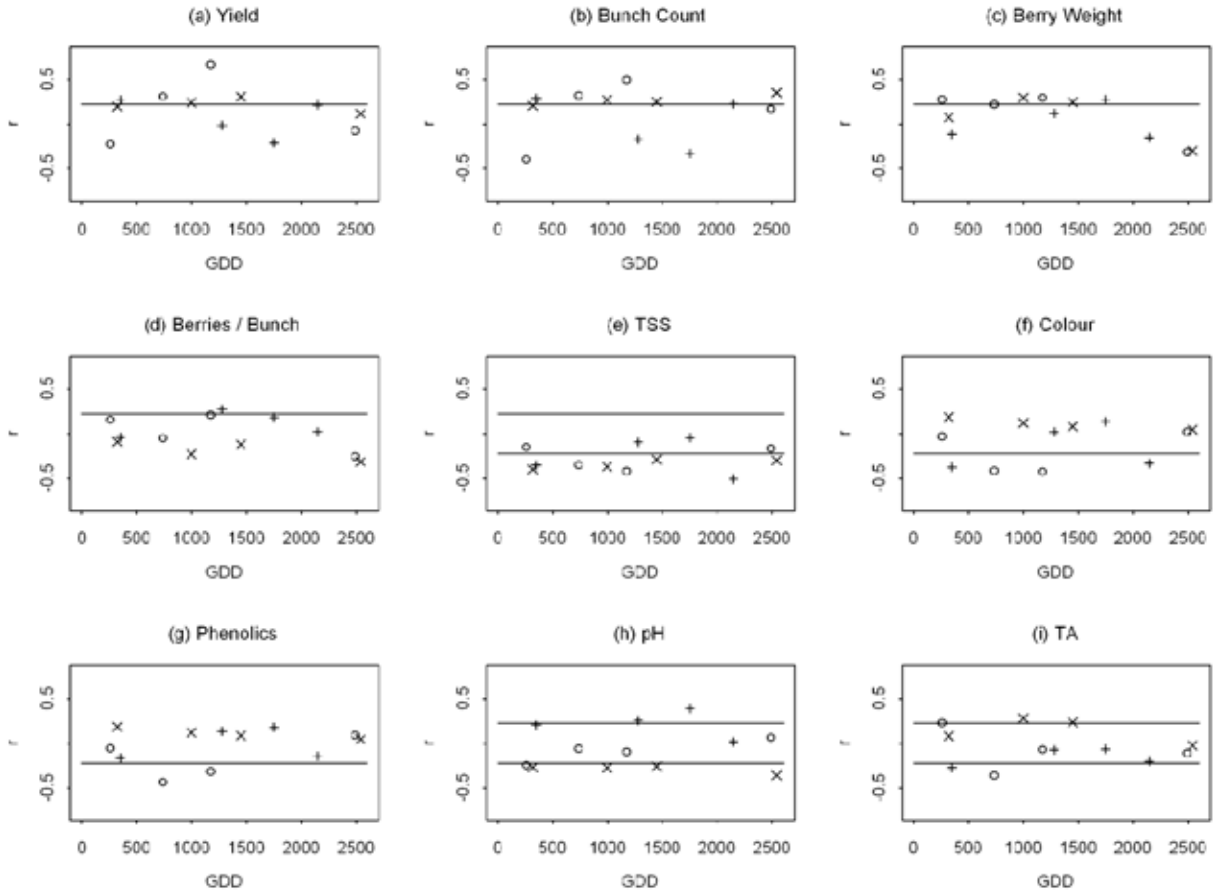


Figure 4.27 Correlation coefficients between canopy described by the triangular vegetation index (TVI) for 54 sample sites in the Hunter Valley vineyard and (a) yield, (b) bunch count, (c) berry weight, (d) berries/bunch, (e) total soluble solids (TSS), (f) anthocyanins (colour), (g) total phenolics, (h) pH, (i) titratable acidity (TA) plotted against accumulated growing degree days (GDD) since budbreak. Symbol type indicates year in which imagery and harvested fruit data described by the point were collected: + year 1; o year 2; × year 3. The horizontal lines at r=±0.225 indicates significant 1-tail correlations at α=0.05.

this VI was the poorest predictor of yield and fruit quality of the sample vines. The VARI, nevertheless, produced canopy descriptors that correlated with fruit yield and quality variables 59 times at the Hunter Valley vineyard and 65 times at the Riverina vineyard (at α=0.05), and it was demonstrated therefore to be useful in predicting patterns of fruit yield and quality using visible wavebands only. The Size vine object descriptor also had relatively fewer significant correlations with fruit quality and yield (166 across both sites at α=0.05, *Table 4.26*). Canopy descriptors derived from Size exhibited the greatest degree of scatter when plotted against the other VIs. Because Size is a simple count of pixels above a threshold NDVI, the canopy descriptors derived from this measure did not contain detailed information on canopy vigour. This loss of information was enough to make Size less suitable for predicting patterns of vineyard fruit quality and yield than the other VIs.

Both the NDVI and SR derived canopy descriptors had more significant correlations with fruit quality and yield than either Size or VARI (182 and 179 cf. 166 and 124, respectively at α=0.05, *Table 4.26*).

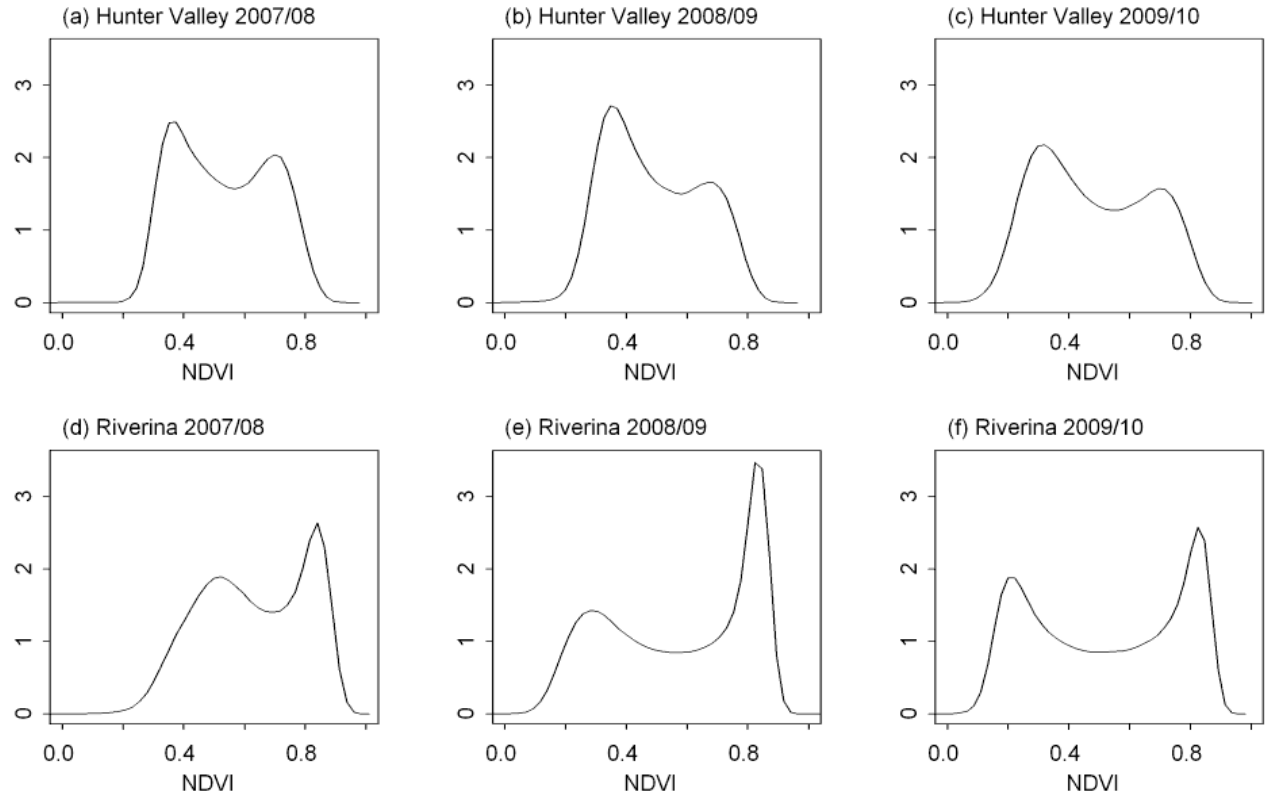


Figure 4.28 Density plots of pixel NDVI values from vineyard imagery acquired closest to veraison at the spur-pruned Hunter Valley vineyard in (a) the 2007-08, (b) the 2008-09 and (c) the 2009-10 seasons, and at the machine-pruned Riverina vineyard in (d) the 2007-08, (e) the 2008-09 and (f) the 2009-10 seasons.

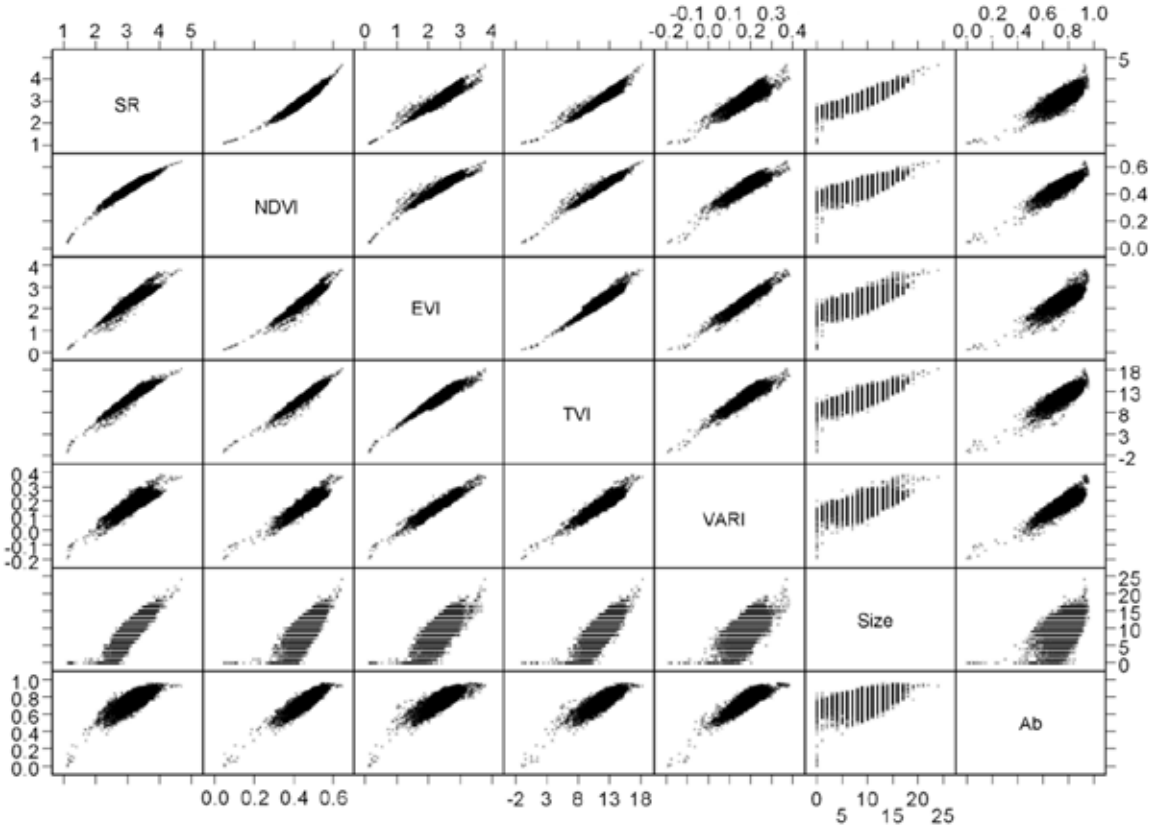


Figure 4.29 Scatter plot matrix of all vine canopy descriptor sets derived from each of the VIs for a single vineyard close to veraison (Riverina, 02/12/2009). The canopy descriptors derived using all VIs are compared for a single image (Riverina vineyard near veraison, 02/12/09) in a scatter plot matrix. The scatter patterns are similar to those produced for the other images.

More information about the density of the vegetation is conveyed by NDVI and SR (compared to Size and VARI) by the inclusion of the NIR band and information of relative vigour levels of all pixels representing each vine unit. Despite SR having greater sensitivity to denser vegetation evident in *Figure 4.29*, there was little difference between them in terms of their predictive power for precision viticulture practice with similar totals at both sites at each significance level (*Table 4.26*).

Canopy descriptors derived from the Abundance measure (Homayouni *et al.* 2008) had similar counts of significant correlations with fruit yield and quality combined over both vineyards to NDVI and SR (*Table 4.26*). Abundance derived canopy descriptors produced the greatest number of significant correlations with fruit quality and yield at the Hunter Valley vineyard at α=0.05 (86 cf. the average count of 74, *Table 4.26*), but had a relatively low count at the Riverina vineyard (93 cf. the average count of 102, *Table 4.26*). The relative difference between the two vineyard sites suggests Abundance may be a superior predictor of vineyard fruit quality and yield spatial variability in vineyards with relatively lower levels of vigour. Overall lower levels of canopy vigour were recorded at the spur-pruned Hunter Valley vineyard than at the machine-pruned Riverina vineyard (*Figure 4.28*).

Differences in correlation strength for different fruit quality and yield attributes

The strongest relationship with canopy vigour, as described by descriptors derived from TVI, was overall yield at the Riverina vineyard. Except for imagery acquired before flowering and after harvest, significant positive correlations between canopy vigour and yield were recorded at each instance (*Figure 4.26a*). The level of correlation was consistently lower at the Hunter Valley spur-pruned vineyard (*Figure 4.27a*). The five significant (positive) correlations at the Hunter Valley vineyard occurred at a similar phenological stage to the strongest correlations achieved at the Riverina vineyard, i.e. from 300 to 1500 growing degree days. The yield component at the Riverina vineyard that correlated most strongly with canopy vigour was berry weight (*Figure 4.26c cf. b and d*). The temporal pattern of correlation level between canopy vigour and yield and between canopy vigour and berry weight was similar (*Figure 4.26a and c*). Berry weight was therefore the main contributing yield component factor co-varying with canopy vigour. It may be concluded that level of canopy vigour in the Riverina vineyard determined berry weight, possibly because greater photosynthetic capacity from the larger canopy allowed for more cell division during berry growth. Bunch count and berries per bunch are largely determined in the preceding season (Watt *et al.* 2008; Dunn and Martin 2007) and so are less likely to be correlated with the harvest-season canopy vigour.

The yield components that most explained the overall yield correlation with canopy at the Hunter Valley vineyard were not clear. Both bunch count and berry weight had some weak significant correlations with canopy vigour but not berries per bunch (*Figure 4.27b, c and d*). Inconsistent and relatively weak correlations between canopy vigour and yield at the Hunter Valley vineyard, due to overall smaller canopy sizes and the consequent effect on accuracy of canopy vigour measures, did not enable identification of potential causes of individual fruit yield and quality relationships with grapevine canopy.

Because colour and total phenolic measures of winegrape composition are often closely related, the pattern of temporally changing correlation strength was similar for both fruit attributes at each vineyard (*Figure 4.27f and g* and *Figure 4.26f and g*). Canopy vigour has a known effect on anthocyanin concentration within harvested red winegrapes, with fruit of high vigour vines containing lower anthocyanin concentrations (e.g. Cortell *et al.* 2007; Smart 1985), and a negative relationship between canopy vigour measurements derived from remotely sensed imagery and anthocyanin concentration of fruit has been demonstrated before in a Cabernet Sauvignon vineyard (Lamb *et al.* 2004). In the present study, the same negative relationship was consistent and strong at the Riverina vineyard. Exceptions to this consistency occurred in year 1 with an anomalous lack of correlation for the imagery collected at about 1000 GDD after budbreak, and lack of negative correlations early and late in the growing season. Anthocyanin accumulation within winegrapes can be more complex than being simply related to sun exposure, with evidence suggesting anthocyanin synthesis is adversely affected by high temperatures and light exposure (Bindon *et al.* 2008). Relatively warmer temperatures and greater light exposure in the fruiting zone (due to the relatively smaller canopies that result from spur-pruning) may explain the lack of consistent significant correlation between anthocyanin content and canopy vigour in the Hunter Valley vineyard (*Figure 4.27f and g*).

In comparison to yield and other quality components, TSS, pH and TA each had relatively low levels of correlation with canopy vigour (*Figures 4.26* and *4.27*). Nevertheless, at the Hunter Valley vineyard, TSS was significantly negatively correlated with canopy with some consistency (*Figure 4.27e* cf. the Riverina vineyard, *Figure 4.26e*). Canopy vigour correlated particularly well with TSS in year 3, the year with the lowest overall yield of 1.5 kg m^{-1} (cf. years 1 and 2 at 4.9 and 2.7 kg m^{-1}, *Table 4.26*). In the relatively low yielding years (at the Riverina vineyard in year 2 and at the Hunter Valley vineyard in year 3, *Table 4.26*), fruit acidity also correlated with high canopy vigour (*Figure 4.27h*). A cause for the possible relationship between canopy vigour and TSS during low yielding years is unclear but may involve rates of ripening. In lower yielding years, fruit ripening may occur more rapidly because of greater photosynthetic capacity to yield ratios.

Within season temporal variability in correlation strengths

This study has extended the findings of Lamb *et al.* (2004) in the examination of the change in strength of correlations between canopy vigour and harvested fruit attributes as a consequence of the changing pattern of canopy vigour variability as grapevine phenology progresses. Lamb *et al.* (2004) investigated imagery taken at times when grapevine canopy was relatively dense at single vineyards over two years only. In the present study, early-stage canopy development (before anthesis) and post-harvest canopy condition (after onset of senescence) were additionally imaged and the study spanned two vineyards and three years. By aggregating all correlation coefficients into single charts plotted against GDD, a picture of the timing of image acquisition for the greatest level of correlation with winegrape fruit composition and yield was revealed (*Figure 4.30*). The fitted lines that describe correlation magnitude variation over time in these charts peak at similar stages: after 64% of season heat accumulation between budbreak and harvest at the Riverina vineyard and after 68% at the Hunter Valley vineyard. Regardless of the differences between the vineyards, including the much lower level of correlation at the Hunter Valley vineyard, a common peak in correlations strengths in terms of GDD accumulation was observed. The timing of the peak corresponded with veraison, the time at which the fruit begins to colour and soften and most canopy growth ends. After harvest and onset of leaf senescence, the correlation magnitudes fell away, suggesting that any spatial difference in rates of senescence and leaf fall had no relationship with within-season fruit quality and yield. Similarly, early-season canopy vigour imagery, which may act as an early indicator of spatial variability in rates of phenological development, was less likely to correlate with fruit yield and quality than imagery acquired when canopy was fully developed.

Section 2b

Table 4.27 presents correlation coefficients calculated for the relationships between the canopy indices and grape yield across both years. Significant correlations existed across both years, typically changing from negative early in the season to positive later in the season. Canopy information derived from imagery acquired after mid-season canopy

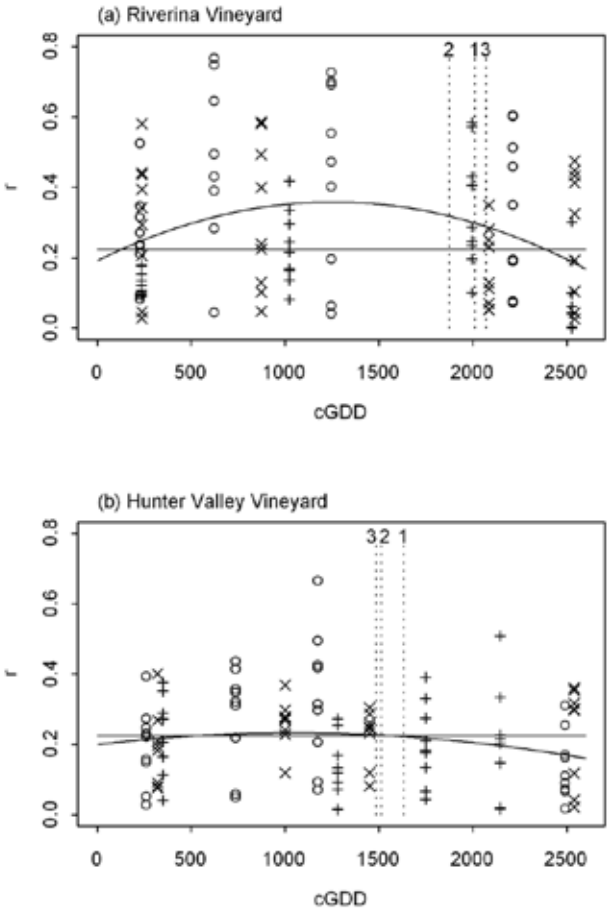


Figure 4.30 Correlation coefficient magnitudes describing relationships between TVI derived canopy descriptors and each of the fruit quality and yield descriptors plotted against accumulated GDD at time of image acquisition. Points plotted above the horizontal lines indicate significant correlations at α = 0.05. The vertical dashed lines indicate harvest times in each of the three study years. The curvilinear line is a least-squares derived second-order polynomial model of correlation strength vs. GDD, using all combined data.

Table 4.27 Correlation coefficients between grapevine canopy descriptors and yield. Formatting indicates significance level: |r| < 0.23, p > 0.05; 0.23 <|r| < 0.32, 0.01 < p < 0.05; **|r| > 0.32, p < 0.01**.

	Year 1			Year 2					
	Flowering	Veraison	Maturity	Post-budbreak	Flowering	Post-flowering	Veraison	Post-veraison	Maturity
CD, Yield Year 1	-0.24	**0.33**	0.26	0.12	-0.28	-0.13	**0.55**	0.26	**0.34**
CD, Yield Year 2	**-0.67**	**0.38**	**0.60**	**-0.36**	**-0.52**	**-0.37**	**0.46**	-0.06	-0.03
CA, Yield Year 1	**0.32**	**0.37**	**0.39**	-0.29	0.10	0.37	0.38	0.23	0.28
CA, Yield Year 2	-0.29	0.25	**0.46**	**-0.69**	**-0.33**	0.20	**0.58**	0.20	0.18

Table 4.28 Correlation coefficients between plant growth rate indices and yield. Formatting indicates significance level: |r| < 0.23, p > 0.05; 0.23 <|r| < 0.32, 0.01 < p < 0.05; **|r| > 0.32, p < 0.01**.

	Year 1		Year 2				
	Flowering to veraison	Veraison to maturity	Post-budbreak to flowering	Flowering to post-flowering	Post-flowering to veraison	Veraison to post-veraison	Post-veraison to maturity
CDC, Yield Year 1	**0.41**	0.31	-0.29	0.16	**0.54**	**0.40**	-0.19
CDC, Yield Year 2	**0.73**	**0.76**	0.01	0.19	**0.56**	**0.57**	-0.04
CAC, Yield Year 1	-0.14	0.20	**0.45**	0.19	0.01	0.03	-0.25
CAC, Yield Year 2	**0.47**	**0.55**	**0.48**	**0.56**	**0.36**	0.24	-0.08

trimming (post-veraison and maturity in year 2) was less consistently significantly correlated with yield, having no significant relationship between either canopy density or canopy area with year 2 yield.

Table 4.28 presents correlation coefficients similar to *Table 4.27*, but calculated for the relationships between the canopy change indices (CAC and CDC). The strengths of the relationships of the canopy change indices with yield were stronger at different times of the season for each different canopy change index. CAC had strong relationships with yield at veraison to maturity and post-budbreak to flowering, whereas CDC had strong relationships with yield for both change periods in year 1 and between post-flowering and veraison in year 2.

Tables 4.29 and *4.30* present truncated results of the best sub-sets regression analyses (the 25 models produced with the greatest adjusted-R^2) using canopy density descriptors and canopy area descriptors respectively. As well as using each set of canopy descriptors in the modelling, yield in year 1 was included as a predictor variable in both variable sets. The correlation coefficient between yield in year 1 and yield in year 2 was 0.49, indicating its potential value as a predictor variable within the models.

There were clear temporal differences in the significant correlations with yield depending on whether the canopy area (CA) descriptors or the canopy density (CD) descriptors were used as the predictors (*Table 4.27*). Overall, there was no clear advantage to using either canopy density or canopy area descriptors in forecasting yield with the number of significant correlations using either CA or CD being similar. Due to the clear pattern of significant and non-significant relationships with yield, the two descriptors may have quantified significantly different characteristics of the grapevine canopies with respect to their relationships with yield.

Rate of canopy growth in year 1 (as described by CDC and CAC for both flowering to veraison and veraison to maturity) was strongly related to yield in year 2 (*Table 4.28*). The canopy density descriptor, rather than the canopy area descriptor, produced the greatest magnitude correlation coefficients of the study (0.73 and 0.76 for flowering to veraison and veraison to maturity, respectively). The rate of foliage growth up to the time at which the first set of images was acquired in either season is described by CD or CA derived from the imagery taken at that point in time. Because there is no canopy vegetation at the start of the season, the rate of change in canopy is directly proportional to the actual canopy foliage at the time. Therefore, the first CD or CA dataset collected in a season is equivalent to CDC or CAC. Correlation coefficients with yield in year 2 for CD and CA at flowering in year 1 were −0.67 and −0.29 respectively (again being stronger in the case of the canopy density descriptor). The rate of canopy growth can be summarised, therefore, as reversing at the stage of average time of anthesis in the vineyard.

A similar pattern of negative followed by positive correlations with yield data collected at the end of

each season is also apparent, although it is not clear at the end of year 2 because of the confounding effect of the mid-season trimming after the veraison imaging mission. Those grapevines in the vineyard that produced fast growing shoots early in the season reached canopy maturity early and any canopy increase subsequently slowed, with the vines finishing the season with relatively smaller canopies (compared to the whole vineyard block) at seasons-end and yielding relatively low fruit weights at harvest. Those grapevines that experienced relatively slower growth rates at the beginning of the season developed canopy throughout the year at a faster rate after anthesis than those grapevines that experienced faster growth at the beginning of the season, becoming the vines with the larger canopies at seasons-end and yielding relatively higher fruit weight at harvest. *Figure 4.31* illustrates the different patterns of canopy growth rates hypothesised to have been experienced in the vineyard. See Hall *et al.* (2008a) for further discussion and implications for explaining the environmental

Table 4.29 Variables (canopy density descriptors) included in models (inclusion indicated by shading), model equations, and coefficients of correlation between the model variables (where *v1* refers to left-most variable, *v2* to middle variable and *v3* to right-most variable as displayed in the respective row of this table) of the 25 models with highest adjusted-R^2 values from best subsets regression analysis. NA signifies less than 3 variables from which to obtain correlations.

Order	Adjusted-R^2	Canopy density variables included in model													Equation	Coefficients of correlation between model variables		
		F1	V1	M1	pB2	F2	pF2	V2	FV1	VM1	pBF2	FpF2	pFV2	yield1		cor(v1,v2)	cor(v1,v3)	cor(v2,v3)
1	0.693				■					■					yield2 = - 50.7pB2 - 56.0VM1 + 0.5yield1 + 103.5	0.28	0.14	-0.27
2	0.689								■	■				■	yield2 = 0.3yield1 - 45.6VM1 - 41.6FV1 + 99.4	0.67	-0.38	-0.27
3	0.679					■				■					yield2 = - 56.0F2 - 50.9FV1 - 38.3VM1 + 150.6	0.31	0.41	0.67
4	0.665									■				■	yield2 = 0.4yield1 - 57.4VM1 - 48.2F2 + 109.2	0.41	-0.25	-0.27
5	0.663	■		■										■	yield2 = - 115.5F1 + 64.8M1 + 0.4yield1 + 52.5	-0.35	-0.23	0.22
6	0.660	■								■				■	yield2 = - 57.2F1 + 0.4yield1 - 46.2VM1 + 103.8	0.77	-0.23	-0.27
7	0.657			■						■				■	yield2 = 0.4yield1 - 89.7VM1 - 58.7M1 + 148.4	-0.87	0.22	-0.87
8	0.656					■			■						yield2 = - 68.5FV1 - 67.4F2 + 53.3M1 + 96.2	-0.28	-0.43	0.31
9	0.655						■			■				■	yield2 = - 45.2pF2 - 60.3VM1 + 0.4yield1 + 108.4	0.29	-0.11	-0.27
10	0.654		■							■				■	yield2 = 0.4yield1 + 36.3V1 - 62.7VM1 + 45.1	-0.19	0.30	-0.27
11	0.654				■				■	■				■	yield2 = - 27.7pB2 - 50.7FV1 - 43.6VM1 + 128.9	0.26	0.28	0.67
12	0.648									■	■			■	yield2 = - 19.4pBF2 + 0.5yield1 - 63.3VM1 + 91.0	0.00	-0.27	0.30
13	0.646								■	■		■			yield2 = - 54.7FV1 - 43.9VM1 - 19.2FpF2 + 132.8	0.67	0.02	0.15
14	0.644						■		■	■					yield2 = - 45.2VM1 - 49.5FV1 - 29.6pF2 + 133.4	0.34	0.29	0.67
15	0.644		■			■				■					yield2 = 56.9V1 - 63.9F2 - 58.0VM1 + 79.9	-0.03	-0.19	0.41
16	0.643								■	■					yield2 = - 46.3VM1 - 52.9FV1 + 113.6	0.67	NA	NA
17	0.643									■			■	■	yield2 = - 60.6VM1 - 13.1pFV2 + 0.3yield1 + 84.7	0.44	-0.27	-0.51
18	0.641									■				■	yield2 = 0.4yield1 - 64.3VM1 + 75.4	-0.27	NA	NA
19	0.641		■	■					■						yield2 = - 77.9V1 - 107.0FV1 + 59.5M1 + 136.5	0.26	-0.71	-0.43
20	0.640								■	■			■		yield2 = - 9.6pFV2 - 46.3VM1 - 45.5FV1 + 115.4	0.67	0.66	0.44
21	0.638	■		■					■						yield2 = - 71.9F1 + 59.5M1 - 48.5FV1 + 73.1	-0.35	0.72	-0.43
22	0.638								■					■	yield2 = 59.8M1 - 66.2FV1 + 0.3yield1 + 30.0	-0.43	0.22	-0.38
23	0.638		■						■	■					yield2 = - 21.1V1 - 64.7FV1 - 42.0VM1 + 138.3	-0.71	-0.19	0.67
24	0.637	■							■	■					yield2 = - 17.2F1 - 42.6VM1 - 49.2FV1 + 120.2	0.72	0.77	0.67
25	0.637			■					■	■					yield2 = - 54.9VM1 - 16.5M1 - 49.8FV1 + 132.5	-0.43	-0.87	0.67

Table 4.30 Variables (canopy area descriptors) included in models (inclusion indicated by shading), model equations, and coefficients of correlation between the model variables (where *v1* refers to left-most variable, *v2* to middle variable and *v3* to right-most variable as displayed on the respective row of this table) of the 25 models with highest adjusted-R^2 values from best subsets regression analysis. NA signifies less than 3 variables from which to obtain correlations.

Order	Adjusted-R^2	Canopy area variables included in model													Equation	Coefficients of correlation between model variables		
		F1	V1	M1	pB2	F2	pF2	V2	FV1	VM1	pBF2	FpF2	pFV2	yield1		cor(v1,v2)	cor(v1,v3)	cor(v2,v3)
1	0.666				■			■						■	yield2 = - 1.9pB2 + 1.6V2 + 0.3yield1 + 6.5	-0.10	-0.22	0.33
2	0.656	■						■						■	yield2 = - 2.2F1 + 0.7yield1 + 1.8V2 + 2.8	0.19	0.33	0.33
3	0.650				■					■				■	yield2 = - 1.3pB2 - 9.0VM1 + 0.5yield1 + 23.1	0.50	-0.22	-0.14
4	0.645				■			■							yield2 = - 4.8VM1 + 1.5V2 - 1.7pB2 + 11.4	-0.10	0.50	-0.45
5	0.632	■		■										■	yield2 = - 2.3F1 + 1.3M1 + 0.7yield1 + 10.1	0.24	0.33	0.39
6	0.632	■			■			■							yield2 = - 0.6F1 + 2.0V2 - 1.8pB2 + 7.2	0.48	0.19	-0.10
7	0.631				■					■		■		■	yield2 = - 10.4VM1 - 12.8FpF2 + 0.5yield1 + 24.0	0.37	-0.14	-0.15
8	0.624					■				■				■	yield2 = 0.6yield1 - 11.1VM1 - 0.9F2 + 22.4	0.26	0.11	-0.14
9	0.624				■			■							yield2 = - 2.1pB2 + 1.9V2 + 6.6	-0.10	NA	NA
10	0.624		■					■							yield2 = 2.1V2 - 0.5V1 - 2.0pB2 + 9.2	0.02	0.59	-0.10
11	0.623				■			■	■						yield2 = - 1.9pB2 + 1.8V2 - 4.7FV1 + 8.5	-0.10	0.52	-0.14
12	0.622			■	■			■							yield2 = 1.6V2 - 2.0pB2 + 0.3M1 + 6.4	-0.21	0.69	-0.10
13	0.620				■	■		■							yield2 = - 1.9pB2 - 0.3F2 + 1.9V2 + 6.6	0.67	-0.10	0.17
14	0.620					■					■				yield2 = - 14.2pBF2 + 2.0V2 - 2.0F2 + 19.2	0.17	-0.32	-0.32
15	0.619				■			■							yield2 = - 2.2pB2 + 1.9V2 + 2.1pBF2 + 4.7	-0.10	0.48	-0.32
16	0.619				■			■				■			yield2 = - 2.8FpF2 + 1.8V2 - 1.9pB2 + 8.0	-0.10	0.64	-0.25
17	0.617				■		■						■		yield2 = - 2.1pB2 + 1.6pF2 - 14.3pFV2 + 23.7	0.17	0.26	0.55
18	0.616				■			■							yield2 = - 0.2pFV2 + 1.8V2 - 2.1pB2 + 7.0	-0.10	0.26	-0.46
19	0.616				■		■								yield2 = - 2.1pB2 - 0.0pF2 + 1.9V2 + 6.7	0.17	-0.10	0.49
20	0.611										■	■	■	■	yield2 = - 13.2pFV2 - 22.4FpF2 - 14.7pBF2 + 54.3	0.03	-0.15	-0.02
21	0.602								■	■	■			■	yield2 = - 14.5FV1 - 8.5VM1 + 0.7yield1 + 21.5	0.60	0.18	-0.14
22	0.599					■		■							yield2 = 0.5yield1 + 1.9V2 - 1.6F2 + 0.8	0.17	0.11	0.33
23	0.598				■				■						yield2 = - 1.2pB2 - 16.4FV1 + 0.6yield1 + 24.8	0.52	-0.22	0.18
24	0.594	■								■					yield2 = - 1.1F1 + 0.7yield1 - 9.7VM1 + 20.4	0.47	0.33	-0.14
25	0.594			■	■									■	yield2 = 0.8M1 - 1.8pB2 + 0.3yield1 + 13.6	-0.21	0.39	-0.22

basis of precision viticulture scale spatial variation in grape yield and composition.

With correlation coefficients for many of the relationships between yield and the canopy descriptors being significant, the canopy descriptors may be valuable in forecasting future grape yield. Using a single canopy descriptor that best correlated with yield in year 2 from all descriptors produced over the lead up two seasons, 58% of the variability in yield can be explained (r=0.76 for CDC from veraison to maturity in year 1, equivalent to R^2=0.58). Because the canopy descriptor sets do not all correlate with each other, extra information that could further indicate yield may be present in canopy descriptors acquired on different occasions. The best subsets regression analyses using all possible sets of 1 to 3 canopy descriptors (for either CA or CD) do produce models that explain significantly greater levels of variability (69%) in year 2 yield than using one canopy descriptor from one time alone (58%). The predictor variables of the model of yield in year 2 with the highest adjusted-R^2 were the rate of increase in CD between veraison and maturity in year 1 (r=0.76), CD at post-budbreak in year 2 (r=−0.36) and yield in year 1 (r=0.49).

Section 3a

The distributions of each of Australia's wine regions' median index values, as they relate to the different categories of climate suitability, are presented in *Table 4.12*. The distribution of wine region median GST index values closely conform to a normal distribution, with the greatest number of regions (28) in the middle *warm* category (17–19°C), a similar number are in the two adjacent *intermediate* and *hot* categories (14 and 16 regions, respectively), and a few GIs were categorised as either *cool* or *very hot* (2 and 3 regions, respectively). No GI had a median GST below 13°C or above 24°C. Similar normal shaped distributions were found for GDD, HI and BEDD. The distribution for median GDD (categories for which were originally developed for the relatively warm climate of California) was slightly positively skewed, whereas median HI (categories for which were originally developed for the relatively cooler climate of France) and median BEDD values were slightly negatively skewed.

The indices calculated for all the regions are compared against each other in *Figure 4.32*. The figure qualitatively illustrates the level of linearity of the relationships and the level of similarity between the different indices by the degree of scatter of the points. For example, *Figure 4.32* suggests GST and GDD are functionally very similar, evidenced by the straight line formed by the points and by the low level of scatter. Linear relationships between GST, GDD and HI are apparent from *Figure 4.32*, whereas a curvilinear relationship exists between BEDD and the other three indices. Models describing the relationships between the indices are presented in *Table 4.31*. First order polynomials were used to model the apparent linear relationships and second-order polynomials were used for the curvilinear relationships (i.e. those involving BEDD). Coefficients of determination (R^2) quantitatively describe the level of scatter of the points

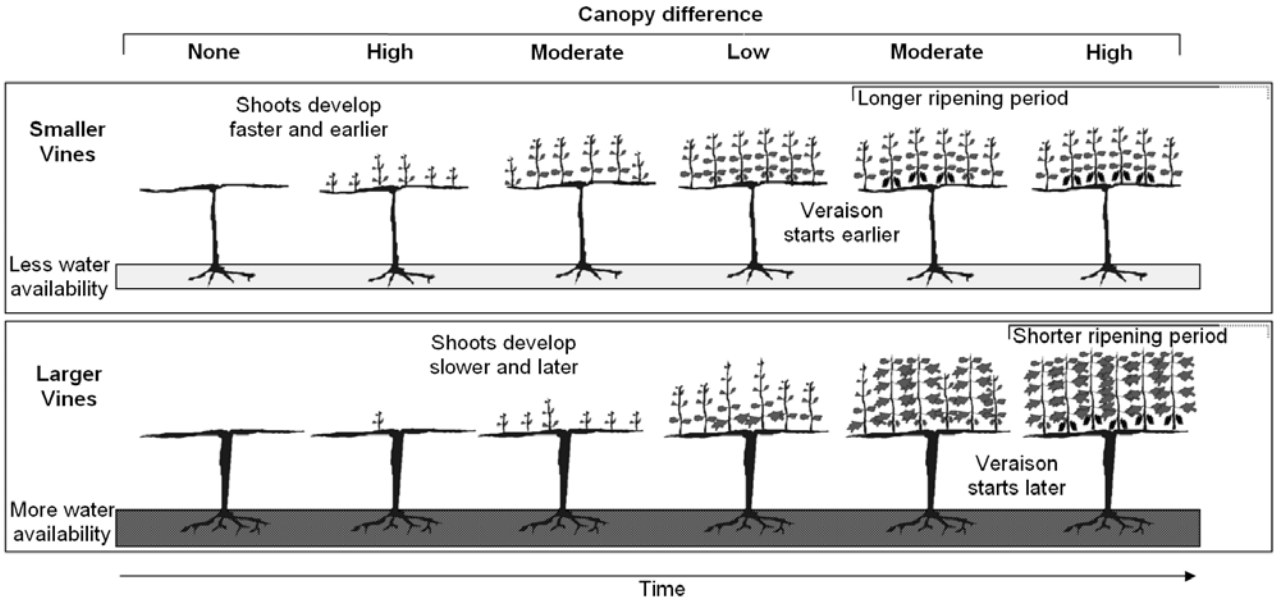


Figure 4.31 Schematic illustrating an hypothesis to explain levels of difference between canopy within a vineyard block caused by differences in average soil moisture. The greatest difference in canopy occurs early in the season and then late in the season (after Hall *et al*. 2008a).

around the model or how accurately the formulae describe the relationship between the two indices.

The greatest influences on differences in index values between GIs are latitude and continentality. Inland GIs are more likely to have greater index values than GIs proximal to the ocean at the same latitude. Although average temperatures are likely to be similar at coincident latitudes using data for whole years, the indices are calculated using temperature data from the summer months only. Summer temperatures deviate more from the annual average with increasing continentality. Daytime temperatures are also likely to be greater with increasing continentality. This increases the rate of change of HI with increasing continentality relative to the other indices, because HI uses an estimate of daytime temperature rather than average diurnal temperature. Latitude has the greatest influence on the indices between the regions. Lower latitudes experience warmer temperatures and consequently greater index magnitudes, leaving much of Australia deemed unsuitable for quality winegrape production based on these climate indices (*Figure 4.20*).

Historically, the seven (or six in the case of the Huglin Index) warmest months of the year have been used to assess suitability for winegrape growing. This provided the best indication of the lower suitability cut-off at the cool end of the climate scale (when using monthly mean temperature). Inclusion of months outside this range can result in a false unsuitable classification of some cool areas with continental climates where the summer months are significantly warmer than winter, early-spring and late-autumn months. In warm regions, however, budbreak often occurs well before 1 October and harvest can occur before February. The temporal extent of the actual growing season for such regions will therefore be quite different to the standard seven month period used to calculate GST. The temperature of the seven month period, nevertheless, can still be used as a guide to potential viticultural unsuitability due to excessive heat, because this figure will be directly related to the temperature of the actual growing season. Continuing use of the seven month period is, therefore, appropriate in guiding long-term suitability of a climate for winegrape production. Calculating indices from a single time period is a simple, consistent method that can be applied to any location,

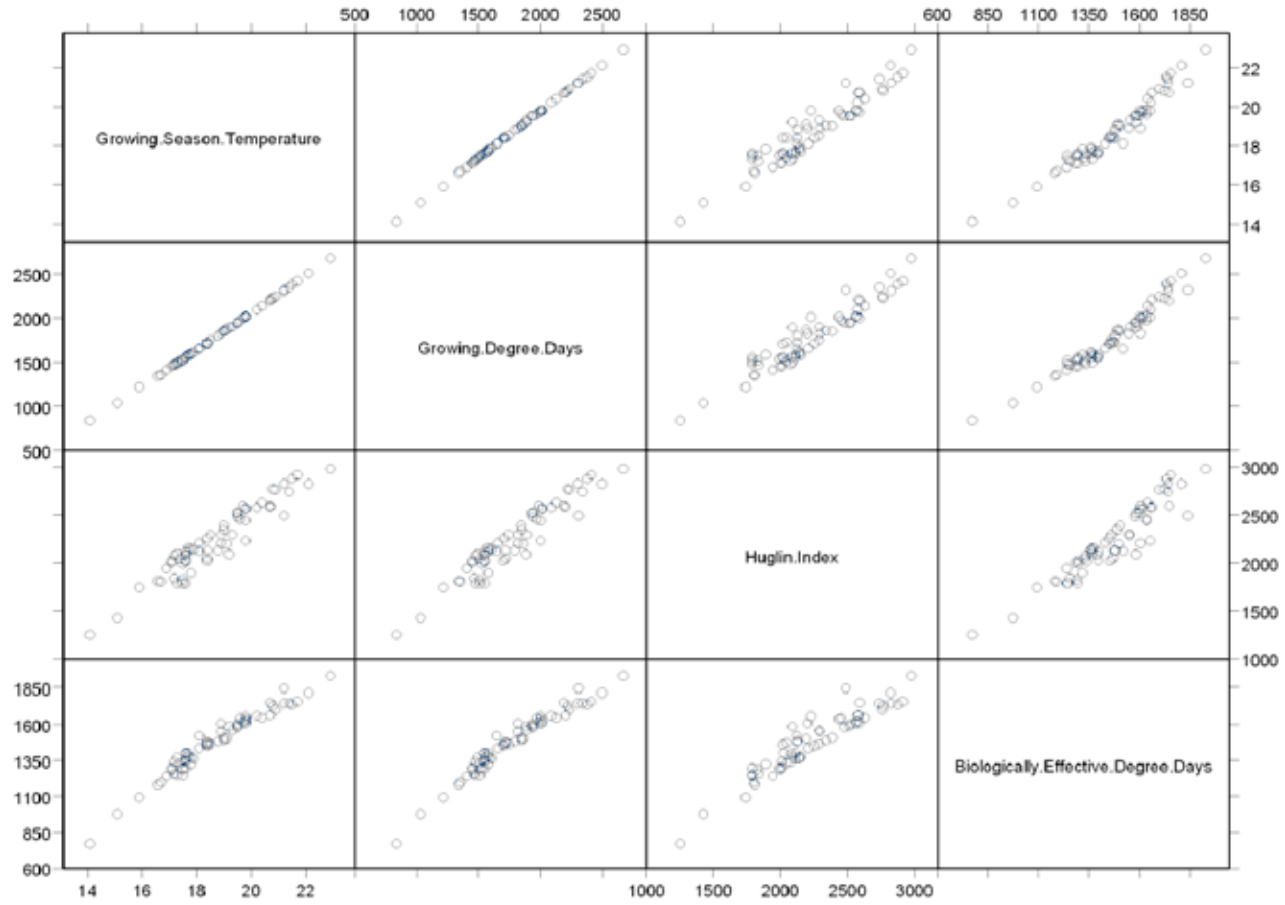


Figure 4.32 Scatter matrix illustrating relationships between GI medians of each of the four indices. Each plotted circle represents one GI.

Table 4.31 Order of polynomial, coefficient of determination (R^2), and formula for each model describing relationships between the different indices.

Function	Order	R^2	Formula
GST = f(*GDD*)	1	0.9995	$GST = 4.78\times10^{-3}GDD + 10.2$
GST = f(*HI*)	1	0.9059	$GST = 4.51\times10^{-3}HI + 8.61$
GST = f(*BEDD*)	2	0.9641	$GST = 2.93\times10^{-6}BEDD^2 - 5.42\times10^{-4}BEDD + 13.0$
GDD = f(*GST*)	1	0.9995	$GDD = 209GST - 2.13\times10^{3}$
GDD = f(*HI*)	1	0.9092	$GDD = 0.946HI - 332$
GDD = f(*BEDD*)	2	0.9476	$GDD = 6.63\times10^{-4}BEDD^2 - 0.255BEDD + 690$
HI = f(*GST*)	1	0.9059	$HI = 201GST - 1.52\times10^{3}$
HI = f(*GDD*)	1	0.9092	$HI = 0.961GDD + 522$
HI = f(*BEDD*)	2	0.8845	$HI = 2.82\times10^{-4}BEDD^2 + 0.782BEDD + 460$
BEDD = f(*GST*)	2	0.9691	$BEDD = -7.31GST^2 + 397GST - 3370$
BEDD = f(*GDD*)	2	0.9710	$BEDD = -1.83\times10^{-4}GDD^2 + 1.25GDD - 142$
BEDD = f(*HI*)	2	0.8981	$BEDD = -1.57\times10^{-4}HI^2 + 1.26HI - 532$

whereas determining climate suitability indices from different time periods (e.g. before October in warm regions) for different locations and varieties would be impractical and lead to incomparability.

Australia has no upper latitudinal limit to viable viticulture. Only Southern Tasmania has marginal conditions based on its median index values (median GST=14.1°C), although an upper GST of 15.6°C indicates Southern Tasmania has areas that fall within the intermediate GST category. Similarly, some of the warmest regions, such as South Burnett, Riverina and Hunter Valley with median GSTs of 22.9, 21.5 and 20.7°C, respectively, contain areas with significantly lower GSTs, indicated by minimum GSTs of 20.9, 19.7 and 13.4°C, respectively. These regions' combinations of large area and/or varied topography cause a high degree of absolute spatial variability in index values and therefore a wide range in cultivar suitability.

The large size of many of the GIs indicates there is scope for spatial variability within each region simply due to changes in latitude or continentality. The greatest effect on temperature variability within each GI is, however, topography. With a decrease in average temperature of 6.5°C km^{-1} of elevation (Donn 1975; Sturman and Tapper 1996) and an average elevation range of 603 m, mean temperature spatially varies by about 3.9°C on average within each of the GIs. The spatial variability within each GI is an important consideration when interpreting data in *Table 4.28*. The GIs with high median index values are likely to have their winegrape growing regions in areas that experience the lower temperatures, such as South Burnett, Riverina and Hunter Valley, thus a more accurate description of their temperature regimes may be described by an index closer to the first quartile. Conversely, GIs with low median index values are likely to have their vineyards sites in areas with relatively warmer temperatures, such as the higher latitude Tasmanian regions, or in regions that include large areas at high elevations, such as Alpine Valleys and Grampians. In such cases, the third quartile index may better describe the effective winegrape growing temperature regime.

The value of knowledge of the full spatial range of indices within a GI can be illustrated with data from three example climate stations. Cape Naturaliste was one of two climate stations with a >95% complete temperature data set in the Margaret River GI for the 1971–2000 period. The range of values for the total GDD produced by the BOM interpolated climate maps were 1702 to 2031 C days. Using the climate data from the Cape Naturaliste climate station produced a GDD of 1880 C days. Cape Naturaliste is located in the very northern-most part of the GI, which places it in a relatively warm location. In the range of GDD values for Margaret River, it is above the third quartile. As well as differences within GIs not being representative, differences between neighbouring GIs can sometimes only be revealed using interpolated data. Padthaway, Wrattonbully and Coonawarra are relatively small GIs that border one another. Only one climate station with >95% complete temperature data set for the 1971–2000 period is closest to all three

GIs. Located in the NW corner of Wrattonbully, the Naracoorte climate station produced a GDD total of 1591°C days. Any difference between the different GIs, which would be likely due to latitudinal variation, cannot be represented by a single station, yet the median GDD total for Padthaway, Wrattonbully and Coonawarra from the interpolated climate data were 1657, 1554 and 1511 C days, respectively. The third example is for the Yarra Valley GI, which contained no climate stations with a >95% record of temperature data for the 1971–2000 period. The Melbourne Airport climate station, which is located within the Sunbury GI, is likely to be the most representative of the Yarra Valley. Using this station to represent the Yarra Valley would not only lead to it being assigned the same GDD total as Sunbury, but also lead to information about the large range of GDDs from the interpolated data within the Yarra Valley not being conveyed. The varying topography of the Yarra Valley GI (with elevation range 251–1339 m asl) is the main contributing factor to the large range of GDD totals within its area (ranging from 623 to 1708°C-days).

The distribution of climate types according to Winkler's GDD classification is illustrated in *Figure 4.33* for nine selected GIs. The Yarra Valley GI crosses four categories, but its climate is predominantly best described as Region II, with 53% of its area falling within this category. For each of the other eight GIs, the spatial variability in climate spans at least two climate categories. The topographically varied Hunter Valley has the most spatially varied climate of the nine GIs spanning a total of five categories, but is mostly Region IV (33%) and Region V (46%), indicating that it is predominantly a warm to very warm GI. The Margaret River and Barossa Valley GIs, on the other hand, mostly fall into a single category (Region III, 84% and 67%, respectively), indicating these regions have relatively spatially homogeneous climates. *Figure 4.33* demonstrates the level of spatial variability in climate within different GIs can be significant, indicating single climate stations are likely to not fully represent the climate within a GI.

Although care is needed to select an appropriate value in the ranges of index values calculated for each GI to effectively compare temperature-regimes across regions, differences between GIs may be assessed using any of the indices. There are, however, subtle differences between the indices with the degree of difference varying. The GST and the GDD indices are very similar. The coefficient of determination of the first-order linear model that describes the relationship between these two indices is close to unity. There is effectively, therefore, no difference between the two indices except in terms of their magnitudes. The Winkler index (GDD) may be useful for determining stages of annual phenological development at time steps within a season, but, in terms of describing a region's growing season temperature, the GST is a simpler index with few methodological issues that produces a similar comparative result when considering the conditions over the whole season (Jones 2006; Jones *et al.* 2010).

The coefficients of determination for the models describing the relationships of HI with GST and GDD ($R^2 \approx 0.91$) indicate a functional difference. The HI differs to GST and GDD because it uses an estimate of the daytime temperature instead of mean diurnal temperature, includes a latitudinal day-length correction (*K*), and employs a slightly different period. The model that describes the relationship is again a first-order polynomial so there is a constant underlying rate of change in HI with respect to either GST or GDD. The GIs with the largest residuals (i.e. the greatest difference between the modelled index and the actual index), Hastings River, Kangaroo Island and Shoalhaven, particularly demonstrate the differences caused by using daytime temperatures in the calculation. These three GIs have the least difference between their daytime temperatures and average diurnal temperatures because their humid coastal climates reduce diurnal temperature ranges.

The BEDD index is the most different to the other three indices. A second-order polynomial best describes the relationship between the BEDD and each of the other indices. The rate of increase in BEDD decreases as the other index values increase. In simple terms, at warmer temperatures, the rate of increase in BEDD is less than that of the other indices. The greatest cause of difference between the BEDD and the other indices, which produces the curvilinear relationship with the other indices, is an adjustment for vine temperature response. Gladstones (1992) cites various sources to derive that grapevine growth rates reach a maximum at 23–25°C, and bases a temperature response curve for grapevine growth on this temperature range. The response curve is approximated for in the calculation of the BEDD by capping degree-day accumulation to a maximum of 9°C-days per day. Gladstones (1992) assumes "growth, as measured by plant weight, and rate of phenological development respond to temperature

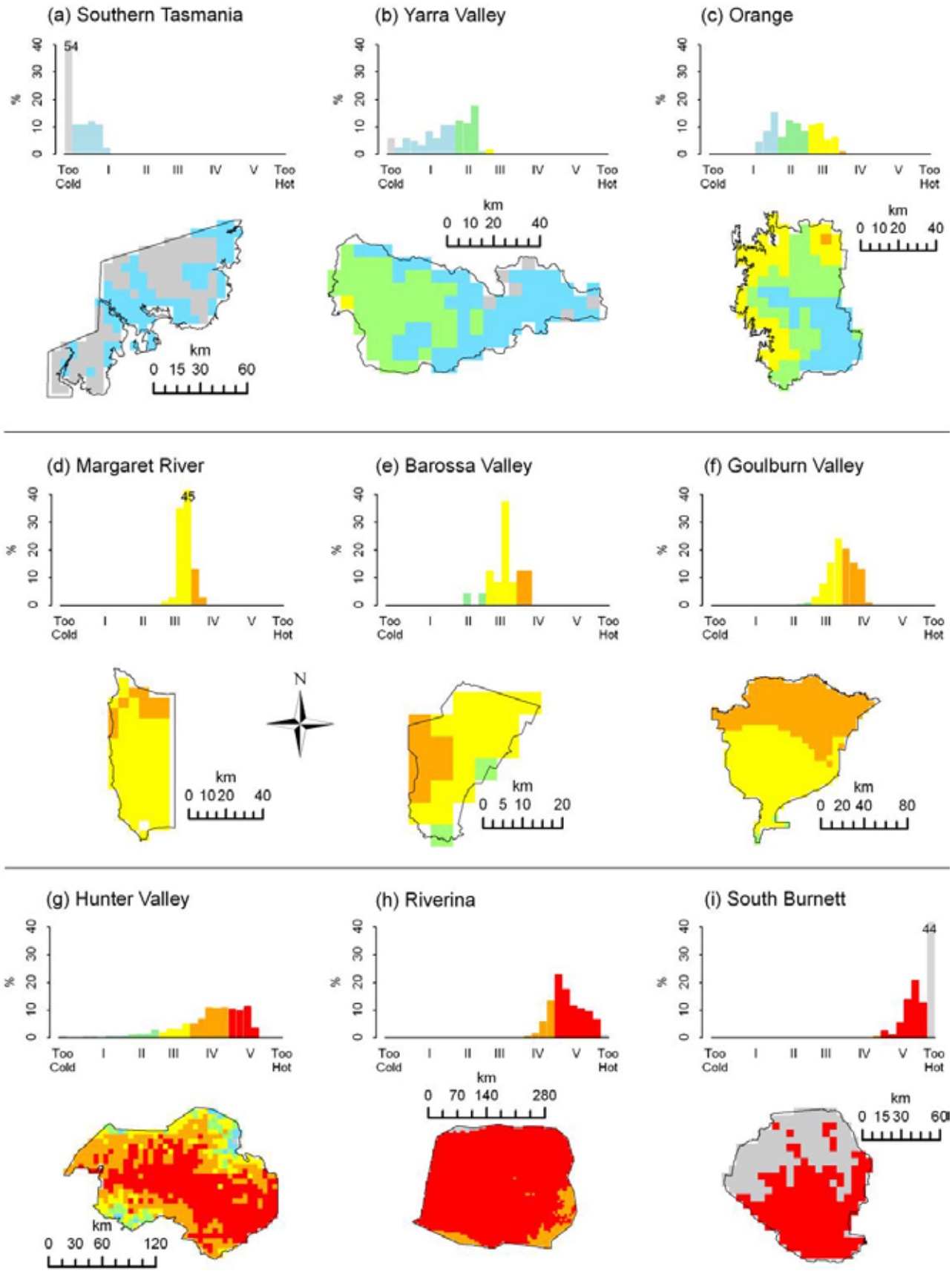


Figure 4.33 Distribution of climate types within nine selected GIs, categorised by Winkler's growing degree-day derived classes, shown as both histograms (with bars at 69.5°C day intervals, approximately 1 quarter the range between the original Winkler categories) and maps (each pixel in the maps is a 0.05 decimal degree square). Histogram bars are restricted to 40% in the chart; those that extend beyond 40% are labelled with the actual percentage. Note: Southern Tasmania is not an officially established GI.

in much the same way", but cites no evidence for the phenological development rate following the plant-weight growth rate. The coefficients of determination for the models between BEDD and the other indices ($R^2 \approx 0.97$ for GDD and GST and $R^2 \approx 0.90$ for HI) suggest there are further differences than the slowing rate of increase in the index for warmer temperatures, caused by the adjustments for latitude and diurnal temperature range. The greatest residuals are for the most southerly and northerly GIs, North and South Tasmania and South Burnett, indicating latitude can have a greater effect on the BEDD than on the other indices.

Section 3b

A full analysis is underway using the climate data and methodology outlines above. Preliminary results for Chardonnay are presented here. Full results will be available in an upcoming publication.

The climate variables identified as having the strongest relationship with regional Chardonnay yield anomalies are presented in *Table 4.33*. Many of the variables identified are temperature related and mostly were at times in seasons 1 or 2 years prior, suggesting a perennial effect from previous seasons that may involve carbohydrate storage and utilisation. The optimised neural network obtained from the variables identified in *Table 4.33* was tested using cross-validation methodology. The predicted and actual yield anomaly data that resulted are presented in *Figure 4.34*. The level of variability in the yield data explained by the neural network model is 53.6%, which is represented by the coefficient of determination of the least squares fitted line.

Outcome and conclusion

Section 1

Yield forecasts for two vineyard blocks were produced at two sites over two years using yield weights hand-harvested from 54 sample locations that most fully represented the spatial variability of the vineyards. The raw estimate (the mean yield per sample multiplied the total vineyard area) was significantly greater than the machine harvested weight, but was relatively consistent across the sites and years (67–75%). A multiplicative correction factor was used to account for this difference in order to produce more accurate forecasts in absolute terms. Using all 54 sample sites the level of error was 6.4% and 4.6% at the two sites in the second year.

A statistical technique called Monte Carlo simulation was used to produce likely confidence intervals of using sub-samples of the 54 sample vines to produce yield estimates. The sub-samples were semi-randomly selected using rules that incorporated knowledge of the spatial variability of the vineyards. This allowed for a comparison of the accuracy of yield forecasting that incorporates spatial information to yield forecasting that uses a random sampling technique. The results suggest that the advantage of incorporating spatial knowledge into sample selection is likely to be significant. Although the method of ascertaining the best sample locations in this study were relatively technically complex, it is likely that sample site selection using some form of spatial data that relates to yield variability will increase the efficiency and/or accuracy of yield forecasting for individual management blocks.

Selecting samples using the spatial information produced significantly lower errors than selecting samples purely randomly. Approximately half the number of samples collected using the spatial information was required to attain the same level of error that would have been produced had the sample locations been selected randomly. The total error, however, was still high, reflecting the high degree of variability common in vineyard blocks. A high number of samples are still required to reduce the confidence interval of an estimate of yield or TSS. A method of adjusting yield estimates from data collected using a consistent sampling system to produce accurate absolute estimates of yield harvested using a consistent method was also achieved.

In future work we aim to increase the level of accuracy of yield estimates by taking into account relationships between rates of canopy growth and yield (see Hall *et al.* 2010) and then modelling the yield for each vine in the vineyard using simple empirical models, and by also improving our knowledge of the causes and predictors of vineyard variability.

Section 2a

Through the development of a row-crop image-segmentation algorithm, grapevine canopy vigour was quantified at the individual grapevine scale at two vineyard sites that were subject to high spatial resolution optical remote sensing four times per year over three years. Measures of vegetative canopy vigour at the individual grapevine scale, derived using a set of remote sensing vegetation indices that could be calculated from a basic 4-band imaging system, were found to correlate with fruit composition and yield variables at a level to enable vineyard maps derived from the algorithm to be potentially useful tools for

Table 4.33 Variables identified for regional Chardonnay winegrape yield anomalies (deviation from the long term mean).

Variable Name	Data	Year	Time	Power	r
SOI1.2	SOI	0	0-100 GDD	2	0.521246
MmeanT50m23.1	Mean Temperature	-2	September	1	-0.520120
MATm1.1	Mean Temperature	-1	Whole Year	1	-0.447570
MmeanT50m33.1	Mean Temperature	-3	September	1	-0.442920
springTm2.1	Mean Temperature	-2	Sep-Nov	1	-0.393340
MIODm21.2	IOD	-2	July	2	0.389367
Chardonnaym1.1	Yield	-1	NA	1	0.387694
MmeanT501.1	Mean Temperature	0	July	1	-0.385110
MATm2.1	Mean Temperature	-2	Whole Year	1	-0.380550
MmeanT502.2	Mean Temperature	0	August	2	0.376269
MmeanT50m13.1	Mean Temperature	-1	September	1	-0.356210
MSOI1.1	SOI	0	July	1	0.337886
autumnTm2.1	Mean Temperature	-2	March-May	1	-0.336690
MATm3.1	Mean Temperature	-3	Whole Year	1	-0.315610
springTm1.1	Mean Temperature	-1	Sep-Nov	1	-0.310620
MHSIm22.2	Heat Stress Index	-2	August	2	0.309952
meanT50m21.1	Mean Temperature	-2	0-100 GDD	1	-0.299290
MmeanT50m24.2	Mean Temperature	-2	October	2	-0.292210
MHSI4.1	Heat Stress Index	0	October	1	0.291030
MTVIm31.2	Temperature Variability Index	-3	July	2	0.288561
autumnT.1	Mean Temperature	0	March-May	1	-0.285810
MmeanT504.2	Mean Temperature	0	October	2	-0.284980
autumnTm1.1	Mean Temperature	-1	March-May	1	-0.283790
Chardonnaym2.1	Yield	-2	NA	1	0.277896
MmeanPm21.1	Precipitation	-2	July	1	0.275551

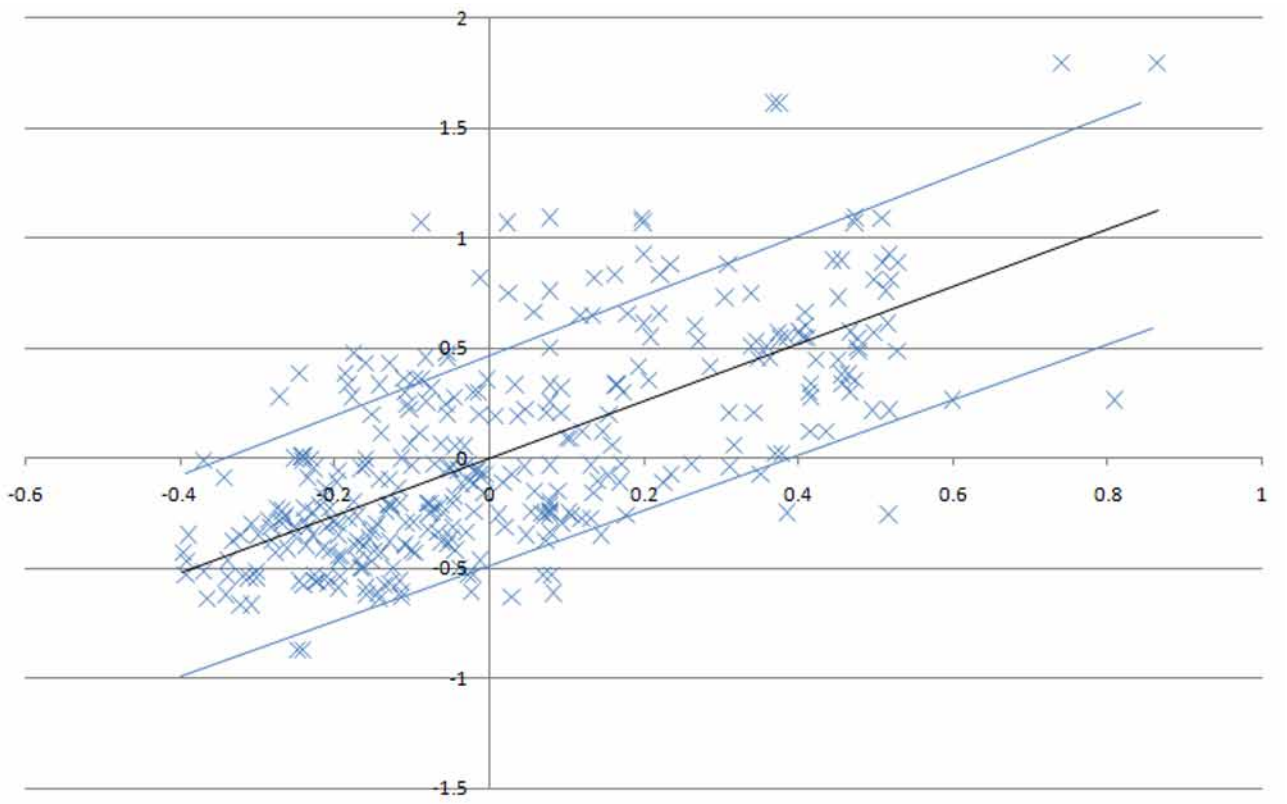


Figure 4.34 Predicted yield anomalies (x-axis) plotted against actual yield anomalies (y-axis) using the optimal neural network determined for the Chardonnay yield anomaly data. Each point represents a unique year and region instance (25 years by 30 regions). Coefficient of determination (r^2) for this relationship is 0.536.

predictive mapping of winegrape quality, yield and ripeness. This study has demonstrated that caution should be exercised when making predictions about winegrape composition and yield based on remotely sensed canopy data due to apparent inconsistency in correlation strengths caused by different vineyard characteristics, especially pruning method and consequent canopy size. This data also suggested that inter-annual variability in correlation strength may also be affected by significant deviations from mean annual production.

An investigation into various vegetation indices for their ability to most accurately describe canopy characteristics in terms of enabling predictive mapping of yield and composition data, demonstrated the triangular vegetation index (TVI) to be superior. Vegetation indices sensitive to differences in dense vegetation, including the enhanced vegetation index, were stronger predictors than the traditionally used normalised difference vegetation index or the simple ratio. Two canopy measures produced in previous studies on vineyard remote sensing were similarly assessed. Canopy metrics based on "vegetation abundance", a measure estimated by a partial spectral unmixing procedure, performed strongly in the vineyard that had overall lower vegetative vigour, producing the greatest number of significant correlations with fruit yield and composition, but produced relatively poor predictions in the high vigour vineyard. A vine canopy size measure, which does not contain detailed information on canopy variability, performed relatively poorly. The only index that did not include any information on reflectance in the near-infrared spectral band, the visible atmospherically resistant index, produced canopy vigour measurements that correlated least with fruit yield and composition, but may still be useful when near-infrared bands are not available in basic imaging systems.

Analysis of canopy vigour descriptors derived from the TVI correlations with winegrape quality, yield and ripeness indicators revealed a degree of inconsistency in correlation strength that appeared to be affected by vineyard type and phenological stage. With all seasons' data combined, at both sites, the strength of correlations peaked at veraison, the time at which most seasonal canopy growth ends, and declined after harvest with the onset of senescence. Images produced early in the season, during early canopy development, were also less likely to correlate with harvested fruit yield and composition variables than imagery acquired around veraison. In the machine-pruned larger canopy vineyard, strong positive correlations with yield and negative correlations with the quality-indicating fruit descriptors, anthocyanin and total phenolic content, were observed, which was consistent with previous studies. In the spur-pruned smaller canopy vineyard, however, these relationships were significantly weaker and less consistent. A possible contributory reason for this was the relative size of canopy. Higher canopy to inter-row space pixel ratios, in the machine-pruned vineyard provided a more accurate average measure for each canopy unit. Large deviations from annual total production may also alter correlation strengths. In particular, fruit total soluble solids correlated with the remotely sensed canopy descriptors in lower yielding years only.

Section 2b

Significant correlations between canopy characteristics derived from remotely sensed high spatial resolution vegetation index imagery of 52 individual Cabernet Sauvignon grapevines and yield were observed over a two year period. In particular, canopy growth rates described by the ratio of canopy density as derived from high spatial resolution remotely sensed vegetation index imagery, were strongly correlated to grapevine yield at the end of the following season. The grapevines that had developed foliage canopies faster and earlier at the start of each season had relatively smaller canopy sizes at the end of each season and relatively less grape yield. Due to the changes in the strength and type (negative or positive) of relationships between the canopy descriptors and yield, the level of spatial variability of within vineyard scale grapevine productivity that can be interpreted from vegetation index imagery is dependent upon the timing of the imaging acquisition missions (see *Figure 4.31*).

Canopy area (CA, number of pixels above a threshold vegetation index) and canopy density (CD, mean vegetation index of the pixels counted as canopy area) achieved different levels of correlation with grape yield depending on the time in the season at which the images used to derive the canopy descriptors were acquired. The differences in the strength of the correlations, using either CA or CD, suggests that one or the other canopy descriptor may be better at quantitatively characterising grapevine canopy depending on the overall vegetative characteristics of the vineyard block.

A best subsets regression using up to three of the canopy descriptors and/or yield in year 1 as predictor variables delivered a model that explained 69% of the spatial variance in yield. This suggests that extra information about spatial variability in grapevine yield may be contained in canopy descriptors acquired at more than one occasion over the previous two years before a harvest. Overall, this study suggests that improvements in grape yield forecasting at the vineyard block scale through the application of remote sensing technologies are achievable.

Section 3a

Temperature indices provide key information for comparing wine region climates, yet, until now, no consistent set of indices has been available to enable direct comparisons between countries. In addition, historical comparisons of the climate characteristics between regions have been done using individual stations, which can vastly under- or over-estimate the true climate structure in a given wine region. The data and methodology presented in this section of the report contribute a set of climate indices and their spatial characteristics for Australia's winegrape growing regions. The results show that spatial variability of the climate indices within regions can be significant; and that understanding their distribution provides a measure of understanding the range of cultivar suitability within wine regions.

Functional differences between the selected temperature indices were identified. Season total growing degree-days (GDD) was nearly functionally identical to growing season temperature (GST), as both indices were calculated using average daily temperature data only. The Huglin Index (HI) was functionally similar to GST and GDD, but varied for some regions because it uses an estimate of daytime temperature (instead of average diurnal temperature) and includes a modification to account for day-length, which varies by latitude. Biologically effective degree-day (BEDD) totals were the most different to the other indices because of the cap placed on the number of degree-day units that can be accumulated on any one day. This resulted in the rate of increase in the BEDD with respect to increases in the other indices slowing at higher temperatures. A consequence of the dissimilarity amongst the indices is that descriptions of temperature regime differences between the same region pairs can vary depending upon what index is employed.

In selecting an index most suitable for indicating economically sustainable winegrape production, there appears to be no advantage in using the indices with more complex formulas than simple average growing season temperature. Capping the heat accumulation component of the biologically effective degree-day index to 9°C, renders the BEDD insensitive to increasing temperatures in already warm regions and would therefore be the least suitable for climate change modelling. Latitude adjustments incorporated within both the Huglin Index and the BEDD are however, likely to be valuable at providing values closer to the actual daily mean temperature, and therefore more representative of a region's viticultural suitability. The Huglin Index does not include a cap on heat accumulation but does include a latitude adjustment factor so is perhaps the most suitable of the four indices for viticultural climate change impact studies. The HI does not include the seventh warmest month (April/October in the Southern/Northern Hemisphere), which is of value when determining limits of production in cool regions. Perhaps the best solution would be an index with the basic simplicity of the GST (of the seven warmest months), but modified for latitude, achieved by simply multiplying the GST by *K* (Eqs. 4–7). To more fully describe the potential suitability of a climate type for long-term commercially successful winegrape production, accompanying indices that describe spring frosts and extreme heat could also be determined, such as the temperature variability index, spring frost index or heat stressfulness index (see Gladstones 1992; Gladstones 2004).

While each of the temperature indices examined in this research have been developed with viticultural suitability in mind (Winkler *et al.* 1974; Huglin, 1978; Gladstones, 1992; Jones, 2006), their applicability to other wine regions from where they were developed has not been fully examined. The data and methods presented here and by others (Jones *et al.* 2010; Jones *et al.* 2009) are providing a more holistic look at climate index characteristics globally and the framework by which regional validation can be examined. Furthermore, it is important that ongoing updates to the spatial characterization of the indices be completed as data becomes available, i.e. more recent data (e.g. 1981–2010) and at a higher spatial resolution, so as to keep these index values up-to-date in a changing climate and at an increasing level of accuracy and precision.

Section 3b

All other things being equal, climate variability is the driver of the variability of grape yields. However,

many factors come into play to cause fluctuations in grape yield besides climate. Since it is the aim of the research presented in this section to determine short-term (inter-annual) climatic factors that affect yield, it is necessary to eliminate factors other than climate that cause yield fluctuations. External markets and demand have a large influence on the price paid for and hence the profitability of grapes. A loss of demand for a particular variety may lead to growers deciding it is not worth maintaining vines of that variety to produce a viable crop. Money otherwise spent of irrigation water, fertilisers, herbicides, canopy management, etc. is deemed to be less than what will be received for grapes produced from that vineyard. Harvesting of grapes may even be abandoned at the end of season, because the cost of harvesting is greater than the value of the crop that would be produced. Nevertheless, we have so far demonstrated that about 50% of the variability in the data can be explained using climate anomaly data. With standard methods for collecting climate data on a large spatial scale, quantitative forecasts of yield were shown to possible, albeit with a large potential error. The ground work has been laid for similar analysis of Cabernet Sauvignon and Shiraz yield along with yield predictions for 2008-2010 actual yields using the 1982 -2007 climate data.

General Conclusions

Data describing environmental, yield and quality components of two vineyard sites (Hunter and Riverina) were collected, over three consecutive seasons. Sampling schemes captured the spatial variability of the two study sites using nested cluster algorithms with either EM38 maps or remotely sensed canopy vigour maps as input. Using spatial data to help select sites significantly increased the sampling efficiency in all three years at both sites. If selected using spatial data approximately 50% the number of sample sites were required to achieve a similar level of error in a yield estimate that would result from using random sampling. The overall potential error for yield forecasts due to vineyard spatial variability was about ±20% using 9 sample sites selected with the aid of spatial information.

Vineyard sample data was collected at both sites at harvest, and associated winemaking and berry analysis has been completed over three years at the two sites. Remotely-sensed vineyard canopy data (collected four times per season over three years at two study sites) were processed using a specially designed remote-sensing imagery discretisation algorithm. Best subset regression analysis revealed that remotely sensed canopy data from the preceding two years in conjunction (with elevation data in the topographically varied vineyard site) can consistently explain 40–50% of the variability in the sampled yield. The best models were applied to whole of vineyard remotely sensed and environmental data to estimate whole of vineyard spatial variability in yield.

Other key results included:

- Use of the Triangular Vegetation Index (rather than commonly used Simple Ratio or NDVI) consistently correlated more strongly with yield and quality attributes than other remotely sensed vegetation indices.
- The strength of the correlations peaked at veraison, and declined rapidly after harvest
- The strength of the correlations varied for the different vineyard types, particularly due to pruning technique, with spur pruned vines consistently having weaker correlations than machine pruned vines.
- Relatively low levels of correlations are required to have a significant impact on segmented harvesting. Using 54 sample sites: at α=0.01, r=0.312, fruit loads from a segmented harvest will have significantly different attributes 74% of the time; at α=10–4, r = 0.475, fruit loads from a segmented harvest will have significantly different attributes 99% of the time.
- Large deviations from annual total production appeared to weaken the strength of correlations, i.e. remotely sensed data collected in years with average productivity was most valuable for precision viticulture practice.

Very large tables (i.e. 616 samples of 4180 variables) of aggregated yield and climate data were produced for all major viticultural regions of Australia. Data from the ABS (grapevine yield data by region and variety for the 1982–2009) and from the BOM (temporally contiguous daily climate data interpolated for the whole of Australia) were acquired. These data were prepared in heat-unit time period summaries. Multivariate analysis was completed to produce yield forecasts. A neural network modelling protocol was developed as a regional yield forecasting tool. The modelling protocol was applied to 1982–2007 Australian Chardonnay yield. Cross-validation techniques indicated that about 50% of the temporal variability in yield was explained by the climate data using the neural network model. Indicators of yield at various stages leading up to harvest were identified from the analysis of the national climate and yield

data, for example temperature at fruit set in the preceding seasons.

A synthesis of key results of the various components of the project produced options for yield forecasting using different methods and data at various times before harvest. Important forecast variables include canopy growth rates in the preceding season, canopy size at around veraison and temperature indicators in late winter/ early spring of previous years.

Social, economic and environmental benefits

- Reduction in harvest, transport and storage costs.
- Resource allocation in the winery better managed through better scheduling, particularly at harvest time.
- Better relationship between growers and wineries will result. With better understanding of the next harvest's vineyard productivity and grape quality, growers and wineries will be able to better negotiate price points.
- The environmental benefits are indirect. With more accurate forecasts, management decisions made from the vineyard to the winery, particularly during vintage, will increase production efficiency, delivering a greater value output to input ratio.

Experiment 4.5
Grapevine nutrient reserves and their impact on grape yield variability and yield estimation

Introduction

Section 1

The seasonal pattern of carbohydrate reserve mobilization and storage by grapevines is strongly influenced by developmental stage, and the extent to which growth and maintenance requirements can be balanced by current photosynthesis. Carbohydrate demands of developing shoots typically cause the most pronounced period of mobilization. However, as the season progresses, reserve dynamics can be strongly influenced by factors such as crop load, canopy size and irrigation, or weather conditions that effect photosynthesis and the net capacity for carbon acquisition (Holzapfel *et al.* 2010). Consequently, the over-wintering carbohydrate reserve status may vary from season to season according to both climatic factors and vineyard management. Nitrogen reserves are also stored in the perennial tissues of grapevines and play an important role in supporting early season canopy growth (Conradie 2005). The nitrogen content of perennial tissues is responsive to nitrogen fertilizer applications, and like carbohydrates, concentrations at dormancy and the changes in concentrations between developmental stages may also vary between seasons (eg. Treeby and Wheatly 2006).

Previous studies have linked carbohydrate and nitrogen reserves with vegetative growth and fruiting responses (eg. Cheng *et al.* 2004; Bennett *et al.* 2005; Weyand and Schultz 2005), raising the possibility that a measure of stored reserves at dormancy could provide an advanced indication of yield and growth potential in the following season. Recently we have also observed that seasonal differences in the composition of Shiraz grapes were associated with a contrasting pattern of carbohydrate reserve storage and mobilization between flowering and harvest. This suggests that monitoring changes in reserve concentrations between key development stages may also assist with understanding the impact of management practice and climatic factors on berry development and fruit quality. For carbohydrate and nitrogen reserve testing to be of value for commercial grapevine management, a number of issues remain to be addressed. One of these is the characterization of existing variation in reserve concentrations, such that some context is provided for the interpretation of any analysis undertaken. Like many other vine based measurements, there is also a need for some characterization of spatial variability in reserve concentrations such that the most effective sampling strategies can be developed for determining a vineyards reserve status.

Current methods of analysis based upon single analyte determination may also be too slow for basing management decisions, or too laborious and expensive for widespread commercial adoption. Hence there is a requirement for a more rapid and lower cost method for measuring carbohydrate and nitrogen concentrations in grapevine tissues. Attenuated total reflectance Fourier transform infrared spectroscopy (ATR-FT-IR) combined with chemometric modelling offers a rapid means for the determination of a range of analytes in powdered or ground samples. This process involves collection of the infrared spectra of samples and correlating the absorbance at specific wavelengths to analyte concentration with predictive models constructed that can be used to determine the concentration of analytes in other samples. ATR-FT-IR offers significant advantages over traditional analysis methods due to the ease of operation, reproducibility and speed of data collection.

Section 2

Modeling of grapevine balance

Vine balance is a term widely used in viticulture to describe the relationship between the vegetative growth and yield of grapevines. Typically this has been quantified in terms of the leaf area to fruit weight ratio, or the more easily determined dormant cane weight to fruit weight ratio (Ravaz 1930; Kliewer and Dokoozlian 2000), providing a simple empirical measure of the relationship between the size of main carbon source (leaves) and main carbon sink (berries) during the ripening period. Vine balance can in turn have a direct influence on berry composition, with sugar accumulation delayed by heavy crop loads or competition with actively growing shoots, and hastened by low but possibly uneconomic yields at the other extreme. The production of key secondary metabolites contributing to wine colour and aroma can also be influenced by vine balance (eg. Petrie and Clingeleffer 2006), indicating that internal carbon availability is important not only for the rate of ripening, but also for the composition and quality of wine produced from the fruit. The flavonoid pathway in developing grape berries, which is responsible for the production of anthocyanins and tannins (eg. Downey *et al.* 2003; Bogs *et al.* 2005), is ultimately regulated at the gene level. However, flavonoids are metabolically expensive to produce, and their amino acid precursor phenylalanine is derived from a pathway that utilizes 20% of the carbon fixed by plants (Haslam 1993). Consequently, characterising the internal availability of carbon during the ripening period may be central to understanding how grapevines can be managed to optimise the accumulation of these key quality attributes.

Many cultural practices currently aimed at improving fruit composition, such as trellis design, pruning, leaf removal, crop thinning and deficit irrigation are techniques that can alter the internal vine carbohydrate availability and sink:source relations. However, despite the relative simplicity of the concept of vine balance, it is a harder to define and use in the day to day management of vineyards. Firstly, leaf area alone does not determine photosynthetic capacity where trellis design can alter the amount of exposed leaf area, or environmental conditions such as temperature and water availability alter the photosynthetic rates of individual leaves. Secondly, a simple ratio between leaf area and fruit weight at one point in time does not take into account changes in internal carbon balance that occur over the whole season, or the contribution from stored carbohydrates in perennial tissues that can influence carbon availability both within seasons. Stored carbohydrates may also vary between vineyards and seasons according management practice and environmental conditions, which can in turn influence vegetative growth and yield (Smith and Holzapfel 2009; Holzapfel and Smith 2011), and lead to potential differences in internal carbon balance from season to season. Consequently, determining the combinations of yield and management driven control over vine assimilation needed to optimize fruit quality is something that can take considerable trial and error, or long term experience with particular vineyards.

An alternative approach to understanding how factors such as weather conditions and trellis design might impact on internal carbon availability is to model their effects on whole vine photosynthesis and carbon assimilation. Existing models for grapevine photosynthesis range in complexity from simple empirical relationships (Bindi *et al.* 1997) to mechanistic based models that scale single leaf photosynthesis responses to the whole canopy level (Poni *et al.* 2006; Lakso *et al.* 2008). More recently, functional-structural models have been developed that superimpose biochemical models of photosynthesis onto individual leaves of measured or statistically re-constructed 3D canopies (Prieto *et al.* 2011). In some cases these models have also been validated with direct measurements of net photosynthesis using whole canopy gas exchange systems (Poni *et al.* 2006). The subsequent internal partitioning of carbon assimilate to the various growth and maintenance is a more complex process to model, and is more developed in other crop species than grapevines (eg. Cieslak *et al.* 2010). However, preliminary work in this area suggests considerable benefit from a modelling approach that allows changes in net internal carbon balance through the season to be related to berry development and composition (Lakso and Poni 2005).

Despite being essential for the re-establishment of the canopy in spring, and providing an alternative source of carbon to current photosynthesis during the season, a factor that has received relatively minor attention in grapevine growth models are carbohydrate reserves. With our research, we have been interested in two particular aspects. The first, as addressed in the previous section of this report, is the contribution of reserves to reproductive development and seasonal yield variation. The second, which is

addressed in part here, is understanding why the internal dynamics of carbohydrate reserve storage can vary between seasons (eg. Holzapfel and Smith 2011) and what implications this may have for berry development and composition. In the longer term, we believe very significant advances can be made in our ability to manage fruit quality through a combined modelling and field based experimental approach that can characterise the effects of internal carbon balance and availability on berry development and wine quality. Here we report on the capacity developed and work undertaken towards meeting this objective.

Section 3

Whole vine gas exchange chambers

The final objective was to develop and test whole vine gas exchange chambers for above ground vine atmosphere studies. Sufficient funding was approved for the purchase of some key chamber components in 2010, but due to time constraints a prototype has not yet been constructed. However, the chambers been designed, and over 100 vines planted in 50 litre pots and trained onto a fixed trellis system (*Figure 4.35*). The future intention is to use these vines to assist with model validation, and also to improve our understanding of climatic conditions and internal carbon availability on berry quality, water use efficiency and whole vine photosynthesis.

Materials and method

Section 1

Fruitfulness and carbohydrate variability–Riverina site

Sample collection for bud-fruitfulness assessments and carbohydrate analysis was undertaken at the Theme 4.2 Riverina Shiraz site at dormancy in 2009 and 2010. These were collected from 54 individual sample vines selected in 2009, and repeated on the same vines in 2010. For the bud-fruitfulness assessments, five canes were randomly selected, and bud-dissections undertaken for nodes 1 to 3. For each bud the number of inflorescences in the primary shoot bud were recorded if the entire bud was alive, or the next largest secondary shoot bud if the primary bud was dead. The incidence of primary bud necrosis (PBN) or completely dead buds was also recorded. In addition to the winter bud-dissections, shoot samples were collected from each of the 54 sample vines on three occasions (9 December, 15 February, 20 April) to examine the progression of primary bud necrosis during the 2009-10 season. Eight buds from each vine (two canes×four buds) were excised from the shoots and stored in 70% ethanol at 4°C. For microscopic analysis the buds dehydrated with series of ethanol solutions (75, 85, 95 and 100%) and then infiltrated with liquid paraffin wax. The buds were then embedded in paraffin wax blocks, sectioned, mounted and stained with toluidine blue following de-waxing and rehydration.

For carbohydrate analysis, root samples (diameter range ~3–7 mm) were manually dug from near the base of each vine. Wood samples were collected with a 4.8 mm drill bit to a depth visually estimated as the centre of the cordon and trunk. Roots were washed in phosphate free detergent and rinsed with de-ionized water, and all tissues were oven dried at 70°C and then ground to 0.12 mm with a heavy duty cutting mill (Retsch ZM2000, Haan, Germany) and ultra-centrifugal mill (Retsch ZM200). Non-structural carbohydrate concentrations were determined on a 20 mg sub-sample of each tissue. Free soluble carbohydrates were extracted using two 1 ml aliquots of 80% ethanol incubated in a water bath at 80°C for 10 min, and a third at room temperature for 10 min. Supernatants were pooled from each extraction following centrifuging at 10,000 rpm for 2 min, and the pooled fraction diluted to 10 mL with ultra-pure water. The concentration of sucrose, D-fructose and D-glucose were determined by commercial enzymatic assay (K-SUFRG, Megazyme International, Bray, Ireland). For starch analysis, the remaining wood sample was re-suspended in 200 µL of dimethylsulfoxide, heated at 98°C for 10 min, and then 300 µL of thermostable α-amylase (29 U mL^{-1}, Megazyme International) in MOPS buffer (pH 7) was added. After incubation for a further 15 min, the samples were allowed to cool, and 400 µL of amyloglucosidase (32 U mL^{-1}, Megazyme International) in sodium acetate buffer (pH 4.5) was added. The samples were then incubated at 50°C for 60 min and then centrifuged at 10,000 rpm for 2 min. The supernatant was diluted 1:6 (wood) or 1:11 (roots), and the glucose concentration determined using a glucose oxidase/peroxidase based assay (K-GLUC, Megazyme International). Starch concentration in the original 20 mg sample was then calculated.

An object based analysis of the remotely sensed colour-infrared images of the vineyard, collected on 12 occasions between October 2007 and March 2010, was used to produce single grapevine sized metrics of canopy vigour. A vegetation index sensitive to high density vegetation was employed, the triangular vegetation index (TVI, see *Table 4.34* in the "Predictive modelling of grapevine production using




Figure 4.35 Potted vines trained to fixed trellis wire in preparation for use with a whole vine gas exchange system. Image on left shows vine for future varietal comparisons (planted 2009, trained onto trellis in 2011) and right, more advanced vines for chamber development (planted 2006, trained onto trellis 2009).

remote sensing techniques" final report). The canopy data of 54 sample vines was subjected to a correlation analysis using the measures of trunk circumference, carbohydrate reserve concentrations, bud fruitfulness and primary bud necrosis that were made for each vine in winter 2009 and 2010.

ATR-FT-IR calibration for rapid measurement of starch and nitrogen reserves

Spectra were collected from a calibration and validation sample set of 1,880 root and wood samples with an ALPHA FT-IR spectrometer (Bruker, Ettlingen, Germany). The sample set consisted of 840 Shiraz, 456 Riesling and 528 Semillon root and wood (cordon and trunk) from the Riverina and SW Slopes regions of New South Wales Australia, and 156 Riesling wood (one and two-year wood) samples from the Rheingau in Germany. Non-structural carbohydrate concentrations were determined on a 20 mg sub-sample of each tissue as described in the previous section. For total nitrogen, an equal proportion of tissue from the five replicate locations in each vineyard was bulked, and the nitrogen content of a 50 mg sub-sample determined with a VarioMAX combustion analyser (Elementar, Hanau, Germany). All samples originated from research trials conducted between 2005 and 2009, including some from the survey described above. Samples were assigned randomly to calibration or test data sets representing two thirds and one third of the samples respectively. Signal preprocessing and calibrations employing support vector-regression were undertaken as described in full detail by Schmidtke *et al.* (2011).

Briefly, each sample was measured once, with the recorded spectra averaged from 64 scans over the region 374–7496 cm^{-1}. Data was converted to ascii format and imported into Matlab version 7.4.0.287 R2007a (The Mathworks, Natick). For the purposes of exploratory data and regression analysis ATR data between 374–3958 cm^{-1} was extracted from each scan and converted to absorbance to correct for differences in sample penetration of the beam at different wavelengths.

Spectra from all samples, and the 95% confidence interval for absorbance, was plotted to identify regions with interesting variation. A principal component analysis (PCA) of the standard normal variate (SNV) scaled and mean centred (MC) spectral data between the regions 875–1800 cm^{-1} was conducted using the singular value decomposition (SVD) algorithm with principal components (PC) 1–2 and associated loadings plotted to identify specific groups of samples. Two approaches to constructing calibration and test data sets were conducted; firstly random assignment of samples to a calibration or test set based so that approximately two thirds of samples were designated calibration and one third as an independent test set. The second approach involved interrogation of the MIR spectra to identify outlier samples.

Calibration and test data were pre-processed using SNV scaling followed by calculating the second derivative using a Savitzky–Golay filter prior to variable selection. Alternatively, multiplicative scatter correction (MSC) or extended multiplicative scatter correction (EMSC) using reference spectra for water and carbon dioxide vapour were applied to the calibration data set using a second order polynomial filter in accordance with described procedures prior to variable selection. Spectra for carbon dioxide were obtained from an online database at a resolution of 0.1 cm-1, were de-resolved and re-sampled to match the reflectance spectra of samples. For the purposes of applying MSC and EMSC, the mean spectra of the

calibration samples were used as the reference spectra. Variable selection within the calibration block was conducted using the forward interval PLS (iPLS) regression for each analyte and model combination. Predictive models of the spectra for nitrogen and starch were constructed using either PLS regression or support vector regression analysis.

To relate the accuracy of the ATR-FT-IR predictive models to seasonal and spatial variation in carbohydrate and nitrogen reserve storage, additional analysis of data collected during project CSU 05/01 was undertaken. In this earlier project, the carbohydrate and nitrogen reserve status of 34 commercially operated vineyards were surveyed during winter in 2005, 2006 and 2007. The sampling strategy employed at these vineyards involved the random selection of five replicate panels of four vine, and sampling wood and root carbohydrate and nitrogen concentrations as described above. The number of vineyards used in the current analysis has been reduced to 32 (16 Shiraz and 16 Chardonnay) where associated management and yield information could not be obtained for the remaining two sites. The same vines were used for sample collection in each season.

Section 2

Photosynthesis response to light and temperature

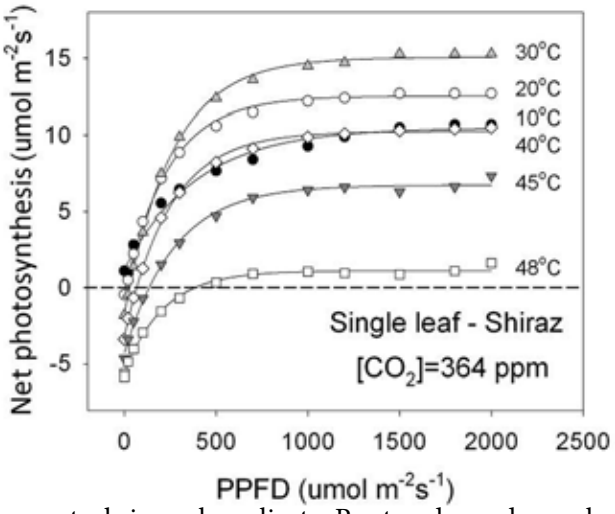
A single leave light and temperature response function was determined using a 3-year-old potted Shiraz grapevine that had been previously been grown outside under non-limiting irrigation (*Figure 4.36*). On the day of measurement the vine was transferred to a controlled environment chamber (Thermoline, Australia), and a light response curve recorded at 10, 20, 30, 40, 45 and 48°C using a LiCOR LI6400 infrared gas analyser (LiCOR, USA). The most recently fully expanded leaf was used for the photosynthesis measurements, with light intensity increased from 0 to 2100 μmol $m^{-2}s^{-1}$. The temperature of the controlled environment chamber was adjusted between each measurement such that the whole plant and measured leaf experienced approximately the same conditions during the measurement period. The vine was watered at regular intervals to avoid any soil water deficits.

Canopy light interception.

A linear array of 15 photodiodes (Silonex, Quebec, Canada) was mounted at 20 cm intervals along a section of aluminium channel (20×20 mm), and wired in reverse bias to provide a linear voltage output response to light intensity. Each sensor was connected to a CR1000 data logger and AM25T solid state multiplexer (Campbell Scientific, Utah, USA). During light interception measurements the output was recorded every five seconds. A six metre long aluminium frame was constructed with fixed markings at 50 cm spacing that could be assembled under the vine to support the sensor array during light interception measurements. Where light interception was to measure on multiple occasions during the season, steel bolts were driven into the ground under each leg of the support frame such the system could be re-assembled in the exact location each time. For each measurement of canopy light interception the sensor array was first used to record light intensity above the canopy, and then at each of the 50 cm intervals along the aluminium frame. An average of six light intensity measurements were made at each position and the mean value calculated. A quantum sensor (Apogee Instruments SQ-110, Utah, USA) was used to record incoming photosynthetic photon flux density (PPFD), such that the voltage output of the sensors could be expressed in terms of actual and relative light intensity. Total light interception was determined from the difference in light intensity above and below the canopy (*Figure 4.37*).

Carbohydrate reserve data

The carbohydrate data used for this study was originally collected as part of the carbohydrate reserve management trial that was conducted with Shiraz between 2007 and 2010. The carbohydrate reserve and viticultural component of this work is presented in a recently submitted manuscript (Holzapfel and Smith 2011), and additional information relation to the experimental winemaking component can be found in the CSU 05/01 final report to GWRDC. In brief, the vineyard was located in the Riverina grape growing region of New South Wales, and the vines were planted in 1997 on own-roots with a 2.7 m vine and 3.6 m row spacing. The trellis system was a single bilateral cordon with a single fixed foliage wire 30 cm above the fruiting wire. Five treatments aimed at either increasing or decreasing carbohydrate reserve accumulation relative to control vines were applied to four replicated panels of eight vines in a fully randomized block design over the 2006-07, 2007-08 and 2008-09 seasons. The treatments comprised of post-harvest hedging (PH-hedge), reduced irrigation (or increased irrigation deficit relative to control RDI vines) in the period post-fruitset to veraison (RI-PS), reduced irrigation from harvest to leaf-fall (RI-PH), and 33% or 66% bunch removal at veraison (BR-33 and 66%). Panels of eight untreated vines were used



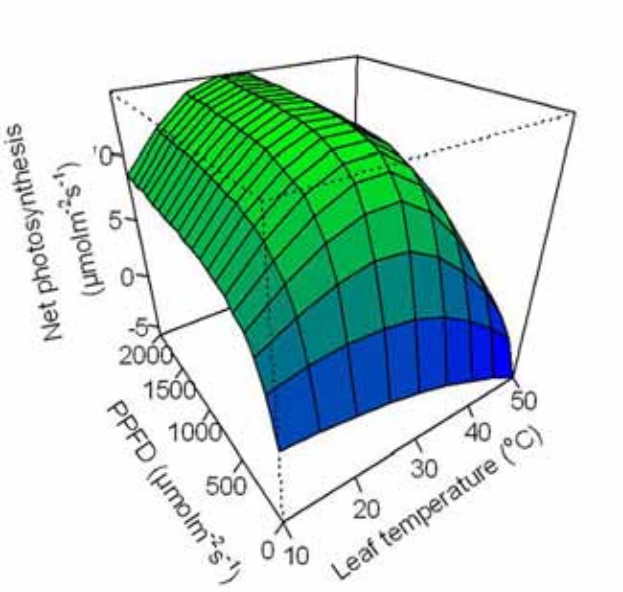


Figure 4.36 Net single leaf photosynthetic response of Shiraz to variation in photosynthetic photon flux density (PPFD) and temperature (a), and fitted function used for modelling whole canopy carbon assimilation (b). (Smith, Field, Auzmendi and Holzapfel, unpublished data).

as controls in each replicate. Root and wood samples were collected at bud-break, flowering, veraison, harvest and leaf-fall, and the concentration of free sugars and starch determined as described in the previous section.

Berry and wine composition

Berry analysis and replicated small-lot winemaking was undertaken with fruit from the Riverina Shiraz trial site in the 2007-08 and 2008-09 seasons. The wines were made from batches of up to 50 kg of hand-picked fruit from the control, RI-PH, BR-66% and RI-PS treatments. The fruit was crushed, de-stemmed and fermented according the NWGIC winemaking protocol in 100 L variable capacity stainless steel tanks at 20°C. The protocol included adjustment to pH 3.5 and adjustment to ±0.5°baume to provide a uniform sugar concentration across treatments. The wines were fermented for 7–10 days and pressed off at dryness (<1 g L^{-1} residual sugar). In the 2009-10 season the treatments were repeated and small lot wine making was undertaken on 80 kg batches of fruit in temperature controlled tanks. Rather than adjust sugar concentrations, each treatment was picked three times over a four week period to produce six treatment wines at three harvest dates. The intent of this harvest process was to firstly to provide a third season of wine data, but also to understand the extent to which the timing of harvest could be used to compensate for crop load effects on fruit composition. The middle harvest date, which was the closest to the timing of harvest in the preceding seasons, is presented in this report. Wine colour density and tannin concentration was determined according to Iland *et al.* (2004) and Sarneckis *et al.* (2006) respectively.

Canopy photosynthesis model

A preliminary canopy photosynthesis model was developed by combining canopy light interception data with the fitted light and temperature photosynthesis response function scaled to the total vine leaf area. The canopy light interception values were based on monthly measurements made on single cordon spur pruned Shiraz vines at solar noon and noon ±3 hours as outlined above. For the purposes of this preliminary model, these values were assumed to be representative of an average canopy in the Riverina. However, single time point measurements were made at other vineyards to confirm that the light interception values were similar (*Figure 4.37*). Net photosynthesis calculations were made at an hourly time step using weather data provided by the Griffith CSIRO Land and Water laboratory for the 2007-08 and 2008-09 growing seasons. The modelled photosynthesis values for each season where then compared carbohydrate reserve data collected during GWRDC project CSU 05/01. The same generic canopy light interception data was used for both seasons, so the model only described variation in photosynthesis due to light and temperature. At this point, no allowance for leaf age or the condition of leaves has been made in the model. Additional 10 cm soil temperature data was sourced from the nearest available Australian Bureau of Meteorology station (Wagga Wagga AMO) for comparative purposes with air temperature.

Structural canopy model

A preliminary structural grapevine canopy model was produced using L-studio (University of Calgary)

by modifying parameters of an earlier version of the kiwifruit model published by Cieslak *et al.* (2010). This was developed largely using shoot growth data from the literature. However, detailed measurements of leaf appearance, internode elongation and lateral shoot growth in Shiraz were made on a weekly basis through the 2010-11 season at the CSU Orange campus vineyard to enable further refinement of the shoot growth routine.

Results and discussion

Section 1

Fruitfulness and carbohydrate variability – Riverina site

Average bud-fruitfulness for nodes 1–3 across the 54 sample vines was similar in both seasons with 1.34 inflorescences per bud in 2009 and 1.31 in 2010. The number of initiated inflorescences was higher in 2009 than 2010 (1.93 compared to 1.63), but this was offset by a higher incidence of primary bud necrosis (PBN) in 2009 than 2010 (34% compared to 16%). The number of initiated inflorescences, which was inferred from the fruitfulness of buds unaffected by PBN, was the least variable of the measured fruitfulness parameters (*Figure 4.38a*). Instead, the variability in the final average fruitfulness values could be largely attributed to the high variability in PBN across the site with significant negative correlations ($p<0.001$) between the two parameters in both seasons. Although an assumption is made that more fruitfulness buds are no less likely to be affected by PBN than non-fruitful buds, this finding suggests that spatial variability in bunch numbers per shoot at this vineyard is more likely to be influenced by the survival of inflorescence primordia after their initiation rather than variability in initiation per se. However, variation in bunch numbers per shoot between seasons may still be influenced by variation in both initiation of inflorescences and the extent of primary or complete bud necrosis.





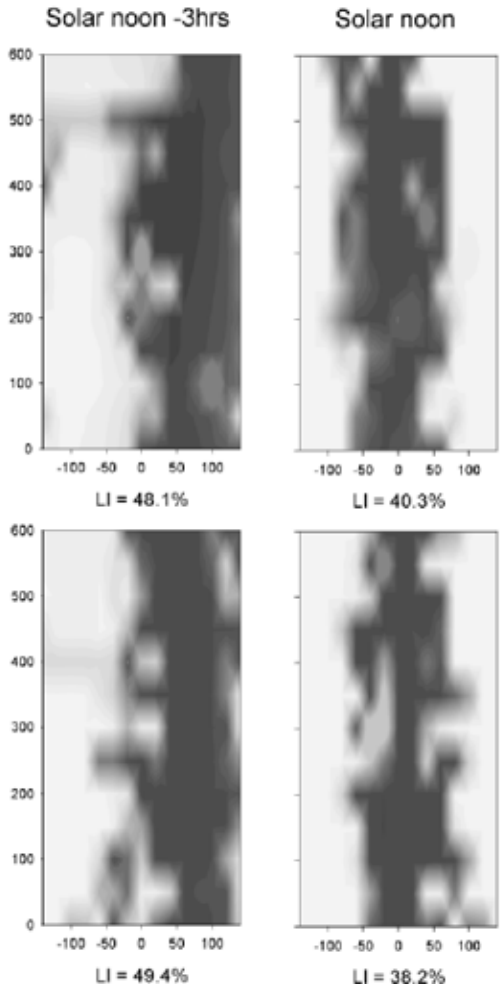


Figure 4.37 Example of canopy light interception measurements at two Riverina vineyards, and corresponding under vine light intensity and solar noon and three hours before solar noon
Upper vineyard: Leaf area 12.7 m^2 $vine^{-1}$, yield 7.8 kg $vine^{-1}$, pruning weight 1.35 kg $vine^{-1}$, pruning weight ratio 5.8.
Lower vineyard: Leaf area 11.4 m^2 $vine^{-1}$, yield 20.2 kg $vine^{-1}$, pruning weight 1.73 kg $vine^{-1}$, pruning weight ratio 11.6 (Smith, Field and Holzapfel, unpublished data).

In our earlier survey of fruitfulness variability across southern NSW Shiraz and Chardonnay (Holzapfel *et al.* 2009) it was also found that the number of initiated inflorescences and subsequent development of PBN contributed to seasonal variability in average bud-fruitfulness. The significant region-level effects on these fruitfulness parameters, which in turn indicate a broader influence of weather conditions on the processes of inflorescence initiation and survival, suggest that climate based yield forecasting models may have the potential to predict seasonal variability in bunch numbers. Direct measures of bud-fruitfulness could provide a physiological input to refine the accuracy of such predictions, but it is important that these distinguish between the separate underlying processes that contribute to the final variation in average bunch numbers per bud.

The analysis of the 1296 bud sections prepared from the trial site in the 2009-10 is still in progress due to the large number of images collected, and the need for some re-sectioning to ensure the structures within each bud could be properly identified. Initial analysis of these images show that clearly differentiated inflorescences are present by early December (*Figure 4.39a*), but at the same time buds affected by PBN were also evident (*Figure 4.39b*). The causes of PBN have not been clearly established, although high shoot vigour, shading within the canopy and low carbohydrates have all been suggested (eg. Wolf and Cook 1992; Dry and Coombe 1994; Vasudevan *et al.* 1998). However, in the present trial we did not see any clear relationship between PBN incidence at dormancy in 2009 and 2010 and any of the remotely sensed canopy size data during the respective seasons (*Table 4.34*). There was a negative relationship between PBN in winter 2009 and canopy size later in the 2009-10 season, suggesting a possible increase in canopy size due to reduced bunch numbers per vine, but no clear evidence of an effect of canopy size on the incidence of PBN.

Variability in carbohydrate concentrations between vines was similar for the roots and wood tissue (*Figure 4.38b*), although absolute concentrations were higher in the roots. The lowest spatial variability in carbohydrate reserve storage was seen in the canes. Total carbohydrate concentrations in the wood in winter 2009 and 2010 showed a significant positive relationship ($r=0.4$, $p<0.001$), but neither wood or cane carbohydrate reserves were correlated across seasons. The use of single vines over multiple seasons limited the amount of root sample that could be collected in the present study, so it is possible that the variability in root reserve concentrations was a reflection of the sampling protocol rather than the real spatial variability in root reserve storage. Previously we have found root as well as wood carbohydrate concentrations to be correlated across seasons when samples have been collected from panels of four vines (Holzapfel *et al.* 2009), suggesting that bulking samples across a number of adjacent vines is more appropriate method for assessing root reserve concentrations.

Spring growth requirements for carbohydrates are initially supported by stored reserves, with

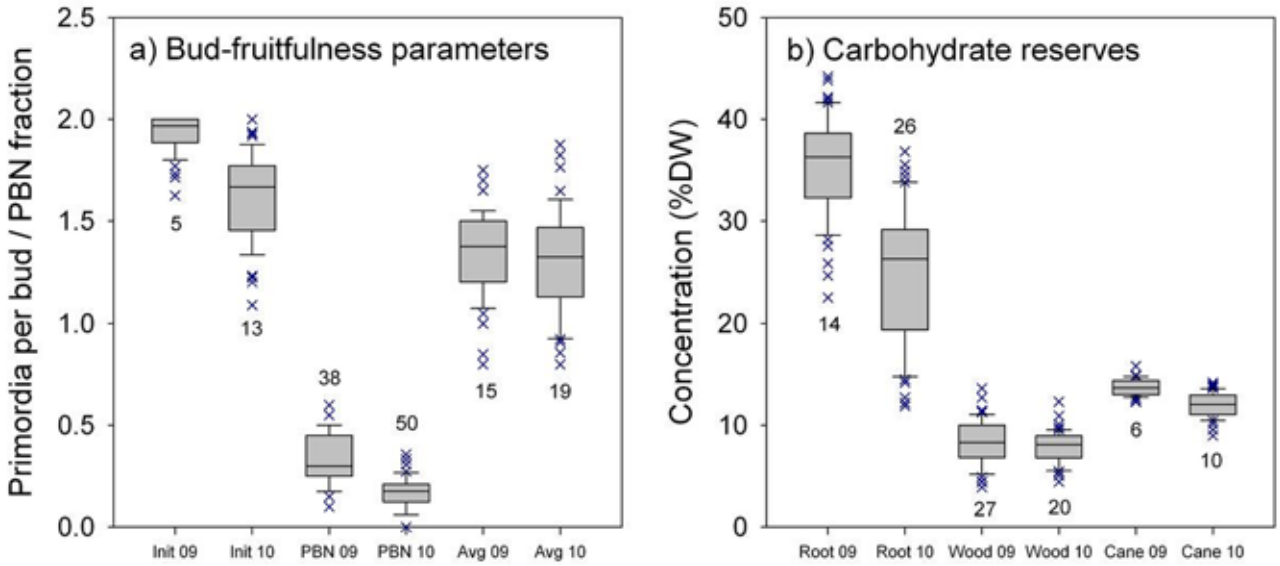


Figure 4.38 Summary bud-fruitfulness parameters for the 54 sample vines across the Yenda Shiraz trial site in winter 2009 and 2010 (a), and total carbohydrate reserve concentrations in root, wood and cane tissue at the same sampling date (b). Boxplots show 10th and 90th percentiles with outliers in blue, while numbers corresponding to each plot show the coefficient of variation (CV%).

mobilization reaching a maximum at the 8 to 10 leaf stage (Yang and Hori 1979; Yang and Hori 1980). If reserves are inadequately replenished prior to leaf fall, then shoot growth rates may be reduced during this period of high carbohydrate demand (Bennett *et al.* 2005; Smith and Holzapfel 2009). In the present study total carbohydrate concentrations in the wood were generally positively correlated with the canopy TVI, with wood reserves in winter 2009 showing a strong positive correlation with canopy density in the following spring (*Table 4.34*), and large canopies in spring 2008 and 2009 in turn associated with higher wood reserves in winter 2009 and 2010 (*Table 4.34*, *Figure 4.40*).

The positive correlation between wood reserves at dormancy in 2009 and canopy TVI in October of the following spring suggests that a measurement of wood reserves at the end of the season could provide a predictor of canopy growth potential in the following spring. In this study we did not find any correlations between carbohydrate reserve status and bud-fruitfulness values, but previous research suggests inflorescence flower numbers and bunch weights may be more responsive than bunch number to variations in carbohydrate reserve status (Smith and Holzapfel 2009 Holzapfel and Smith 2011). Therefore, while not providing a direct yield prediction tool, a measure of carbohydrate reserve status could give an indication of a vines capacity to express full yield potential in a given season. The positive relationship observed between the canopy TVI in spring and wood reserves at the end of the season in 2009 and 2010, and also between wood reserves across the two seasons, would also suggest that the spatial variability in reserve status may be self-sustaining.

ATR-FT-IR calibration for rapid measurement of starch and nitrogen reserves

Predictive models were successfully produced for nitrogen and starch, with an error of prediction of 0.08% DW (R^2=0.976) and 1.43% DW (R^2=0.950) respectively, that were independant of variety, tissue type and location of vineyard (*Figure 4.41*). The predictive models were tested using a process of cross validation and an independent test set of samples spanning the analytical range, and indicate that nitrogen and starch can be rapidly determined with high levels of accuracy. Calibration and validation of predictive models for the rapid determination of glucose, fructose and sucrose are in progress, and preliminary results suggest that ATR-FT-IR spectroscopy will also be suitable for the measurement of free sugars. Thus the quantification of total non-structural carbohydrates along with starch and total nitrogen will be able to be performed in approximately 60 seconds per dried and ground sample enabling high throughput data collection and vineyard monitoring.

Within season changes in starch concentrations of perennial tissues typically range between 2 and 30% DW, while nitrogen concentrations fluctuate between approximately 0.1 and 1.8% DW (e.g. Winkler and Williams 1945; Bates *et al.* 2002; Weyand and Schultz 2005; Treeby and Wheatly 2006). The concentration ranges observed between vineyards in the present study are in general agreement with these earlier works (*Figure 4.42*), and suggest that ATR-FT-IR spectroscopy presents a sufficiently accurate method to quantify changes in reserve storage between development stages. In the surveyed vineyards, the maximum seasonal fluctuations in nitrogen concentrations were 0.46, 0.17 and

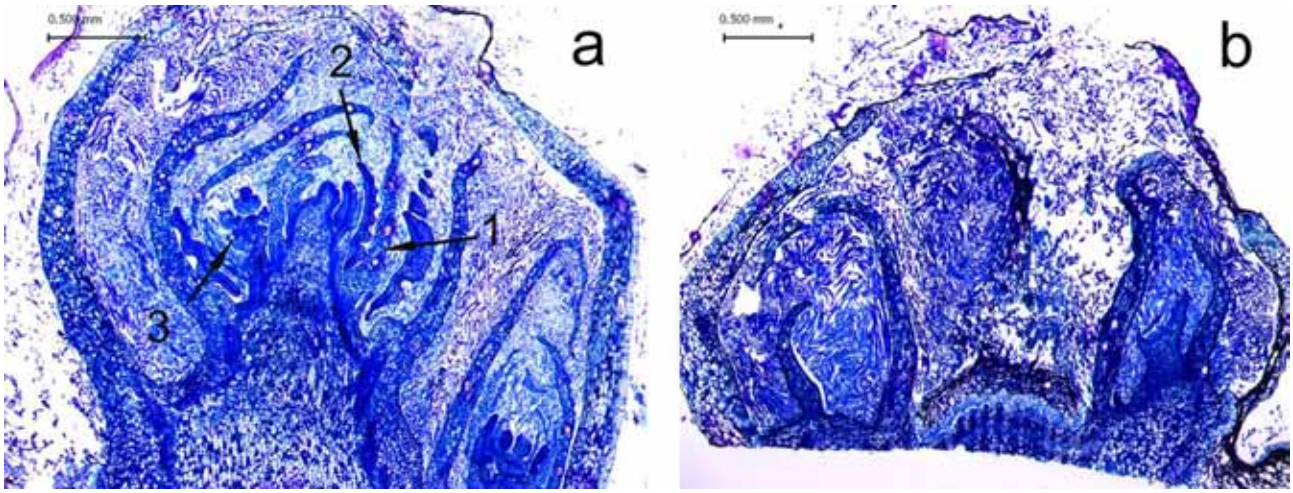


Figure 4.39 Stained sections of wax embedded Shiraz buds collected from the Riverina trial site on December 9 in 2009 showing a healthy bud (a), and bud from the same vineyard affected by primary bud necrosis (b). Numbered structures in the first image are stipules (1), leaf primordia (2) and inflorescence primordia (3).

0.52% DW respectively for the roots, wood and spurs (*Figure 4.42a*). For starch, the values were 14.0, 6.0 and 4.9% DW respectively (*Figure 4.42b*). Therefore, with a RMSEP of 0.06% DW for total nitrogen and 1.43% DW for starch, it would also be expected that the method would be sufficiently accurate to identify seasons where the replenishment of carbohydrate or nitrogen reserves has been significantly higher or lower than normal. Based on the sampling strategy employed during the carbohydrate reserve and fruitfulness survey, where five replicate panels of four vines were tagged and sampled each year, a change in root starch of 3.5% DW or more would be required for a statistically significant difference to be detected. For wood and cane starch the change between seasons would need to be 0.94% DW or higher. At this stage only nitrogen analysis for the cane tissue has been completed at the individual replicate level, and for this nitrogen reserve component a change

Table 4.34 Correlation matrix between remotely sensed canopy density measures (TVI) and various carbohydrate and bud fruitfulness measures. The photosynthetic biomass is determined by using TVI, the formatting indicates significance level p = 0.05 at r = ±0.225 (regular); p=0.01 at r = ± 0.312 (bold). Yellow highlight corresponds to *Figure 4.40*.

		TC09	PBN09	AVG09	PBN10	AVG10	RootTot09	WoodTot09	RootTot10	WoodTot10
TVI	17/10/07	-0.119	0.282	-0.308	0.158	-0.216	0.052	**0.408**	-0.208	0.185
TVI	17/12/07	0.238	0.243	-0.216	0.065	0.033	0.134	0.238	-0.105	0.277
TVI	19/02/08	0.233	0.201	-0.287	**0.353**	-0.046	**-0.328**	0.019	-0.138	0.249
TVI	31/03/08	0.066	-0.072	-0.040	0.207	-0.021	-0.217	-0.035	-0.091	0.083
TVI	15/10/08	-0.060	0.052	0.050	-0.222	-0.119	0.123	**0.521**	-0.310	0.226
TVI	25/11/08	0.265	0.125	-0.138	0.158	0.008	-0.237	0.256	-0.250	**0.416**
TVI	13/01/09	0.207	0.146	-0.190	0.107	0.009	-0.202	**0.397**	-0.227	**0.469**
TVI	17/03/09	0.106	0.163	-0.180	0.051	0.106	-0.127	0.308	-0.141	0.265
TVI	19/10/09	-0.074	0.102	-0.056	-0.006	-0.215	-0.032	**0.532**	-0.215	**0.370**
TVI	2/12/09	0.235	0.146	-0.132	-0.085	0.190	0.058	**0.405**	0.056	**0.409**
TVI	16/02/10	-0.016	0.100	-0.301	0.277	-0.037	-0.138	0.095	0.236	0.220
TVI	22/03/10	0.000	0.273	**-0.338**	0.279	0.053	0.140	-0.087	0.157	0.146

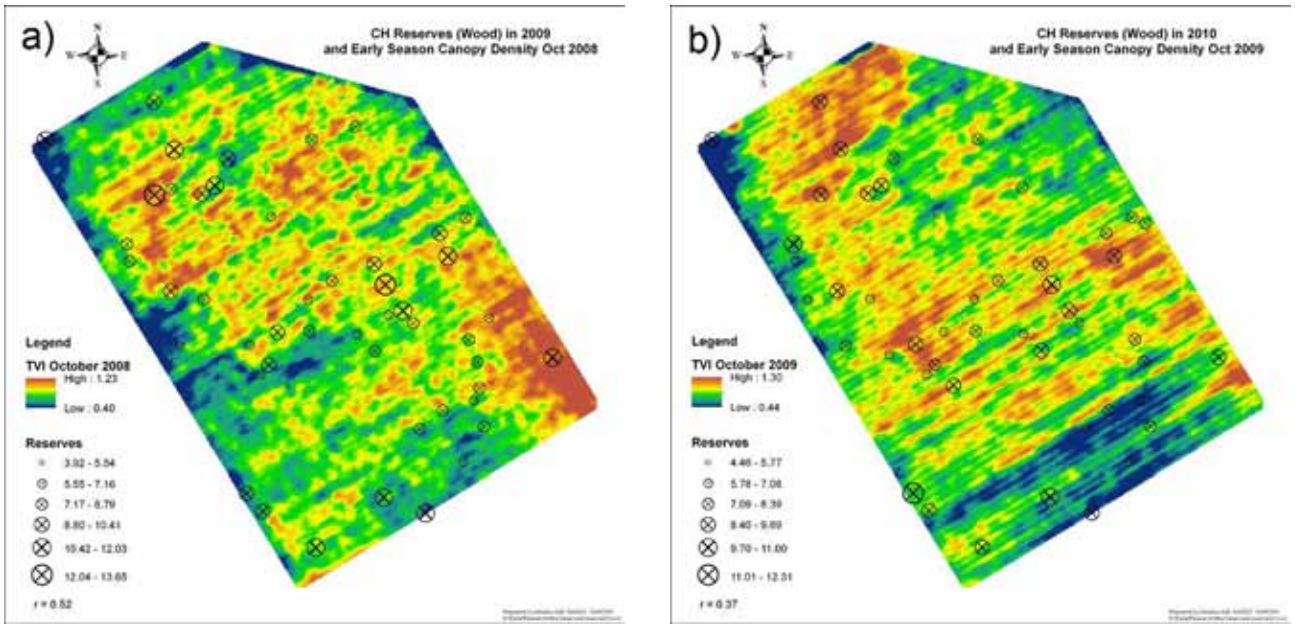


Figure 4.40 Relationship between canopy triangular vegetation index (TVI) in spring 2008 (a) and spring 2009 (a), with total carbohydrate reserve concentration (%DW) in the wood at the end of each season. Individual symbols show the location of the 54 sample vines.

of 0.06% DW or more would be required for a statistically significant difference.

Section 2

Carbohydrate reserve dynamics and net photosynthesis

Growth stage had the single largest effect on TNC concentrations, with changes between sampling dates accounting for 95% of the variation in the roots and 70% in the wood. Treatment×growth stage interactions accounted for only 3.4% and 9.1% of the variation in root and wood TNC concentrations respectively, while treatment effects alone explained less than 1% of the variation in the wood and none of the variation in the roots. Consequently, the total carbohydrate reserve concentrations have been averaged to highlight the differences between sampling dates and season (*Figure 4.43e*). Between bud-break and flowering in the 2007-08 and 2008-09 average total non-structural reserve concentrations of the roots, and to a lesser extent the wood, declined as carbohydrates were utilized to support early season growth. However, for the remainder of the season root reserve dynamics showed significantly different patterns of carbohydrate mobilization and storage. In 2008-09 root reserves increased between flowering and veraison, declined during the ripening period, and then increased again in the post-harvest period. Conversely, reserves continued to decrease between flowering and veraison in 2007-08 but then increased during both of the subsequent measurement periods.

The modelled values of net canopy photosynthesis, which have been presented here to show the relative difference between seasons (*Figure 4.43c*), suggest that until approximately half way through the ripening period carbon assimilation was generally higher in the 2008-09 season than in 2007-08. This suggests that the recovery of root reserves by veraison in the 2008-09 season may have been due to an increase in carbohydrate availability during this period. It has previously been shown that the mobilization of starch from the root system is significantly increased at warmer soil temperatures due to increased utilization for shoot growth, higher respiration or promotion of root growth (Field *et al.* 2009; Rogiers *et al.* 2011). Although soil temperature was not recorded at the site, 10 cm values at the nearest BOM weather station where the parameter was recorded (Wagga Wagga AMO) indicate that soil temperatures were warmer in the spring and early summer of 2007-08 than in 2008-09. Therefore, the combination of higher soil temperatures and lower net assimilation may have caused the greater depletion of root reserves following bud-break the first season. Wood reserves showed a similar trend, but the absolute difference in concentrations between seasons was small.

From approximately halfway through the ripening period, there was a distinct change in the net assimilation rate between seasons (*Figure 4.43c*). Whereas assimilation was higher prior to that point in 2008-09, there was a drop in net photosynthesis due to high temperatures in heat wave that was experienced across SE Australia in February 2009. The soil temperature difference also peaked at nearly 15°C higher during this period (*Figure 4.43d*), suggesting that reduced photosynthesis, carbohydrate demands from ripening fruit and increased root respiration may have all contributed to a decline in root reserves during the ripening period of the 2008-09 season. During the post-harvest the restoration of reserves was greater in the 2008-09 season despite similar modelled values for photosynthesis and slightly

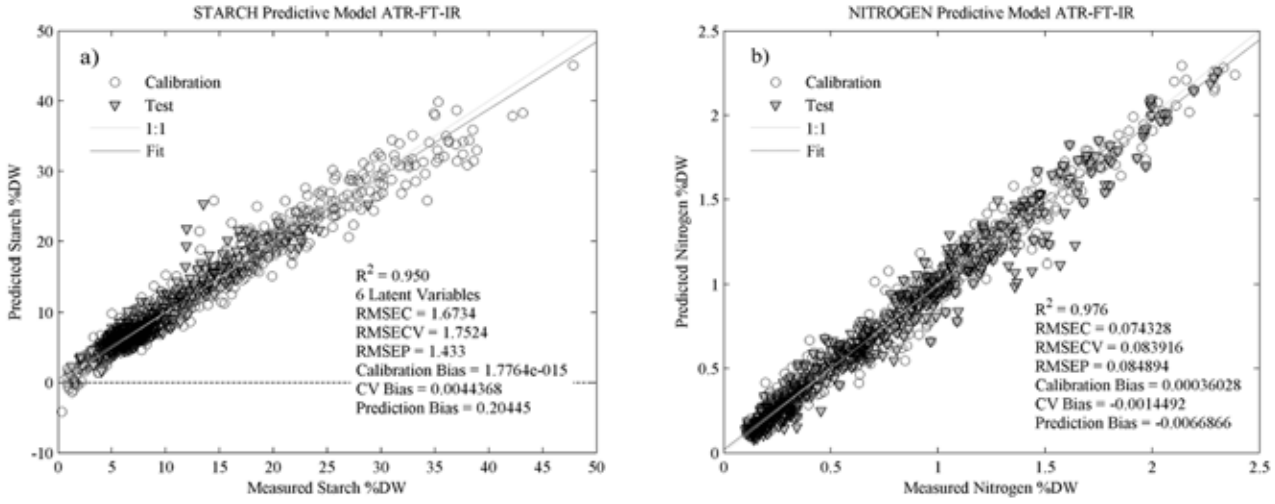


Figure 4.41 Predicted and measured values of total nitrogen (a) and starch concentration (b) of grapevine roots and wood (1 year, 2 year, trunk and cordon) from ATR-FT-IR spectra of dried ground tissue samples (n=1880).

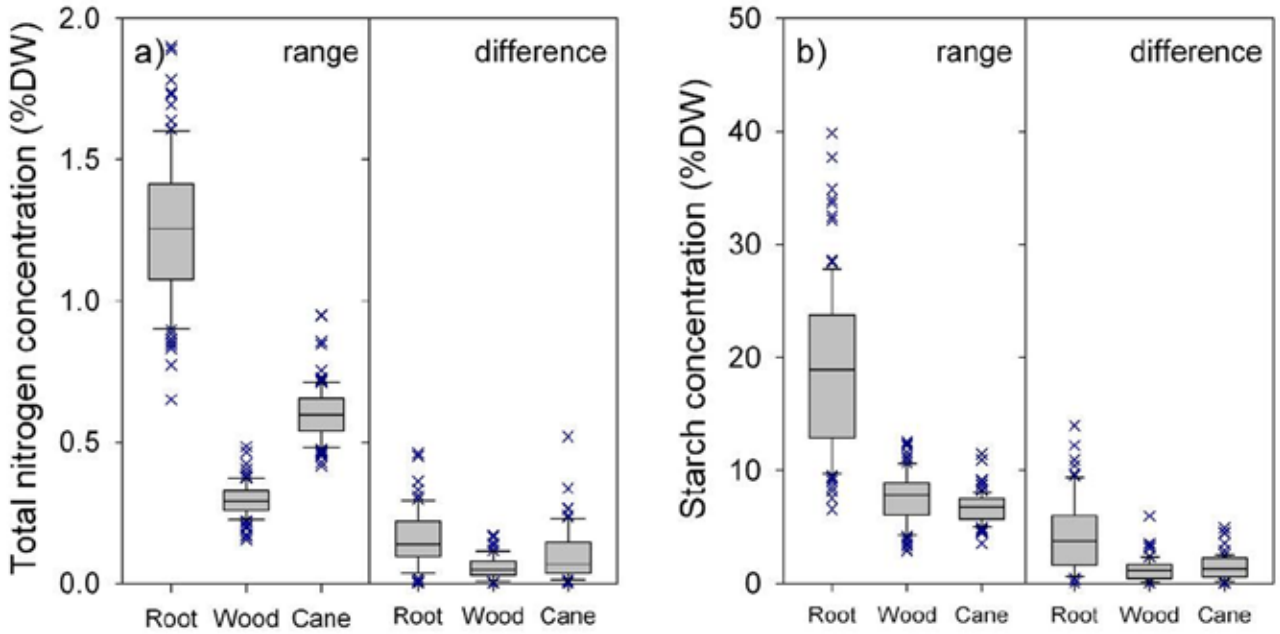


Figure 4.42 Summary of total nitrogen (a) and starch (b) concentrations measured at during winter at 32 vineyards over 3 seasons. Range indicates absolute concentration range (n=96), while difference indicates magnitude of change in concentration between seasons at each vineyard (n=64). Boxplots show 10th and 90th percentiles with outliers in blue.

warmer soil temperatures. This highlights a limitation of a model that takes no account of leaf age or the actual conditions of the canopy. However, the absence of any treatment effect on root reserve accumulation in the post-harvest period, and the differences in post-harvest reserve accumulation rates across seasons, suggest that climatic factors play a significant role in determining the extent of the post-harvest recovery.

Berry and wine composition

Despite the lack of treatment effects on root carbohydrate concentrations and minor impact on wood reserve dynamics, clear differences between fruit and in particular wine composition were observed (*Table 4.35*). In 2008 and 2009 the BR-66% treatment had both the highest wine colour density and tannin concentration, and in 2009 also had the highest sugar concentration at harvest. Wines were made from both bunch removal treatments in 2010, and these were again associated with higher sugar content at harvest (second date), and higher wine colour density and tannins. Water stress (in addition to the commercial RDI practice at the vineyard) caused a slight increase in colour and berry sugar content, but generally did not affect tannin concentration. The post-harvest deficit irrigation treatment significantly delayed sugar accumulation and colour development in 2008-09 due to reduced shoot growth and high crop load (not shown), but was similar to the control in the other two seasons.

The original intent of the bunch removal treatments was to promote a cumulative increase in reserve accumulation, and this was observed in the wood with an average increase of 7% after two seasons of treatment and 20% after three seasons (individual treatment data not presented). However, there was no effect on root reserve concentrations, and the estimated increase in reserve storage of 200–400 g DW vine^{-1} was significantly lower than the 1.3–2.5 kg vine^{-1} difference in berry sugar production between the thinned an control vines. The only other treatment to impact on reserve storage was the post-harvest hedging, and this only resulted in a transient reduction in wood reserves during the 2007-08 season. This was associated with a decrease in bunch numbers relative to control vines (213 compared to 156 vine^{-1}), and a lower yield which allowed reserves to recover by the end of the 2008-09 season. Neither water stress treatment had any effect on reserve concentrations or dynamics relative to control vines.

Previous studies have shown that reserve accumulation can be significantly altered with severe crop or leaf removal treatments (Bennett *et al.* 2005; Smith and Holzapfel 2009), but these recent findings imply there is less scope for manipulating carbohydrate reserve accumulation in the vineyard through moderate changes in management practice. Down regulation of photosynthesis following cluster removal has been reported by numerous authors (eg. Iacono *et al.* 1995, Naor *et al.* 1997), and it possible

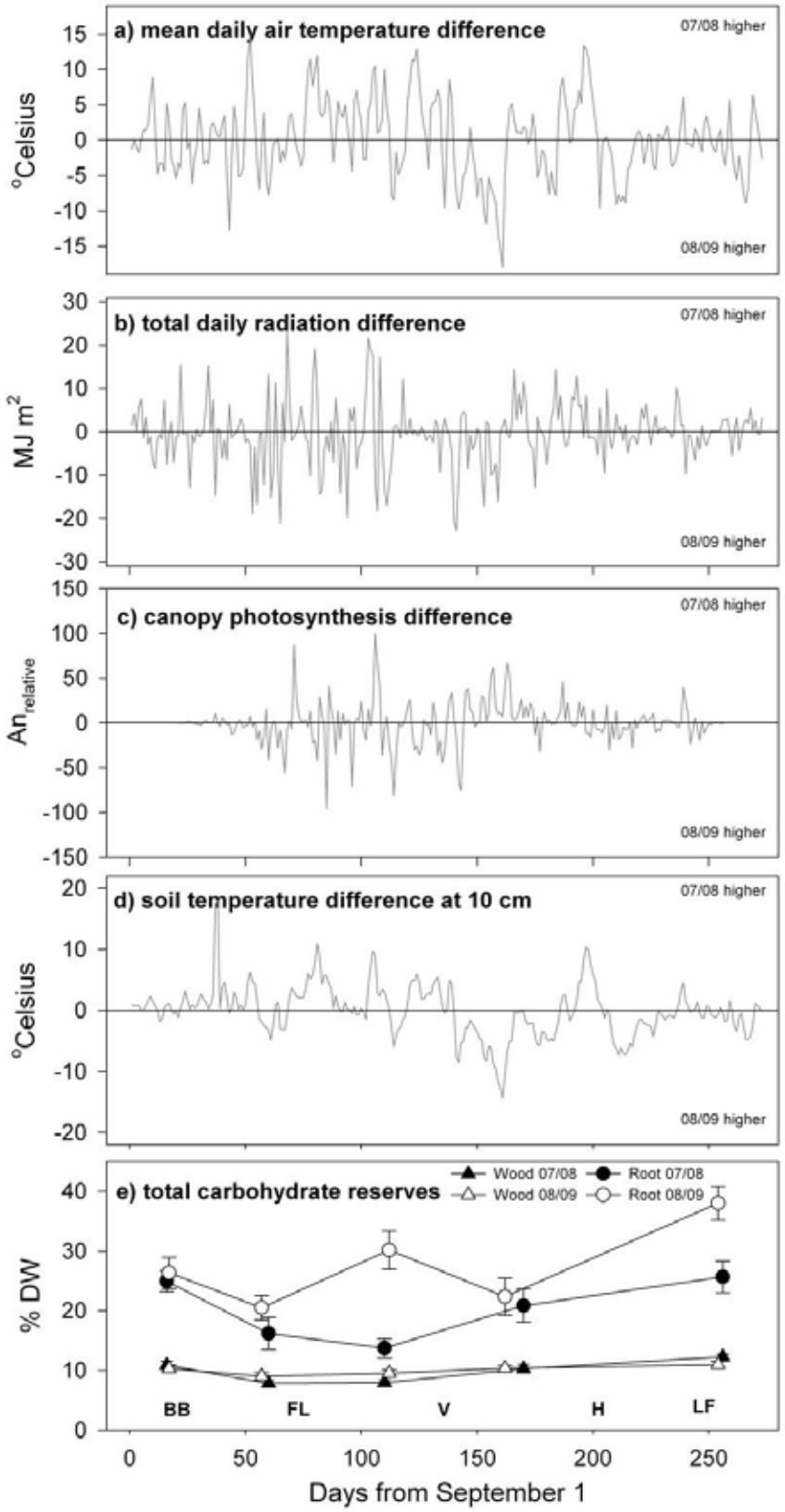


Figure 4.43 Comparison of seasonal difference in: (a) mean air temperature; (b) total radiation; (c) modelled canopy photosynthesis; (d) soil temperature; and (e) corresponding measured carbohydrate concentrations, for the Riverina Shiraz trial site in the 2007-08 and 2008-09 season.

Table 4.35 Impact of crop thinning (66% bunch removal at veraison) and deficit irrigation (flowering to fruit-set and post harvest) on berry sugar concentration at harvest, and the colour density and tannin concentration of wines make from 50 kg batches of fruit from each treatment.

	Berry sugar (°Baume)			Wine colour density ($A_{420}+A_{520}$)			Wine tannins (mg L^{-1})		
	2008 Feb 19	2009 Feb 10	2010 Feb 16	2008 Feb 19	2009 Feb 10	2010 Feb 16	2008 Feb 19	2009 Feb 10	2010 Feb 16
Control	13.6	12.8 ba	13.3	3.6 a	6.9 b	5.06	0.39 b	0.59 b	0.66
BR-33%			13.4			7.40			0.68
BR-66%	13.9	14.7 d	13.4	5.1 b	11.1 c	7.12	0.42 c	1.01 c	0.57
RI-PH	13.6	12.2 a	12.8	3.7 a	4.0 d	6.00	0.15 a	0.33 a	0.24
PH-Hedge			13.1			6.16			0.56
RI-PS	14.1	13.3 c	13.0	4.6 ab	7.0 b	6.34	0.38 b	0.63 b	0.48
	ns	***b	-	*	***	-	*	***	-

a Means separated within columns using Fisher's LSD test. Different letters within a indicate a significant difference (p=0.05).

b *, **, ***, and ns indicate significance at p<0.05, <0.01, <0.001 and not significant, respectively.

that the BR-33% and BR-66% treatment induced a similar response in our current study. Therefore, instead of diverting excess carbohydrates to reserve storage, the vines may have reduced their total carbon assimilation capacity in response to reduced demand from the fruit. Recently it has also been shown that stomatal density is responsive to the carbohydrate reserve concentrations of the perennial tissues (Rogiers *et al.* 2011). Therefore, vines with depleted reserves may respond to a perceived carbon limitation by increasing stomatal density of newly formed leaves, while a high reserve status may lead to the development of leaves with reduced stomatal density. Such mechanisms could provide the vine with sufficient flexibility in carbon assimilation capacity to buffer the effects of more moderate treatments on carbohydrate reserve dynamics, and provide some explanation as to why our treatments were not able to cause a substantial change in the prevailing pattern of carbohydrate reserve dynamics at the trial site.

Despite our inability to substantially alter reserve accumulation or dynamics, the differences in fruit and wine composition suggest the treatments (and bunch removal in particular) did have sufficient impact on internal carbon availability to influence berry development. The results of the 2007-08 and 2008-09 seasons initially suggested a cumulative improvement in wine colour and tannin concentration. However, in the 2009-10 seasons the colour and tannin concentrations decreased relative to the previous season, and the relative difference between treatments were also reduced. This finding suggests that like carbohydrate reserve dynamics, there may have been an overriding seasonal influence on berry composition in the 2007-08 and 2008-09 seasons.

The flavonoid pathway in developing grape berries is responsible for the production of anthocyanins, flavonols and tannins. Skin tannins are produced between flowering and veraison, flavonols around flowering and prior to harvest, while anthocyanins are produced from veraison onwards. Seed tannin production can continue for a few weeks after veraison, but the period between veraison and harvest is predominately one of tannin maturation (Downey *et al.* 2003). Ultimately the synthesis of these compounds is regulated at the gene level, and through the activity of associated enzymes. However, flavonoids are metabolically expensive to produce, and their amino acid precursor phenylalanine is derived from a pathway that utilizes 20% of the carbon fixed by plants (Haslam 1993). Consequently, the accumulation of anthocyanins, tannins and flavonols, and the flow of metabolites through these pathways, may be sensitive to the internal availability of carbon during their respective periods of production.

In the 2008-09 season our photosynthesis model indicated total carbon availability was higher than in 2007-08, and also that there may have been less demand for root reserves due either to the higher canopy assimilation or lower soil temperatures. Although we can't rule out the possibility that the differences in wine tannin concentration were related to the winemaking conditions, the winemaking protocol was identical in each season. Therefore, the possibility is raised that the higher tannin content across all treatments in the 2008-09 season was associated with increased carbon availability in the

period between flowering and veraison. The greater relative difference between treatments in 2008-09 might have then been due to the high temperatures through the February heat wave. During this period predicted net assimilation rates were lower than in 2007-08, and the mobilization or loss or carbohydrate reserves suggested the vines experienced a period of carbon deficit during this period. Unfortunately, we did not undertake sufficiently detailed analysis of the berry samples and wine to explain the difference in wine colour density between seasons. Berry colour of the control treatment each season did not differ significantly (data not shown), but the wine colour density was almost double in the 2008-09 vintage.

Structural canopy model

A preliminary grapevine model, with shoot growth and leaf appearance driven by thermal time, was produced to assess the potential application of L-Studio software for the development of a vine balance model (*Figure 4.44*). Functional-structural plant growth models using L-studio are becoming increasingly prevalent (eg. Allen *et al.* 2005; Cieslak *et al.* 2010), and further work will be undertaken at the NWGIC to produce a model that incorporates carbon acquisition and whole vine carbon balance. From an industry adoption perspective this approach to modelling has advantages in that the process can be better visualized, and parameters such as retained bud numbers quickly modified to match particular vineyards or proposed management changes. A negative aspect is a full carbon balance model can take a day to run a growth simulation for a full season (I. Auzmendi, personal communication), whereas the simple model presented in the previous section can be run in a much shorter time period.

Outcome and conclusion

Carbohydrate reserve dynamics

Measurements of carbohydrate reserves at dormancy may provide an indicator of canopy growth in the following spring, and also the capacity of the vine to express full yield potential as determined by the extent of inflorescence initiation and differentiation in the preceding season. To facilitate incorporation of a carbohydrate reserve test into commercial vineyard management practices or future yield forecasting models, a rapid ATR-FT-IR method was developed for starch (and also nitrogen reserves) in root, wood and cane tissue. Further work is required to quantify the effects of seasonal variation in reserve accumulation on vine productivity at the regional level. However, based on research carried out at the individual vineyard level, the ATR-FT-IR method and proposed sampling strategy based on permanently tagged replicated vine panels would detect changes in reserve storage below that expected to impact on canopy growth or reproductive development. In our earlier research, reserve accumulation, inflorescence initiation and primary bud necrosis were all found to vary at the regional level and work is currently underway to identify an approach by which direct measurement of the parameters at a regional level could be used a refinement for climate data based yield forecasting models.

Carbohydrate reserves: measurement versus management

Based on our previous research and additional analysis undertaken as part of the current project, we suggest that carbohydrate reserve dynamics are predominantly driven by developmental stage and climatic factors. Carbohydrate reserve mobilization or restoration can be manipulated in the vineyard, but severe defoliation or crop removal treatments



Figure 4.44 Cross section of a Shiraz canopy in the CSU vineyard (a) and a preliminary version of the same canopy produced using L-Studio (Guissard, Smith, Holzapfel and Hannan, unpublished).

appear to be required to achieve this. For more realistic management practices such as crop thinning or deficit irrigation, there appears to be little scope to deliberately alter carbohydrate reserve status in the shorter term. However, changes in carbohydrate reserve concentrations between growth stages may be a directly measurable indicator of variability in internal carbon availability during the growing season. In the previous section we described a rapid method for assessing starch concentrations in perennial tissues, and expect that the technique will also be suitable for the free sugar fraction of the non-structural carbohydrate reserves. Measurement of over-wintering reserves has considerable potential as a predictor of canopy growth and yield potential if a database is complied over multiple seasons. However, measurements of reserve dynamic during the season may be a predictor of fruit quality, or at least provide an indicator of when crop load adjustments would result in a fruit quality response.

Grapevine balance model

At the present there is insufficient knowledge of the physiological processes underlying flowering and berry development for models to make accurate yield or fruit quality predictions. However, with the ability of existing models to accurately simulate photosynthesis (eg. Schultz 2003), and the availability of software to model canopy structure in three dimensions, the ability to estimate the likely effects of weather conditions or water availability on net photosynthetic capacity could in itself be a valuable management tool for growers. Our concept for a vine balance model is one that allows parameters such as trellis shape, shoot numbers, shoot length, trunk / cordon volume and bunch weight to be directly entered in the model. These are parameters that can be directly measured, and in software such as L-Studio, factors such as shoot bending or leaf angles can also be changed with relative ease such that the model could start with a canopy that was a realistic representation of the vineyard of interest. Defining such parameters would then reduce the complexity and computing time of the model, and allow more effort to be placed on accurately quantify the effects of weather conditions or management changes on net carbon availability. We suggest that a model could start at the end of the active shoot growth period where the size of the canopy and potential crop load is already known. Hourly or daily time step photosynthesis calculations could then be made depending on the availability of weather data, and air and soil temperature effects on respiration also determined. Direct measurements of stored reserves could provide an additional starting input to the model, and if these were made again later in the ripening period provide a method for validating the model output. It is known that reserves can be mobilized to support berry ripening, but the consequence for secondary berry metabolite production is unknown. The challenge also remains to relate the internal carbohydrate availability to berry composition and ripening rate. In the preliminary model output data shown in this report we have presented net canopy photosynthesis in a manner that highlights the differences between seasons. It is proposed that such an approach, whereby seasons are compared and related to fruit composition, may offer grape growers with a chance to predict seasonal variations in fruit composition and provide some advanced warning for management intervention in the vineyard.

Outcomes/conclusions

Theme outcomes

	Outcome	Achieved
1	Compare use of different moisture sensors to schedule irrigation and develop case studies showing how to get the best out of them in terms of water management and crop performance for a range of soil/cultivar/ vine age combinations	Y
2	Reduce environmental and ecological impacts of irrigation and fertiliser practices per unit production	Y
3	Reduce water inputs per unit production	Y
4	Model grapevine yield using spatial analysis tools.	Y
5	Predict grapevine yield using spatial analysis tools	Y*
6	Identify zonal variability within vineyards: vigour zones and quality zones.	Y
7	Reduce zonal variability within vineyards: management zones	Y
8	Offer cost savings in comparison to existing industry best-practice	Y
9	Make data available to CSIRO for further development (i.e. VineLOGIC).	In progress

Theme outputs

	Output	Achievement
1	Dissemination of results through written publications and extension programs such as On-Farm Trials, RITA demonstration sites, Research to Practice Training and integration into customised MIA EnviroWise® courses in conjunction with Murrumbidgee Irrigation (MI).	Where possible
2	Report outcomes from CRV Theme S2.3.6 (December 2006).	Achieved
3	Six industry/technical articles across lifetime of theme	Exceeded - 13
4	Five refereed journal articles across lifetime of theme.	Exceeded - 14
5	Presentations at Australian Wine Industry Technical Conferences (2007 and 2010).	Achieved
6	Presentations at the annual NWGIC Industry Symposium (2007 to 2010).	Achieved
7	Presentations to industry associations in the theme regions and at NWGIC Road shows	Achieved
8	Undergraduate training of students enrolled in CSU wine science and viticulture degree courses.	Achieved – 12 seminars/ lectures/ workshops
9	Short course and certificate programs offered as part of training programs offered by the NWGIC and its partner organizations in various wine regions.	Achieved
10	Postgraduate training of students enrolled in higher degrees at CSU (coursework Masters and research degrees).	1 PhD student trained

Theme milestones

	Milestone	Achieved
1	Form technical advisory panel and complete site selection (September 2006)	Y
2	Develop uniform soil moisture depletion system (June 2007 and 2008).	Y
3	Recommend options to manage zonal variability of yield and quality (Annual update in December 2008, 2009 and 2010.	Y
4	Yield models evaluated (March 2009, June 2009, March 2010, June 2010 and March 2011).	Y
5	Develop threshold values for water volume and soil nutrient export to be incorporated into a viticultural EMS (June 2010).	N*

* WFA moved away from advocating an EMS approach but the information is available

Recommendations

The results from the projects conducted in this Theme have shown the interactive effects of irrigation and N fertiliser management on movement of soluble N, which ultimately affects wine quality and losses beyond the vineyard system due to leaching. It is essential for vineyard managers to monitor and analyse their management strategies and the possibilities of these decisions affecting overall vineyard sustainability.

The original aim to incorporate the results from this work into the industry-wide EMS VERA (Viticare Environmental Risk Assessment), was not progressed with the approval of the Steering Committee after the wine sector's peak body the Winemakers' Federation of Australia adopted a different approach viz. Entwine. Nevertheless we strongly recommend the continuing promotion of best practice recommendations, benchmark indicators and monitoring procedures (see Appendix 9, Other Relevant Materials), arising from this research in this Theme as part of the ongoing development of regional best management practices and environmental risk management guidelines.

The research in this Theme was confined to warm, wholly irrigation-dependent vineyards in the Riverina. We envisage further requirements for development of regionally specific water and nutrition management practices and indicators, adapted for regional soil and climatic conditions, and driven by regional groups across Australia. We recognise strong synergies between soil nutrition and water management and the biological qualities of soil for grape and wine production and strongly recommend that these aspects be researched simultaneously from a regional perspective.

Aerial remote sensing for yield forecasting

Targeted sampling through the use of EM38 soil or aerial canopy surveys lead to better prediction of yield and fruit quality

Selecting samples using the spatial information produced significantly lower errors than selecting samples purely randomly. Approximately half the number of samples collected using the spatial information was required to attain the same level of error that would have been produced had the sample locations been selected randomly. The total error, however, was still high, reflecting the high degree of variability common in vineyard blocks. A high number of samples are still required to reduce the confidence interval of an estimate of yield or TSS. A method of adjusting yield estimates from data collected using a consistent sampling system to produce accurate absolute estimates of yield harvested using a consistent method was also achieved.

Uptake of new technology enables greater understanding of vineyard variability

Through the development of a row-crop image-segmentation algorithm, grapevine canopy vigour was quantified at the individual grapevine scale at two vineyard sites that were subject to high spatial resolution optical remote sensing four times per year over three years. Measures of vegetative canopy vigour at the individual grapevine scale, derived using a set of remote sensing vegetation indices that could be calculated from a basic 4-band imaging system, were found to correlate with fruit composition and yield variables at a level to enable vineyard maps derived from the algorithm to be potentially useful tools for predictive mapping of winegrape quality, yield and ripeness. This study has demonstrated that caution should be exercised when making predictions about winegrape composition and yield based on remotely sensed canopy data due to apparent inconsistency in correlation strengths caused by different vineyard characteristics, especially pruning method and consequent canopy size.

Vegetation indices that are more sensitive to high photosynthetic biomass levels (e.g. the triangular vegetation index) are more suitable for precision viticulture practice

An investigation into various vegetation indices for their ability to most accurately describe canopy characteristics in terms of enabling predictive mapping of yield and composition data, demonstrated the triangular vegetation index (TVI) to be superior. Vegetation indices sensitive to differences in dense vegetation, including the enhanced vegetation index, were stronger predictors than the traditionally used normalised difference vegetation index or the simple ratio. Two canopy measures produced in previous studies on vineyard remote sensing were similarly assessed. Canopy metrics based on "vegetation abundance", a measure estimated by a partial spectral unmixing procedure, performed strongly in the vineyard that had overall lower vegetative vigour, producing the greatest number of significant correlations with fruit yield and composition, but produced relatively poor predictions in the high vigour vineyard. A vine canopy size measure, which

does not contain detailed information on canopy variability, performed relatively poorly. The only index that did not include any information on reflectance in the near-infrared spectral band, the visible atmospherically resistant index, produced canopy vigour measurements that correlated least with fruit yield and composition, but may still be useful when near-infrared bands are not available in basic imaging systems.

Imagery acquired at veraison confirmed as most valuable information for yield and quality forecasting

Analysis of canopy vigour descriptors derived from the TVI correlations with winegrape quality, yield and ripeness indicators revealed a degree of inconsistency in correlation strength that appeared to be affected by vineyard type and phenological stage. With all seasons' data combined, at both sites, the strength of correlations peaked at veraison, the time at which most seasonal canopy growth ends, and declined after harvest with the onset of senescence. Images produced early in the season, during early canopy development, were also less likely to correlate with harvested fruit yield and composition variables than imagery acquired around veraison. In the machine-pruned larger canopy vineyard, strong positive correlations with yield and negative correlations with the quality-indicating fruit descriptors, anthocyanin and total phenolic content, were observed, which was consistent with previous studies.

Trellising systems that allow for large canopy growth are more suitable for remote sensing data collection

In the spur-pruned smaller canopy vineyard, however, these relationships were significantly weaker and less consistent. A possible contributory reason for this was the relative size of canopy. Higher canopy to inter-row space pixel ratios, in the machine-pruned vineyard provided a more accurate average measure for each canopy unit.

Unusual events during a season lowers yield forecast skill

The data suggested that inter-annual variability in correlation strength may also be affected by significant deviations from mean annual production. In particular, fruit total soluble solids correlated with the remotely sensed canopy descriptors in lower yielding years only.

Incorporating data from the previous season adds considerable skill to yield forecasting models

A best subsets regression using up to three of the canopy descriptors and/or yield from current and previous season as predictor variables delivered a model that explained 69% of the spatial variance in yield. This suggests that extra information about spatial variability in grapevine yield may be contained in canopy descriptors acquired at more than one occasion over the previous two years before a harvest. Overall, this study suggests that improvements in grape yield forecasting at the vineyard block scale through the application of remote sensing technologies are achievable.

There are functional differences between common temperature indices

Season total growing degree-days (GDD) was nearly functionally identical to growing season temperature (GST), as both indices were calculated using average daily temperature data only. The Huglin Index (HI) was functionally similar to GST and GDD, but varied for some regions because it uses an estimate of daytime temperature (instead of average diurnal temperature) and includes a modification to account for day-length, which varies by latitude. Biologically effective degree-day (BEDD) totals were the most different to the other indices because of the cap placed on the number of degree-day units that can be accumulated on any one day. This resulted in the rate of increase in the BEDD with respect to increases in the other indices slowing at higher temperatures. A consequence of the dissimilarity amongst the indices is that descriptions of temperature regime differences between the same region pairs can vary depending upon what index is employed.

In selecting an index most suitable for indicating economically sustainable winegrape production, there appears to be no advantage in using the indices with more complex formulas than simple average growing season temperature. Capping the heat accumulation component of the biologically effective degree-day index to 9°C, renders the BEDD insensitive to increasing temperatures in already warm regions and would therefore be the least suitable for climate change modelling. Latitude adjustments incorporated within both the Huglin Index and the BEDD are however, likely to be valuable at providing values closer to the actual daily mean temperature, and therefore more representative of a region's viticultural suitability. The Huglin Index

does not include a cap on heat accumulation but does include a latitude adjustment factor so is perhaps the most suitable of the four indices for viticultural climate change impact studies. The HI does not include the seventh warmest month (April/October in the Southern/Northern Hemisphere), which is of value when determining limits of production in cool regions. Perhaps the best solution would be an index with the basic simplicity of the GST (of the seven warmest months), but modified for latitude, achieved by simply multiplying the GST by *K* (Eqs. 24-27). To more fully describe the potential suitability of a climate type for long-term commercially successful winegrape production, accompanying indices that describe spring frosts and extreme heat could also be determined, such as the temperature variability index, spring frost index or heat stressfulness index (see Gladstones 1992; Gladstones 2004).

Climate anomaly data are valuable for winegrape yield forecasting

All other things being equal, climate variability is the driver of the variability of grape yields. However, many factors come into play to cause fluctuations in grape yield besides climate. Since it is the aim of the research presented in this section to determine short-term (inter-annual) climatic factors that affect yield, it is necessary to eliminate factors other than climate that cause yield fluctuations. External markets and demand have a large influence on the price paid for and hence the profitability of grapes. A loss of demand for a particular variety may lead to growers deciding it is not worth maintaining vines of that variety to produce a viable crop. Money otherwise spent of irrigation water, fertilisers, herbicides, canopy management, etc. is deemed to be less than what will be received for grapes produced from that vineyard. Harvesting of grapes may even be abandoned at the end of season, because the cost of harvesting is greater than the value of the crop that would be produced. Nevertheless, we have so far demonstrated that about 50% of the variability in the data can be explained using climate anomaly data. With standard methods for collecting climate data on a large spatial scale, quantitative forecasts of yield were shown to be possible, albeit with a large potential error. The ground work has been laid for similar analysis of Cabernet Sauvignon and Shiraz yield along with yield predictions for 2008-2010 actual yields using the 1982 -2007 climate data.

Future research should concentrate on carbohydrate storage and utilisation in order to inform vineyard management that would eliminate much of the year-to-year variability in yield, thus eradicating the need for yield forecasting

Forecasting grapevine yield is difficult due to the inherent spatial and temporal variability currently exhibited within vineyards. Although accurate estimates (±5%) can be achieved, the process requires much time and requires uncommon technical skills. Much of the research presented in this report contains results that infer clear influence of grapevine carbohydrate storage/utilisation/depletion on yield. Understand grapevine carbohydrate dynamics in order to manage vineyards to stabilise yield.

The work undertaken in Project 4.5 has further consolidated and extended the findings of project CSU 05/01 'Management of carbohydrate reserve accumulation as a tool for regulating vine productivity and fruit quality'. One area of research focused on within season carbohydrate reserve dynamics, and whether changes in concentrations between developmental stages may offer an insight into the impact of management and climatic factors on internal carbon balance and the cropping capacity of vines within a particular season. A second component of the research concerned reserves as a yield forecasting tool, and whether a measure of carbohydrate reserve concentrations at key developmental stages may provide growers with an advanced indication of yield and canopy growth potential in the following season.

Overall it was found that the pattern of carbohydrate reserve dynamics, and the amount of reserves stored by leaf-fall, can vary significantly between seasons. Carbohydrate mobilization can be manipulated by management intervention, but within and between season variation appears to be predominately determined by developmental stage and climatic factors. Preliminary modelling suggests that the seasonal variations in fruit composition and perennial tissue reserve concentrations are associated with variations in carbon assimilation capacity, and that stored reserves can be mobilized to support berry ripening during periods of reduced photosynthesis. High winter carbohydrate concentrations have previously been associated with increased shoot vigour and yield, suggesting that an adequate replenishment of reserves is required to attain full growth and yield potential. However, during the processes of initiation, inflorescence branching and fruit-set, reserves

appear to compete with reproductive development for carbohydrates. Measurements of reserves within a season may give an indication of yield potential in the following season. Winter carbohydrate reserve concentrations may provide an indication of vine capacity to support shoot growth and express full yield potential in the following season.

The NWGIC extension team has recognised specific topics arising from this Theme of high interest for future workshop presentation.

- Irrigation and nutrient management in vineyards
- Application of nutrient modelling to better understand fertigation and irrigation strategies.
- EMS risk management of nutrients in surface and ground water runoff.
- Use of remote sensing as a tool for vineyard management (precision viticulture)
- Use of remote sensing for yield and crop estimation could be limited but other more conventional crop estimation techniques could be further extended.
- Data from remotely sensed yield estimation trials show a very clear story in variation across a site for vigour, yield, quality and soil. This is complemented with wine-making from sections of the vineyard showing these variations.

Specifically we recommend further research to:

- Validate and facilitate the use of deep drainage measurement in a broad range of Australian viticultural soils.
- Define grapevine water use in terms of vine balance within different regional environments ('terroirs')

Appendix 1
Communications

Refereed articles

Barlow, K., Bond, W., Holzapfel, B., Smith, J. and Hutton, R. (2009). Nitrogen concentrations in soil solution and surface run-off on irrigated vineyards in Australia. *Australian Journal of Grape and Wine Research* **15**: 131-143.

Guisard, Y., Birch, C. J. and Tesic, D. (2010). Predicting the leaf area of grapevines (*Vitis vinifera* L.) cvs Cabernet Sauvignon and Shiraz *American Journal of Enology and Viticulture* **61**: 272-277.

Hall, A. and Jones, G.V. (2009). Effect of potential atmospheric warming on temperature based indices describing Australian wine grape growing conditions. *Australian Journal of Grape and Wine Research* **15**: 97-119.

Hall, A. and Jones, G.V. (2010). Spatial analysis of climate in wine grape growing regions in Australia. *Australian Journal of Grape and Wine Research* **16:** 389-404.

Hall, A., Lamb, D.W., Holzapfel, B. and Louis J. (2011). Within-season temporal variation in correlations between vineyard canopy and wine grape composition and yield. *Precision Agriculture* **12**: 103-117.

Hall, A. and Louis, J. (2009). Vineclipper: A proximal search algorithm to tie GPS field locations to high resolution grapevine imagery. In: *Innovations in* Remote *Sensing and Photogrammetry.* Eds. S. Jones and K. Reinke, (Springer, Berlin Heidelberg), pp. 361-372.

Hall, A., Louis, J. and Lamb, D.W. (2008). Low-resolution remotely sensed images of wine grape vineyards map spatial variability in planimetric canopy area instead of leaf area index. *Australian Journal of Grape and Wine Research* **14**: 9-17.

Holland, J. and Charlton, P. (2010). Transfer function modelling of bromide under drip irrigated vines. *Soil Science Society of America Journal* (submitted)

Holzapfel, B., Field, S., and Mueller, M. (2008). Nitrogen and water management implications on grape production in the Riverina wine grape regions of South Eastern Australia. *Le Bulletin de le Organisation Internationale de la Vigne et du Vin* **81**: 17-25.

Holzapfel, B.P., Smith, J.P., Field, S.K. and Hardie, W.J. (2010). Dynamics of carbohydrate reserves in cultivated grapevines. *Horticultural Reviews* **36**: 143-211.

Jones, G.V., Duff, A., Hall, A. and Myers, J. (2010). Spatial analysis of climate in wine grape growing regions in the western United States**.** *American Journal of Enology and Viticulture* **61:** 313-326.

Jones, G.V., Moriondo, M., Bois, B., Hall, A. and Duff, A. (2009). Analysis of the spatial climate structure in viticulture regions worldwide. *Le Bulletin de le Organisation Internationale de la Vigne et du Vin* **82**: 507-518.

Smith, J.P. and Holzapfel, B.P. (2009). Cumulative response of grapevine (*Vitis vinifera L.*) To Late season perturbation of carbohydrate reserve status. *American Journal of Enology and Viticulture* **60**: 461-470.

Smith, J.P. and Holzapfel, B.P. (2011). Developmental stage and climatic factors impact more on carbohydrate reserve dynamics of Shiraz than cultural practice. *American Journal of Enology and Viticulture* (submitted).

Technical reports and industry journal articles

Hall, A. and Hardie, W.J. (2008). Using precision viticulture to improve grape yield forecasting. *Australian and New Zealand Grapegrower and Winemaker* **538**: 20-24.

Holzapfel, B.P. and Smith, J.P. (2009). The relationship between vine carbohydrates and reproductive development. *Australian Viticulture* **1**: 56-57.

Quirk, L.F., Smith, J., Holzapfel, B., Holland, J., Hutton, R. (2008). Monitoring Soil nutrient in irrigated Chardonnay vineyards of the Riverina, NSW. *Australian and New Zealand Grapegrower and Winemaker* December 50-51.

Research Conference – Papers and/or Presentations

Barlow, K. and Nash, D. (2008). Managing the risk of nitrogen leaching from vineyards using a Bayesian network for decision analysis. Soils 2008 Conference, Palmerston North, New Zealand, 1-5 December 2008.

Hall, A. (2009). Forecasting grape yield with high spatial resolution optical remote sensing presentation at: 8th International Symposium of Information and Technology for the Sustainable Production of Fruit, Vegetables, Nuts, Wines and Olives. Frutic 2009, Concepción, Chile, 06/01/09.

Holland, J. and Charlton, P. (2010). The effect of applied irrigation volume and antecedent soil moisture on bromide movement in a drip irrigated vineyard. World Congress of Soil Science, Brisbane, Australia.

Holzapfel, B., Hall, A. and Smith, J. (2010). Impact of Management Practice and Environment on Carbohydrate Reserves and the Implications for Grape Production. 7th International Cool Climate Symposium, Seattle, Washington, USA, June 20-22.

Holzapfel, B., Smith, J., Hutton, R. and Holland, J. (2010). Nitrogen management in irrigated vineyards in SE Australia. International Intervitis Interfructa Conference, Stuttgart, Germany, March 24-28.

Holzapfel, B. and Smith, J. (2011). The influence of various management practices on nitrogen reserves of the perennial structure in Shiraz grapevines in South-Eastern Australia. Proceedings of the XVIIth International Symposium GIESCO, Asti – Alba, Italy, August 29 – September 2, 427-430.

Smith, J., Quirk, L., Müller, M., Schmidke, L. and Holzapfel, B. (2011). Variation in starch and nitrogen reserve storage by grapevines and measurement by ATR-FT-IR spectroscopy. Proceedings of the XVIIth International Symposium GIESCO, Asti – Alba, Italy, August 29 – September 2, 263-266.

Leaflets / brochures / technical guides

Hall, A., Quirk, L., Wilson, M. and Hardie, J. (2009). Increasing the efficiency of forecasting wine grape yield by using information on spatial variability to select sample sites, *Grapevine Management Guide 2009-10* (National Wine and Grape Industry Centre, Wagga Wagga) pp.11-12.

Holland, J. (2009). Where is all my phosphorus? A brief update on P in vineyard soils. *Grapevine Management Guide 2009-10* (National Wine and Grape Industry Centre, Wagga Wagga) pp. 24-25.

Holland, J. Charlton, P. and Wilson, M. (2010). Investigating the effect of drip emitter rate on the movement of mobile nutrients through drip-irrigated vineyard soils. *Grapevine Management Guide 2010-11* (National Wine and Grape Industry Centre, Wagga Wagga) pp. 31-32.

Holzapfel, B.P., Quirk, L., Hutton, R. and Holland, J. (2009). Wine grape nutrition and use of fertilisers and other nutritional supplements to sustain production. *Water and Vine - Managing the Challenge.* Technical Notes and Fact Sheet.

Holzapfel, B., Smith, J.P., Hutton, R. and Hackett, S. (2010). Nitrogen management in Chardonnay vineyards in the Riverina. *Grapevine Management Guide 2010-11* (National Wine and Grape Industry Centre, Wagga Wagga) pp. 25-28.

Holzapfel, B., Smith, J.P. and Quirk, L. (2010). Vineyard management effects on Shiraz vine performance and grape composition. *Grapevine Management Guide 2010-11* (National Wine and Grape Industry Centre, Wagga Wagga) pp 22-24.

Smith, J., Holzapfel, B., Hackett, S. and Hutton, R. (2006). Matching nutrients and other nutrients inputs to vine requirements. *Grapevine Management Guide 2006* (National Wine and Grape Industry Centre, Wagga Wagga) pp. 58-60.

Smith, J., Quirk, L., Field, S., Müller, M .and Holzapfel, B. (2009). Understanding the importance of the post harvest period in hot – climate vineyards. *Grapevine Management Guide 2009-10* (National Wine and Grape Industry Centre, Wagga Wagga) pp. 13-17

Smith, J.P., Quirk, L and Holzapfel, B. (2010). Fruitfulness assessments and primary bud necrosis of grapevines. *Grapevine Management Guide 2010-11*, National Wine and Grape Industry Centre,WaggaWagga. pp. 11-15.

Industry conference and workshop presentations

Hall, A. (2007). Space: the final frontier for grape yield forecasting? Winegrowing Futures Steering Committee meeting – Hunter Valley, Cessnock. 29/10/07.

Hall, A. (2007). Space: the final frontier for grape yield forecasting? NWGIC Industry Advisory Board meeting, Wagga Wagga. 12/11/07.

Hall, A. (2008). Grapes in space: Precision viticulture and yield forecasting. Mudgee Wine and Grape Growers Association, Mudgee, 30/4/08.

Hall, A. (2008). Grapes in space: precision viticulture and vineyard sampling. North East Victorian Grapegrowers and Winemakers Association, Charles Sturt University, Thurgoona, 11/7/08.

Hall, A. (2008). Grapes in space: precision viticulture and vineyard sampling : Hanwood Growers Association, Catholic Club, Hanwood, 21/10/08.

Hall, A. (2008). Grapes in space: precision viticulture and vineyard sampling. Yarra Valley Wine Growers Association, Healesville, 26/11/08.

Hall, A. (2009). Effect of potential atmospheric warming on temperature based indices describing Australian wine grape growing conditions. National Wine and Grape Industry Centre Seminar Series, Ron Potter Centre, Wagga Wagga. 21/1/09.

Hall, A. (2009). Effect of potential climate change on Australian wine grape growing conditions. National Wine and Grape Industry Centre Extension Managers meeting, Ron Potter Centre, Wagga Wagga, 15/4/09.

Hall, A. (2009). Vineyard sampling for yield estimation Riverina Field Days, Griffith, 8/5/09.

Hall, A. (2009). Climate change projections for regional Australia. Riverina Field Days, Griffith, 9/5/09.

Hall, A. (2009). Climate change projections for viticulture in the Canberra district. Murrumbateman Grapegrowers Association, Murrumbateman, 11/5/09.

Hall, A. (2009). Targeted vineyard sampling for accurate yield estimation and some climate change projections for Australian viticulture. Orange region Vignerons Association, Orange, 20/5/09.

Hall, A. (2009). Understanding the enhanced greenhouse effect is easy… forecasting temperature change effects on grapevines is not so easy. Department of Innovation, Industry, Science and Research "Science in the Bush", Charles Sturt University, Wagga Wagga, 22/6/09.

Hall, A. (2009). Warming scenario modelling of viticulture-region climate indices. GWRDC Climate Change Workshop, Wine Innovation Cluster, Adelaide. 12/10/09.

Hall, A. (2010). Within-season temporal variation in correlations between vineyard canopy and wine grape composition and yield. NWGIC seminar series, Ron Potter Centre, Charles Sturt University. Wagga Wagga, 3/3/10.

Hall, A. (2011). Climate change and impacts on NSW regions. NWGIC Industry Showcase Day: Winegrowing Futures and More, National Wine and Grape Industry Centre. 16/6/11

Hall, A. and Wilson, M. (2011). The role of vineyard spatiotemporal variability in grapevine yield forecasting, National Wine and Grape Industry Centre, Industry Showcase Day: Winegrowing Futures and More, Wagga Wagga, 16/6/11.

Hall, A. (2011). Temperature index modelling for viticulture climate change planning using spatial analogues climate 11 – impacts and adaptations symposium. NSW Department of Primary Industries, Convention Centre, Charles Sturt University, Wagga Wagga, 22/6/11

Holzapfel, B. (2010). Post-harvest management of grapevines - nutrient and carbohydrate reserves. Southern Tablelands Winemakers Association. Canberra, ACT, 28/05/10.

Holzapfel, B., Hall, A., and Smith, J. (2010). Influence of vineyard management and environment on carbohydrate reserves and vine performance. Workshop presentation. How weather and carbohydrate availability control grapevine yields. 14th Australian Wine IndustryTechnical Conference, Adelaide, July 4-7.

Holzapfel, B.P., Hall, A. and Smith, J. (2011). Influence of vineyard management and environment on carbohydrate reserves and vine performance. Climate 11 – Impacts and Adaptations symposium. NSW Department of Primary Industries, Convention Centre, Charles Sturt University, Wagga Wagga, 23/6/11

Smith, J. (2009). Understanding carbohydrates reserves in relation to vine growth and balance. Southern Tablelands Winemakers Association meeting. Canberra, ACT, 02/02/09.

Smith, J. (2009). Can carbohydrate reserves provide a physiological indicator of vine balance in hot climate vineyards? National Wine and Grape Industry Centre seminar series, Wagga Wagga, NSW, 05/08/09.

Smith, J. (2009). Carbohydrates and vine balance: some insights for the management of berry sugar accumulation. GWRDC workshop: Handling high sugar levels in the vineyard and winery. Bendigo, Victoria, 18/11/2009.

Smith, J., Field, S., Quirk, L. and Holzapfel, B. (2009). Post-harvest care of vines: irrigation, nutrition and salinity. Module 1, Water and Wine workshop: Cowra, NSW, 30/01/09.

Smith, J., Field, S., Quirk, L. and Holzapfel, B. (2009). Post-harvest care of vines: irrigation, nutrition and salinity. Module 1, Water and Wine workshop: Canberra, ACT, 27/02/09.

Smith, J., Field S., Quirk L, and Holzapfel, B. (2009). Post-harvest care of vines: irrigation, nutrition and salinity. Module 1, Water and Wine workshop: Langhorne Creek, SA, 06/11/09.

Smith, J., Holzapfel, B., Barlow, K., Bond, W., Blackney, E., Hutchinson, P. and Hutton, R. (2007). Nitrogen management in irrigated vineyards: balancing vine nutritional requirements with environmental impact. XIIIth Australian Wine Industry Technical Conference. Adelaide, 28 July – 2 August 2007.

Smith, J., Holzapfel, B. and Rogiers, S. (2011). Grapevine carbohydrate reserves: regional variation, soil temperature and management impacts. NWGIC Industry Showcase Day Winegrowing Futures and More. National Wine and Grape Industry Centre, Wagga Wagga, 16/6/2011

Smith, J., Quirk, L. and Holzapfel, B. (2010). Crop load and irrigation effects on Shiraz grape and wine composition. Irrigation and nutrition science for Riverina wine production workshop. Griffith, NSW, 8/6/2010.

Media reports

14/4/09 A. Hall, CSU media release: Climate change and growing wine grapes - http://News.CSU.Edu.Au/Director/Regionalnews.Cfm?Itemid=A2bff52ea76bdf191c5251f2aba90dc4&Printtemplate=Release

15/4/09 Andrew Hall, Interviewed for news item on win television relating to the climate change and growing wine grapes

17/4/09 Andrew Hall, Reported on for article in Riverina daily advertiser on research - http://Www.Dailyadvertiser.Com.Au/News/Local/News/General/The-Future-Of-Grape-Growing/1489190.Aspx

25/5/09 Andrew Hall, Climate change projections for viticulture in the Hunter Valley 30 minute video recording. Written and performed by: Andrew Hall; produced and directed by: Shayne Hackett and Leo Quirk

Other communications

Hall, A. (2008). Precision agriculture -from a viticulture perspective. Chinese delegation tour program – irrigation and water entitlements and allocation study tour, Charles Sturt University, Wagga Wagga, 19/09/08.

Hall, A. (2008). Precision viticulture, lecture to Charles Sturt University Viticulture 211 students, Food and Wine Industry Training Centre, Wagga Wagga, 30/9/08.

Hall, A. (2010). Earth's Atmosphere, annual Seniors' Week lecture, Joyes Hall, Charles Sturt University, Wagga Wagga, 22/3/10.

Holzapfel, B., Hall, A. and Smith, J. (2010). Influence of vineyard management and environment on carbohydrate reserves and vine performance. Guest lecture, Charles Sturt University Viticulture 301, 22/8/2010.

Smith J. (2009). Can carbohydrate reserves provide a physiological indicator of vine balance in hot climate vineyards? Guest lecture, Charles Sturt University Viticulture 303, 25/9/2009

Appendix 2
Intellectual property

Information generated from this research has been freely disseminated and no intellectual property has been identified from research conducted in this Theme.

Appendix 3
References

Acevedo-Opazo, C., Tisseyre, B., Guillaume, S. and Ojeda, H. (2008). The potential of high spatial resolution information to define within-vineyard zones related to vine water status. *Precision Agriculture* **9**: 285-302.

Ackers, P., White, W.R., Perkins, J.A. and Harrison, A.J.M. (1978). Weirs and Flumes for Flow Measurement. (John Wiley and Sons: Chichester).

Allen, R.G., Pereira, L.S., Raes, D. and Smith, M. (1998). Crop Evapotranspiration: Guidelines for Computing Crop Water Requirements, FAO Irrigation and Drainage Paper 56, FAO, Rome, Italy.

Allen M., Prusinkiewicz P. and Dejong T. (2005). Using L-systems for modelling source-sink interactions, architecture and physiology of growing trees: the L-peach model. *New Phytologist* **166**: 869-880.

Anon., (2004). model environmental management system, http://www.Environment.Gov.Au/Sustainability/Government/Ems/Index.Html, 7/9/2009.

ANZECC and ARMCANZ (2000). National Water Quality Management Strategy. Australian and New Zealand Guidelines for Fresh and Marine Water Quality.

Arheimer, B. and Liden, R. (2000). Nitrogen and phosphorus concentrations from agricultural catchments - influence of spatial and temporal variables, *Journal of Hydrology* **227**: 140-159.

ATECH Group (2000). Aggregated Nutrient Emissions to the Murray Darling Basin, Report prepared for the National Pollutant Inventory. (Environment Australia: Canberra.

Australian Bureau of Meteorology (2010). Australian water availability - temperature archive. Available online at: http://Www.Bom.Gov.Au/Jsp/Awap/Temp/Archive.Jsp (Accessed 24/02/2010).

Australian Government (2004). National Water Quality Management Strategy - Australian Drinking Water Guidelines. (National Health and Medical Research Council: Canberra).

Australian Wine and Brandy Corporation (2008). Australian geographical indications: regions [electronic resource]. (Australian Wine and Brandy Corporation: Adelaide).

Baker, D. (2001). Framework for a wine and grape industry approach to environmental management, Cooperative Research Centre for Viticulture, Proceedings of 11th Australian Wine Industry Technical Conference, Adelaide.

Baker, D. (2004). Viticulture environmental risk assessment tool (VERA), CRCV, Adelaide.

Bandaranayake, W.M. and Arshad, M.A. (2006). Soil profile distributions of water and solutes following frequent high water inputs, *Soil and Tillage Research* **90**: 39-49.

Barlow, K. (2003). Paddock to farm scaling of phosphorus export from irrigated agriculture (farm drains as a source or sink of phosphorus), PhD Thesis, University of Melbourne.

Barlow, K., Bond, W., Holzapfel, B., Smith, J. and Hutton, R. (2009). Nitrogen concentrations in soil solution and surface run-off on irrigated vineyards in Australia, *Australian Journal of Grape and Wine Research* **15**: 131-143.

Barrow, J. (1989). Surface reactions of phosphorous in soil, *Agricultural Science Research Journal* **2**: 33-38.

Bates, T.R., Dunst, R.M. and Joy, P. (2002). Seasonal dry matter, starch and nutrient distribution in 'concord' grapevine roots, *Hortscience* **37**: 313-316.

Bennett, J., Javis P., Creasy, G.L. and Trought, M.C.T. (2005). Influence of defoliation on overwintering carbohydrate reserves, return bloom, and yield of mature Chardonnay grapevines. *American Journal of Enology and Viticulture* **56**: 386-393.

Bergqvist, J., Dokoozlian, N. and Ebisuda, N. (2001). Sunlight exposure and temperature effects on berry growth and composition of Cabernet Sauvignon and Grenache in the central San Joaquin valley of California. *American Journal of Enology and Viticulture* **52**: 1-7.

Biggar, J.W., and Nielsen, D.R. (1976). Spatial variability of the leaching characteristic of a field soil, *Water Resource Research* **12**: 78-84.

Bindi, M., Miglietta F., Gozzini B., Orlandini S. and Seghi L. (1997). A simple model for simulation of growth and development in grapevine (*Vitis vinifera L.*). i. Model description. *Vitis* **36**: 67-71.

Bindon, K., Dry, P. and Loveys, B. (2008). Influence of partial rootzone drying on the composition and accumulation of anthocyanins in grape berries (*Vitis vinifera* cv. Cabernet Sauvignon). *Australian Journal of Grape and Wine Research* **14**: 91-103.

Birth, G. S. and Mcvey, G. (1968). Measuring the colour of growing turf with a reflectance spectroradiometer. *Agronomy Journal* **60**: 640-643.

Blaschke, T. (2010). Object based image analysis for remote sensing. *ISPRS Journal of Photogrammetry and Remote Sensing* **65**: 2-16.

Bogs, J., Downey M.O., Harvey J.S., Ashton A.R., Tanner G.J. and Robinson S.P. (2005). Proanthocyanidin synthesis and expression of genes encoding leucoanthocyanidin reductase and anthocyanidin reductase in developing grape berries and grapevine leaves. *Plant Physiology* **139**: 652-663.

Bramley, R.G.V and Lanyon, D.M. (2002). Vineyard leakiness, Proceedings of a GWRDC Workshop, Adelaide, January pp. 31-37.

Bramley, R. G. V. and Hamilton, R. P. (2004). Understanding variability in wine grape production systems 1.Within vineyard variation in yield over several vintages. *Australian Journal of Grape and Wine Research* **10**: 32-45.

Broge, N. H. and Leblanc, E. (2000). Comparing prediction power and stability of broadband and hyperspectral vegetation indices for estimation of green leaf area index and canopy chlorophyll density. *Remote Sensing of the Environment* **76**: 156-172.

Butler, B.E. (1979). A soil survey of the horticultural soils in the Murrumbidgee Irrigation Areas, New South Wales, CSIRO Division of Soils No. 289.

Butters, G.L. and Jury, W.A. (1989). Field scale transport of bromide in an unsaturated soil 2. Dispersion modelling, *Water Resources Research* **25**: 1583-1589.

Cheng L., Xia G. and Bates T. (2004). Growth and fruiting of young 'concord' grapevines in relation to reserve nitrogen and carbohydrates. *Journal of the American Society of Horticultural Science* **129**: 660-666.

Christen, E. and Hutchinson, P. (2002). Vineyard leakiness, Proceedings of a GWRDC Workshop, Adelaide, January pp. 9-23.

Christen, E. and Skehan, D. (1999). Design and management of subsurface drainage for improved water quality: a field trial, CSIRO Land and Water Technical Report 6/99, (CSIRO Land and Water: Griffith, NSW).

Cieslak, M., Seleznyova A.N. and Hanan J. (2011). A functional-structural kiwifruit vine model integrating architecture, carbon dynamics, and effects of the environment. *Annals of Botany* **107**: 747-764.

Clingeleffer, P. R., Dunn, G., Krstic, M. and Martin, S. (2001). Crop development, crop estimation and crop control to secure quality and production of major wine grape varieties: a national approach. (Grape and Wine Research and Development Corporation: Adelaide).

Conradie, W.J. (2005). Partitioning of mineral nutrients and timing of fertilizer application for optimum efficiency. In: Proceedings of the Soil Environment and Vine Mineral Nutrition Symposium. Eds. J.P. Christensen and D.R. Smart. (American Society For Enology and Viticulture: Davis, California) pp. 68-81.

Cortell, J. M., Halbleib, M., Gallagher, A. V., Righetti, T. L. and Kennedy, J. A. (2007). Influence of vine vigor on grape (*Vitis vinifera* L. cv. Pinot Noir) anthocyanins. 1. Anthocyanin concentration and composition in fruit. *Journal of Agricultural and Food Chemistry* **55**: 6575-6584.

Cottingham, P. (1995). Algal Bloom and Nutrient Status of Victorian Inland Waters, (Department of Conservation and Natural Resources: Melbourne).

Cunha, M., Marcal, A. R. S. and Silva, L. (2010). Very early prediction of wine yield based on satellite data from vegetation. *International Journal of Remote Sensing* **31**: 3125-3142.

Da Costa, J. P., Michelet, F., Germain, C., Lavialle, O. and Grenier, G. (2007). Delineation of vine parcels by segmentation of high resolution remote sensed images. *Precision Agriculture* **8**: 95-110.

Daly, C., Halbleib, M., Smith J.I., Gibson, W.P., Doggett, M.K., Taylor, G.H., Curtis, J. and Pasteris, P.A. (2008). Physiographically-sensitive mapping of temperature and precipitation across the conterminous United States. *International Journal of Climatology* **28**: 2031-2064.

Delenne, C., Durrieu, S., Rabatel, G., Deshayes, M., Bailly, J. S., Lelong, C. and Couteron, P. (2008). Textural approaches for vineyard detection and characterization using very high spatial resolution remote sensing data. *International Journal of Remote Sensing* **29**: 1153-1167.

Department of Natural Resources and Environment (1996). Blue Green Algae and Nutrients in Victoria: a resource handbook, (Department of Natural Resources and Environment, Victoria: Melbourne, Australia).

Dobrowski, S. Z., Ustin, S. L. and Wolpert, J. A. (2002). Remote estimation of grapevine canopy density in vertically shoot- positioned vineyards: determining optimal vegetation indices. *Australian Journal of Grape and Wine Research* **8**: 117-125.

Dokoozlian, N.K. and Kliewer, W.M. (1996). Influence of light on grape berry growth and composition varies during fruit development. *Journal of the American Society of Horticultural Science* **121**: 869-874.

Donn, W. (1975). Meteorology. (Mcgraw-Hill: New York, USA).

Downey, M.O., Harvey J.S. and Robinson S.P. (2003). Analysis of tannins in seeds and skins of Shiraz grapes throughout berry development. *Australian Journal of Grape and Wine Research* **9**: 15-27.

Dry, P. R and Coombe, B. G. (1994). Primary bud-axis necrosis of grapevines. i. Natural incidence and correlation with vigor *Vitis* **33**: 225-230.

Dunn, G. M. and Martin, S. R. (1998). Optimising vineyard sampling to estimate yield components. *The Australian Grapegrower and Winemaker* **414a**: 102-107.

Dunn, G. M. and Martin, S. R. (2003). The current status of crop forecasting in the Australian wine Industry. Proceedings of the ASVO Seminar Series: Grapegrowing at the Edge, Tanunda, Barossa Valley, South Australia, July 2003 pp. 4-8.

Dunn, G. M. and Martin, S. R. (2007). A functional association in Vitis vinifera L. Cv. Cabernet Sauvignon between the extent of primary branching and the number of flowers formed per inflorescence. *Australian Journal of Grape and Wine Research* **13**: 95-100.

Ellsworth, T.R., Shouse, P.J., Skaggs, T.H., Jobes, J.A. and Fargerlund, J. (1996). Solute transport in unsaturated soil: experimental design, parameter estimation, and model discrimination, *Soil Science Society of America Journal* **60**: 397-407.

Fauske, K.M. (2006). example: neural network, http://www.texample.net/tikz/examples/neural-network/, [accessed 15/8/2011].

Field, S. K., Smith, J. P., Holzapfel, B. P., Hardie, W. J., Emery, R. J. N. (2009). Grapevine response to soil temperature: xylem cytokinins and carbohydrate reserve mobilization from budbreak to anthesis. *American Journal of Enology and Viticulture* **60**: 164-172.

Fisher, J. (2004). Regional environmental best practices for viticulture – Yarra Valley, Department of Primary Industries, Victoria.

Fleming, J.B. and Butters, G.L. (1995). Bromide transport detection in tilled and nontilled soil: solution samplers vs. soil cores. *Soil Science Society of America Journal* **59**: 1207-1216.

Flury, M. and Paprtiz, A. (1993). Bromide in the natural environment: occurrence and toxicity, *Journal of Environmental Quality* **22**: 747-758.

Freund, J. E. and Simon, G. A. (1997). Modern Elementary Statistics. (Prentice-Hall International: Upper Saddle River, New Jersey).

Fridgen, J. J., Kitchen, N. R., Sudduth, K. A., Drummond, S. T., Wiebold, W. J. and

Fraisse, C. W. (2004). Management zone analyst (mza): Software for subfield management zone delineation. *Agronomy Journal* **96**: 100-108.

Gasser, M.O., Caron, J., Laverdiere, M.R. and Lagace, R. (2002). Solute transport modelling under cultivated sandy soils and transient water regime **31**: 1722-1730.

Gee, G.W. and Or, D. (2002). Particle-Size Analysis. In: Methods of Soil Analysis. Eds. J. H. Dane and G. Clarke Topp. (Soil Science Society of America: Madison, Wisconsin). Part 4. Physical methods. pp. 255-293.

Gitelson, A. A., Kaufman, Y. J., Stark, R. and Rundquist, D.,(2002). Novel algorithms for remote estimation of vegetation fraction. *Remote Sensing of Environment* **80**: 76-87.

Gladstones, J. (1992). Viticulture and Environment. (Winetitles: Adelaide).

Gladstones, J.S. (2004). Climate and Australian Viticulture. In: 'Viticulture', Volume 1 - Resources. Eds. P. R.Dry and B.G. Coombe (Winetitles: Adelaide, Australia) pp. 90-118.

Glarner, H. (2006). Length of day and twilight (formulas). Http://herbert.gandraxa.com/herbert/lod.asp [accessed 28 July 2009].

Goodwin, I. (2002). Traditional approaches for measuring vine and vineyard water requirements. In: Vine and Vineyard Water Requirements. Eds. R.R. Walker and M.R. Gibberd (Cooperative Research Centre for Viticulture: Adelaide, South Australia).

Grace, M.R., Hart, B.T., Oliver, R.L. and Rees, C.M. (1997). Algal blooms in the Darling River - Are phosphates to blame? *Chemistry in Australia* **64**: 2-5.

Hall, A., Lamb, D. W., Holzapfel, B. and Louis, J. (2002). Optical remote sensing applications in viticulture - a review. *Australian Journal of Grape and Wine Research* **8**: 36-47.

Hall, A., Louis, J. and Lamb, D. (2003). Characterising and mapping vineyard canopy using high-spatial-resolution aerial multispectral images. *Computers and Geosciences* **29**: 813-822.

Hall, A., Louis, J. P. and Lamb, D. W. (2008). Low-resolution remotely sensed images of wine grape vineyards map spatial variability in planimetric canopy area instead of leaf area index. *Australian Journal of Grape and Wine Research* **14**: 9-17.

Hamilton, R. P. and Coombe, B. G. (1988). Harvesting of Wine Grapes. In: Viticulture. Volume 2, Practices. Eds. B. G. Coombe and P. R. Dry (Winetitles: Adelaide).

Hamilton, R. P., Partridge, S. J. and Wall, G. S. (2003) Grapegrowing at the edge. In: Proceedings of Australian Society of Viticulture and Oenology Seminar series: Tanunda, South Australia.

Harbertson, J. F. and Spayd, S. (2006). Measuring phenolics in the winery. *American Journal of Enology and Viticulture* **57**: 280-288.

Harrison, J. (1994). CSIRO Water Series: No 11, ISBN 0 643 05652 1.

Haselgrove, L., Botting, D., Heeswijck, R., Høj, P.B., Dry, P.R., Ford, C. and Land, P.G.I. (2000). Canopy microclimate and berry composition: The effect of bunch exposure on the phenolic composition of *Vitis vinifera* L. cv. Shiraz grape berries. *Australian Journal of Grape and Wine Research* **6**: 141-149.

Haslam, E. (1993). Shikimic Acid: Metabolism and Metabolites. (Wiley. Chichester, New York) 387p.

Heathwaite, A.L., Haygarth, P., Matthews, R., Preedy, N. and Butler, P. (2005). Evaluating colloidal phosphorous delivery to surface waters from diffuse agricultural sources, *Journal of Environmental Quality* **34**: 287-298.

Hillel, D. (1998). Environmental Soil Physics. (Academic Press, San Diego).

Holford, I. (1989). Phosphate behaviour in soils. *Agricultural Science* **2**: 15-21.

Hoiland, P., Gago, P. (1997). Australian Wine from the Vine to the Glass. (Patrick Iland Wine Promotions, Adelaide, Australia).

Holzapfel, B. and Treeby, M. (1999). Proceedings of the. 10th Australian Wine Industry. Technical Conference, Sydney.

Holzapfel, B. P., Smith, J. P., Field, S. K. and Hardie, W. J. (2010). Dynamics of carbohydrate reserves in cultivated grapevines. *Horticultural Reviews* **37**: 143-211.

Holzapfel, B. P., Smith, J. P., Mandel, R. M. and Keller, M. (2006). Manipulating the postharvest period and its impact on vine productivity of Semillon grapevines. *American Journal of Enology and Viticulture* **57**: 148-157.

Holzapfel B.P. and Smith J.P. (2011). Developmental stage and climatic factors impact more on carbohydrate reserve dynamics of Shiraz than cultural practice. *American Journal of Enology and Viticulture* (in press).

Homayouni, S., Germain, C., Lavialle, O., Grenier, G., Goutouly, J. P., Van Leeuwen, C. and Da Costa, J. P. (2008). Abundance weighting for improved vegetation mapping in row crops: applications to vineyard vigour monitoring. *Canadian Journal of Remote Sensing* **34**: S228-S239.

Howell, G. S. (2001). Sustainable grape productivity and the growth-yield relationship: A review. *American journal of Enology and Viticulture* **52**: 165-174.

Huete, A., Didan, K., Miura, T., Rodriguez, E. P., Gao, X. and Ferreira, L. G. (2002). Overview of the radiometric and biophysical performance of the modis vegetation indices. *Remote Sensing of Environment* **83**: 195-213.

Huete, A. R., Justice, C. and Van Leeuwen, W. J. (1999). Modis vegetation index (mod 13) algorithm theoretical basis document (version 3). Available online at: Http://Modis.Gsfc.Nasa.Gov/Data/Atbd/Atbd_Mod13.Pdf (Accessed 5/11/2010).

Huete, A. R., Liu, H. Q., Batchily, K. and Van Leeuwen, W. J. (1997). A comparison of vegetation indices over a global set of tm images for eos-modis. *Remote Sensing of Environment* **59**: 440-451.

Huglin, P. (1978). Nouveau mode d'évaluation des possibilités héliothermiques d'un milieu miticole. *Comptes Rendus de L'Académie D'Agriculture de France* 1117-1126.

Huglin, P. Schneider C (1998). Biologie Et Écologie De La Vigne.' (Lavoisier: Paris, France).

Hutchinson, P.A. and Bond, W.J. (2001). Routine measurement of the soil water potential gradient near saturation using a pair of tube tensiometers, *Australian Journal of Soil Research* **39**: 1147-1156.

Hutton, R., Holzapfel, B., Smith, J., Hutchinson, P., Barlow, K. and Bond, W. (2007). Influence of irrigation and fertiliser management on the movement of water and nutrients within and below the rootzone of vines for sustainable grape production, Final report to Cooperative Research Centre for Viticulture, September 2007.

Iacono, F., Reniero, F. and Scienza A. (1995). Carbon isotope discrimination, fluorescence emission and gas exchange in the genus vitis during adaptation to water stress. definition of an index of genotypic drought tolerance. *Rivista-di-Viticoltura-e-di-Enologia* **48**: 5-34.

Iland, P., Bruer, N., Edwards G., Weeks, W. and Wilkes, E. (2004). Chemical Analysis of Grapes and Wine: Techniques and Concepts. (Patrick Iland Wine Promotions). 110 pages.

IPCC (2007). Summary for policymakers. in: 'Climate Change 2007: The physical science basis. Contribution of Working Group 1 to the Fourth Assessment Report of the Intergovernmental Panel on Climate Change'. Eds. S. Solomon, D. Qin, M. Manning, Z. Chen, M. Marquis, K.B. Averyt, M. Tignor and H.l. Miller. (Cambridge University Press: Cambridge, United Kingdom and New York, USA).

Intrieri, C., Poni, S., Rebucci, B. and Magnanini, E. (1997). Effects of canopy manipulations on whole-vine photosynthesis: results from pot and field experiments *Vitis*, **36**: 167-173.

Isbell, R.F. (1996). Australian Soil Classification. (CSIRO Publishing, Melbourne, Australia).

Isbell, R.F. (2002). The Australian Soil Classification. revised edition (CSIRO Publishing, Melbourne, Australia).

Jet Propulsion Laboratory (2004). Seamless shuttle radar topography mission (srtm) 3 arc second version 2. Ftp://E0srp01u.Ecs.Nasa.Gov/Srtm/Version2/Srtm3/Australia/ [Accessed 18 March 2006].

Johnson, L. F., Bosch, D. F., Williams, D. C. and Lobitz, B. M. (2001). Remote sensing of vineyard management zones: implications for wine quality. *Applied Engineering in Agriculture* **17**: 557-560.

Johnson, L., Lobitz, B., Armstrong, R., Baldy, R., Weber, E., Debenedictis, J. and Bosch, D. (1996). Airborne imaging aids vineyard canopy evaluation. *California Agriculture* **50**: 14-18.

Johnson, L., Lobitz, B., Bosch, D., Wiechers, S., Williams, D. and Skinner, D. (1998). Of Pixels and Palates: Can geospatial technologies help produce a better wine? In: Proceedings of the 1st International Conference on Geospatial Information in Agriculture and Forestry. Lake Buena Vista, Florida, pp.469-476.

Johnson, L. F., Roczen, D. E., Youkhana, S. K., Nemani, R. R. and Bosch, D. F. (2003). Mapping vineyard leaf area with multispectral satellite imagery. *Computers and Electronics in Agriculture* **38**: 33-44.

Jones, G.V. (2006). Climate and terroir: impacts of climate variability and change on wine. in: 'Fine Wine and Terroir - the Geoscience Perspective'. (Eds R.W. Macqueen, and L.D. Meinert) Geological Association of Canada: St. John's, Newfoundland, Canada pp. 203-216.

Jones, G.V, Duff, A., Hall, A. and Myers, J. (2010). Spatial analysis of climate in wine grape growing regions in the western United States. *American Journal of Enology and Viticulture* (in press).

Jones, G.V., Moriondo, M., Bois, B., Hall, A., Duff, A. (2009). Analysis of the spatial climate structure in viticulture regions worldwide. *Le Bulletin de l'Organisation Internationale de la Vigne et du Vin* **82**: 507-518.

Jury, W.A. and Roth, K. (1990). Transfer functions and solute movement through soil: theory and applications, Hirkhauser Verlag, Basle, Switzerland.

Jury, W.A. and Sposito. G. (1985). Field calibration and validation of solute transport models for the unsaturated zone, *Soil Science Society of America Journal* **49**: 1331-1341.

Kirkby, C.A., Smyth, L.J., Cox, J.W. and Chittleborough, D.J. (1997). Phosphorous movement down a toposequence from a landscape with texture contrast soils, *Australian Journal of Soil Research* **35**: 339-417.

Kitchen, N. R., Sudduth, K. A., Myers, D. B., Drummond, S. T. and Hong, S. Y. (2005). Delineating productivity zones on claypan soil fields using apparent soil electrical conductivity. *Computers and Electronics in Agriculture* **46**: 285-308.

Kliewer, H. and Dokoozlian, N.K. (2005). Leaf area/crop weight ratios of grapevines: influence on fruit composition and wine quality. *American Journal of Enology and Viticulture* **56**: 170-181.

Kohavi, R. (1995). A study of cross-validation and bootstrap for accuracy estimation and model selection. Proceedings of the Fourteenth International Joint Conference on Artificial Intelligence, Montreal. (Morgan Kaufmann, San Mateo, California, USA) pp. 1137-1143.

Lamb, D. W., Weedon, M. M. and Bramley, R. G. V. (2004). Using remote sensing to predict grape phenolics and colour at harvest in a Cabernet Sauvignon vineyard: timing observations against vine phenology and optimising image resolution. *Australian Journal of Grape and Wine Research* **10**: 46-54.

Lakso, A.N. and Poni, S. (2005). Vitisim – a simplified carbon balance model of a grapevine. Proceedings of the XIVth GESCO Symposium. pp 478-484.

Lakso, A.N., Intrigliolo, D.S. and Eissenstat, D.M. (2008). Modeling 'Concord' grapes with Vitisim, a simplified carbon balance model: understanding pruning effects. *Acta Horticulturae* **803**: 243-250.

Loveys, B., Stoll, M., Dry, P. and McCarthy, M. (1998). *Australian Grapegrower and Winemaker* **414a**:108-113.

Mabrouk, H. and Sinoquet, H. (1998). Indices of light microclimate and canopy structure of grapevines determined by 3d digitising and image analysis, and their relationship to grape quality. *Australian Journal of Grape and Wine Research* **4**: 2-13.

Mallawatantri, A.P., and Mulla, D.J. (1996). Uncertainties in leaching risk assessments due to field average transfer function parameters, *Soil Science Society of America Journal* **60**: 722-726.

Marschner, H. (1995). Mineral Nutrition of Higher Plants. (Academic Press, London).

Martin, P., Zarco-Tejada, P. J., Gonzalez, M. R. and Berjon, A. (2007). Using hyperspectral remote sensing to map grape quality in 'Tempranillo' vineyards affected by iron deficiency chlorosis *Vitis* **46**: 7-14.

Martin, S., Dunstone, R. and Dunn, G. (2003). How to forecast wine grape deliveries., (Department of Primary Industries, Tatura, Victoria).

Masarik, K.C., Norman, J.M., Byre, K.R. and Baker, J.M. (2004). Improvements to measuring water flux in the vadose zone **33**: 1152-1158.

May, P. (1965). Reducing inflorescence formation by shading individual Sultana buds. *Australian Journal of Biological Science* **18**: 463-473.

May, P. (2004). Flowering and Fruitset in Grapevine. (Lythrum Press: Adelaide).

McCaffery, A. (1999). The Murrumbidgee Irrigation Area tile drainage monitoring scheme 1998/99, 1997/98 National Heritage Community Group Theme Progress Report. (Murrumbidgee Irrigation Ltd, Griffith, NSW).

McCarthy, M. (1998). *Australian Grapegrower and Winemaker* **414a:** 65-71.

Mcintyre, G.N, Kliewer, W.M., Lider, L.A. (1987). Some limitations of the degree-day system as used in viticulture in California. *American Journal of Enology and Viticulture* **38**: 128-132.

Mckenzie, N.J., Coughlan, K.J. and Cresswell, H.P. (2002). Soil Physical Measurement and Interpretation for Land Evaluation. (CSIRO Publishing: Melbourne).

Mengel, K. (1991). Ernährung and Stoffwechsel Der Pflanze (Gustav Ficsher Verlag, Jena).

Meyer, W.S., Smith, D.J. and Shell, G. (1999). Estimating reference evaporation and crop evapotranspiration from weather data and crop coefficients, CSIRO Land and Water, Technical Report 34/98, (CSIRO: Canberra, Australia).

Metternicht, G. (2003). Vegetation indices derived from high-resolution airborne videography for precision crop management. *International Journal of Remote Sensing* **24**: 2855-2877.

Morais, R., Fernandes, M. A., Matos, S. G., Serodio, C., Ferreira, P. and Reis, M. (2008). A zigbee multi-powered wireless acquisition device for remote sensing applications in precision viticulture. *Computers and Electronics in Agriculture* **62**: 94-106.

Muller, K. (1993). Mineralization of organically bound nitrogen in vineyard soils. Part ii. seeping water, nitrate concentration and nitrate washout *Vitis* **32**: 23-34.

Muller, W., Gartel and Zakosek, H. (1985). Leaching of plant nutrients from vineyard soils of the middle-mose, *Journal of Plant Nutrition and Soil Science* **148**: 417-428.

Naor, A., Gal Y. and Bravdo, B. (2002). Crop load affects assimilation rate, stomatal conductance, stem water potential and water relations infield-grown Sauvignon Blanc grapevines. *Journal of Experimental Botany* **48**: 1675-1680.

Neja, R.A., Wildman, W.E., Ayers, R.S. and Kasimatis, A.N. (1977). Grapevine response to irrigation and trellis treatments in the Salinas Valley. *American Journal of Enology and Viticulture* **28**: 16-26.

Newton, P.J. and Hastings, M. Y. (2003). Barwon Basin Environmental Management System. (Department of Primary Industry: Victoria).

Nicholas, P. (2004). Soil, Irrigation and Nutrition. (South Australian Research and Development Institute: Adelaide).

Ollat, N., Diakou-Verdin, P., Carde, J.P., Barrieu, F., Gaudillere, J.P. and Moing, A. (2002). Grape berry development: a review. *Journal International des Sciences de la Vigne et du Vin* **36:** 109-131.

Pedroso, M., Taylor, J., Tisseyre, B., Charnomordic, B. and Guillaume, S. (2010). A segmentation algorithm for the delineation of agricultural management zones. *Computers and Electronics in Agriculture* **70**: 199-208.

Petrie, P.R. and Clingeleffer, P.R. (2006). Crop thinning (hand versus mechanical), grape maturity and anthocyanin concentration: outcomes from irrigated Cabernet Sauvignon (*Vitis vinifera* L.) in a warm climate. *Australian Journal of Grape and Wine Research* **12**: 21-29.

Picard Rr, Cook Rd (1984). Cross-validation of regression models. *Journal of the American Statistical Association* **79**: 575-583.

Piper, C. (1942). Soil and Plant Analysis. (University of Adelaide).

Poni, S., Palliotti, A. and Bernizzoni, F. (2006). Calibration and evaluation of a stella software-based daily co_2 balance model in *Vitis vinifera* L. *Journal of the American Society of Horticultural Science* **131**: 273-283.

Prieto, J.A., Louarn, G., Perez Pena, J., Ojeda, H., Simonneau, T. and Lebon, E. (2011). Assessing whole vine canopy gas exchange through a functional-stuctural plant model for grapevine (cv. Syrah). Proceedings of the XVII GESCO Symposium, pp. 367-370.

Proffitt, T., Bramley, R., Lamb, D. and Winter, E. (2006). Precision viticulture: a new era in vineyard management and wine production. (Winetitles: Ashford, South Australia).

Ramos, M.C. and Martinez-Casasnovas, J.A. (2006). Nutrient losses by runoff in vineyards of the Mediterranean Alt Penedes region (NE Spain). *Agriculture, Ecosystems and Environment* **113**: 356-363.

Ramos, M.C. and Martinez-Casasnovas, J.A. (2004). Nutrient losses from a vineyard soil in North eastern Spain caused by an extraordinary rainfall event, *Catena* **55**: 79-90.

Ravaz, L. (1930). Influence de la taille sur la vigeur et la production de la vigne. *Progres Agricole et Viticulture* **2**: 537.

Rayment, G.E. and Higginson, F.R. (1992). Australian Laboratory Handbook of Soil and Water Chemical Methods (Australian Soil and Land Survey Handbook Vol.3). (Inkata Press: Melbourne).

Reedman, P. (2001). Environmental component of consumer perceptions in the UK market. In: Proceedings of the 11th Australian Wine Industry Technical Conference. Adelaide. p165.

Ribolzi, O., Valles, V., Gomez, L. and Voltz, M. (2002). Speciation and origin of particulate copper in runoff water from a Mediterranean vineyard catchment, *Environmental Pollution* **117**: 261-271.

Ridely, A.M., Paramore, T.R., Beverly, C.R., Dunin, F.X and Froelich, V.M.C (2003). Developing environmental monitoring tools from sustainability indicators in the southern Riverina, *Australian Journal of Experimental Agriculture* **43**: 271-284.

Robinson, J.B., Treeby, M.T. and Stephenson, R.A. (1997). Fruits, vines and nuts. In: Plant Analysis: an interpretation manual. Eds D.J. Reuter and J.B. Robinson. (CSIRO Publishing: Collingwood, Australia) pp. 249-382.

Rogiers S.Y., Smith J.P., Holzapfel B.P. and Hardie W.J. (2011). Soil temperature moderates grapevine carbohydrate reserves after bud-break and conditions fruit set responses to photoassimilatory stress. *Functional Plant Biology* **38**: 899-909

Rouse, J. W., Haas, R. H., Schell, J. A. and Deering, D. W. (1973). Monitoring vegetation systems in the Great Plains with ERTS. In: Third Earth Resource Technology Satellite (ERTS) Symposium, Freden. Eds. S. C., Mercanti, E. P. and Becker, M. A. (NASA: Washington, D, USA) NASA Special Publication SP-351.

Rupp, D. (1996). Green cover management to optimise the nitrogen supply of grapevines.In: First International Society for Horticultural Science workshop on strategies to optimise wine grape quality. pp. 57-62.

Sanchez, L.A. and Dokoozlian, N.K. (2005). Bud microclimate and fruitfulness in *Vitis vinifera* L. *American Journal of Enology and Viticulture* **56**: 319-329.

Sarneckis, C.J., Dambergs R.G., Jones P., Mercurio M., Herderich M.J. and Smith P.A. (2006). Quantification of condensed tannins by precipitation with methyl cellulose: development and validation of an optimised tool for grape and wine analysis. *Australian Journal of Grape and Wine Research* **12**: 39-49.

Schaller, K. (1991). Groundwater pollution by nitrate in viticultural areas. Proceedings of International Symposium on Nitrogen in Grapes and Wine. pp. 12-22.

Schaller, K. (2000). Intensive viticulture and its environmental impacts: nitrogen as a case study. *Acta Horticulturae* **512**: 39-46.

Schaller, K., Löhnerts, O., Bertold, K, Emde, K. and Jagoutz, H.(1993). Proceeding of the 8th Australian Wine Industry Technical Conference, Melbourne, 18-28.

Schepers, A. R., Shanahan, J. F., Liebig, M. A., Schepers, J. S., Johnson, S. H. and Luchiari, A. (2004). Appropriateness of management zones for characterizing spatial variability of soil properties and irrigated corn yields across years. *Agronomy Journal*, **96**: 195-203.

Sharma, M.L., Byrne, J. and Herne, D., Kin P. (1996). Nutrient leaching beneath horticultural land use - West Australian examples. In: Agricultural impacts on groundwater quality. (Australian Centre for International Agricultural Research: Malaysia) pp. 82-89.

Sharpley, A.N. and Tunney, H. (2000). Phosphorous research strategies to meet agricultural and environmental challenges of the 21st century. *Journal of Environmental Quality* **29**: 176-181.

Šimůnek, J., Jacques, D., Van Genuchten, M.Th. and Mallants, D. (2006). Multicomponent geochemical transport modelling using the hydrus computer software packages. *Journal of the American Water Resources Association* **42**: 1537-1547.

Skaggs, T.H., Jaynes, D.B., Kachanoski, R.G., Shouse, P.J. and Ward, A.L. (2002). Solute transport: data analysis and parameter estimation. In: Methods of Soil Analysis Part 4, Physical Methods. Eds. J. H. Dane and G. Clarke Topp, (Soil Science Society of America, Madison, Wisconsin) pp. 1403-1431

Smart, R. E. (1985). Principles of grapevine canopy microclimate manipulation with implications for yield and quality. A review. *American Journal of Enology and Viticulture*, **36**: 230-239.

Smart, R. E. and Sinclair, T. R. (1976). Solar heating of grape berries and other spherical fruits. *Agricultural Meteorology* **17:** 241-259.

Smithyman, R.P., Howell, G.S. and Miller, H.L. (1998). The use of competition for carbohydrates among vegetative and reproductive sinks to reduce fruit set and botrytis bunch rot in Seyval Blanc grapevines. *American Journal of Enology and Viticulture* **49**: 163-170.

Smith, J.P. and Holzapfel, B.P. (2009). Cumulative response of grapevine (*Vitis vinifera* L.) To late season perturbation of carbohydrate reserve status. *American Journal of Enology and Viticulture* **60**: 461-470

Soil Survey Staff (2010). Keys to Soil Taxonomy, 11th ed. (USDA-Natural Resources Conservation Service: Washington, D.C.).

Spayd, S. E., Tarara, J. M., Mee, D. L. and Ferguson, J. C. (2002). Separation of sunlight and temperature effects on the composition of *Vitis vinifera* cv. Merlot berries. *American Journal of Enology and Viticulture* **53**: 171-182.

Steel, R. G. D., Torrie, J. H. and Dickey, D. A. (1997). Principles and Procedures of Statistics: a biometrical approach. (McGraw-Hill: New York).

Sturman, A.P., Tapper, N.J. (1996). The Weather and Climate of Australia and New Zealand. (Oxford University Press: Melbourne, Australia; Oxford, UK; Auckland, New Zealand; New York, USA).

Tibco Software (2008). Tibco spotfire s+ version 8.1.1 for linux 2.6.9-34.el, 64-bit. 8.1.1 ed. Palo alto, California, Tibco software inc.

Tilahun, K., Botha, J.F. and Bennie, A.T.P. (2005). Transport of bromide in the bainsvlei soil: field experiment and deterministic/stochastic model simulation. I. Continuous water application. *Australian Journal of Soil Research* **43**: 73-80.

Tisseyre, B., Mazzoni, C. and Fonta, H. (2008). Within-field temporal stability of some parameters in viticulture: potential toward a site specific management. *Journal International des Sciences de la Vigne et du Vin* **42**: 27-39.

Tisseyre, B., Ojeda, H. and Taylor, J. (2007). New technologies and methodologies for site-specific viticulture. *Journal International des Sciences de la Vigne et du Vin* **41**: 63-76.

Treeby M.T. and Wheatly D.M. (2006). Effect of nitrogen fertilizer on nitrogen partitioning and pool sizes in irrigated Sultana grapevines. *Australian Journal of Experimental Agriculture* **46**: 1207-1215.

United States Federal Government (2008). Code of federal regulations: alcohol, tobacco products, and firearms (Title 27, parts 1-199). Part 9 - American Viticultural Areas, pp. 101-223 (National Archives and Records Administration: Washington, D,C, USA).

United Nations(2003). Water for people, water for life, The United Nations Water Development Report. (United Nations World Water Assessment Programme: Paris, France).

Van Grinsven, J.J.M., Booltink, H.W.G., Dirksen, C., Van Breemen, N., Bongers, N. and Waringa, N. (1988). Automated in situ measurement of unsaturated soil water flux, *Soil Science Society of America Journal* **52**: 1215-1218.

Vanderborght, J., Vanclooster, M., Mallants, D., Diels, J. and Feyen. J. (1996). Determining convective lognormal solute transport parameters from resident concentration data, *Soil Science Society of America Journal* **60**: 1306-1317.

Vasconcelos, M.C., Greven, M., Winefield, C.S., Trought, M.C.T., Raw, V. (2009). The flowering process of *Vitis vinifera*: a review. *American Journal of Enology and Viticulture* **60**: 411-434.

Vasudevan, L. Wolf, T. K. Welbaum, G. G. Wisniewski, M. E. (1998). Reductions in bud carbohydrates are associated with grapevine bud necrosis *Vitis* **37**: 189-190.

Venables, W.N., Ripley, B.D. (2002). 'Modern Applied Statistics with S.' (Springer science+business media inc.: new york, ny, usa).

Wade, J, Holzapfel, B., Keller, M. and Tesic, D. (2000). *Australian Grapegrower and Winemaker* **442**: 77-80.

Wade, J., Holzapfel, B., Keller, M. and Degaris, K. (2001). Proceedings of the 11th Australian Wine Industry Technical Conference, Adelaide.

Wade, J., Holzapfel, B., Degaris, K., Keller, M. and Williams, D. (2002). Acta Horticulturae, XXVIth International Horticultural Congress, Toronto, Canada, August 11-17.

Wahl, K., Schwab, A. and Peternel, M. (1997). New experiences about nitrogen dynamics in permeable soils - environmental aspects and wine quality. In Proceedings of the 4th International Symposium on Cool Climate Viticulture and Enology, Rochester, New York. pp. 6-9.

Walter, V. (2004). Object-based classification of remote sensing data for change detection. *ISPRS Journal of Photogrammetry and Remote Sensing* **58**: 225-238.

Wang, Q., Adiku, S., Tenhunen, J. and Granier, A. (2005). On the relationship of NDVI with leaf area index in a deciduous forest site. *Remote Sensing of Environment.* **94**: 244-255.

Wermelinger, B. (1991). International Symposium on Nitrogen in Grape and Wine pp. 23-31.

Watt, A. M., Dunn, G. M., May, P. B., Crawford, S. A. and Barlow, E. W. R. (2008). Development of inflorescence primordia in *Vitis vinifera* L. cv. Chardonnay from hot and cool climates. *Australian Journal of Grape and Wine Research* **14**: 46-53.

Went Fw (1957). Experimental Control of Plant Growth. (Chronica Botanica Co.: Walthan, Massachusetts, USA).

Weyand, K.M. and Schultz, H.R. (2006). Long-term dynamics of nitrogen and carbohydrate reserves in woody parts of minimally and severely pruned Riesling vines in a cool climate. *American Journal of Enology and Viticulture* **57**: 172-182.

White, R.E. (1987). Introduction to the Principles and Practice of Soil Science. (Blackwell Scientific Publications: London, England).

White, R.E., Dyson, J.S., Haigh, R.A., Jury, W.A. and Sposito. G. (1986). A transfer function model of solute transport through soil. 2. Illustrative applications. *Water Resources Research* **22**: 248-254.

Wild, A. (1988). Plant nutrients in soil: nitrogen. In: Russell's Soil Conditions and Plant Growth. Ed. A. Wild (John Wiley and Sons, Inc.: New York) pp. 652-694.

Winkler, A. J., Cook, J. A., Kliewer, W. M. and Lider, L. A. (1974). General Viticulture (University of California Press: Berkeley, Los Angeles, London).

Wolf, T. K. and Cook, M. K. (1992). Shoot growth and shade affect budnecrosis in Virginia. *American Journal of Enology and Viticulture* **43**: 394.

Wolpert, J. A. and Vilas, E. P. (1992). Estimating vineyard yields: introduction to a simple, two-step method. *American Journal of Enology and Viticulture* **43**: 384-388.

Yasuda, M., Umemiya, Y. and Sato, Y. (1988). Fate of nitrogen applied to soils cultivated with grapevines. *Bulletin of the Fruit Tree Research Station* **15**: 59-67.

Zarco-Tejada, P. J., Berjon, A., Lopez-Lozano, R., Miller, J. R., Martin, P., Cachorro, V., Gonzalez, M. R. and De Frutos, A. (2005). Assessing vineyard condition with hyperspectral indices: leaf and canopy reflectance simulation in a row-structured discontinuous canopy. *Remote Sensing of Environment* **99**: 271-287.

Appendix 4
Staff

Theme 4 leader

Dr Bruno Holzapfel

Key staff

Dr Inigo Auzmendi (From March 2011).

Dr John Gray

Dr Yann Guisard

Dr Andrew Hall

Dr Jonathan Holland

Dr Ron Hutton

Leo Quirk

Dr Jason Smith

Dr Leigh Schmidtke

Mark Wilson

Technical support

Phil Armstrong, NWGIC

Harry Creecy, NWGIC

Rob Giason

Kirstina Lamont, NWGIC

Peter Carey, NWGIC

Ned Sharkey, NWGIC

Markus Müller, NWGIC

Rob Lamont, NWGIC

Chris Haywood, NWGIC

K. Wilson, NWGIC

Andrew Drumm, CSU Winery

C. Scheffre

Emily Rouse, NWGIC

Chris Haywood, DPI NSW

Gail Fuller, Spatial Data Analysis Network, Charles Sturt University

Gary Mckenzie, Spatial Data Analysis Network, Charles Sturt University

Craig Poynter, Spatial Data Analysis Network, Charles Sturt University

Collaborators

Dr Kirsten Barlow, DPI Victoria

Dr Warren Bond, CSIRO

Dr Paul Hutchinson, Hussat Irrigation Services

Jeff Dance

Geoff McCorkelle

Anthony Pitt

Dr Greg Jones, Oregon State University

A/ Prof David Lamb, University of New England

Dr Jim Hannan

Louise Eather, Wyndham Estate Wines

Rod Muldune, Wyndham Estate Wines

John Hornbuckle, CSIRO Griffith

David Smith, CSIRO Griffith

Appendix 5
Other relevant material

Draft Guidelines For Irrigation Management

- Sampling can readily begin at time zero (i.e. application of the radiotracer), offering a broad window of continuous data sampling.
- Obtain Information About Crop Water Needs And Critical Growth Stages, Soil Characteristics And Irrigation System Efficiency To Properly Schedule Irrigations.
- Know How Much Water The Crop Uses On A Daily Or Weekly Basis. This Is The Evapotranspiration Estimated From Weather Data.
- Determine The Soil's Moisture Content In The Effective Root Zone And Its Maximum Water Holding Capacity.
- The Difference Between The Maximum Water Holding Capacity And The Actual Water Content Is The Net Amount Of Water To Be Applied.
- Determine The Application Efficiency Of Your Irrigation System.
- The Gross Amount Of Water To Be Applied Is The Net Amount Divided By The Application Efficiency Of The Irrigation System.
- Use Water Meters To Determine How Much Water Is Being Applied.
- Monitor Soil Moisture Before And After Irrigation To Determine Depth Of Water Penetration.
- With Surface Irrigation, Use Cutback Practices To Reduce Deep Percolation And Runoff.
- When Fertigating, Leave Room In The Soil Profile (10 To 20 Percent) To Store Potential Rainfall To Avoid Runoff Or Leaching

These guidelines are for fertiliser management:

- Use on-farm yield records and soil maps (em38) to determine site variability for calculating fertilizer rates in relation to yield performance
- Soil analysis should be used in conjunction with petiole analysis to determine fertilizer application rates.
- Split nitrogen applications to improve uptake efficiency and yield return for fertilizer investment. Apply one-third at or prior to the spring break and the balance before the critical flowering stage for the crop development. This is especially important for sandy soils which may leach nitrate.
- Avoid high application rates of nitrogen during autumn.
- Incorporate urea or ammonium sulphate n fertilizers into the soil to prevent volatilisation losses of ammonia gas.
- Place nitrogen and phosphorus in the same band to increase yields, as well as uptake efficiencies.
- Only apply nitrogen in irrigation water where irrigation efficiency and uniformity is high.
- Keep good records of nitrogen fertilizer to help make nitrogen management decisions later.

These guidelines should be implemented into an on-farm ems plan-do-check-act cycle that best suits specific vineyard practices. The benefits of implemented ems on-farm include:

- Better understanding of the environment, risks and liabilities
- Improved management and record keeping skills
- Reduced offsite impacts from the production system, including water and nutrient movement off site.

Appendix 6
Budget Reconciliation

See *Winegrowing Futures Final Report, Theme 1*